75.65

DIRECT NUCLEAR REACTIONS

INVOLVING NUCLEONS

by

KENNETH A. AMOS B.Sc.(Hons)
Department of Mathematical Physics
The University of Adelaide
South Australia

Submitted July, 1964

A Thesis submitted in accordance with the requirements of the degree of Doctor of Philosophy.

TABLE OF CONTENTS

193209

SUMMARY

The direct reaction theory for the inelastic scattering of nucleons from nuclei is developed using a two-body reaction mechanism. Factors which influence the relative contributions from the nuclear interior and surface are identified and studied.

The purely optical model effects of "phase averaging" which reduces the contribution from the nuclear interior, and "focussing", which emphasises the surface region more with increasing incident energy, are defined. It will be shown that phase averaging does not remove the contribution from the nuclear interior, although it does give a reduction from the plane wave situation, and that focussing has a large effect on the angular distributions especially on the extreme angle cross-sections.

Defining a surface reaction as one in which the region $r < R_f$ is weighted by the value f=0, significant differences in shape are found between this surface and complete volume calculations. Here R_f is a suitably defined radius. In many cases these differences cannot be removed by any reasonable adjustment of the optical model parameters.

These effects are extensively analysed in two reactions. The first is the reaction $F^{19}(p,p')F^{19*}$ to the first excited level, a parity changing case with a small Q-value.

It must be stressed that although we do not expect the single particle model to be a correct description of the F^{19} bound states, we use this model for simplicity

as we are concerned with optical model effects in these angular distributions. Further, because of this and the fact that the absolute strength of the two-body interaction inside nuclear matter is an unknown parameter, we will not be concerned with absolute magnitudes of cross-sections.

The second is the reaction $C^{13}(p,n)N^{13}$ to the ground state. In both of these cases, the differences between volume and surface mechanism calculations are significant and cannot be reproduced by variations of any optical model properties. This leads to the conclusion that the density dependence of the two-body force for reactions proceeding by a two-body, collision mechanism may be identified by the angular distributions and the energy dependence of the extreme angle cross-sections, which are particularly sensitive to the foci in the optical model wave functions.

Preliminary calculations show that the inclusion of a realistic finite range form for the two-body interaction potential will not invalidate these conclusions.

Finally, calculations are reported for the inelastic scattering of protons exciting first state by Y^{89}. This is expected to be a single particle transition between two almost shell model states and involves a change of parity.

It will be seen that the conclusions drawn from the case for lighter nuclei are borne out for this reaction

which we expect to be described in our model of the reaction, possibly with the extensions mentioned in the text.

It is hoped that with this reaction that we will be able to fit the experimental results still to be obtained and thus determine the two-body force strength and exchange features.

I hereby declare that this thesis contains no material which has been accepted for the award of any other Degree or Diploma in any University, and that to the best of my knowledge and belief, the thesis contains no material previously published or written by another person, except where due reference is made in the text.

ACKNOWLEDGEMENTS

I wish to thank Professor I.E. McCarthy for many helpful discussions and suggestions and, also, for his unfailing and understanding encouragement throughout the course of this work. His supervision was greatly appreciated.

I also wish to express my gratitude -

(a) to Dr. K.L. Lim for his assistance in building the direct reaction code and in discussion of the results and to Dr. C.A. Pearson for many useful discussions.

(b) for the guidance and encouragement given to me by Professor H.S. Green, Dr. C.A. Hurst, Dr. P.W. Seymour and other members of the Mathematical Physics Department.

(c) to Drs. Melkanoff, Nodvik, Saxon and Cantor for the use of their optical model wave function code, SCAT4.

(d) for the co-operation and help of Drs. P.E. Hodgson, J.R. Rook, B.A. Robson, A. Agodi and G. Schiffrer in checking the distorted wave code, as well as that given by the staff of the Adelaide University computing centre and Weapons Research Establishment, Salisbury, S.A., in particular Mr. B. McDowell, in overcoming computing problems.

In addition, I wish to thank the Australian Atomic Energy Commission, the Australian Institute for Nuclear Science and Engineering and the U.S. Atomic Energy Commission for their financial support.

LIBRARY OF THE UNIVERSITY OF ADELAIDE

CHAPTER 1 INTRODUCTION

Section 1.1 of this introduction covers the background development of Nuclear Reaction Theory, relevant to the work presented in this thesis, up to the stage of discussing the direct reaction theory in particular. Section 1.2 deals with the development of the direct reaction theory, Section 1.3 with distortion in the optical model and Section 1.4 considers the localization of the reaction region and its significance.

1.1 BACKGROUND

The complexity of the nuclear many-body problem has led nuclear physicists to investigate nuclear properties by the introduction of particular simplifying models. A model is an approximate representation either of the nucleus or, for some scattering problems, of the reaction mechanism, or a combination of both. A chosen model is constructed so that some known information about nuclear properties is contained within its construction. This can then be investigated to obtain further information about the nucleus, and, if this information is verified by experiment, the model can be considered as a factual representation within its range of validity.

In fact, a prime object of the nuclear model approach is to gain from the characteristics of the model, a better understanding of more fundamental nuclear properties, such as knowledge about the two-body force inside nuclear matter. The process is one of extrapolation, and its success in a given case depends upon the limitat-

ions and complexity of calculation of the model chosen.

For scattering problems, two extreme representations have been particularly successful, namely, the compound nucleus and the direct reaction theories. The elastic scattering problem often can be well described by using the optical model. Using this model, the fitting of experimental results was quite remarkable in many cases. This is not considered as a third representation because direct reactions can be thought of as extensions of the optical model theory.

However, the compound nucleus and optical models are related, because the scattering matrix for each can be derived from the same basic expression,[*1] the difference depending on just how large an energy interval, I, is used to form the average. When this energy interval is large enough, the scattering matrix, which can be expanded as a sum of the contributions from the compound levels, can be separated into an average and a fluctuation term. This average can be represented by the optical model. Many authors have found this relationship using slightly differing approaches. References to these are given by G.E. Brown[*1].

Direct nuclear reactions are defined as processes in which only a few degrees of freedom of the nucleus are excited. Two interpretations of these excitation processes have been extensively investigated in the past. One is the collective excitation of many bound nucleons by the incident particle[*2], causing the nucleus, or some

part of the nucleus, to vibrate or rotate. Good fits to angular distributions, both in magnitude and shape, are obtained by this method, and, as this theory does not involve the particle forces explicitly, the accuracy of the results obtained indicates that the first order Distorted Wave Born Approximation (hereafter abbreviated to D.W.B.A.) is a good approximation, at least for these reactions.

The other direct reaction process which has been extensively investigated assumes that the reaction proceeds by a two-body collision between the incident unbound particle and one of the target nucleus particles, a bound particle. Obviously, this involves the two-body potential in nuclear matter and we seek information about the density distribution of this effective two-body force. The two-body results however, may be influenced by collective excitations[*3], and therefore, be difficult to isolate.

This type of prediction can, of course, only be attempted when satisfactory expressions for the initial and final states of the nuclear system are used. The computer code described in the Appendix does not include either an exchange character for the two-body force, or a spin-orbit interaction effect in the optical model representations of the wave functions of the unbound particles. Further, most results reported here involve a zero-range two-body force. Some calculations have been performed using a Yukawa finite range potential and their discussion is contained in Section

4.3. Our analysis using this two-body potential is not yet extensive and, consequently, unless stated, all results and conclusions refer to the zero-range D.W.B.A. calculations. Nevertheless, results obtained with this zero-range code indicate that on taking into account the density dependence by weighting the interaction region appropriately there are significant differences in both magnitude and shape of the angular distribution when these results are compared with those in which the whole volume is considered. The energy variations of the backward peaks in angular distributions are also affected by this weighting of the interaction region. These differences cannot be produced by any sensible variations of the parameters of the theory. This, of course, supposes the reaction studied does occur via a two-body interaction mechanism and that the results of experiments are not enhanced by any collective excitation effect.

However, there is some evidence, based on the applicability of the shell model, that excitations by a two-body interaction do in fact exist. For example, there are cases where the shell model predicts small collective admixtures of wave functions and correct γ-ray transition probabilities. Such a case is the ground state and first excited state of Y^{89}.

In general, as both compound nucleus and direct reaction mechanism contribute to the reaction results, the relative contributions and interference of the two

processes cannot be accounted for. However, there are two ways of achieving some measure of separation. Further, in many cases, under appropriate conditions, one or other of the contributions can be made negligible. The two ways are:-

(1) The use of poor energy resolution in an energy region where the compound nucleus has sufficient levels. In this case the characteristic fluctuations due to the compound nucleus will be averaged out and the statistical model applied. This means that the compound nucleus contribution is nearly isotropic and can be subtracted incoherently from the experimental results.

(2) The use of good energy resolution. Here the contributions from the two processes add coherently and so cannot be separated. However, consistent features in the results as a function of energy can be attributed to the direct reaction process.

In the poor resolution case, it has been shown by Dodd and McCarthy[*4] that the "Parity" rule of Kromminga and McCarthy[*5,6], described in some detail in Chapter 3, can be used, provided the very restrictive conditions of this rule are satisfied experimentally, to separate the compound nucleus and direct reaction contributions and thereby normalize the direct reaction contribution. At least, we expect to identify the non-D.W.B.A. term to within a few millibarns. Essentially they show that

for poor resolution the compound nucleus contribution to the angular distribution is given by the statistical model and so the angular distribution for this mechanism is then symmetric about 90^{o}. Hence, for a parity changing reaction, the direct reaction contribution at zero scattering angle is zero so that any experimental value at zero scattering angle must be solely that of the compound nucleus. This value then must be that of the compound nucleus at the backward scattering angle. Hence, the difference between the experimental cross-section values for the scattering angles of 180^{o} and 0^{o} is the value of the direct reaction cross-section at 180^{o}.

The reaction $F^{19}(pp')F^{19*}$ (first excited level) would appear to be just such a process. But, the Q value of 0.11 MeV, together with the fact that the second excited level of F^{19} has a Q value of approximately 0.2 MeV, means that experiments must have extremely good energy resolution.

1.2 DEVELOPMENT OF THE DIRECT REACTION THEORY

Scattering is a relatively infrequent process, and so analysis by means of first order perturbation theory is possible.

Weisskopf[*7] has described the direct reaction process for inelastic scattering as follows:-

Stage 1 - The incident particle is scattered elastically by the target nucleus.

Stage 2 - The interaction occurs and energy and momentum are transferred within the total system.

Stage 3 - The emerging particle is elastically scattered by the resultant nucleus.

Viewing the direct reaction inelastic process in such a fashion means that the cross-sections can be described in terms of the overlap of the initial and final states of the system without the introduction of possibly undetermined intermediate states. In other words, all measurable quantities can be expressed in terms of matrix elements having the form -

$$\eta = \langle \text{final} | \text{Interaction} | \text{Initial} \rangle \quad (1.1)$$

where in general the initial and final states of the system are expressed as an appropriate product of two wave functions, one describing the unbound particle, the other the bound particle or particles. The anti-symmetrization of these total states of the system is not neglected, but is most often taken into account by appropriately defining the form of the interaction.

The wave functions for the bound and unbound particles are derived from a suitable representation of the nucleus. The bound states have been most successfully defined in terms of the nuclear shell model[*8]. Improvement on this can be obtained by using, for example phenomenological mixtures of configurations.

However, the wave functions of the unbound particles

are of most importance for a given angular momentum transfer, because these are primarily responsible for the shape of angular distributions[*10,11]. Since the angular distributions are not so sensitive to the bound state wave function, relatively simple forms are adopted for the shell model to reduce the complexity of computation. Even then, using the best representation available for the unbound particle wave functions (provided by the optical model), the calculations require a large and fast computer and so computing facilities and economics can be a considerable problem.

The first attempts to evaluate these matrix elements used plane waves for the unbound particle wave functions. This Plane Wave Born Approximation was used to describe stripping and heavy particle reactions. It predicted the correct angular momentum transfer by fitting some general features of the angular distributions[*12]. However, it did not yield detailed fits in most of these cases and proved most inadequate for nucleon-induced reactions.

The success of the optical model[*13] in fitting elastic scattering[*14] indicated that this might give a better representation of the unbound particle wave function. Now, although elastic scattering only depends on the values of the optical model wave functions at large distances from the nucleus, the success of the D.W.B.A.[*11], especially for well known collective

excitations[*2], indicated that the optical model wave function is a good representation also near to and inside the nucleus.

1.3 DISTORTION IN THE OPTICAL MODEL

The optical model represents the nucleus by means of a complex potential well -

$$\emptyset\,(r) = V(r) + iW(r) \qquad (1.2)$$

which strongly distorts in both amplitude and phase the plane wave functions. It is known that the real part of the potential causes refraction and reflection of the partial waves, while the imaginary part attenuates the wave as it progresses through the nuclear volume. The effect of reflection on the optical model wave functions is to give parts of them a standing wave appearance. Attenuation accounts for the loss of probability into channels other than the entrance channel.

McCarthy[*15,43] has shown how this distortion is most pronounced for the surface partial waves, where, in the partial wave expansion for the optical model, the surface partial waves are defined as those with angular momenta $l \approx kR$, k being the wave number, R the nuclear radius. He also has shown how the phase relationships between the partial waves in and near the diffuse nuclear surface, result in constructive interference to produce the "focus". The focus is a region of large probability amplitude on the axis on the side of the nucleus opposite that of the collision surface. The

axis is defined by the direction of the incident particle at a great distance from the nucleus. These features of the optical model wave functions, together with a more explicit background discussion, are described in Section 2 of Chapter 3. It was shown*16 that flux and ray calculations inferred the existence of this focus, because, although the probability of a particle being present in the focal region on any trajectory is small, many trajectories lead to this region.

This*16 and other calculations*17,18 showed that the distortion described above smoothed out the angular distributions from that obtained by plane wave calculations, whilst often retaining all the salient features of the plane wave results, and also in many cases, produced extreme angle peaking. Because angular distributions are measures of momentum transfer, these effects can be understood from the fact that distortion causes a localization of the interaction region which is not present in the plane wave theory. This localization, in view of the uncertainty principle, implies that momentum is less resolved and so the angular distributions are smoothed out.

The predominant features of the localization are a front "surface" term and the "focal" term. Using an approximate wave function based on these two terms, McCarthy and Pursey*18 had considerable success in fitting (α, α') experiments and expected reasonable nucleon induced scattering results. McCarthy and

Kromminga[*21] later showed that the angular distribution for (p, p') reactions could often be understood on the basis of this localization. Now in an inelastic scattering process, at least two such wave functions are needed and so their overlap is greatest in the two extreme directions. For the scattering angle $\theta_{sc} = 180^{\circ}$, the two focus terms overlap as do the two surface terms; likewise for $\theta_{sc} = 0^{\circ}$ the focus term of one wave function overlaps the surface term of the other. Hence at these two scattering angles, the overlap of the magnitudes of the wave functions is expected to be a maximum. Then if the phase relationships both within and between the two regions where the overlap of the two unbound particle wave functions has a large value (that is when $\theta_{sc} = 0^{\circ}$ or 180°), are constructive, extreme angle peaking will clearly result.

1.4 LOCALIZATION OF THE REACTION REGION

Early D.W.B.A. calculations considered the reaction mechanism to be a surface phenomenon[*10] i.e., the matrix elements were calculated by replacing the radial integrals, extending from r=0 to r=∞, by a thin shell of the nuclear surface. Elton and Gomes[*19] suggested that these calculations should be successful because internal reaction products could be totally internally reflected at the nuclear surface, and so the nuclear interior would not contribute to the reaction's angular distribution.

However, this interpretation is inadequate as it prohibits any focus phenomena*16. Later, Austern*20 investigated the optical model wave function in more detail, and discovered that the interior region may not contribute to reaction values because the phases of the low angular momenta partial waves (the only ones that have appreciable magnitude in the interior) vary smoothly with radius and so would average out. McCarthy*15 investigated this "phase averaging" effect in greater detail, covering the low energy results specifically excluded in Austern's paper, and found that this phenomenon persisted.

By calculating the exact matrix element expressions, we will show that, while phase averaging still exists, the reduction of internal contributions caused by this effect is not as great as may have been expected. The contribution to the matrix elements from the low partial waves involved in phase averaging should not be influenced by focal contributions, as the focus is mainly generated by the surface partial waves.

Hence, in cases where this purely optical model effect of phase averaging is not severe, where surface and volume calculations have differences that cannot be overcome by realistic changes in the parameters of the theory or understood in terms of focal contribution

alone, comparison of the theory and experiment will yield information about the reaction mechanism. Hereafter, surface calculations are defined as those in which the radial integrants values from r=0 to $r=R_f$ are taken as zero. R_f will often be chosen to be the Saxon Well radius. It will be seen that parameter variation cannot convert surface to volume results, and, since the differences persist and sometimes amplify as energy increases, the focus, which moves further out into the surface region with increasing energy, cannot bring about this conversion.

Now, although the incorporation of the focus is not expected to invalidate the above, it is the most important localization feature and has marked effect on angular distributions. Since the focus is energy and potential dependent, it was first thought that, for low energies, it would be a probe into the nuclear interior*[16,6]. This may still be the case for heavy targets, but for nuclei of low mass number, the foci of wave functions for energies in the 5 MeV range and lower are spread over both the nuclear interior and surface regions. Nevertheless in the picture proposed above, it should be still possible to obtain information about the nuclear interaction mechanism.

Although the focus is spread, its effects are still decisive features that should contain information about the nuclear interaction. The extreme angle peaking is the most sensitive feature of the focal effect and we

will report here the results of analysis of the reaction $C^{13}(p,n)N^{13}$ data of Dagley, Haeberli and Saladin[*21]. We attempt to fit the extreme angle peak versus energy variation but find that the limitations of our calculations are too severe. It is expected that inclusion of a finite range interaction with an exchange character will improve the situation. The analysis by Agodi and Schiffrer[*22,23] of the $Si^{28}(n,p)Al^{28}$ reaction indicates this fact. In particular, these authors find that exchange effects can have pronounced effects on the backward peaks. Nevertheless, our calculations indicate the extent to which focussing affects the angular distributions.

A sidelight to the fitting of the backward peaks variation with energy is evidence of the well known $V R^n$ ambiguity where, in our calculations n is 2.

CHAPTER 2 MATHEMATICAL DESCRIPTION

2.1 INTRODUCTION

Direct reactions can be described in terms of the initial and final states of the total system without intervention of any intermediate compound states. Thus observable quantities can be theoretically discussed in this mechanism in terms of matrix elements of the form -

$$\mathcal{M} = \langle \text{final} | \text{Interaction} | \text{Initial} \rangle \qquad (2.1)$$

It is also known that the first order Born approximation[*24] is applicable and can be improved by introducing distortion into the unbound particles description as given by the optical model. This is then the D.W.B.A., a two channel first order approximation[*11].

The differential cross section can then be expressed as -

$$\sigma(\theta) = \text{Normalization} \sum_{\text{ave}}' |\mathcal{M}|^2 \qquad (2.2)$$

where $\sum_{\text{ave}}'$ refers to an average over the unmeasured quantum numbers of the entrance channel and a summation over the quantum numbers of the exit channel. In the particular case of describing a nucleus as a closed shell core plus or minus one extra core nucleon, the $\sum_{\text{ave}}'$ is then simply an average over the initial bound state projections and a summation over the final bound state projections -

$$\sum_{\text{ave}}' = \frac{1}{2j+1} \sum_{m_j, m_j'}' \qquad (2.3)$$

In section 2.2, we discuss the three constituents of

the matrix elements namely the representation of the unbound particles, the representation of the bound particles, and expressions for the two-body interaction. Exact expressions are derived in section 2.3 for the direct interaction involving a two-body collision mechanism, including a finite range and exchange form of the interaction, but neglecting any spin-orbit coupling. Finally, in section 2.4, the simplified expression for a delta function interaction without any exchange feature is derived from the results of section 2.3. The expression of the matrix element in this case is shown to be equivalent to that as calculated by Glendenning*[10], assuming spinless unbound particles.

2.2 THE COMPONENTS OF THE MATRIX ELEMENTS

In the following three sub-sections we discuss the mathematical expressions for the components of the matrix elements as are calculated in the code described in the Appendix. Hereafter, the reaction mechanism is considered as having the two-body form.

(a) The Bound States

To describe the bound states, we use the pure j-j coupling shell model. In particular, the initial and final nuclei are considered as closed shell nuclei with one extra core particle, or the equivalent closed shell with one hole configuration. Then the total spin and most properties of the nuclei are described by the values associated with the extra-core particle.

The closed shell core of nucleons in the target or residual nucleus enters the calculations only through the potential wells, with which we represent the nuclei and which distort the unbound particle's wave functions from the plane wave appearance. We describe the bound states as -

$$\psi_i(\underline{r}) = R_{np}(r)\,|p\,j\,m_j\rangle$$

$$\psi_f(\underline{r}) = R_{n'p'}(r)\,|p'j'm_j'\rangle \qquad (2.4)$$

where n, n' - are the initial and final prime quantum numbers.

p, p' - are the initial and final orbital quantum numbers.

j, j' - are the initial and final total spin quantum numbers.

m_j, m_j' - are the initial and final total spin projection quantum numbers.

In particular, the radial wave functions, $R_{np}(r)$ $R_{n'p'}(r)$, that are used in our calculations, are those of the Harmonic Oscillator. The expression for these are -

$$R_{np}(r) = \frac{2^{p-n+2}}{\pi^{1/4}} \left[\frac{(2p+2n+1)!}{(n-1)!\,(p+n-1)!}\right]^{\frac{1}{2}} \frac{p!}{(2p+1)!}\,\nu^{3/4}$$

$$(\sqrt{\nu}\,r)^p\, e^{-\frac{1}{2}\nu r^2} \sum_{k=0}^{n-1} (-)^k \binom{n-1}{k} \frac{(2p+1)!!}{(2p+2k+1)!!}\,(2\nu r^2)^k \qquad (2.5)$$

where following the notation of Glendenning,[*10] -

$$\nu = \frac{2\,[2(n-1)+p]+3}{R_{INT}^2}$$

$$\binom{a}{b} = \text{binomial coefficient} \qquad (2.6)$$

R_{INT} is what we shall call hereafter the "average interaction radius". This parameter controls the spread of these bound state expressions in space and is a measure of the binding energy of the nucleon within the target. The Saxon well radius, if used for R_{INT}, corresponds to a binding energy of about 10 MeV.

The angular dependence of these expressions for the bound states are -

$$|p\,j\,m_j\rangle = \sum_{\mu}^{\cdot} C\,(p, m_p, \tfrac{1}{2}, \mu; j, m_j)\, Y_{p,m_p}(\Omega) \times \chi_{\frac{1}{2},\mu}(s) \qquad (2.7)$$

where the three terms in the summation are notations for the Clebsch-Gordan coefficients, normalized spherical harmonics and normalized intrinsic spin wave functions respectively.

The Clebsch-Gordan coefficient -

$$C\,(a, \alpha, b, \beta; c, \gamma)$$

couples the state described by the angular momentum quantum number a and its projection α to a state with the quantum numbers b, β giving a new state described by the quantum numbers c, γ. The selection rules for these coefficients are then -

$$|a-b| \leq c \leq a+b$$

$$\alpha + \beta = \gamma \qquad (2.7)$$

This description of the bound states can be much improved, but as well as having simplicity, it is adequate to specify the change of nuclear state. Further, angular distributions are far more sensitive to the localizations of the unbound particles and complicating the bound state's calculation is unwarranted.

(b) The Wave Functions of the Unbound Particles

The wave functions for the unbound particles are calculated from the optical model. These are the solutions of the Schroedinger Equations for particles moving in complex potential wells. The calculations reported in this thesis ignore spin-orbit terms in this complex potential. The complex well form used most often is of the Eckart type -

$$V(r) = [V_0 + i W_0] \left[1 + \exp((r-R)/a)\right]^{-1} \qquad (2.8)$$

V_0, W_0 are the well depths in MeV

R is the Saxon well radius in fermis

a is the surface thickness parameter in fermis.

This optical model successfully predicts elastic scattering results and total reaction cross-sections but is not sufficient to discuss inelastic processes. To do so requires the incorporation of a reaction mechanism.

Glendenning[*10] and Levinson and Banerjee[*11] have shown that direct reaction matrix elements are accurate if we consider the wave functions of the incident and emergent particles as the solutions of the optical model representations of the initial and residual nuclei.

In the partial wave expansion, the wave function for the unbound particle in this representation has the form -

$$\phi(r) = \sum_l [4\pi(2l+1)]^{\frac{1}{2}} e^{i\sigma_l} i^l f_l(kr) |l, m_l\rangle \qquad (2.9)$$

σ_l are the coulomb phase shifts

Defining $\rho = kr$, the $f_l(\rho)$ satisfy -

$$\left[\frac{\partial^2}{\partial r^2} + \left\{k^2 - \frac{2\mu}{\hbar^2}(V(r) + iW(r)) - \frac{l(l+1)}{r^2}\right\}\right] f_l(\rho) = 0 \qquad (2.10)$$

where $k = \sqrt{\frac{2\mu E}{\hbar^2}}$ is the wave number (2.11)

At this point, we can describe the total state of the system as -

$$\Psi = \psi(r_1)\,\phi(r_2) \qquad (2.12)$$

where ψ is as given by equations (2.4) to (2.7) and ϕ by equations (2.8) to (2.12). Of course the co-ordinate system for the unbound particle is different from that of the bound particle.

(c) <u>The Interaction</u>

We consider the two-body collision and express this interaction as -

Interaction = $V(|\underline{r}_1 - \underline{r}_2|)\, P_x$

$$= \sum_L^{\prime} A_L \nu_L(r_1 r_2)\, P_L(\cos\theta_{12})\, P_x \qquad (2.13)$$

where the subscripts 1 and 2 distinguish the unbound particle co-ordinates from the bound particles co-ordinates.

P_x is the exchange operator. It is this that effectively includes the antisymmetrization of the wave functions.

L is the angular momentum transfer in the reaction.

$\nu_L(r_1 r_2)$ is the radial two-body interaction for a given angular momentum transfer quantum number L.

(i) The $\nu_L(r_1, r_2)$

Including the expansion of the $P_L(\cos\theta_{12})$ into spherical harmonics, there are two forms in which we can express this. The first is an expression in which the interaction has zero range, the delta function interaction. The second involves a finite range. The finite range Yukawa interaction appears to be the most realistic although a Gaussian form is often used. Recent (p,2p) studies[*25] have shown that at high energies (the order of 100 MeV) the Gaussian form is not acceptable.

The three expressions are -

Delta function $\nu_L(r_1, r_2) = \delta(r_1 - r_2)\, 4\pi / r_1^2$

Gaussian $\nu_L(r_1, r_2) = i^L e^{-\alpha(r_1^2 + r_2^2)} j_L(2i\alpha r_1 r_2)$

(2.14)

Yukawa $\nu_L(r_1, r_2) = j_L(i\mu r_<)\, h_L^{(1)}(i\mu r_>)$

where μ, α give measures of the range of the forces

$r_<, r_>$ are respectively the smaller and larger co-ordinate of r_1 and r_2

j_L are Spherical Bessel functions

$h_L^{(1)}$ are Hankel functions of the first kind.

Now each of these interactions must be normalized by a strength value, in the delta function case by V_0/μ^3 and the Yukawa case by V_0/μ.

(ii) The Exchange Operator P_x

$$P_x = W + BP^\sigma - MP^s - HP^H \qquad (2.15)$$

where P^σ = Bartlett Exchange Operator (Spin Exchange)

P^s = Majorana Exchange Operator (Space Exchange)

$P^H = P^\sigma P^s$ Heisenberg Exchange Operator.

The constants W,M,B and H are not independent, but satisfy the following equation -

$$W + B + H + M = 1 \qquad (2.16)$$

The following table gives values for these constants as suggested by Rosenfeld*26 and Peaslee*27.

	Rosenfeld	Peaslee
W	-.13	.0575 + .245 ω
M	+.93	.4425 - .145 ω
B	+.46	.0425 - .01 ω
H	-.26	.4575 - .09 ω

Where $1 \leq \omega \leq 3.5$

For a Yukawa shape, with $\mu = 1.04, \omega \approx 1.5 \pm .003$. This was evaluated from nuclear saturation conditions. Peaslee also defined the two-body strength of interaction as -

$$V_0 = 46 + \frac{1}{7}(7\omega - 2.5)^2 \qquad (2.17)$$

These values for the exchange operators are those for free nuclear nucleon data. If we wish to include antisymmetry into our calculations, then this can be done by simply changeing the values for W, M, B and H. For total antisymmetry, because the two-body interaction in our matrix element is symmetric in $\underline{r}_1$ and $\underline{r}_2$, we need only consider one state, the initial or final state, for total antisymmetry. Hence

$$V(|\underline{r}_1 - \underline{r}_2|)\,[W + BP^\sigma + HP^\sigma P^S - MP^S]\quad[1 - P^\sigma P^S]\Psi(\underline{r}_1, \underline{r}_2)$$

$$= V(|\underline{r}_1 - \underline{r}_2|)\,[(W-H) + (B+M)P^\sigma - P^S(B+M) - (W-H)P^\sigma P^S]\,\Psi(\underline{r}_1 \underline{r}_2)$$

using $P^{\sigma\,2} = P^{S\,2} = 1$

(2.17a)

Thus we can now calculate the matrix elements and therefore the differential cross-section under the following approximations -

(i) The D.W.B.A. is used. That is, consider only a first order perturbation theory with a two channel approximation.

(ii) The optical model, without a spin-orbit potential, describes the probability amplitude of the unbound particles within the nuclear region.

(iii) The pure j-j coupling shell model describes the wave functions of the bound particles. In particular, we consider a nucleus as a closed shell core plus either an extra core particle or a hole in the closed shell core. The radial form is that of a Harmonic Oscillator with parameters chosen to fit the Binding Energy as was done by Glendenning*10.

(iv) The interaction is of the two-body form, having either zero or finite range.

In the next section we shall find expressions for the matrix elements associated with a reaction under these approximations. The last section considers the simplification in the delta function interaction case and derives from this the expressions as given by Glendenning*10.

The majority of our calculations have used this simplified form as it is sufficient to describe the optical model effects of interest. Further, these effects are more clearly defined if this simplified expression is used.

2.3 THE EXPLICIT FORM OF THE MATRIX ELEMENTS

In the partial wave expansion, the wave functions of the unbound particles have the form -

$$\phi_i(\underset{\sim}{r}_1) = \sum_l' [4\pi(2l+1)]^{\frac{1}{2}} i^l e^{i\sigma_l} f_l(k_i r_1) \times \sum_{\rho\sigma}' C(l,0,\tfrac{1}{2},\sigma;\rho,\sigma)\, Y_{l,0}(\Omega_1)\, \chi_{\frac{1}{2},\sigma}(\xi_1)$$

$$\phi_f^*(\underset{\sim}{r}_1) = \sum_{l'}' 4\pi\, i^{-l'} e^{i\sigma_{l'}} f_{l'}(k_f r_1) \sum_{m_{l'}}' Y_{l',m_{l'}}(\theta_{sc}) \times \sum_{\rho'\sigma'}' C(l',m_{l'},\tfrac{1}{2},\sigma';\rho'_f\nu')\, Y^*_{l',m_{l'}}(\Omega_1)\, \chi^*_{\frac{1}{2},\sigma'}(\xi_1) \quad (2.18)$$

where θ_{sc} = scattering angle, the angle between $\underset{\sim}{k}_i$ and $\underset{\sim}{k}_f$. The expansion -

$$P_L(\cos\theta_{12}) = \frac{4\pi}{2L+1} \sum_M' Y^*_{L,M}(\Omega_1)\, Y_{L,M}(\Omega_2) \quad (2.19)$$

has been used in the partial wave expansion.

The initial and final bound states are described by:-

$$\psi_i(\underset{\sim}{r}_2) = R_{np}(r_2) \sum_\mu' C(p,m_p,\tfrac{1}{2},\mu;J,m_J)\, Y_{p,m_p}(\Omega_2)\, \chi_{\frac{1}{2}\mu}(\xi_2)$$

$$\psi_f^*(\underset{\sim}{r}_2) = R^*_{n'p'}(r_2) \sum_{\mu'}' C(p',m_{p'},\tfrac{1}{2},\mu';J',m_{J'})\, Y^*_{p',m_{p'}}(\Omega_2) \times \chi^*_{\frac{1}{2}\mu'}(\xi_2) \quad (2.20)$$

where $R^*_{ab} = R_{ab}$ if we use radial Harmonic Oscillator wave functions. Some calculations were performed using the corresponding square well wave functions adjusted to give the correct R.M.S. radius.

Then, without specifying the interaction, the matrix elements for this case are, in general, functions of θ_{sc}, m_J and $m_{J'}$.

$$\mathcal{M} = \iint d^3r_1\, d^3r_2\, d\xi_1\, d\xi_2\, \phi_f^*(\underset{\sim}{r}_1)\, \psi_f^*(\underset{\sim}{r}_2)\, V_{int} P_x \times \phi_i(\underset{\sim}{r}_1)\, \psi_i(\underset{\sim}{r}_2) \quad (2.21)$$

where V_{int} represents the interaction and P_x the exchange properties to be used. Substituting (2.18)

and (2.20) using (2.13) for V_{int}, and defining E_x^s, E_x^{spin} as operators that exchange the space and spin co-ordinates of the final bound state wave function with those of the final unbound state wave function, the matrix element is -

$$\begin{aligned}
\mathcal{M} = {} & \Sigma'(l,l',L,M,\sigma,\sigma',\rho,\rho',\mu,\mu',m_{l'}) \; (4\pi)^{5/2} \, i^{l-l'} e^{i(\sigma_l+\sigma_{l'})} \\
& \times (2l+1)^{\frac{1}{2}} \; C(l,0,\tfrac{1}{2},\sigma;\rho,\sigma) \; C(l',m_{l'},\tfrac{1}{2},\sigma';\rho',\nu') \\
& \times C(p,m_p,\tfrac{1}{2},\mu;j,m_j) \; C(p',m_{p'},\tfrac{1}{2},\mu';j',m_{j'}) \\
& \times \iint r_1^2 dr_1 \, r_2^2 dr_2 \; f_{l'}(k_f r_1) R_{n'p'}(r_2) \, V_L(r_1,r_2) \left[1+E_x^s\right] f_l(k_i r_1) R_{np}(r_2) \\
& \times (-)^M \iint d\Omega_1 \, d\Omega_2 \left[Y^*_{l',m_{l'}}(\Omega_1) \; Y^*_{p',m_{p'}}(\Omega_2) \right. \\
& \qquad \left. \times Y_{L,-M}(\Omega_1) \, Y_{L,M}(\Omega_2) \left[1+E_x^s\right] Y_{l,0}(\Omega_1) \, Y_{p,m_p}(\Omega_2) \right. \\
& \times \iint ds_1 \, ds_2 \; \chi^*_{\frac{1}{2}\mu'}(s_2) \, \chi^*_{\frac{1}{2}\sigma'}(s_1) \, \chi_{\frac{1}{2}\mu}(s_2) \, \chi_{\frac{1}{2}\sigma}(s_1) \left[1+E_x^{sp}\right] \\
& \times Y_{l',m_{l'}}(\theta_{sc})
\end{aligned} \tag{2.22}$$

E_x^s occurs twice in this expression, but this has been done to stress that both radial and angular integrals are affected by space exchange.

For the sake of clarity we will use the following notation.

$$I_{\ell L \ell'} = \iint r_1^2 dr_1 r_2^2 dr_2 \, f_{\ell'}(k_f r_1) R_{n'p'}(r_2) \, V_L(r_1, r_2) \, f_\ell(k_i r_1) R_{np}(r_2) \tag{2.23}$$

and $I^S_{\ell L \ell'}$ is the above integral under the operation of the space exchange E^S_x

$$\langle a\alpha | c\gamma | b\beta \rangle = \int d\Omega \, Y^*_{a,\alpha}(\Omega) \, Y_{c,\gamma}(\Omega) \, Y_{b\beta}(\Omega) \tag{2.24}$$

$$= \left[\frac{(2c+1)(2b+1)}{4\pi(2a+1)}\right]^{\frac{1}{2}} C(b,0,c,0;a,0) \, C(b\beta, c\gamma; a\alpha)$$

(See Rose[*28])

$$\langle \chi_{\frac{1}{2}\tau'} | \chi_{\frac{1}{2}\tau} \rangle = \int d\delta \, \chi^*_{\frac{1}{2}\tau'}(\delta) \, \chi_{\frac{1}{2}\tau}(\delta) \tag{2.25}$$

$$= \delta_{\tau\tau'}$$

$$\Sigma'_T = \Sigma'(\ell, \ell', L, M, \sigma, \sigma', \rho, \rho', \mu, \mu', m_{\ell'}) \tag{2.26}$$

And, whenever they are used, the superscripts S, Sp, SSp refer to Space Exchanged, spin exchanged and both space and spin exchanged quantities respectively.

(a) <u>The matrix element without exchange</u>

$$\mathcal{M}(m_j, m'_j, \theta_{sc}) = \Sigma'_T \, (4\pi)^{5/2} \, i^{\ell - \ell'} e^{i(\sigma_\ell + \sigma_{\ell'})} \, I_{\ell L \ell'}$$
$$\times (2\ell+1)^{1/2} \, C(\ell, 0, \tfrac{1}{2}, \sigma; \rho, \sigma) \, C(\ell', m_{\ell'}, \tfrac{1}{2}, \sigma'; \rho', \nu')$$
$$\times C(p, m_p, \tfrac{1}{2}, \mu; J, m_j) \, C(p', m_{p'}, \tfrac{1}{2}, \mu'; J', m_{j'})$$
$$\times \langle \ell', m_{\ell'} | L, -M | \ell, 0 \rangle \, \langle p', m_{p'} | L, M | p, m_p \rangle$$
$$\times \langle \chi_{\frac{1}{2}\sigma'} | \chi_{\frac{1}{2}\sigma} \rangle \, \langle \chi_{\frac{1}{2}\mu'} | \chi_{\frac{1}{2}\mu} \rangle \, Y_{\ell' m_{\ell'}}(\theta_{sc}) \tag{2.27}$$

Now using the expressions given in (2.23) to (2.26), the matrix element (2.27) reduces to -

$$\mathcal{M}(m_j, m_j', \theta_{sc}) = \sum'_{\ell\ell' L M \sigma \mu \rho \rho'} (4\pi)^{3/2} i^{\ell-\ell'} e^{i(\sigma_\ell + \sigma_{\ell'})} I_{\ell L \ell'}$$
$$\times (2\ell+1)(2L+1)\left[\frac{(2p+1)}{(2p'+1)(2\ell'+1)}\right]^{1/2} C(\ell, 0, \tfrac{1}{2}, \sigma; \rho, \sigma)\, C(p, 0, L, 0; p', 0)$$
$$\times C(\ell, 0, L, -M; \ell', -M)\; C(p, m_p, L, M; p', m_{p'})$$
$$\times C(\ell, 0, L, 0; \ell', 0)\; C(\ell', -M, \tfrac{1}{2}, \sigma; \rho', \nu')$$
$$\times C(p, m_p, \tfrac{1}{2}, \mu; j, m_j)\; C(p', m_{p'}, \tfrac{1}{2}, \mu; j', m_j')$$
$$\times Y^*_{\ell', M}(\theta_{sc}) \qquad (2.28)$$

where the summation over the quantum numbers is greatly reduced by the selection rules associated with the various coefficients[*28] in (2.28). These selection rules are, firstly for the angular momentum quantum numbers,

$$l+L \geqslant l' \geqslant |l-L|$$
$$l+l'+L = \text{even}$$
$$p+L \geqslant p' \geqslant |p-L|$$
$$p+p'+L = \text{even} \qquad (2.29)$$
$$\rho, \rho' \text{ can have the values } \ell \pm \tfrac{1}{2}, \ell' \pm \tfrac{1}{2} \text{ respectively}$$

Secondly, the projection quantum numbers must satisfy the following -

$$m_{l'} = -M$$
$$m_{\rho'} = -M + \sigma$$

$$m_p + \mu = m_j$$

$$m_p' + \mu = m_j'$$

$$|M| \leq 1'$$

$$m_\rho = \sigma \qquad (2.30)$$

Further, σ and μ can have only the values $+\frac{1}{2}$ and $-\frac{1}{2}$.

(b) The matrix element for space exchange

This is achieved by changing the co-ordinates in the final state description. That is equation (2.22) is now -

$$\eta^S(m_j, m_{j'}, \theta_{sc}) = \Sigma'_{\Gamma} (4\pi)^{5/2} i^{l-l'} e^{i(\sigma_l + \sigma_{l'})} (2l+1)^{\frac{1}{2}} I^S_{lL l'}$$

$$\times C(l, 0, \tfrac{1}{2}, \sigma; \rho, \sigma) \quad C(l', m_{l'}, \tfrac{1}{2}, \sigma'; \rho', \nu')$$

$$\times C(p, m_p, \tfrac{1}{2}, \mu; j, m_j) \quad C(p', m_{p'}, \tfrac{1}{2}, \mu'; j', m_{j'})$$

$$\times \langle p' m_{p'} | L, -M | l, 0 \rangle \langle l', m_{l'} | L, M | p, m_p \rangle$$

$$\times \langle \chi_{\frac{1}{2}\mu'} | \chi_{\frac{1}{2}\mu} \rangle \langle \chi_{\frac{1}{2}\sigma'} | \chi_{\frac{1}{2}\sigma} \rangle \; Y_{l', m_{l'}}(\theta_{sc}) \qquad (2.31)$$

Using the relations given in (2.24), (2.25) and (2.26), this becomes -

$$\eta^S(m_j, m_{j'}, \theta_{sc}) = \Sigma'_{l, l', L, M, \rho, \rho', \sigma, \mu} (4\pi)^{3/2} i^{l-l'} e^{i(\sigma_l + \sigma_{l'})}$$

$$\times (-)^M I^S_{lLl'} (2l+1)(2L+1) \left[\frac{(2p+1)}{(2p'+1)(2l'+1)}\right]^{1/2} C(p, 0, L, 0; l', 0)$$

$$\times C(l, 0, L, 0; p', 0) \quad C(l, 0, L, -M; p', -M)$$

$$\times C(p, m_p, L, M; l', m_{l'}) \quad C(l, 0, \tfrac{1}{2}, \sigma; \rho, \sigma)$$

$$\times C(l', m_j-\mu+M, \tfrac{1}{2}, \sigma; \rho', \nu') \; C(p', -M, \tfrac{1}{2}, \mu; J', m_{j'})$$

$$\times C(p, m_j-\mu, \tfrac{1}{2}, \mu; J, m_j) \; Y_{l', M+m_j-\mu}(\theta_{sc}) \qquad (2.32)$$

The selection rules for this expression are as follows. For the angular momenta -

$$\begin{aligned} &l + p' + L = \text{even} \\ &L + l \geq p' \geq |l-L| \\ &p + L + l' = \text{even} \\ &p + L \geq l' \geq |p-L| \end{aligned} \qquad (2.33)$$

and again ρ, ρ' can have the values $l \pm \frac{1}{2}$, $l' \pm \frac{1}{2}$ respectively, except, of course, $\rho = -\frac{1}{2}$, $\rho' = -\frac{1}{2}$ are prohibited if $l, l' = 0$ respectively.

For the projections, the selection rules are -

$$\begin{aligned} m_p' &= -M \\ m_j' &= \mu - M \\ m_p &= m_j - \mu \\ m_l' &= m_j - \mu + M \\ m_\rho &= \sigma \\ m_{\rho'} &= m_j - \mu + M + \sigma \end{aligned} \qquad (2.34)$$

(c) <u>The matrix element for spin exchange</u>

Since we neglect spin-orbit coupling, for spin exchange only, the contribution to the matrix element from the spin wave functions change from $\delta_{\sigma\sigma'}\delta_{\mu\mu'}$ to $\delta_{\sigma\mu'}\delta_{\mu\sigma'}$. Hence, the matrix element for spin exchange is given by

equation (2.28) with the coefficients -

$$C(l', -M, \tfrac{1}{2}, \sigma; \rho', \nu')\ C(p', m_{p'}, \tfrac{1}{2}\mu; j', m_{j'})$$

replaced by the coefficients -

$$C(l', -M, \tfrac{1}{2}, \mu; \rho', \nu'')\ C(p', m_{p'}, \tfrac{1}{2}, \sigma; j', m_{j'})$$

Of course this change weights the partial contributions to the matrix element for spin exchange differently from the no exchange case, and alters some of the selection rules for the projection quantum numbers.

(d) <u>The matrix elements for space and spin exchange</u>

As for the case of spin exchange alone, the matrix element for this case is simply the expression for space exchange alone, equation (2.32), with the coefficients -

$$C(l', m_j - \mu + M, \tfrac{1}{2}, \sigma; \rho', \nu')\ C(p', -M, \tfrac{1}{2}, \mu; j', m_{j'})$$

replaced by -

$$C(l', m_j - \mu + M, \tfrac{1}{2}, \mu; \rho', m_j + M)\ C(p', -M, \tfrac{1}{2}, \sigma; j', m_{j'})$$

and the appropriate selection rules for the projection quantum numbers changed.

Defining the matrix elements for the four cases stated above by -

$$\mathcal{M} = \mathcal{M}(m_j, m_{j'}, \theta_{sc})$$

$$\mathcal{M}^S = \mathcal{M}^S(m_j, m_{j'}, \theta_{sc})$$

$$m^{Sp} = m^{Spin}(m_j, m_j', \theta_{sc})$$

$$m^{SSp} = m^{SSpin}(m_j, m_j', \theta_{sc})$$

the total matrix element for the reaction is found by adding them with the weight defined in the exchange character chosen for the interaction as per equation (2.17a) -

$$m^{Tot} = (W-H)\left[m - m^{SSp}\right] + (B+M)\left[m^{Sp} - m^{S}\right] \quad (2.35)$$

2.4 SIMPLIFICATION TO SPINLESS PARTICLES AND ZERO RANGE

Under the zero range delta function form of the interaction, the double radial and angular integrals of the preceding section reduce to single integrals. This means that space exchange is irrelevant. Further, if we also assume that the unbound particles are not just unpolarised but are spinless, then spin exchange is also irrelevant. Hence, in this section, we merely need consider the direct matrix element expression given by equation (2.28)

The two assumptions stated here affect the expressions for the unbound particle's descriptions and the interaction form given by (2.18) and (2.14) respectively.

The unbound particles now are described by -

$$\phi_i(r_1) = \Sigma_l' \left[4\pi(2l+1)\right]^{\frac{1}{2}} i^l e^{i\sigma_l} f_l(k_i r_1)\, Y_{l,0}(\Omega_1)$$

$$\phi_f^*(r_1) = \Sigma_{l'}' 4\pi i^{-l'} e^{i\sigma_{l'}} f_{l'}(k_f r_1) \sum_{m_{l'}}' Y^*_{l',m_{l'}}(\Omega_1)\, Y_{l',m_{l'}}(\theta_{sc}) \quad (2.36)$$

and the radial integrals $I_{\ell L \ell'}$ become -

$$I_{\ell L \ell'} = \int r^2 dr \, f_{\ell'}(k_f r) \, R_{n'p'}(r) \, f_{\ell}(k_i r) \, R_{np}(r) \qquad (2.37)$$

Thus the matrix elements now have the form -

$$\begin{aligned} \mathcal{M}(m_j, m_j', \theta_{sc}) = {} & \sum'_{l,l',L,M,\mu} (4\pi)^{3/2} \, i^{l-l'} \, e^{i(\sigma_\ell + \sigma_{\ell'})} \\ & \times I_{l L l'} \, (2l+1)(2L+1) \left[\frac{(2p+1)}{(2p'+1)(2l'+1)} \right]^{\frac{1}{2}} \\ & \times C(l, 0, L, 0; l', 0) \; C(p, 0, L, 0; p', 0) \\ & \times C(l, 0, L, -M; l', -M) \; C(p, m_p, L, M; p', m_{p'}) \\ & \times C(p, m_p, \tfrac{1}{2}, \mu; j, m_j) \; C(p', m_{p'}, \tfrac{1}{2}, \mu; j', m_{j'}) \\ & \times Y^*_{l', +M}(\theta_{sc}) \end{aligned} \qquad (2.38)$$

The term -

$$\sum'_{pp'\sigma} C(l, 0, \tfrac{1}{2}, \sigma; p, \sigma) \; C(l', -M, \tfrac{1}{2}, \sigma; p', \nu') \qquad (2.39)$$

has disappeared under the assumption of spinless particles.

Now Edmonds[*28] has shown that the following relationship exists -

$$\sum_{\beta} C(a,\alpha,b,\beta;c,\gamma)\, C(d,\delta,c,\gamma;J,\mu)\, C(b,\beta,c,\gamma;e,\varepsilon)$$

$$= [(2d+1)(2e+1)]^{\frac{1}{2}}\, W(a,b,J,c;d,e)\, C(a,\alpha,e,\varepsilon;J,\mu) \qquad (2.40)$$

where the $W(a,b,J,c;d,e)$ is a Racah function.

This relationship can be used to generate the matrix element expression as given by Glendenning*10. In particular we define -

$$a = j \qquad c = p' \qquad e = L$$
$$b = p \qquad d = \tfrac{1}{2} \qquad \beta = \tau \qquad (2.41)$$

Then

$$\sum_{\tau} C(j,m_j,p,\tau;\tfrac{1}{2},\mu)\, C(\tfrac{1}{2},\mu;p',m_{p'};J',m_{J'})\, C(p,\tau,p',m_{p'};L,M)$$

$$= [2(2L+1)]^{\frac{1}{2}}\, W(j,p,J',p';\tfrac{1}{2},L)\, C(j,m_j,L,M;J',m_{J'}) \qquad (2.42)$$

Using the symmetry properties of the Clebsch-Gordan coefficients, the right-hand side of (2.42) can be written as -

$$\text{R.H.S.} = \sum_{\tau} (-)^{\frac{1}{2}-J'+L+p}\, C(p,-\tau,\tfrac{1}{2},\mu;J,m_j) \left[\frac{2}{(2J+1)}\right]^{\frac{1}{2}}$$

$$\times C(p',m_{p'},\tfrac{1}{2},\mu;J',m_{J'})\, C(p,-\tau,L,M;p',m_{p'}) \left[\frac{(2L+1)}{(2p'+1)}\right]^{\frac{1}{2}} \qquad (2.43)$$

Hence by defining $\tau = -m_p$ and since the sum rule for these coefficients shows $m_p + \mu = m_j$, the summation over τ can be replaced by one over μ, since for this bracket of terms in the matrix elements, m_j is considered fixed.

$$\sum_{\mu}' C(p, m_p, \tfrac{1}{2}, \mu; j, m_j) \, C(p', m_{p'}, \tfrac{1}{2}, \mu; j', m_{j'}) \, C(p, m_p, L, M; p', m_{p'})$$

$$= (-)^{\frac{1}{2}-j'+L+p} \left[\frac{(2p'+1)(2j+1)}{2(2L+1)} \right]^{\frac{1}{2}} [2(2L+1)]^{1/2}$$

$$\times \, W(j, p, j', p'; \tfrac{1}{2}, L) \, C(j, m_j, L, M; j', m_{j'}) \tag{2.44}$$

Hence the matrix element given by (2.38) can now be expressed as -

$$\mathcal{M}(m_j, m_{j'}, \theta_{sc}) = \sum_{l, l', L, M}' (4\pi)^{3/2} \, i^{l-l'} \, e^{i(\sigma_l + \sigma_{l'})} \, I_{lLl'}$$

$$\times (-)^{\frac{1}{2}-j'+L-p} (2l+1)(2L+1) \left[\frac{(2p+1)(2j+1)}{(2j'+1)} \right]^{\frac{1}{2}}$$

$$\times \, C(l, 0, L, 0; l', 0) \, C(p, 0, L, 0; p', 0) \, C(l, 0, L, -M; l', -M)$$

$$\times \, C(j, m_j, L, M; j', m_{j'}) \, W(p, j, p', j'; \tfrac{1}{2}, L) \, Y^{*}_{l', M}(\theta_{sc}) \tag{2.45}$$

where the rearrangement of the order of the quantum numbers within the Racah coefficient is allowable by its symmetry. Further, the matrix element given above is not a function of three variables but only of two. This is because of the sum rule -

$$m_j + M = m_j \tag{2.46}$$

This is extremely beneficial for numerical calculations and computer economics.

However, this expression, which agrees with

Glendenning's formulation, can be made somewhat simpler from the point of view of calculation. The simplifications arise from the particularly simple form for the Racah coefficient used. More basically, the particular form that is used in the Wigner-Eckart theorem for this calculation can be simplified.

Using the relationships reported by Glendenning, we find the following expressions -

$$M(m_j, \theta_{sc}) = \sum'_{l,l',L,M} (4\pi)^{3/2} i^{l-l'} e^{i(\sigma_l + \sigma_{l'})} (2l+1)(2L+1)$$

$$\times I_{ll'} \left[\frac{2j+1}{(2j'+1)(2l'+1)}\right]^{1/2} C(l,0,L,0;l',0)$$

$$\times C(j,\tfrac{1}{2},L,0;j',\tfrac{1}{2}) \quad C(l,0,L,-M,l',-M)$$

$$\times C(j,m_j,L,M;j',m_{j'}) \quad Y^*_{l',M}(\theta_{sc}) \qquad (2.47)$$

It is this expression we first coded for the IBM 7090 computer, and most of the results reported here have been obtained with this spinless and zero range approximation code.

CHAPTER 3 DEFINITION OF EFFECTS

3.1 INTRODUCTION

An object of these calculations is to see whether angular distribution shapes contain further information about the effective two-body force. In particular we ask whether the density dependence of the effective two-body force in nuclear matter rather than any optical model property causes the surface mechanism reaction to occur, and whether the surface reaction results are significantly different from the volume calculations, so that the type of reaction could be identified experimentally.

The analysis to be presented will be consistent with the following points -

(i) There exist measurable differences between surface and volume calculations.

(ii) These differences cannot be explained by any sensible variation of the optical model parameters or by any optical model effect present in the matrix elements.

(iii) The compound nucleus properties for the system do not over-ride the direct reaction features.

The analysis reported here centres around two reactions. The first is $F^{19}(p,p')F^{19*}$ to the first excited level with a Q value of 0.11 MeV. This is a parity changing reaction with a small Q-value. Hence the parity rule of McCarthy and Kromminga[*5] should hold and, within the approximations used, it does. This then could indicate the normalization of the direct reaction

contributions, as suggested by Dodd and McCarthy*4 and described in Section 1.1. In any event, it is hoped that this will be able to give insight into point (iii) above in relation to points (i) and (ii). Of course, the parity rule limitations must be fully understood and each case reviewed to see whether conditions are within these limitations.

The second reaction studied extensively is $C^{13}(p,n)N^{13}$ to the ground state of N^{13}, Q-value = 3.005 MeV. This experiment has been performed by Dagley et al*21 over the range of energies from 5 MeV to 12 MeV with good energy resolution. We attempt to fit general features of this data. In particular, we investigate the energy variation of the extreme angle peaks and try to evolve the angular distributions whose shape does not vary rapidly with energy.

In both of these reactions, the surface to volume calculation differences are pronounced and should be sufficient to recognize the reaction mechanism property under question.

The next section of this chapter is devoted to a short discussion of the optical model wave functions, and the effect of the optical model wave functions, and the effect of the optical model parameters on them. Then we define, in more detail, the optical model properties of focussing, phase averaging and the parity involved in the matrix elements. These detailed

definitions are necessary for our interpretation of the results presented in Chapter 4.

3.2 THE OPTICAL MODEL WAVE FUNCTION*29

Before discussing the magnitude and phase pictures of the totaloptical model wave functions at different energies and potentials and for various nuclei, for completeness we shall review the background of its development more fully than was done in Chapter 1.

By 1953, the compound nucleus as postulated by Bohr had been extended by changing its basic assumptions slightly, thereby permitting a more rigorous mathematical structure*30. This led to the Breit-Wigner formula. Within this framework, two extreme situations exist. One was the case for isolated resonances which gave the Breit-Wigner one level formula. The other was the overlapping resonance situation which was described by the many level Breit-Wigner formula and gave cross-sections dependent upon the unknown phase relationships between these overlapping resonances.

In the latter case, Weisskopf and Ewing*31, assuming constant partial widths and random phases were able to calculate cross-sections by defining some reasonable mechanism to find the probabilities of formation and decay of the compound system. However, while the statistical model, as it was called, agreed with some experimental results*32, for the nuclear wave functions describing this system of complete chaos,

the cross-sections are smooth functions of energy when, as described in Chapter 1, an averaging is made over several resonances. This is not in agreement with some observed cross-sections*33, and further, the model cannot explain the large asymmetric angular distributions as found by Gugelot*34.

In fact, such features could not be explained by any compound nucleus theory. However, the single particle models had more success in this regard. In particular, by representing the target nucleus by a complex potential well, a good account of high energy nucleon scattering*35 as well as low energy elastic scattering*36 was found, and its usefulness was further shown by the agreement with the total and differential cross-sections of Walt et al*37.

The fundamental assumption in the optical model is that the scattering of particles by nuclei is a problem of the motion of the particle in a time independent complex potential well, which cannot give information on the detailed structure of the nucleus. Hence it cannot describe changes in the target. Also, because it contains no details of the interaction, the model can only produce the averaged values for the cross-sections and not show compound nucleus resonance features.

The wave functions for the unbound particle in this model are, therefore, solutions of the Schroedinger equation -

$$\left[\nabla^2 + k^2 + \frac{2m}{\hbar^2} V(\underset{\sim}{r})\right] \psi(\underset{\sim}{k}, \underset{\sim}{r}) = 0 \qquad (3.1)$$

where $$k^2 = \sqrt{\frac{2mE}{\hbar^2}} \qquad (3.2)$$

and, in its most general form -

$$V(r) = -V_0 f(r) - iW_0 g(r) + \left(\frac{\hbar}{\mu c}\right)^2 [V_{so} + iW_{so}] \times \frac{1}{r}\frac{df}{dr}\underset{\sim}{\sigma}\cdot\underset{\sim}{L} \qquad (3.3)$$

V_0, W_0, V_{so}, W_{so} are the real and imaginary parts of the central and spin-orbit potentials

$\hbar/\mu c$ = π- meson Compton wave length.

Defining R as the radius at which the potential has a magnitude one half of its central value, a as the surface thickness parameter and b as a gaussian spread parameter, the form factors f(r) and g(r) have two generally accepted forms -

(a) for Volume absorption -

$$f(r) = g(r) = \left[1 + \exp((r-R)/a)\right]^{-1} \qquad (3.4)$$

(b) for surface absorption -

$$f(r) = \text{Saxon form factor (3.4)}$$

$$g(r) = \exp(-(r-R)^2/b^2) \qquad (3.5)$$

In the calculations we have made, spin-orbit coupling is neglected and the volume absorption is used.

From equations (3.1) to (3.5) it can be seen that, in its simplest form, the optical model theory contains at least four parameters. They are V_c, W_c, a and R. It is usual to consider the radius parameter as -

$$R = r_o A^{1/3} \qquad (3.6)$$

Hence one test of the theory would be to find a consistency between the sets of parameters for various cases. Unfortunately these were found to vary from reaction to reaction as well as being energy dependent. However, Bjorklund and Fernbach*[14] found that the following set of parameters were at least a good starting point for analysis.

r_o = 1.25f

a = 0.65f

b = 1f

V = 52 MeV for E → 0 MeV and decreasing as E increases

W = 3 MeV for E → 0 MeV and increasing to 20 MeV for E=100 MeV and slowly decreasing for E > 100 MeV.

A recent evaluation*[41] as well as the advent of the non-local optical model potential, has advanced the parametrization of the model. Most important is the fact that these results show a fairly smooth monotonic variation with A, and, with the non-local potential calculations some marked closed shell effects are noticed.

Nevertheless, defects still exist in the parametrization. Two noticeable flaws are the following -

(a) There is a Vr_o^2 ambiguity. This is quite evident in figure 13 in Chapter 4 and reference will be made

to it then.

(b) Many sets of parameters give equivalent fits to results and with higher incident energies, calculations are far less sensitive to changes in the potential V. Saxon*[38] cites the case that, for E≈135 MeV, the elastic scattering data can be fitted with any value of V between 10 MeV and 40 MeV. However, this number of sets of parameters can be reduced if other reactions are considered.

While these features detract from the model, its success is not doubted so that it well describes the wave function of the unbound particle not only in the external region of the nucleus, but, as stated in Chapter 1, also inside the nucleus.

Figure 1 shows the moduli of the optical model wave functions for 5, 10 and 20 MeV protons on C^{13}. These pictures are (a), (b) and (c) respectively. Also in Figure 1, contour maps of the phases of the 10 and 20 MeV cases are shown in (d) and (e) respectively. The parameters used in these calculations are -

$V = 50MeV$, $W = 6MeV$, $a = 0.55f$ and $r_o = 1.2f$.

The surface region, that is the region of space in which the nuclear potential has a value between 10% and 90% of its central value, is shown in black in the magnitude pictures, and the nuclear radius and the surface region by a dotted line and brackets in the phase pictures. In all these photographs, the focus

FIGURE 1

(a), (b) and (c) are the magnitude pictures of the optical model wave functions for 5, 10 and 20 MeV on C^{13}.

(d) and (e) are the phase pictures for the 10 and 20 MeV incident energy cases.

The parameters used were -

V = 50MeV W = 6MeV a = 0.55f r_o = 1.2f

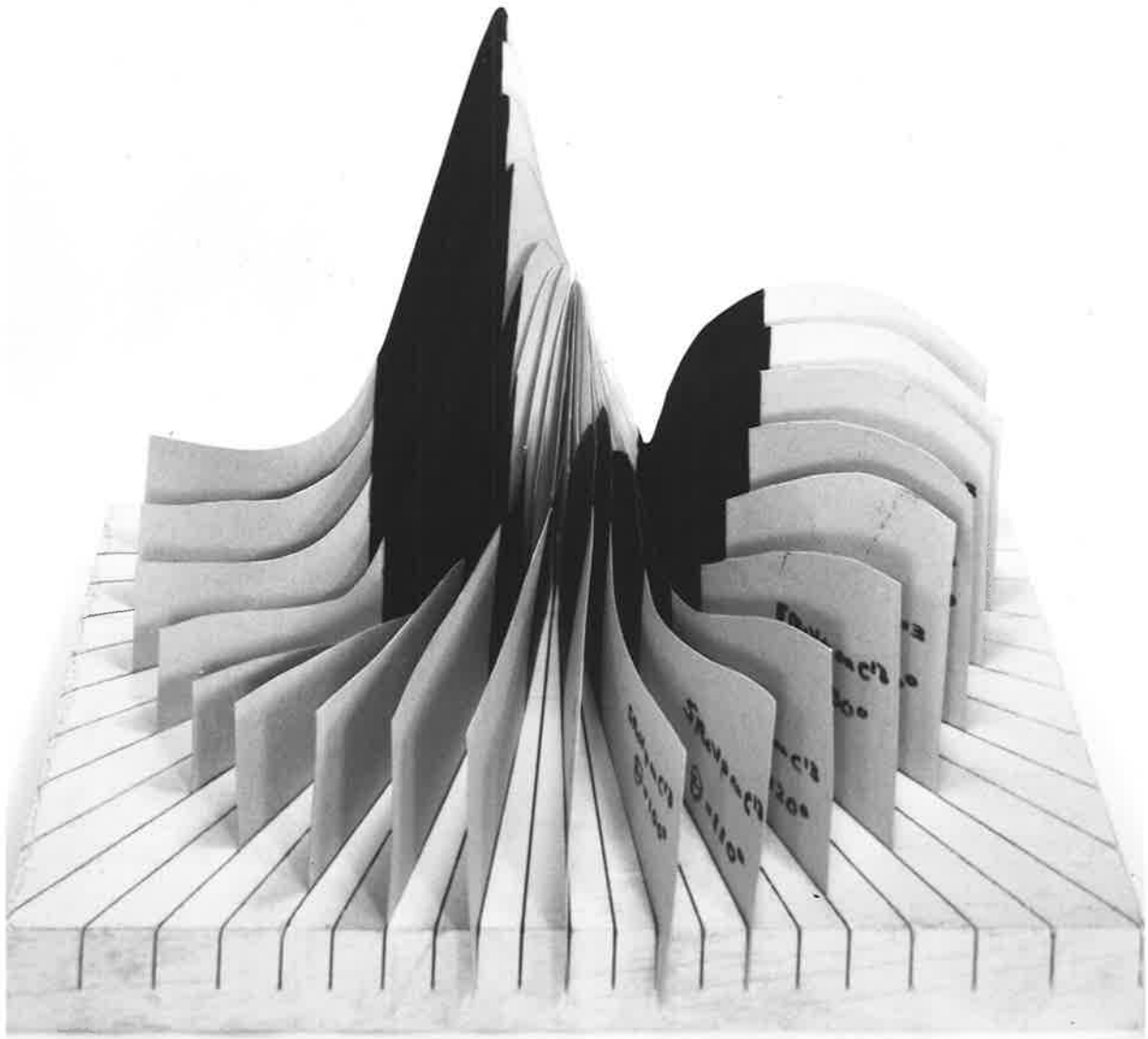

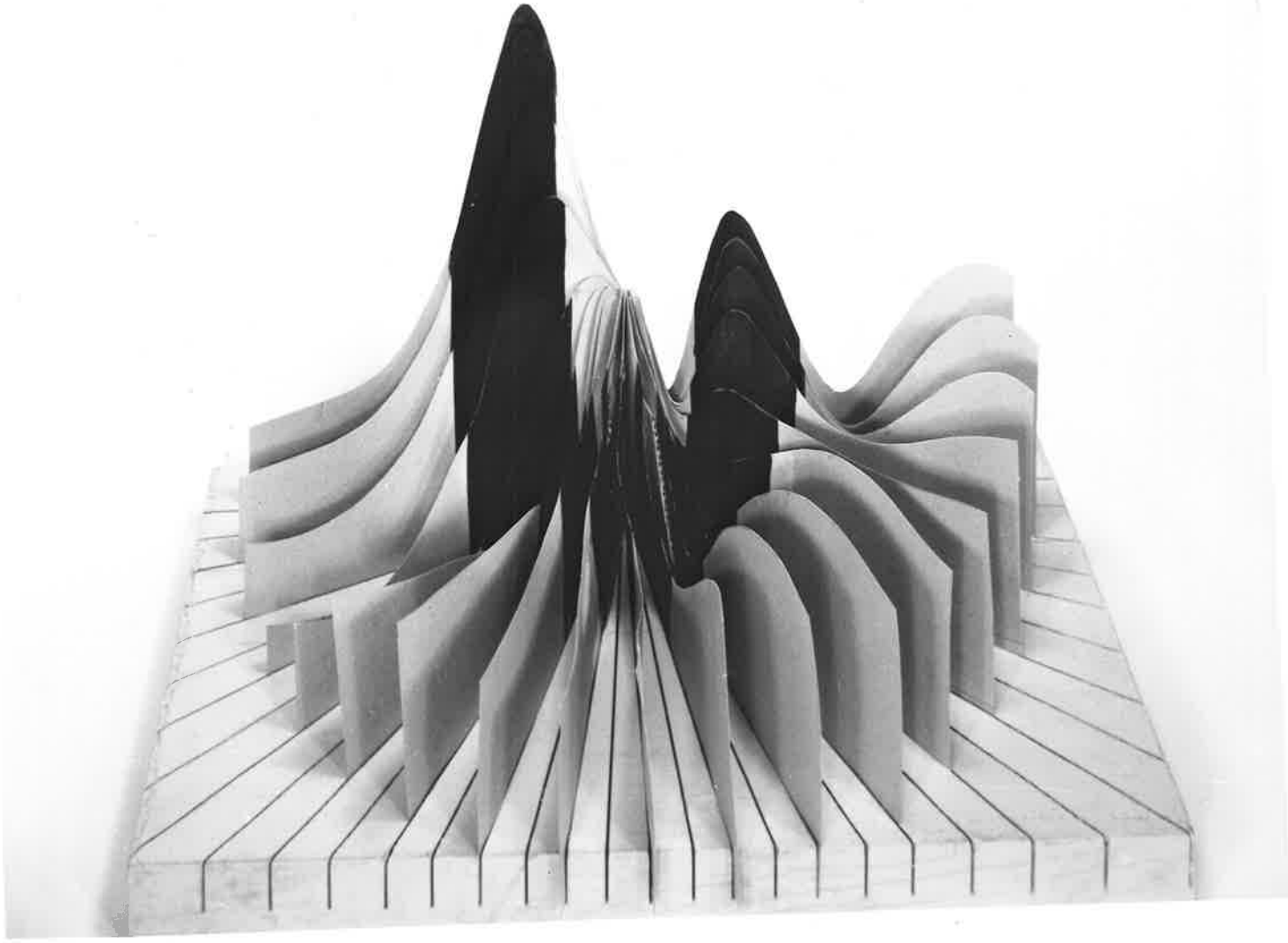

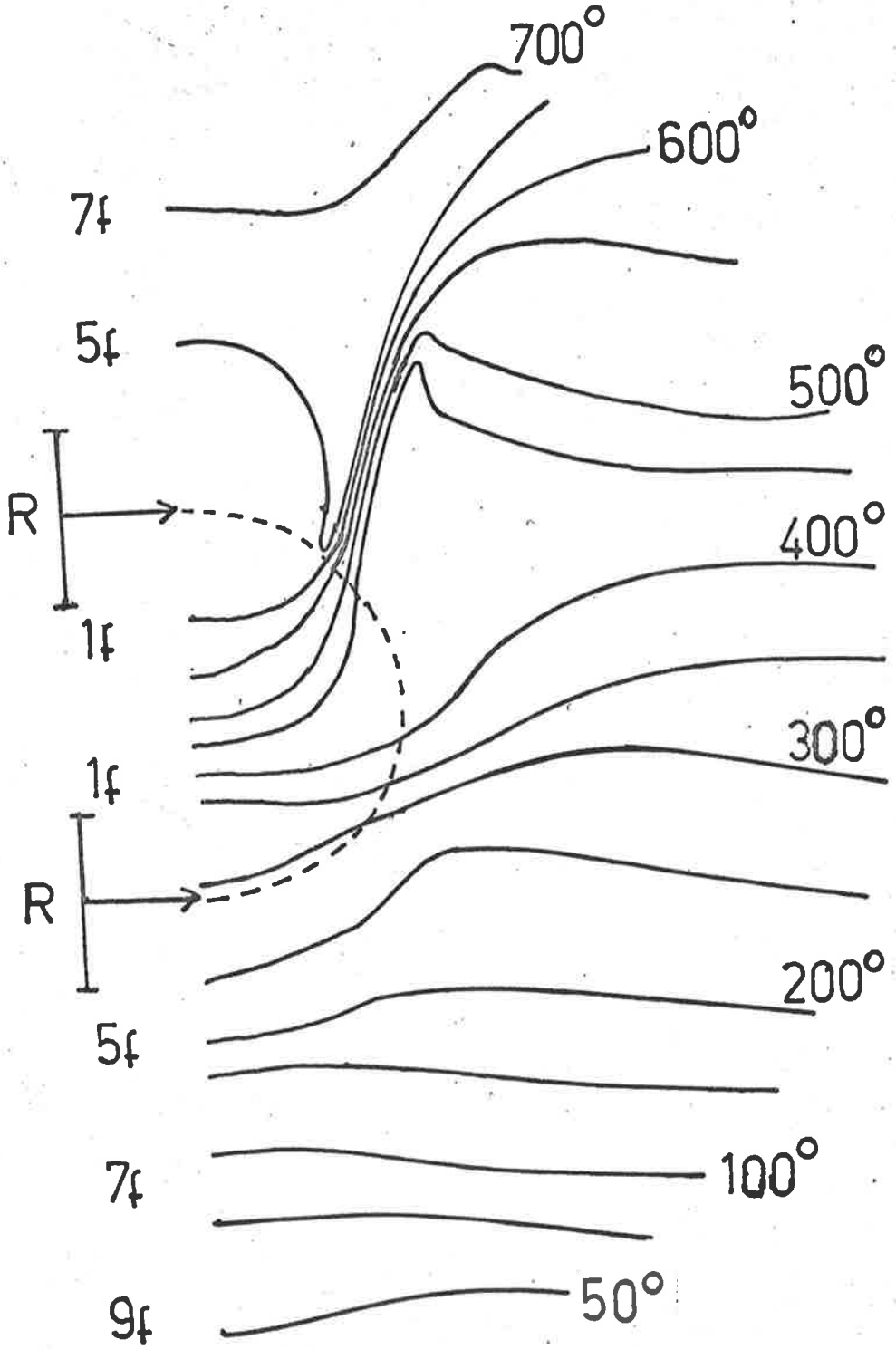
700°
600°
7f
5f
500°
R
400°
1f
300°
1f
R
200°
5f
7f
100°
9f
50°

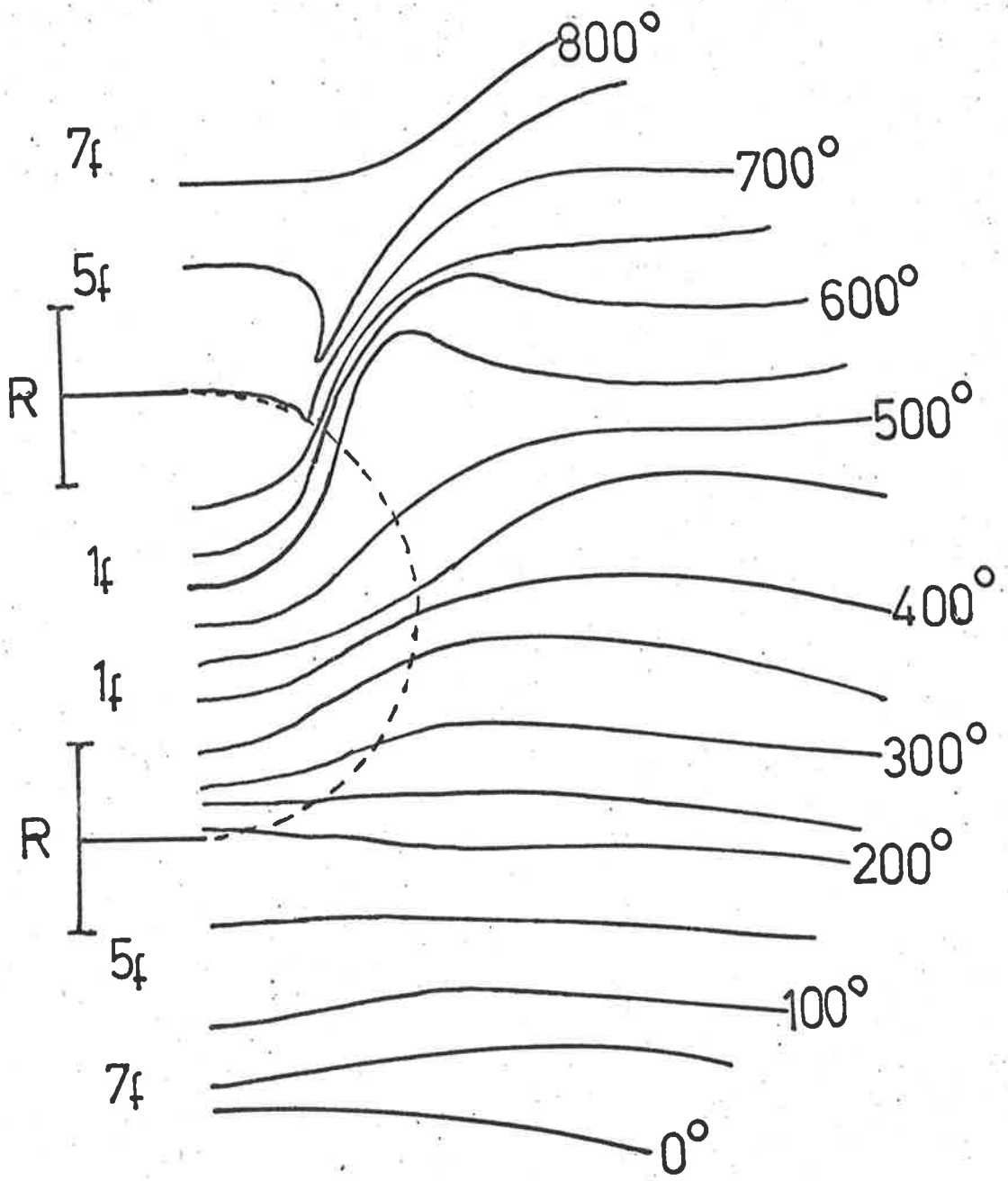
800°
7f
700°
5f
600°
R
500°
1f
400°
1f
300°
R
200°
5f
100°
7f
0°

is most pronounced and the incident direction is always taken as from the top of the page down. The maximum magnitudes of the foci increase with energy from 2.9, 3.07 to 3.258, but more important than this are the structural changes.

The most obvious structural change is the extra peak for higher incident energy in the 0° - 180° line. This is accompanied by outward shift of the position of the maximum of the focus and an inward shift of the front surface peak position. Increased structure and decreased magnitude in the 90° area is also a feature of increasing energy.

In the phase pictures of Figure 1, the formation of the focus is quite evident and, while diffraction effects are present, the main distortion of the phase from that of the plane wave case occurs within the nuclear surface region and bears out the theoretical discussion of the next section. As is expected, with increase in energy, the phase changes are more rapid and are less severe. However an important feature of these results is that phase lines crowd together in those regions of space where the magnitudes of the wave functions are small and there are relatively small phase changes in regions of maxima in the magnitudes of the wave functions. It is because of this that the plane wave theory in many cases gives results not as wildly divergent from those of the

distorted wave theory as the magnitude pictures seem to indicate.

Figure 2(a) and (b) are the magnitude and phase pictures for 10 MeV protons on F^{19} using the following parameters -

V = 55MeV, W = 4MeV, a = 0.55f and r_o = 1.2f

Figure 2(c) and (d) are the same pictures but for the case of V = 45 MeV. The maximum magnitudes of the foci are 3.37 for the V = 55 MeV case and 2.88 for the V = 45 MeV case but the position of the maximum in the V = 45 MeV case is further inside the nuclear volume than the higher V case. While this is not as might be expected there is more structure along the 0^o - 180^o line for the V = 55 MeV case indicating that the relationships between partial waves is more complex than for the lower V case.

However, both wave functions have considerable structure in their magnitudes but, in the lower V case this is more sharply defined, especially in the spread in space of the focus.

The phase pictures (b) and (d) once again show the crowding of phase lines in the regions of small magnitudes and are similar except in the focal region where in the higher potential case a closed loop of phase exists. This is connected with the fact that the focal region for this case is more extensive than in the lower potential case where no such closed phase

FIGURE 2

The magnitude and phase pictures for 10 MeV protons on F^{19}. Plates (a) and (b) are the wave functions for V = 55 MeV. Plates (c) and (d) are the wave functions for V = 45 MeV.

The other parameters were -

W = 4 MeV a = 0.55f r_o = 1.2f

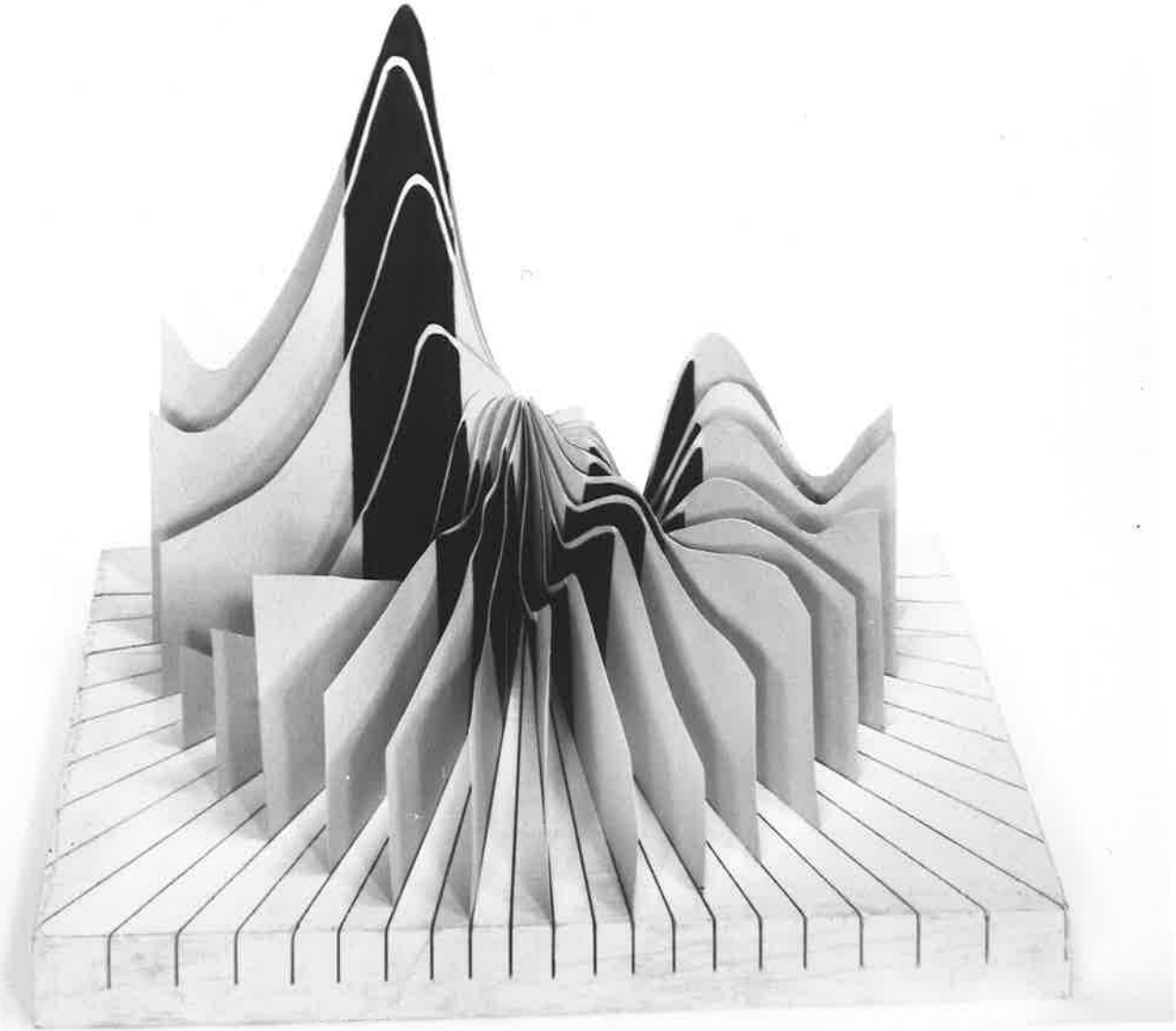

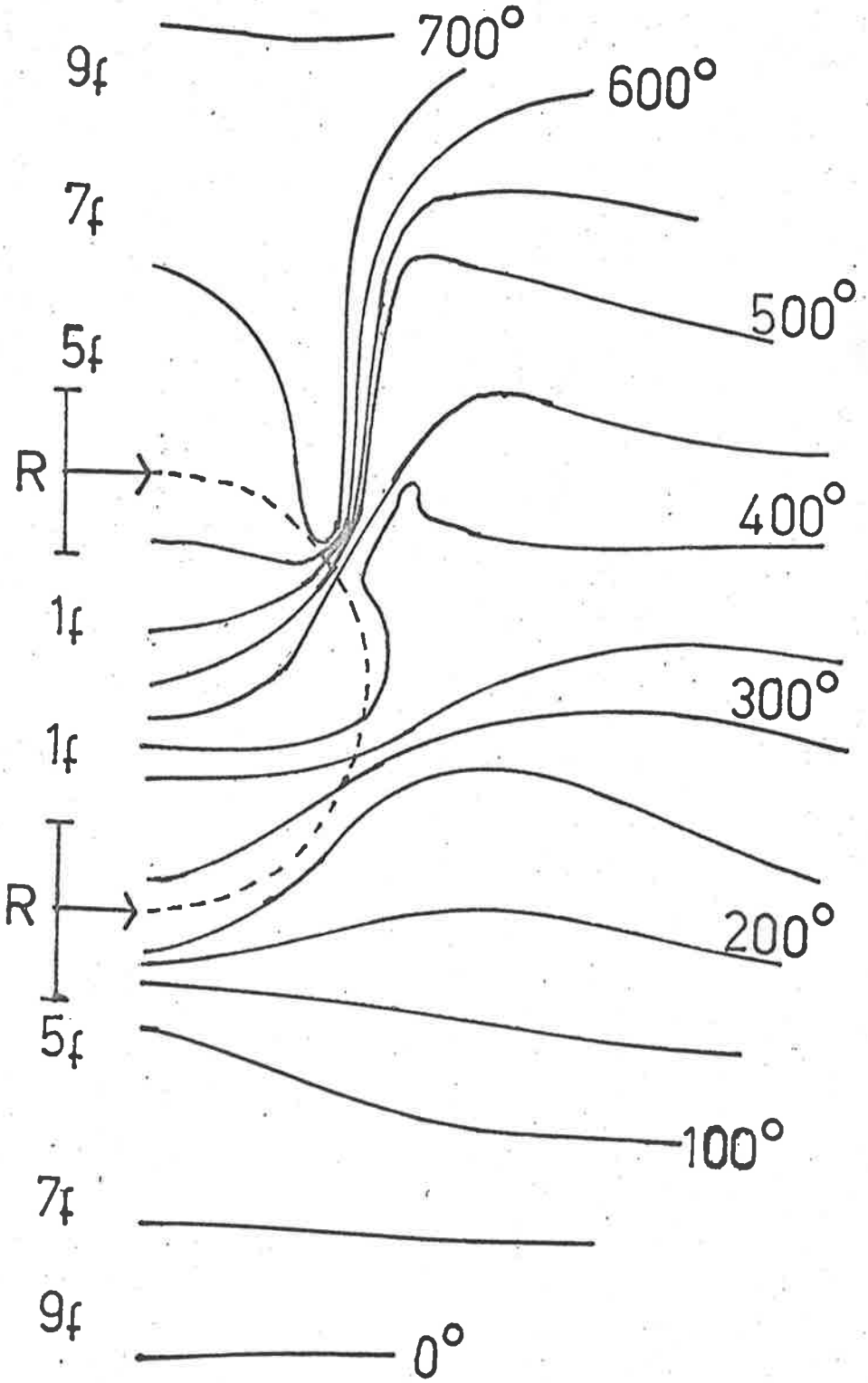
700°
600°
500°
400°
300°
200°
100°
0°
9f
7f
5f
R
1f
1f
R
5f
7f
9f

loop exists.

Figure 3 shows the magnitude (a) and phase (b) pictures of the optical model wave function for 60 MeV protons on F^{19}. Except in the focal region the magnitude throughout most of the nuclear volume shows little deviation from that of a plane wave with a modulus of near 0.85. In the focus, the magnitude rises fairly smoothly to about 2.37. The reflection effects can be seen most clearly in the front surface region (at top of page) while diffraction seems evident at back of the nuclear volume, especially the start of the second peak at about 2 to 3 nuclear radii. The focal region shows a peculiar double peak effect which most likely is a combination of diffraction around, and refraction through the nuclear volume. The phase picture bears out the plane wave tendency, and the characteristic increase in the rate of phase change with increase in energy can easily be seen if this is compared with the corresponding diagrams of Figure 2. Diffraction may appear more probable in this case because relative absence of crowding of phase lines.

Figure 4 shows the optical model wave for 24 MeV neutrons on Sn^{118}. For this heavy nucleus we see that most of the nuclear interior has the flat plane wave shape as for the previous figure, with again, the exception of the focal region. The magnitude of the

FIGURE 3

The modulus (a) and phase (b) of the optical model wave function for 60 MeV protons on F^{19}. The parameters are -

V = 40 MeV W = 8 MeV a = 0.5f r_o = 1.2f

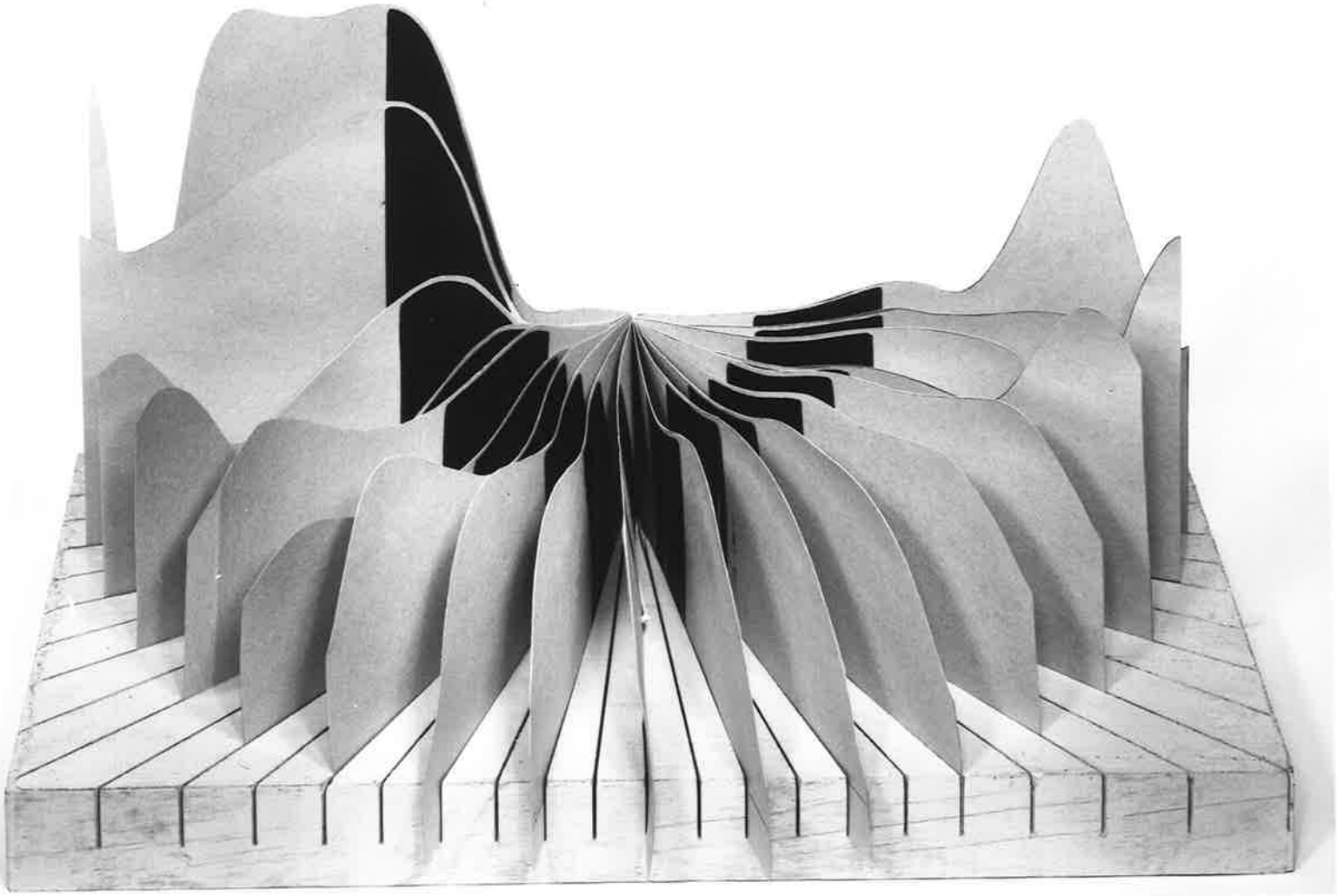

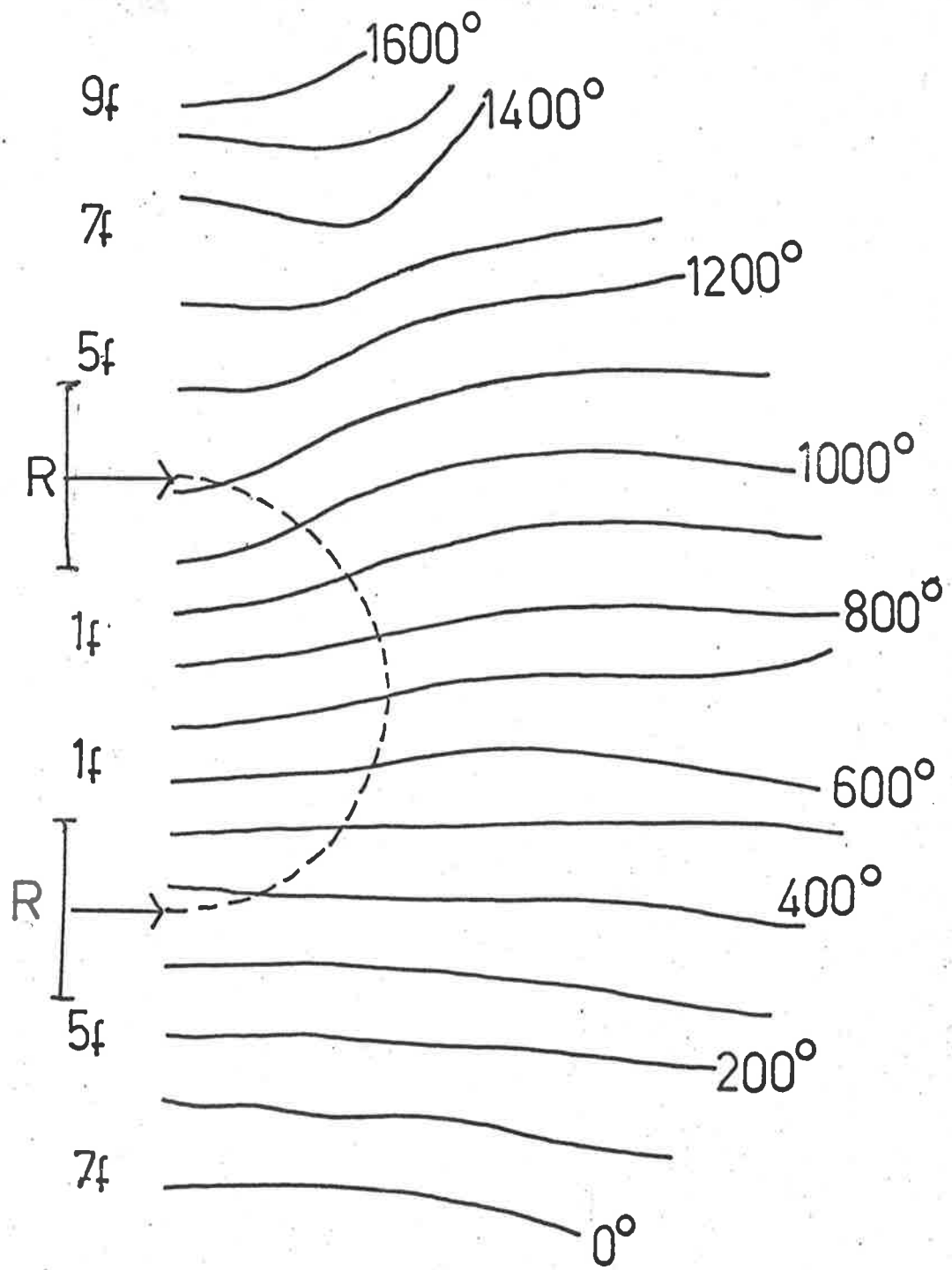
1600°
9f
1400°
7f
1200°
5f
R
1000°
800°
1f
1f
600°
R
400°
5f
200°
7f
0°

internal region here is about 0.6 and all structure of this wave function is fairly well contained in the nuclear surface. The front side, $\theta = 180^{o}$, exhibits slight reflection effects while the focus is most pronounced (magnitude 2.8) and centred on the nuclear radius. Comparing the magnitude picture with the previous figures we can see that this focus is well defined in angle but quite spread radially. In this wave function, the focus subtends about a 30^{o} angle whereas in the 10 MeV protons on F^{19}, for example, it subtends about a 50^{o} angle.

In the phase picture the plane wave appearance can be readily seen as can the fact that structuring is only pronounced in the focal region and the small angle parts of the nuclear surface.

These two diagrams point to the fact that refraction of the waves through the nuclear surface produces the focus. The parameters used for this figure were v = 40 MeV, W = 11 MeV, a = 0.7f and r_{o} = 1.25f.

Figure 5 shows a square well calculation with parameters V = 40 MeV, W = 0 MeV, r_{o} = 1.2f for the case of 10 MeV protons on F^{19}. Again a focus appears which must be due to wave effects through the nuclear interior. It has a magnitude of 3.0. In this case the wave function is very structured, presumably due to reflection effects, and this is borne out by the phase picture.

FIGURE 4

The magnitude (a) and phase (b) of the optical model wave function for 24 MeV neutrons on S_n^{118} . The parameters used were -

V = 40MeV, W = 11MeV, a = 0.7f, r_o = 1.25f

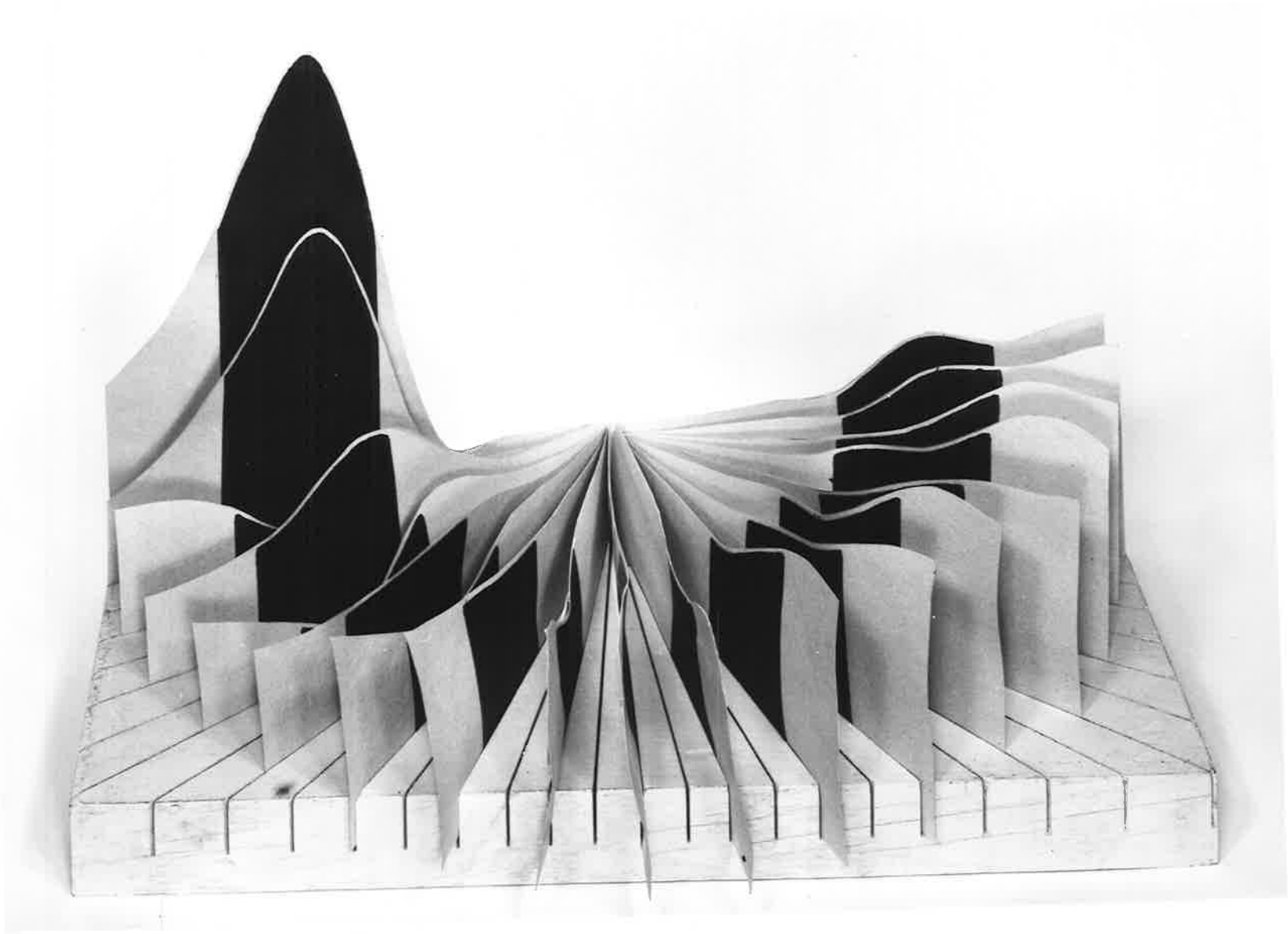

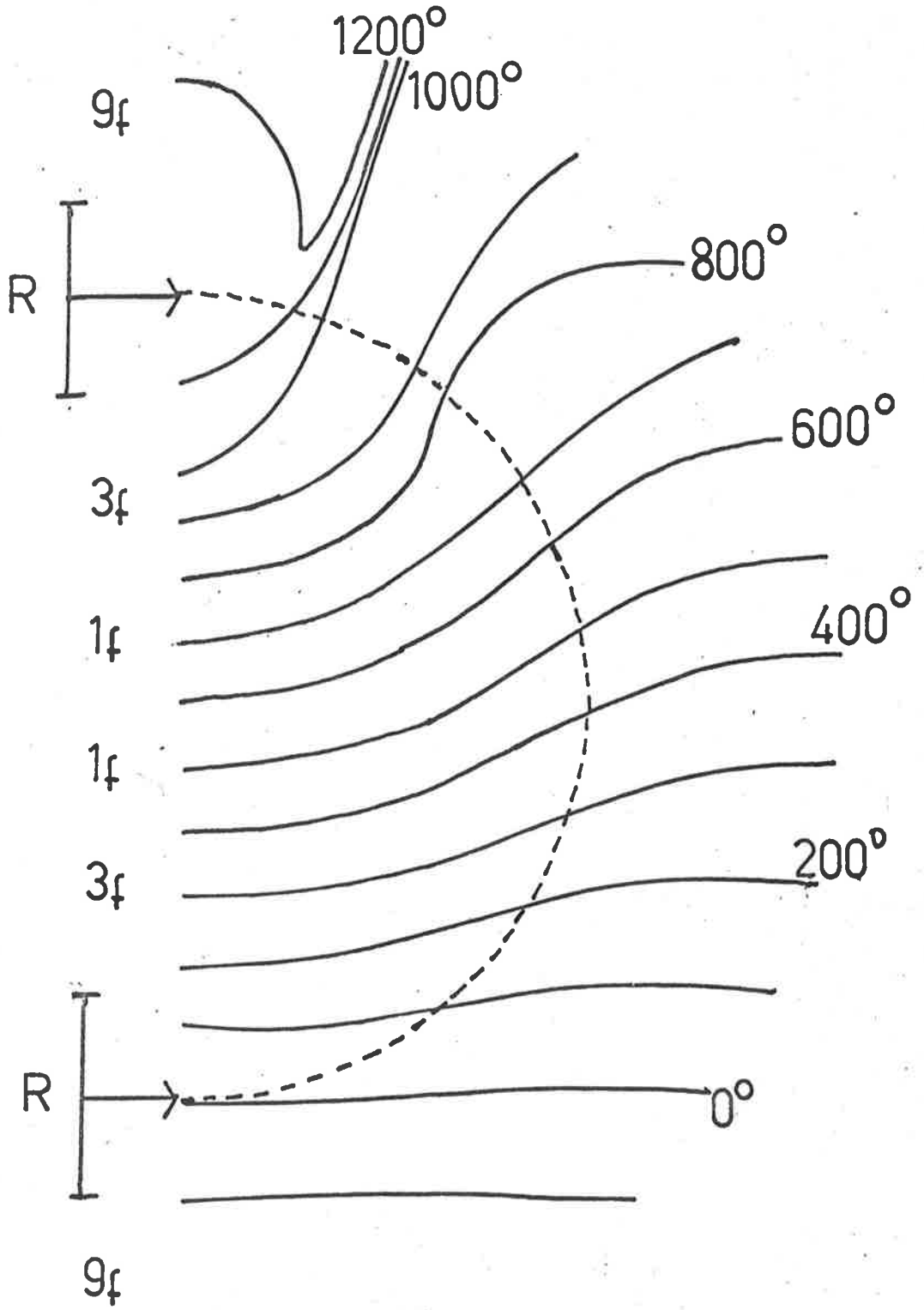
1200°
1000°
9f
R
800°
600°
3f
400°
1f
1f
200°
3f
R
0°
9f

FIGURE 5

The magnitude (a) and phase (b) of the optical model wave function for 10 MeV protons on F^{19} using a Square potential well with parameters -

V = 40 MeV, W = 0 MeV, r_o = 1.2f

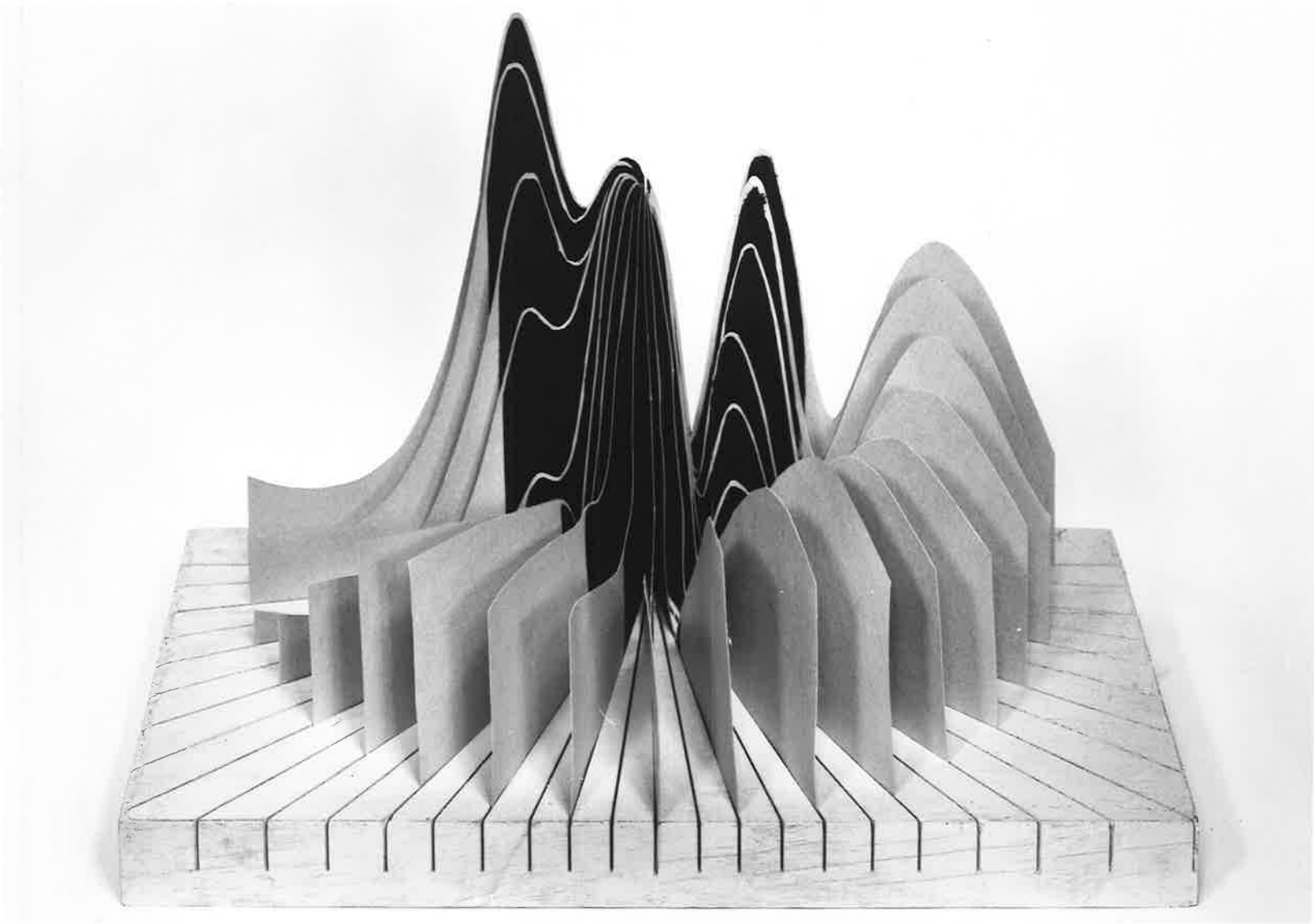

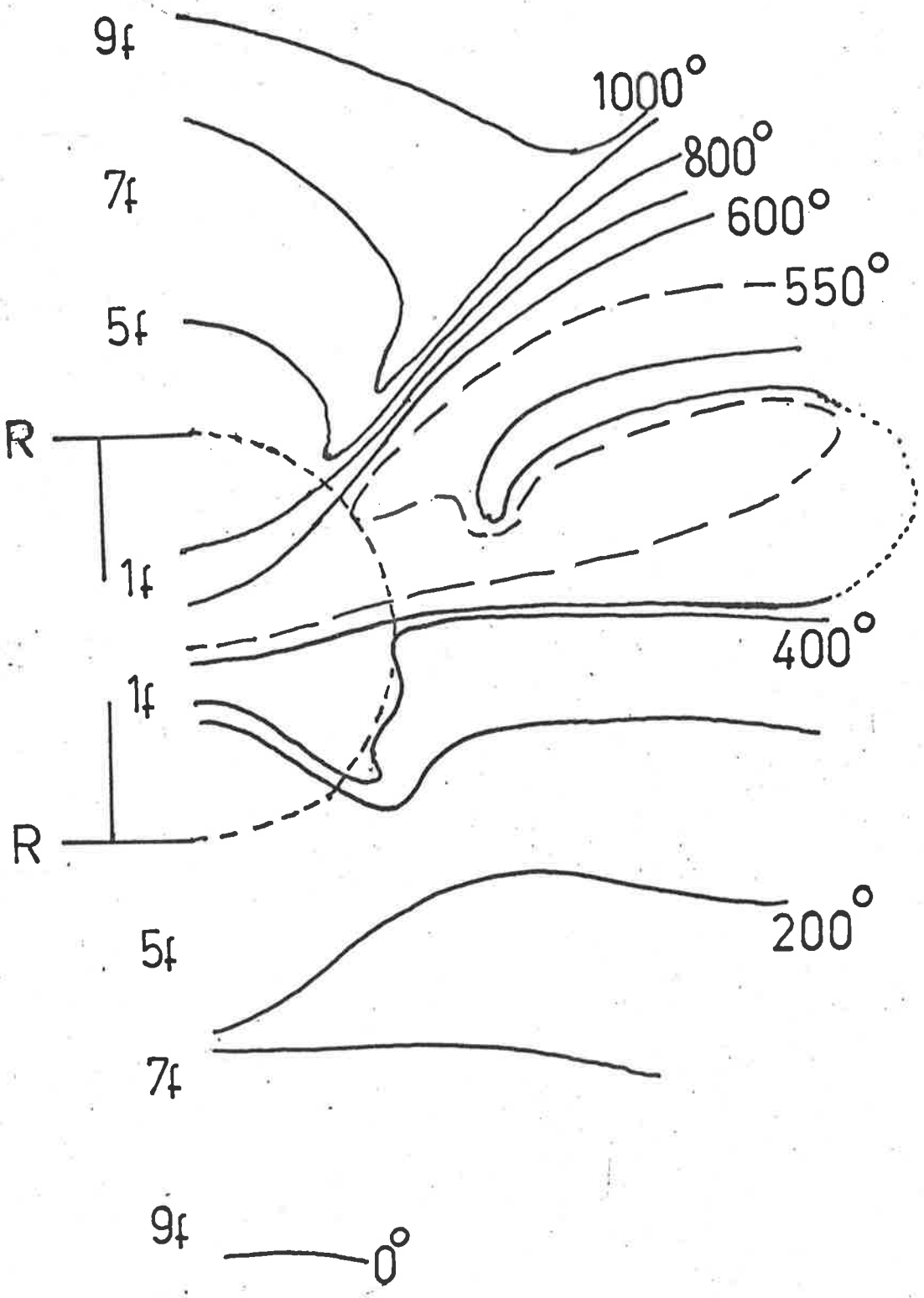
9f
1000°
7f
800°
600°
5f
550°
R
1f
400°
1f
R
5f
200°
7f
9f
0°

Hence the optical model wave function has a structure far removed from that of the plane wave picture (although the phase properties in the low energy case may offset this to some extent), and only will tend to plane wave situation for higher incident energies or when heavier nuclei are used as the target except in the focal region.

In fact, the approximate wave function of McCarthy and Pursey appears to be more adequate in these cases. This is borne out by results obtained by this method.

If a square well potential is used the structure of the wave function becomes more extreme than for the Saxon Well case but the phase properties are far removed from the diffuse edge calculations and, in view of the role played by the phase in the next section, this may be a serious objection to the use of a square well.

3.3 THE INTERFERENCE EFFECTS IN THE PARTIAL WAVE FORMALISM

We will show here how the terms "focus", "phase averaging" and "parity rule" arise from the mathematical description of the optical model wave functions and the direct reaction theory when the partial wave expansion technique is used.

(a) The Focus and Phase Averaging

This discussion follows closely that given by McCarthy*[15,43].

In the partial wave representation, the optical model wave function for a particle of energy E, impinging on a nucleus characterised by a radius R, has the form -

$$\psi^{(+)}(k,r) = \sum_{l=0}^{\infty} \psi_l^{(+)}(kr)\, P_l(\cos\theta) \qquad (3.7)$$

$$\psi_l^{(+)}(\rho) = i^l (2l+1)\, e^{i\sigma_l} f_l(\rho) \qquad (3.8)$$

where, as before, $\rho = kr$

In the limit as $r \to \infty$, the functions $f_l(\rho)$ have the assymptotic form

$$f_l(\rho) \xrightarrow[r\to\infty]{} \frac{1}{\rho}\left[F_l(\rho) + C_l\{G_l + iF_l\}\right] \qquad (3.9)$$

where the F_l, G_l taken at the origin are the regular and irregular coulomb or spherical bessel functions for the charged and uncharged incident particle cases respectively. The coefficients C_l are related to the nuclear phase shifts δ_l, and the reflection coefficient η_l, by the following expression -

$$\eta_l = e^{2i\delta_l} = 2iC_l + 1 \qquad (3.10)$$

For large angular momenta the reflection coefficient

$$\eta_l = 1 \qquad (3.11)$$

For small angular momenta -

$$\eta_\ell \to 0 \qquad (3.12)$$

For surface partial waves of intermediate angular momenta -

$$0 \leq \eta_\ell \leq 1 \qquad (3.13)$$

This means that very nearly full reflection of partial waves characterizes the nuclear exterior, so that these are standing waves. In contrast, the partial waves characterizing the nuclear interior are not appreciably reflected, and so these are incoming in form.

Between these limits we have the intermediate partial waves, which give rise to the dependence, at least for elastic scattering, of the scattering amplitudes on the details of the potential.

For the incoming partial waves, it was originally thought that the smallness of η_ℓ was a property of absorption. This, according to Austern[*20] and later McCarthy[*15], is not the case, and these authors show that the small η_ℓ for these partial waves is the result of phase averaging. Using the W.K.B. approximation, Austern calculated these reflection coefficients from the expression -

$$\eta_\ell = \int_\infty^{r} (k'(s) - k)\, ds. \qquad (3.14)$$

where $$k'(s) = \left[k^2 - \frac{l(l+1)}{r^2} - \frac{2m}{\hbar^2} U(r)\right]^{\frac{1}{2}} \qquad (3.15)$$

and $U(r)$ is the representative potential of the nucleus. The integrand in the above is complex. For low l, that is for interior partial waves where the classical turning point is well inside nuclear matter, this integrand has a rapid smooth variation of phase with radius. Consequently, the integration value is small.

Consider the plane wave uncharged projectile case -

$$f_l(\rho) = j_l(\rho) \; ; \; \sigma_l = 0 \qquad (3.16)$$

where $j_l(\rho)$ is a spherical bessel function, hence the phase of successive partial waves $\psi_l(\rho)$ are 90° apart. So we now consider

$$\arg \psi_l(\rho) = l\pi/2 + \phi_l \qquad (3.17)$$

where ϕ_l is the phase difference between the optical model partial wave function and the uncharged incident particle plane wave case. Further, in the plane wave case, each partial wave has sudden drops of 180° in phase at the zeros of the appropriate spherical bessel function. This is evident from the phase of the large (external) partial waves, which tend to the plane wave situation, as shown in Figure 6.

These waves are expected to be of plane wave form,

FIGURE 6

The phase of the ℓ^{th} partial wave in the optical model wave function for the scattering of 30 MeV neutrons from C^{12}, using the parameters.

$$V = 40 \text{ MeV}$$

$$W = 8 \text{ MeV}$$

$$r_o = 1.2f$$

$$a = 0.5f$$

The phase is plotted against $\rho = kr$. The curves are labelled with the corresponding value of ℓ.

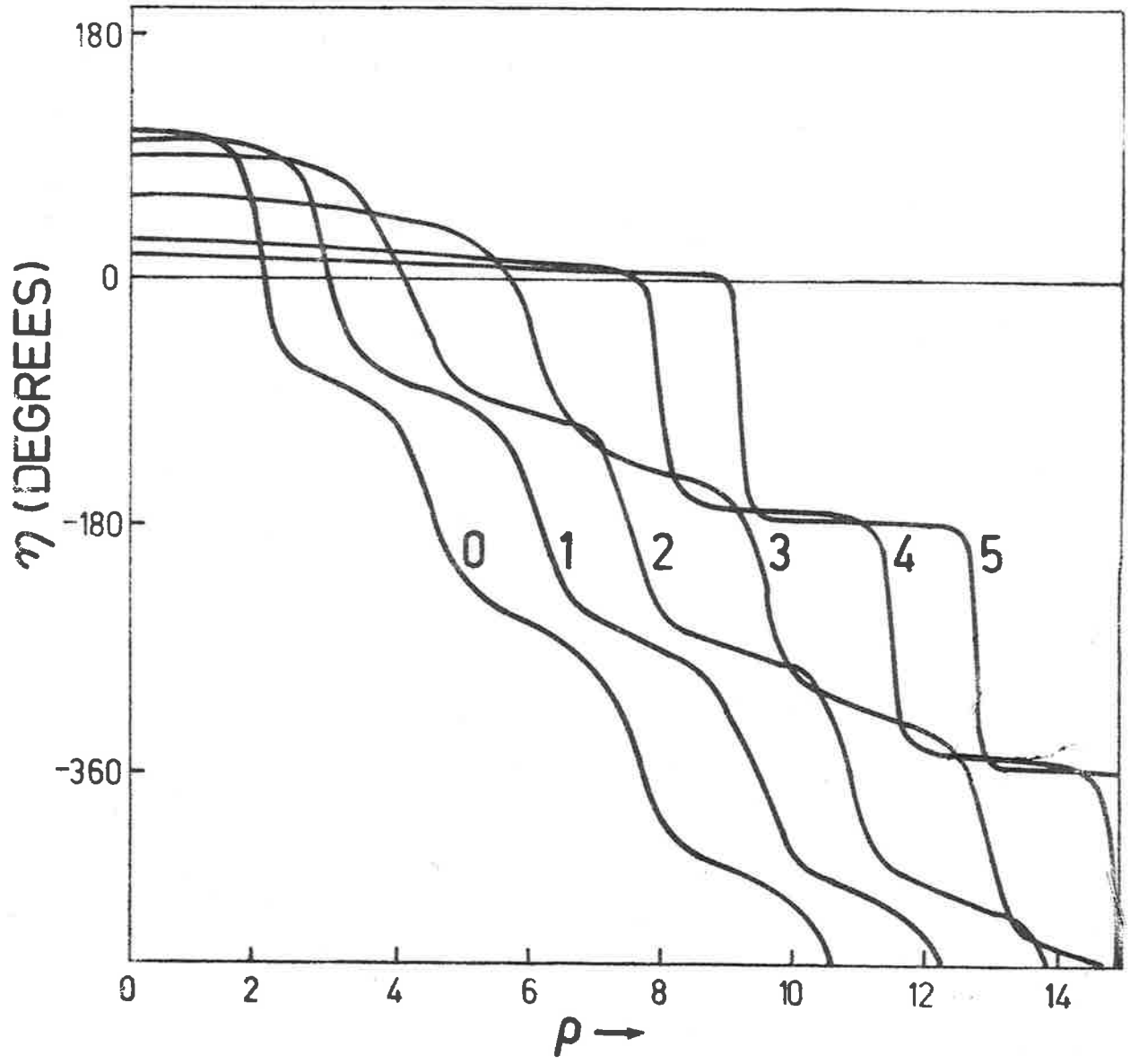
180
0
-180
-360
η (DEGREES)
0
1
2
3
4
5
0
2
4
6
8
10
12
14
ρ →

as they have influence at distances larger than the nuclear potential radius. The numerical solution of the Schroedinger equation for the partial waves, Figure 6, also shows the phase variation of the low waves that leads to the phase averaging mentioned above.

Since the nuclear interior extends to $\rho \approx 2$ (Figure 7), the phase of the partial waves can be taken as their central value, and the changes of π at the zeros of the corresponding spherical bessel functions can be ignored, since for any given value of ρ, the optical model wave function is a summation of the values of all the partial waves for that chosen value of ρ only.

Further, from the magnitude consideration, only those partial waves given by $l, l \pm 1$ where $l \approx \rho$ for any given value of ρ, are major in the evaluation of the optical model wave function as per equation (3.7). The rest of the partial waves providing contributions to the summation for the given value of ρ, which are negligible for the purpose of a qualitative discussion of interference.

Consider only the two directions $\theta = 0^{\circ}, 180^{\circ}$ measured from the direction of the incident beam and the effect of assuming -

$$\phi_{l+1} < \phi_l \qquad (3.18)$$

For $\theta = 0^\circ$, $P_\ell(0^\circ)=1$ and so from equation (3.17) the phase of a given partial wave is $\phi_\ell + \ell\pi/2$ its neighbour is $\phi_{\ell+1} + \frac{(\ell+1)\pi}{2}$ and the effect of these is as shown in Diagram 1. There is an overall reinforcement and so larger probability amplitude at $\theta = 0^\circ$ if the rule, equation (3.18) is obeyed.

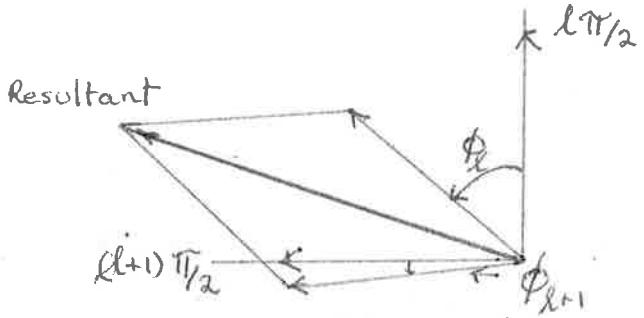

Diagram 1

For $\theta = 180^\circ$, $P_\ell(180^\circ) = (-1)^\ell$. (3.19)

Hence there is a reflection of the directions associated with all odd ℓ partial waves. This results in an overall destructive interference reducing the probability amplitude at $\theta = 180^\circ$ if the rule, equation (3.18) is obeyed (c.f. diagram 2 in which ℓ is taken even for convenience of presentation.

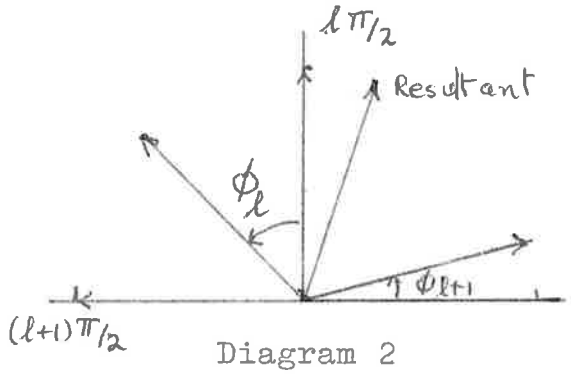

Diagram 2

For small values of ℓ, the magnitude of the partial waves Figure 8, shows that only the interior values of ϕ_ℓ are important and from Figure 7 we see that all the ϕ_ℓ involved here have small separation and the rule, equation (3.18), is satisfied. Hence, from the above description, there is slight constructive and destructive interference, at $\theta = 0$ and 180° respectively. This slight effect can be reversed by the Coulomb term.

The same argument for large ℓ values shows that all ϕ_ℓ involved, are near zero, have small separations, and, reserving the fact that the coulomb term may invert the inequality, the rule, equation (3.18) is obeyed, again implying slight effects as for the small ℓ case.

For the surface partial waves, however, the rule, equation (3.18), always holds and the difference $\phi_\ell - \phi_{\ell+1}$ is appreciable, often as much as 90°. Hence, there is a strong constructive interference at $\theta = 0^\circ$ and a strong destructive interference at $\theta = 180^\circ$. This means a large probability amplitude results in the wave function along the $\theta = 0^\circ$ line and this is the focus discovered by McCarthy et al from their flux and classical ray calculations. The strong destructive interference at $\theta = 180^\circ$ means that the probability amplitude along the collision surface is due only to the other partial

FIGURE 7

The phases of the first few partial waves for the scattering of 30MeV neutrons from C^{12}. The parameters are given in Figure 6 .

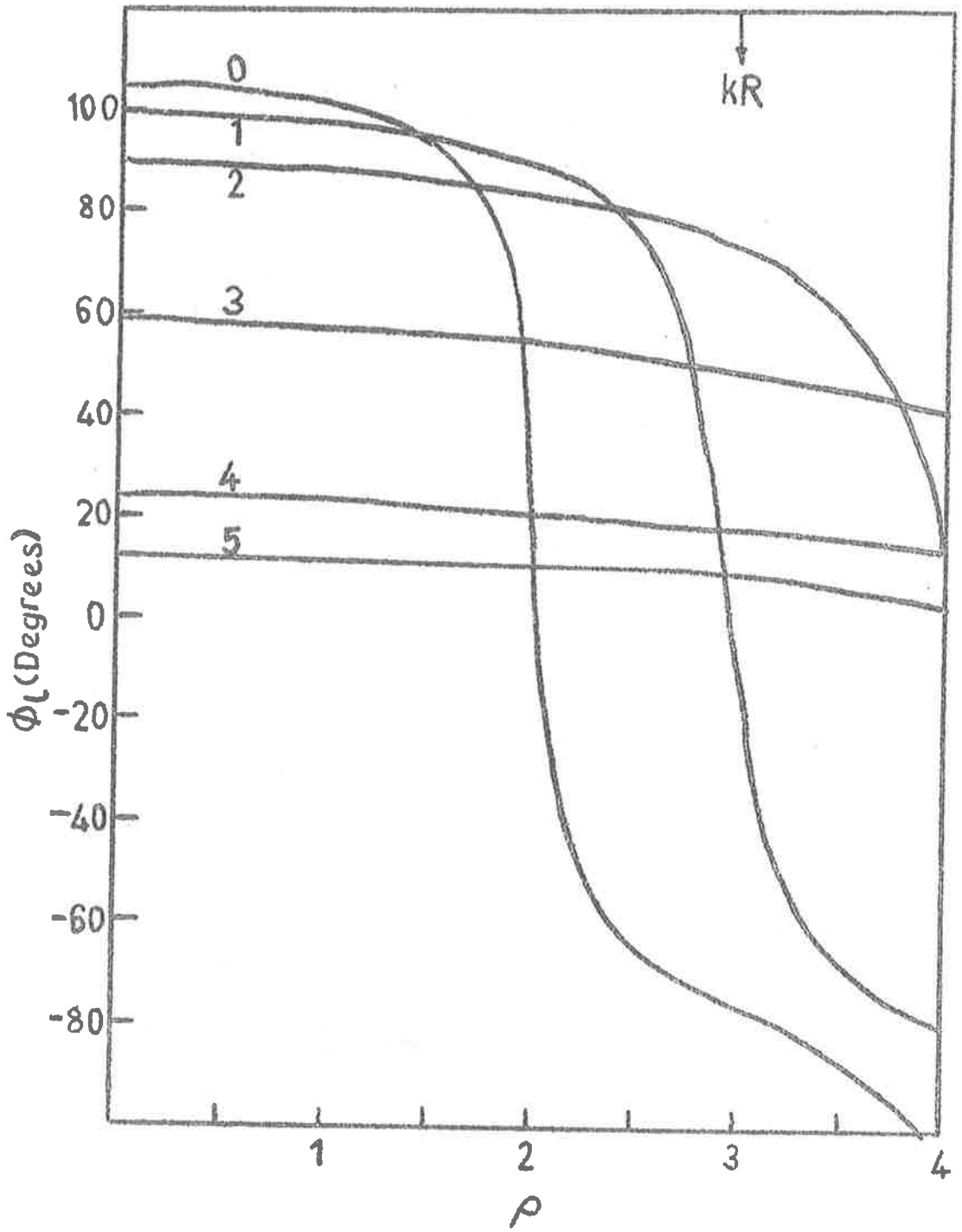
kR
0
1
2
3
4
5
100
80
60
40
20
0
-20
-40
-60
-80
ϕ_l (Degrees)
1
2
3
4
ρ

FIGURE 8

The magnitudes of the first few partial waves for the scattering of 30 MeV neutrons from C^{12}. R is the Saxon Well Radius. The parameters are those given in Figure 6 .

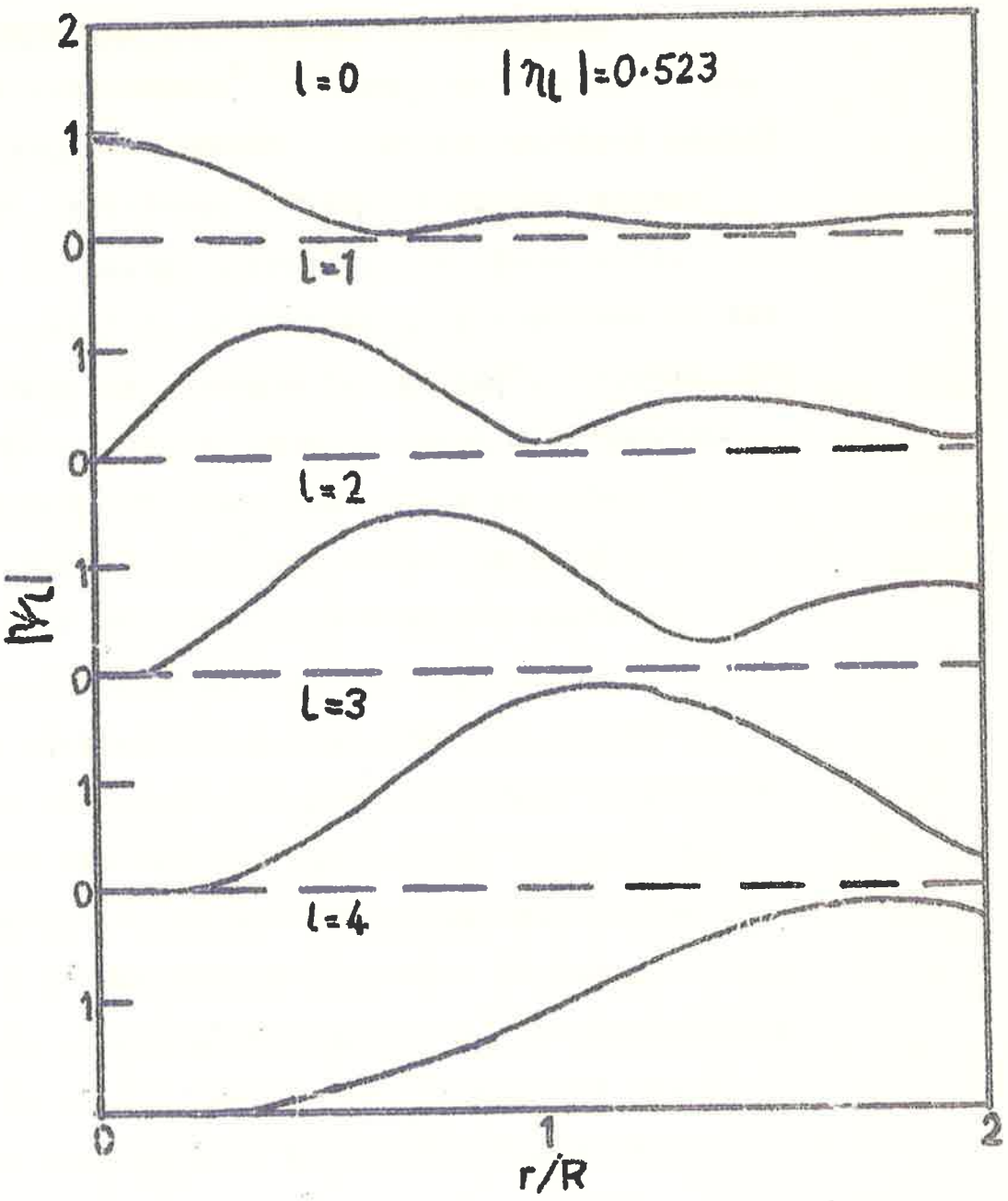
l=0
|η_l|=0.523
l=1
l=2
l=3
l=4
|η_l|
r/R
0
1
2

waves. When attenuation is considered it is therefore not surprising that ratio of the focus to front surface value of probability amplitude is 3 to 1, or less.

(b) Phase Averaging and Angular Distributions

Previous discussions*[18,21] use, as a general rule, the following statement. "For low incident energy < 10 MeV, the focus is located inside nuclear matter. As energy increases, the focus moves outwards until it is located in the surface of the nucleus and its strength is reduced". However, the numerical solutions, some of which are reported in section (3.2), show that while in principle this is correct, viz, the radial location and strength of the focus increases and decreases respectively with energy, the magnitudes of the changes that one visualizes from the statement above do not occur. It has been seen, in Section 3.2, that the foci for the 5-10MeV energy range are spread, and in fact an appreciable amount of them lie in the nuclear surface. Furthermore, for the light nuclei to be considered, the probability amplitude in the nuclear interior is not small and this results from the low ℓ value partial waves. Hence for these cases, the overlap integrals of the form shown below for any ℓ values are not small in magnitude, and if one set is to

predominate, an effect other than magnitude overlap must be present. This effect is phase averaging. Under the conditions stated in Chapter 2 for section 2.4, the differential cross-section for a direct reaction process with zero range interaction has the form -

$$\frac{d\sigma(\theta_{sc})}{d\Omega} = \frac{k'}{k}\left(\frac{\mu}{2\pi\hbar^2}\right)^2 \frac{1}{2j+1} \sum_{m_j} \left| \mathcal{M}(m_j, \theta_{sc}) \right|^2 \qquad (3.20)$$

where μ is the reduced mass of the incident particle, all other quantities as previously defined, and $\mathcal{M}(m_j, \theta_{sc})$ as given by equation (2.47). In this expression for the matrix element, overlap integrals of the following form are involved -

$$I_{l l'} = \int r^2 dr \, f_{l'}(k'r) R_{n l' p'}(r) f_l(kr) R_{n l p}(r) V(r) \qquad (3.21)$$

where $V(r)$ is the radial density factor to be associated with the interaction. In this thesis this is taken to be either a constant or a single step function. For the discussion of this section we will consider it to have a constant value of one.

The phase properties of the optical model partial wave functions as illustrated in Figures 6, 7 and 8 for 30 MeV protons on C^{13}, exhibit the phase averaging form for the interior partial waves. Thus the product of two partial wave functions of

low angular momenta l,l' not only will exhibit oscillations in magnitude, but also have a phase that falls smoothly and quickly with radius. Consequently, any integrals involving the low angular momenta should give little contribution to the matrix element because these integrals, by phase averaging, should be small. As these partial waves have their predominant magnitude within the nuclear volume, this can be interpreted as a small reaction contribution from the nuclear interior. For heavy particles, such as α -particles this is the case, and surface reaction theories give good results, even though the magnitude of the α -particle wave function is not small inside the target nucleus. However, while phase averaging always gives a reduction of the contribution from the nuclear interior, this reduction is not particularly large in the case of nucleons in the entrance and exit channels. This is illustrated in Figure 9, where the $I_{ll'}$ for the reaction 60MeV protons on F^{19} to the first excited level, are plotted against l for the particular quantum numbers L=1, M=0, $m_j=\frac{1}{2}$, and are compared with coulomb excitation values.

While phase averaging effects are not especially large for the nuclear interior, the distortion of the wave functions of the unbound particles associated with the optical model creates phase

FIGURE 9

The overlap integrals $I_{\frac{1}{2}}01,\ell\ell'$ and $I_{\frac{1}{2}}01,\ell'\ell$ plotted against ℓ. ℓ' has values $\ell+1$, $\ell-1$ respectively. The reaction is the inelastic scattering of 60 MeV protons from F^{19} for L = 1. The Q-value is -0.11 Mev.

Circles → case for V = 30 MeV

W = 15 MeV

r_o = 1.2f

a = 0.55f

Crosses → case of coulomb potential only, i.e.

V = W = 0.0

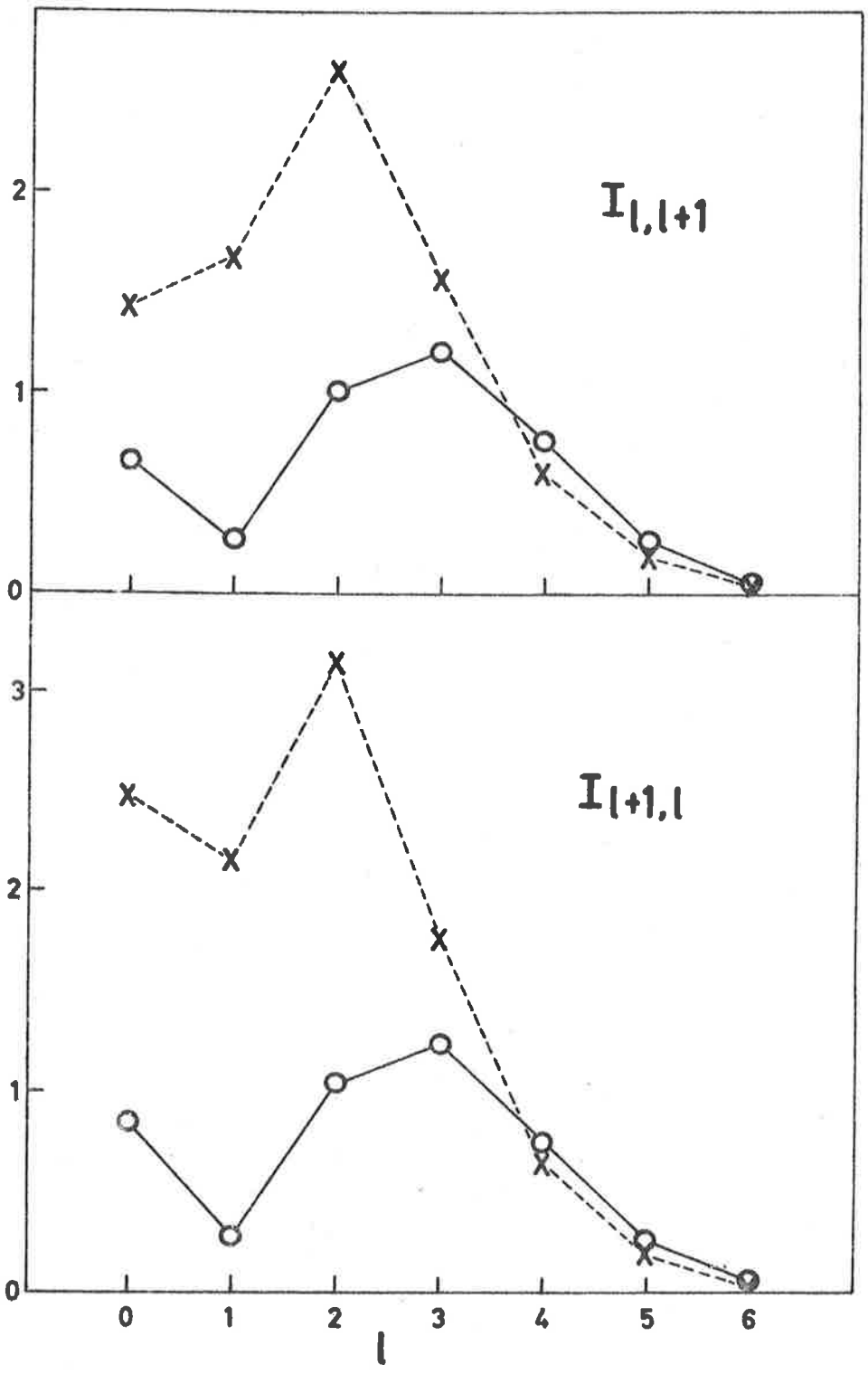
$I_{l,l+1}$
$I_{l+1,l}$
0
1
2
3
0
1
2
3
4
5
6
l

differences between the various $I_{ll'}$ and thereby cause their partial cancellation. These differences are often only important for the surface partial wave values of l,l' for, in these cases the phase differences are large and can often be of the order of 90^{o}. Hence if we consider the backward scattering angles, the large phase differences for the partial waves producing the focus term and those producing the surface term can reverse the directions for some of the $I_{ll'}$ with respect to others, and thereby produce the large backward peaks often observed in the direct reaction process. This means that for any case where the distortion effects are well localized to the nuclear surface, that is, for reasonably high incident energies in this work, any dependence of the reaction angular distribution on the nuclear interior must be due to some property of the reaction mechanism or bound state description, and not to any optical model effect.

(c) The Parity Rule

In his thesis, Glendenning found that angular distributions for some parity changing reactions had small forward values. In general, direct reactions have forward cross-sections which if not peaked are certainly not zero.

McCarthy and Kromminga[*5] were able to show how

the decrease in angular distribution in the parity changing reactions is present in the D.W.B.A. Their argument considers the matrix element in the form -

$$\mathcal{M} \propto \int d^3r\, \phi^{(+)}(\underset{\sim}{k},\underset{\sim}{r})\, \phi^{(-)*}(\underset{\sim}{k}',\underset{\sim}{r})\, \Psi(r) \qquad (3.22)$$

where the $\Psi(r)$ contains the description of the initial and final bound states and of the interaction. The two-body interaction is always even in parity whether it be of zero or finite range and so $\Psi(r)$ carries the parity of the initial and final nuclear states. In other words $\Psi(r)$ has the parity change of the nucleus.

Now for the scattering angle tending to zero, $\underset{\sim}{k} \doteq \underset{\sim}{k}'$ so that -

$$\phi^{(+)}(\underset{\sim}{k},\underset{\sim}{r}) \simeq \phi^{(-)*}(\underset{\sim}{k}',\underset{\sim}{r}) \qquad (3.23)$$

Hence the product $\phi^{(+)}(\underset{\sim}{k},\underset{\sim}{r})\, \phi^{(-)*}(\underset{\sim}{k}',\underset{\sim}{r})$ is even in parity at this angle and so for the parity changing reactions, the matrix element tends to zero as θ_{3c} tends to zero.

Recently McCarthy*[43] by considering the partial wave expansion expression for (3.22), has been able to extend this rule to define cases where no parity change occurs. By using the partial wave expansion, he finds that for odd L transfer reactions the partial matrix elements cancel

leading to small forward cross-sections, and that the gradient of the angular distribution for small scattering angles should be positive, whereas for an even L transfer reaction just the opposite is the case.

The complexity with which terms add in the L even case forces a restriction into the argument, namely, that for any given radius only those partial waves for which $l, l' \approx kr, k'r$ respectively are considered in similar fashion to the method of Section 3.3(a). The extent to which this rule is obeyed depends critically on two factors. The first is the expression for the matrix element, for the inclusion of an exchange term may well invalidate these results. The second and more critical factor is the equivalence of the wave functions for the unbound particles. For this second factor there are three points to consider. First, how large can the scattering angle, which determines the overlap of the optical model functions, become before the parity rule can no longer be identified experimentally? Second, the similarity of the wave functions implies a small Q-value, so that the momentum transfer is small, i.e. $|k| \approx |k'|$. This imposes a limit of about 2MeV on the Q-value. Third, even when the momentum transfer is small, the description of the unbound

particles may require different potentials in the entrance and exit channels and this would certainly be the case if the reaction changed the structure of the nucleus. For instance, it may be that the ground state of F^{19} is described by $O^{16} + H^3$ and the first excited state by $N^{15} + He^4$. Another point that may influence this rule is the coulomb field effect in the case of dissimilar particles in the entrance and exit channels.

CHAPTER 4 RESULTS

This chapter has been divided into four sections. the first two sections are closely related however, and the results reported in these were found using the delta function form for the two-body interaction. Section 4.1 reports and discusses the energy variation results and is almost exclusively concerned with the $C^{13}(p,n)N^{13}$ reaction. In Section 4.2, the surface weighting postulate is shown to influence the angular distributions. Section 4.3 contains the results found using a finite range interaction of a Yukawa form with the parameter $\mu = 0.87 f^{-1}$. Finally Section 4.4 contains a discussion of the results so far obtained for the (p,p') reaction on Y^{89} to the first excited state. From spectroscopy, we believe that the simple j-j coupling shell model should be adequate and so expect the analysis of the experiments to give definite information about the reaction mechanism.

4.1 THE OPTICAL MODEL EFFECT ON EXTREME ANGLE CROSS-SECTIONS

Many direct reaction experiments exhibit large values for the cross-sections at one or both of the extreme scattering angles, 0° and 180°. This effect cannot be explained by the plane wave theory of direct reactions, which predicts small cross-sections at these scattering angles for reasonably small momentum transfers. The case of zero angular momentum transfer

is an exception but, for the conditions specified above, the backward cross-section even in this case is small.

However, it is well known that the distorted wave theory can predict large values for the extreme angle cross-sections.*16,17,18. But the D.W.B.A. can also predict small values for the extreme angle cross-sections, and one case of this is in parity changing reactions for forward cross-sections, as discussed in the previous chapter. McCarthy and Kromminga*6 found this to be a general feature of this class of reactions provided certain conditions were satisfied. Hintz et al*39 confirmed this parity rule for a (p,p') reaction exciting a known 3-level in Ni^{58} and Ni^{60} Figures 16 and 17 in the next Section verify the parity rule for a two-body collision reaction mechanism.

As mentioned before, the F^{19} experiment needs a good energy resolution apparatus, hence the energy variation of the forward cross-section should allow a study of the statistical fluctuations and resonances without contamination from the direct reaction. Also since the normalization procedure of Dodd & McCarthy*4 requires poor resolution, we can average the experimental results over energy thereby meeting their conditions.

Figures 16 to 21 in the next Section show that a finite Q-value does not invalidate this rule. Of course, all Q-values reported here are fairly small, so that the limiting value for preservation of the

parity rule is not yet known. However, more important is the fact that the rule seems evident for angles up to about 15^{o}. The F^{19} experiment may be most evident as the ratio of the values of the cross-sections at 5^{o} and at the first peak is of the order of 1 to 50.

Nevertheless, there is no reason why the potentials of the entrance and exit channels should be the same. Figure 22 also in the next Section shows that if the potentials of the channels differ by 10 MeV at low energies, the parity rule does not suppress the forward cross-section, although the derivative still has the right sign. In fact the sufficient condition for the parity rule to be effect is that the entrance and exit channel wave functions are similar in configuration space. Further, this discussion involves only a contact interaction, and the inclusion of a more realistic two-body force with an exchange character, into the reaction may well affect the parity rule. The effect of a finite range force is indicated in Section 4.3. The extension of the code reported in the Appendix to include an exchange character in the two-body force is being undertaken at present. We have seen that the extreme angle peaks observed in the D.W.B.A. arise from -

(a) the overlap of the two foci and the two surfaces in the entrance and exit channel wave functions for the backward scattering, and

(b) the overlap of the focus in one wave function with the surface term of the other in the case of 0^{o} scattering angle.

Except when specifically stated, what follows will be related to the backward cross-section values as the forward cross-section behaves in a similar way for non-parity changing reactions.

The backward cross-section value is the result of the phase relationship between two essentially distinct regions, the focal and surface overlap terms in the matrix elements. It is the interference between these regions that leads to the energy variation of the backward peak values. Because of the division of the reaction region into two contributing parts, the energy variation of the extreme angle peaks depends on the optical model properties. One such property is the positions of the foci. These are determined by the energyof the unbound particle and the real parts of the optical model potentials, and are important in determining the position of the peak in the energy variation and, to a lesser extent, the relative magnitudes of the values of the extreme angle cross-sections for different energies. This relative magnitude is more sensitive, though, to the energy variation of the imaginary parts of the optical model potentials, and hence absorption, because of the intensity of the focus in an optical model wave function is reduced with larger W.

Besides these optical model properties, the bound state description will influence the energy variation. To show this, one must recall that, for low energies or large V, the focus is centred inside the nucleus, and as energy increases or V decreases, it is centred further out in the nucleus, eventually being mainly contained in the nuclear surface region. So, as energy increases, it is possible that the centre of the focal term will move through the value of the radius of the peak in the bound state product description, and so the magnitude of overlap, and hence of the integrand, in the matrix element for the reaction, exhibits a peak in the range of incident energies considered. The position of this peak in energy is dependent on the radial description of the bound state.

For the $C^{13}(p,n)N^{13}$ reaction the initial and final bound states are described by the same 1p Harmonic Oscillator function and so their product exhibits one peak in configuration space. Hence, using focal language, a peak in the energy variation will occur when the focal region in the product of the optical model wave functions moves through the maximum in the bound state product. A double peak in the energy variation could result if the two foci involved in the focal region only overlap to the extent that a double peak shape appears in the focal

region of the product of the optical model wave functions.

Pearson*[40] has studied this using a semi-classical model and has found remarkable results although the bound state radius used gives too small a value of the root-mean square radius. However, this semi-classical approach assumes that the focus is sharp, and further, that in this model the changes of phase throughout the focus and its neighbourhood are not inconsistent with this assumption.

In fact in the optical model wave function, the focus is not that sharply defined, and the phase changes throughout the region of its spread are not large as shown in Chapter 3. Hence it is not too surprising to find that the D.W.B.A. does not reproduce the sharp variations of the semi-classical treatment without inclusion of features that localize the optical model wave functions more than shown in the previous Section. It appears that this localization could only be produced by a spatial dependence of the interaction.

Figure 10 is a plot of the experimental cross-sections of Dagley et al*[21] for the reaction $C^{13}(p,n)N^{13}$ with incident energies in the range 3.5 MeV to 13 MeV. The angular distributions in the region of 5.91 MeV show small variations over a large energy spread, and so we expect this to be a direct reaction cross-section. The energy variation of the extreme

FIGURE 10

The differential cross-sections for the Reaction $C^{13}(p,n)N^{13}$ for incident energies between 3.39 MeV and 12.86 MeV.

(Reproduced from the paper by P. Dagley et al. Nucl. Phys.24,353,(1961)).

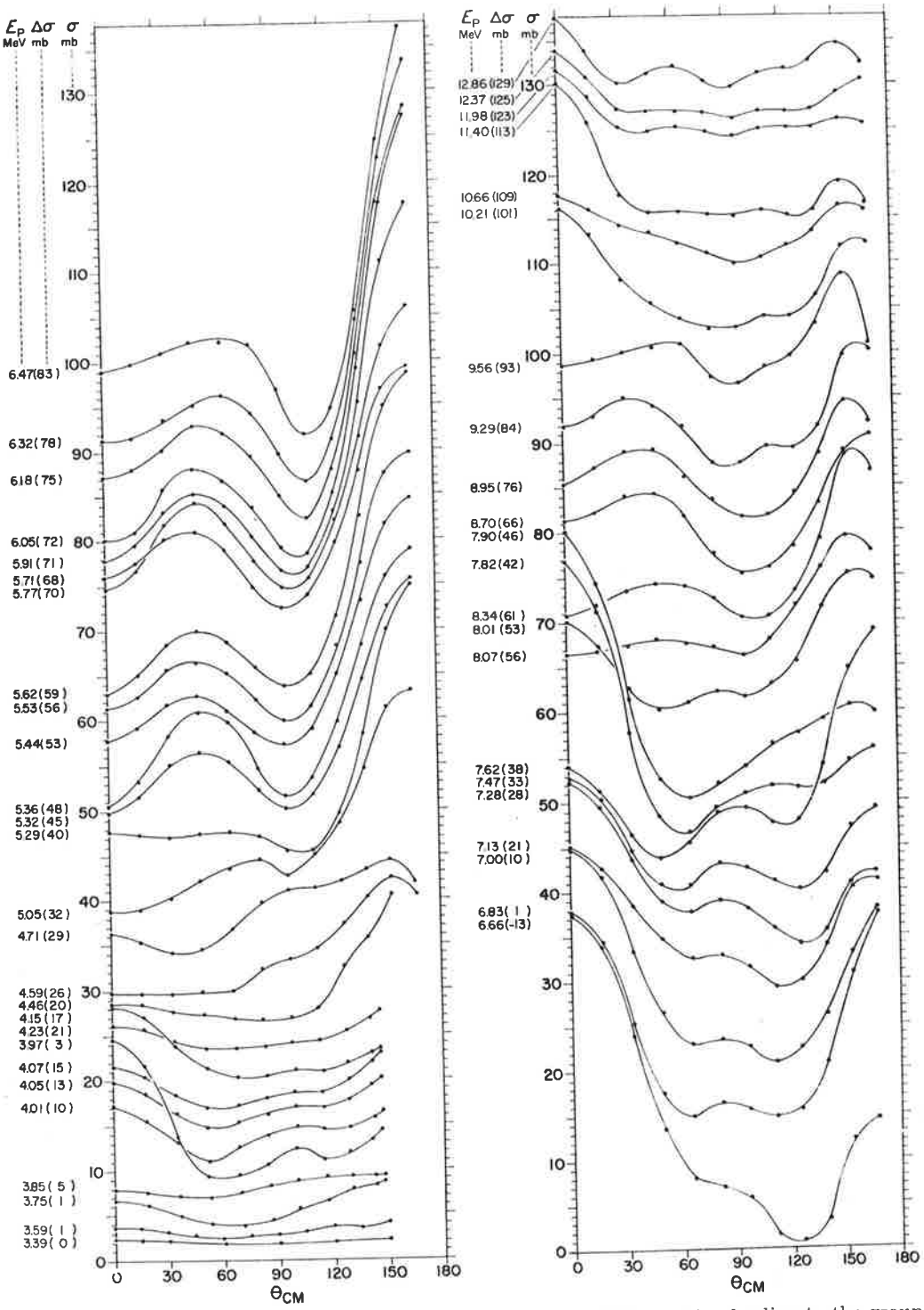

Angular distributions of the neutrons from the $C^{13}(p, n)N^{13}$ reaction leading to the ground state of N^{13}. The cross sections (per unit solid angle) and the scattering angles are given in the centre-of-mass system. The bombarding energy refers to the laboratory system. The curves are displaced vertically by an amount indicated for each curve by $\Delta\sigma$. To obtain the cross section subtract $\Delta\sigma$ from the value given by the ordinate.

FIGURE 11

The experimental values for the energy variation of the extreme angle differential cross-sections of the Reaction $C^{13}(p,n)N^{13}$.

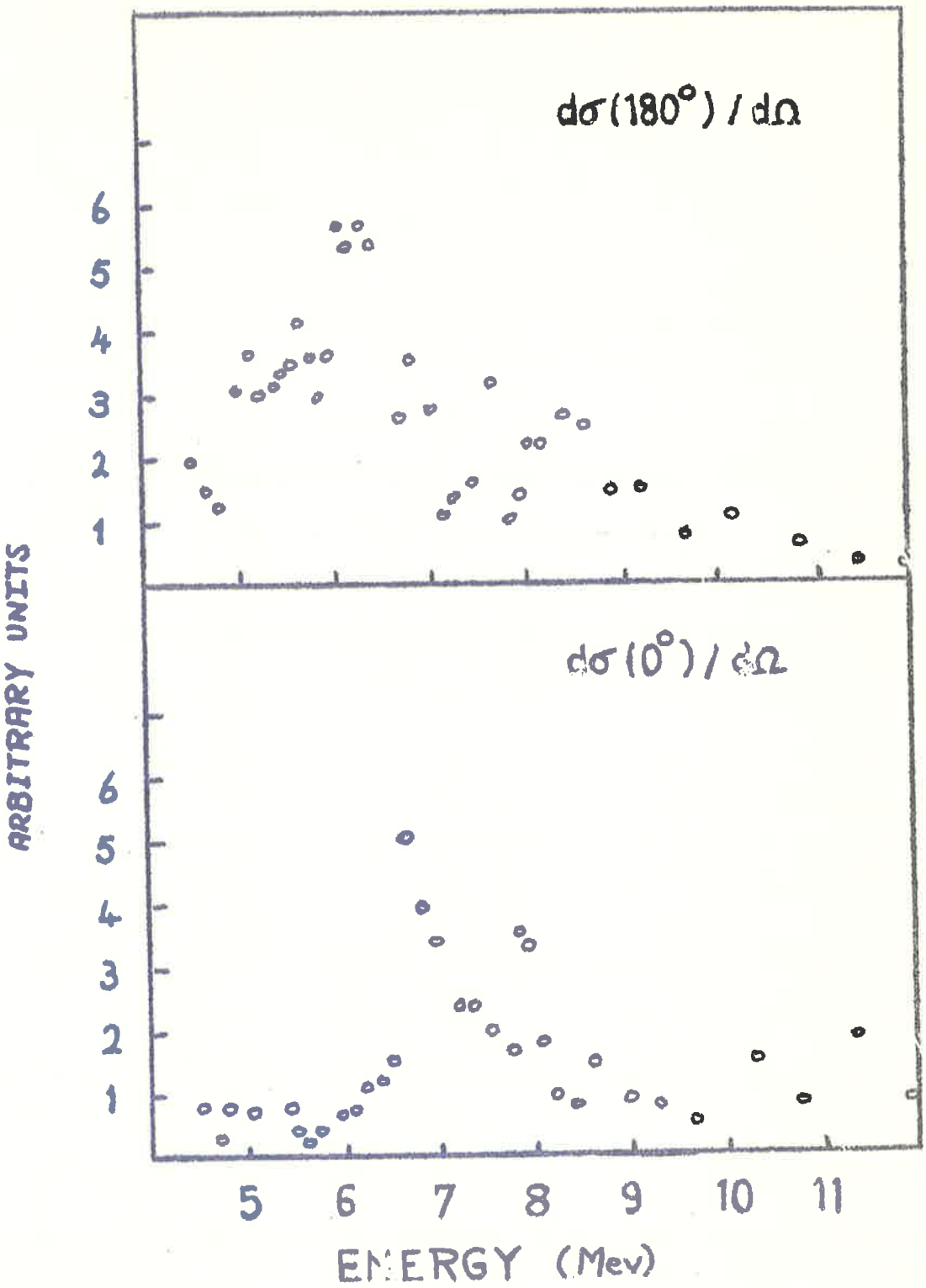
dσ(180°) / dΩ
dσ(0°) / dΩ
ARBITRARY UNITS
1
2
3
4
5
6
5
6
7
8
9
10
11
ENERGY (Mev)

angle cross-sections are shown in Figure 11. The backward cross-section energy variation shows a strong peak centred at 6MeV and possibly a second smaller peak between 8 and 9 MeV, and, although the points are widely scattered, probably due to resonance effects, the general trend of the energy variation is expected to be given by the direct reaction theory. The energy variation of the forward cross-section shows a strong peak at about 7 MeV and a tail that may be oscillatory.

The first attempts to fit the backward peak energy variation for the reaction $C^{13}(p,n)N^{13}$ are shown in Figure 12. The parameters used are the same in both entrance and exit channels. Curves A and C were calculated using V=50MeV, curve B used V=47MeV. The other parameters, W=6MeV, r_o=1.2f, a=.55f were the same for all curves. Curves A and B are volume calculations, curve C is a surface weighted calculation with R_f, the weighting radius, 2.2f and weight F=1/16. The bound states were 1P Harmonic Oscillator wave functions with radius R_b=2.3 for curves A and B and R_b=2.2 for curve C. These radii give too small a root mean square radius, but the results are sufficient to show the general features needed here. The centre weight value for curve C is the case where the surface and volume parts of the integrand contribute with the same order of magnitude.

FIGURE 12

The energy variation of the backward scattering differential cross-section for the $C^{13}(p,n)N^{13}$ calculation using a zero-range two-body force.

CURVE A	CURVE B	CURVE C
V = 50MeV	V = 47 MeV	V = 50 MeV
W = 6MeV	W = 6 MeV	W = 6 MeV
r_o= 1.2f	r_o= 1.2f	r_o= 1.2f
a = 0.55f	a = 0.55f	a = 0.55f
R_b= 2.3f	R_b = 2.3f	R_b= 2.2f
R_f= 2.3f	R_f= 2.3f	R_f= 2.2f
f = 1.0	f = 1.0	f = 0.0625

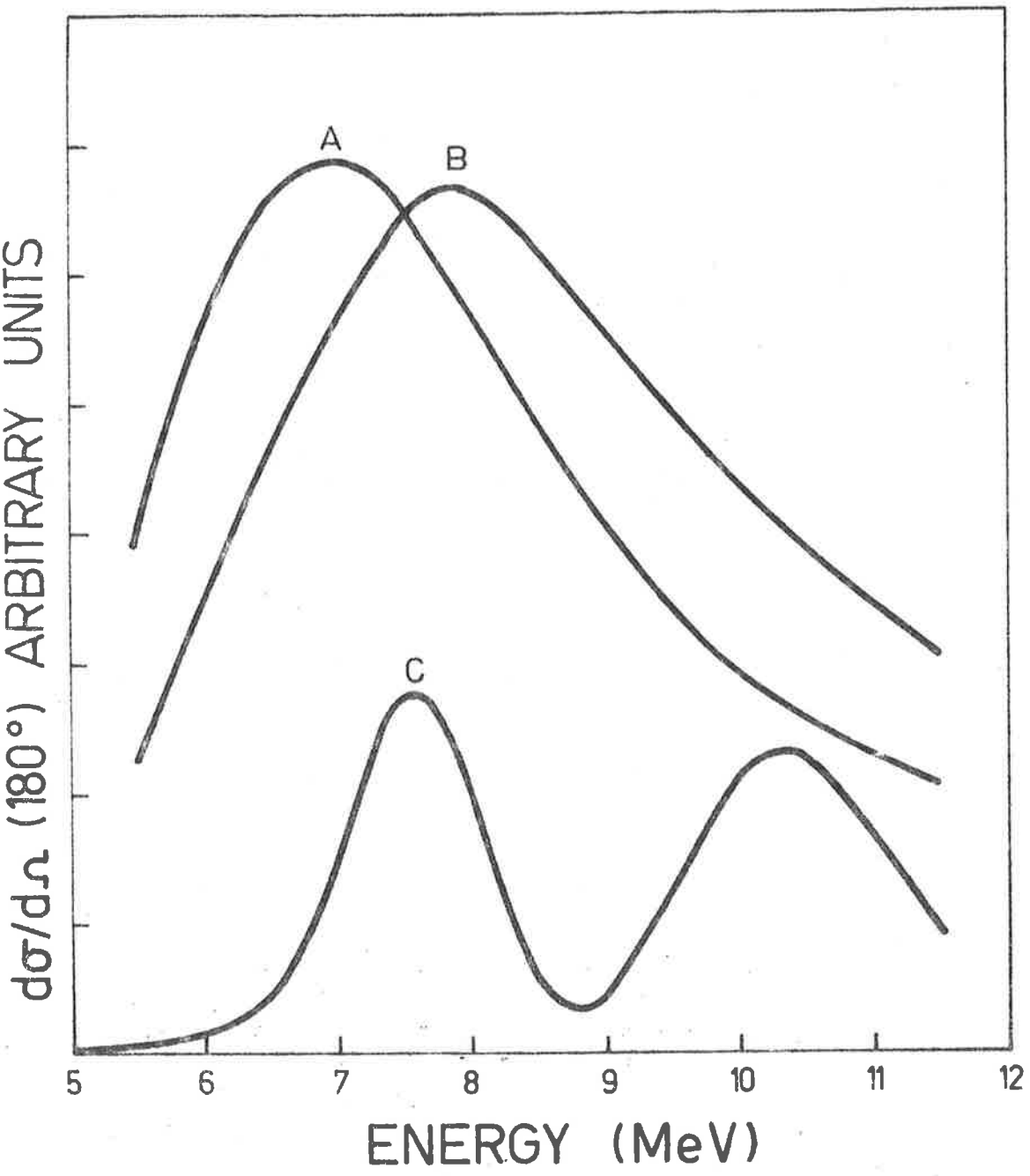
A
B
C
dσ/dΩ (180°) ARBITRARY UNITS
5
6
7
8
9
10
11
12
ENERGY (MeV)

The relative position of curves A and B is contrary to that expected from the fact that the foci are centred further out in the nucleus for lower values of V. However, many factors complicate the situation and it is not surprising to find the relative position of curves A and B as shown. First, the relative phases of the surface and focal terms change with V and energy. Secondly, the entrance and exit channels will not have identical foci, partially due to the coulomb potential, but in the main because the Q value is fairly large (-3.005MeV). Hence, the unbound particles have different energies. Thirdly, (and perhaps to some extent combining the first two factors), the energy variation of the optical model potentials has not been included. An energy plot of the parameters used by many authors to fit elastic scattering of nucleons was made, and calculations of the angular distributions for incident energies from 4.5MeV to 11.5 MeV in 1MeV steps are reported in Figure 13, with the parameters V and W varying with energy. These parameters are given in Table 1. A more realistic bound state radius has been used here, and a single peak again results in the energy variation of the backward scattering cross-section. Figure 13 contains two graphs, the top graph reports values of r_o=1.2, the bottom graph for r_o=1.25. Comparison of these two graphs in conjunction with the data of Table 1, shows

TABLE 1

THE PARAMETERS USED IN FIGURE 13, THE VARIATION OF $\sigma(180^{\circ})$ WITH ENERGY FOR THE REACTION $C^{13}(p,n)N^{13}$ (PRIMES REPRESENT FINAL STATE QUANTITIES)

	$a = a' = .65f$		$r_o = 1.2f$	$R_b = 4.3f$
E(MeV)	V(MeV)	W(MeV)	V′(MeV)	W′(MeV)
4.5	64.3	5.5	54.1	0.6
5.5	63.5	6.5	52.9	2.0
6.5	62.8	7.2	51.9	3.4
7.5	62.0	7.7	50.8	5.0
8.5	61.2	8.1	49.8	6.0
9.5	60.5	8.3	49.1	6.9
10.5	59.7	8.5	48.4	7.5
11.5	58.7	8.7	47.8	7.9

FIGURE 13

The Energy Variation of the backward scattering cross-sections for variation of potential and radius.
Parameters are as given in Table 1.
The continuous lines show the results using the above parameters. The broken lines use values of V,V' 2MeV larger than in the table. The dotted lines use values of V,V' 4MeV larger than in the table.

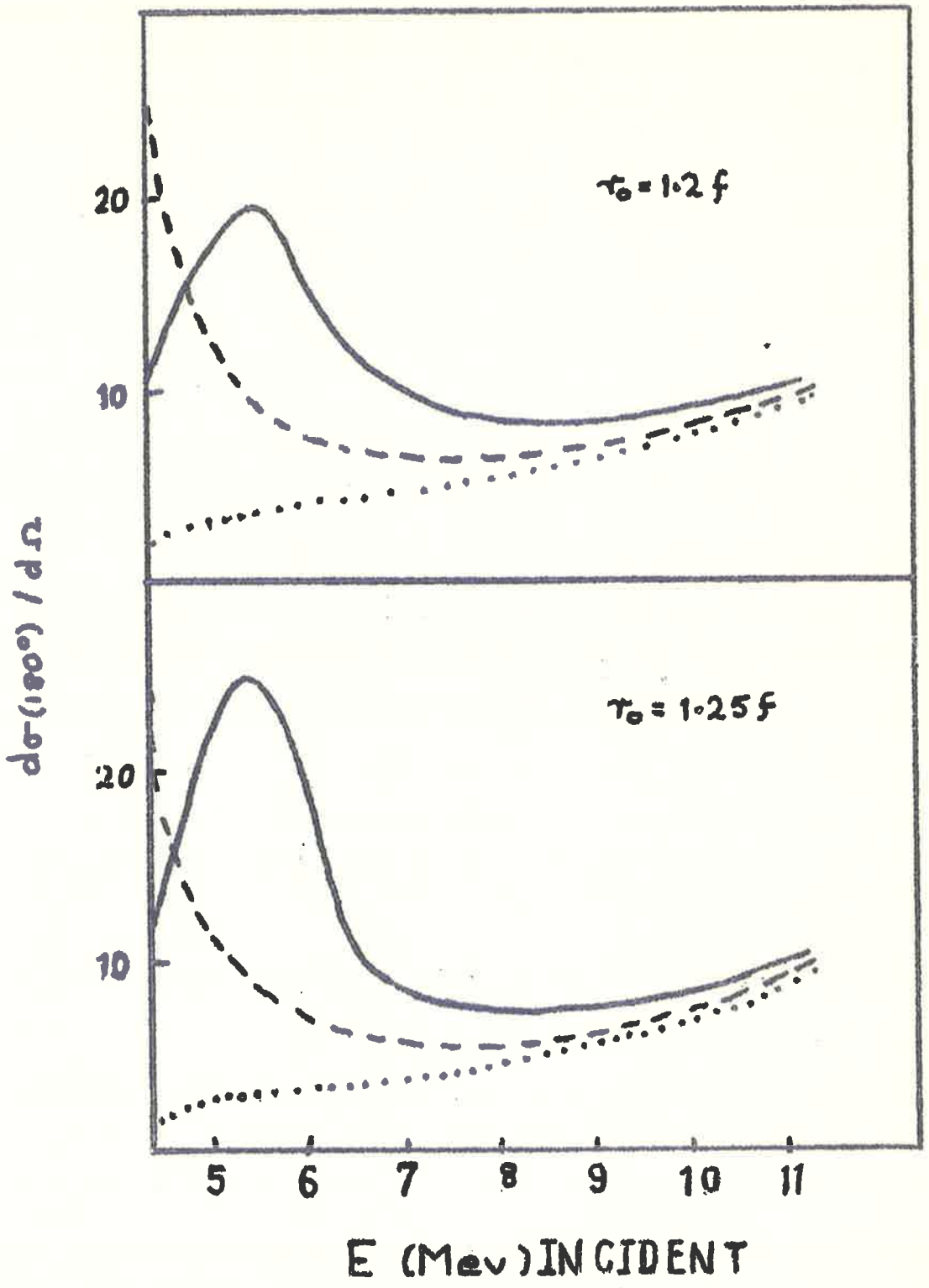
$r_0 = 1.2$ f
$r_0 = 1.25$ f
20
10
20
10
5
6
7
8
9
10
11
E (Mev) INCIDENT
dσ/dΩ (180°)

very clearly the Vr^n ambiguity, where $n \approx 2$.

The most striking feature of these results is the quite sensitive variation with potential V. Further, while the volume calculations can reproduce the general shape of the energy variation of the extreme angle peaks, no vestige of a second peak can be found. Of course the second peak must be a direct reaction feature for the above to hold. It is felt that this is so in view of the semiclassical results of Pearson*[40]. Further, it is known that the imaginary potentials, W, vary with energy. If this variation is faster than that used in Table 1, the values of the backward cross-sections decrease more rapidly with energy than shown in Figure 13. This can be understood since the foci for the higher incident energies then have a much smaller amplitude than those used in the calculations of Figure 13.

However, as the energy variation of the optical model potentials should at least be monotonic, the appearance of the second peak in the energy variation indicates that a reaction property weighting the surface region is required. The curve C of Figure 12 shows that surface weighting does in fact produce a second peak.

Hence the parameters V,V′ primarily determine the positions of the major peak in the energy data; their difference may possibly affect the relative positions

of the two peaks; W and W′ determine the relative size of the cross-sections for different energies, and weighting the interaction region determines the shape of the energy variation.

It can be seen in Figure 10 that there is a 2 to 3 MeV energy range centred about 5.91 MeV for which the angular distributions all have approximately the same shape. Hence, as stated before, we expect that this shape is a direct reaction result, and so the parameters giving best fit to the energy variation of the backward cross-section should give this angular distribution. Using the volume interaction form, no semblance of a fit was found. In fact no fit was found for the parameters listed in Table 2, all curves exhibiting W shape whereas the experiment has a N shape. The calculation using V=67MeV and V=59MeV was least divergent from the experiment, and this calculation was repeated using W=5MeV. Little change in shape results.

Calculations using 1P Harmonic Oscillator wave functions with a characteristic radius R_b=4.3f also gave W-shaped angular distributions for all incident energies between 4.5MeV and 11.5MeV inclusive. These calculations used the parameters listed in Table 3. The values of V and V′ were increased by 2MeV and 4MeV for each energy and although significant changes in normalization were found for the lower energy

TABLE 2

PARAMETERS USED IN THE ANALYSIS OF THE 5.91MeV REACTION $C^{13}(p,n)N^{13}$ USING A VOLUME INTERACTION. (PRIMES DENOTE FINAL STATE QUANTITIES)

V values ranged from 52MeV to 67MeV in 1MeV steps

V' values ranged from 46MeV to 59MeV in 1MeV steps

W = 6.83MeV W' =3.68MeV $a = a' = .65f$

$r_o = 1.25f$

1P square well wave functions were also used to describe the bound states, and were calculated using the following parameters -

V_B = Square well depth = 38.4MeV

E_B = Binding Energy = 16MeV

R_o = Radius of Well = 3.5f

TABLE 3

PARAMETERS USED IN THE VOLUME CALCULATIONS FOR INCIDENT ENERGIES BETWEEN 4.5MeV AND 11.5MeV. (PRIMES DENOTE FINAL STATE QUANTITIES).

E(MeV)	V(MeV)	V′(MeV)	W(MeV)	W′(MeV)
4.5	59.3	49.9	5.5	0.6
5.5	58.5	48.8	6.5	2.0
6.5	57.9	47.7	7.2	3.4
7.5	57.1	46.8	7.7	5.0
8.5	56.4	45.9	8.1	6.0
9.5	55.8	45.3	8.3	6.9
10.5	55.0	44.6	8.5	7.5
11.5	54.1	44.1	8.7	7.9

$r_o = 1.25f$ $\quad a = a' = .65f$ $\quad R_b = 4.3f$

results, little variation in shape and normalization was found above an incident energy of 6MeV.

The calculations were also performed using r_o=1.2f, 1.3f and 1.35f adjusting the potentials in Table 3 by the Vr^2=constant law. It was found that, except for the lowest incident energy, no significant changes in shape occurred. This was also the case for angular distributions with r_o=1.35f and with the optical model potentials larger and more rapidly changing with energy. Finally calculations with a smaller bound state radius, R_b=2.3f, were found to be slightly better in some cases for incident energies below 6MeV. In all, 285 angular distributions were calculated with the volume interaction form without fitting either the energy variation of the extreme angle cross-sections or the experimental angular distributions.

Figure 14 shows the angular distributions for incident energies between 4.5MeV and 11.5MeV using the surface weighting mechanism and parameters of Figure 12. Although these calculations are still not very good fits to the experimental results, the angular distributions in the 5MeV to 6MeV incident energy region are more appropriate than the volume calculations, and the energy variation of the backward scattering cross-section contains two peaks.

The obvious calculations to perform are surface weighted calculations using a more realistic set of

FIGURE 14

The calculated differential cross-sections for the $C^{13}(p,n)N^{13}$ reaction with energy variation and a surface weighting assumption. The parameters are those as for Figure 12, Curve C.

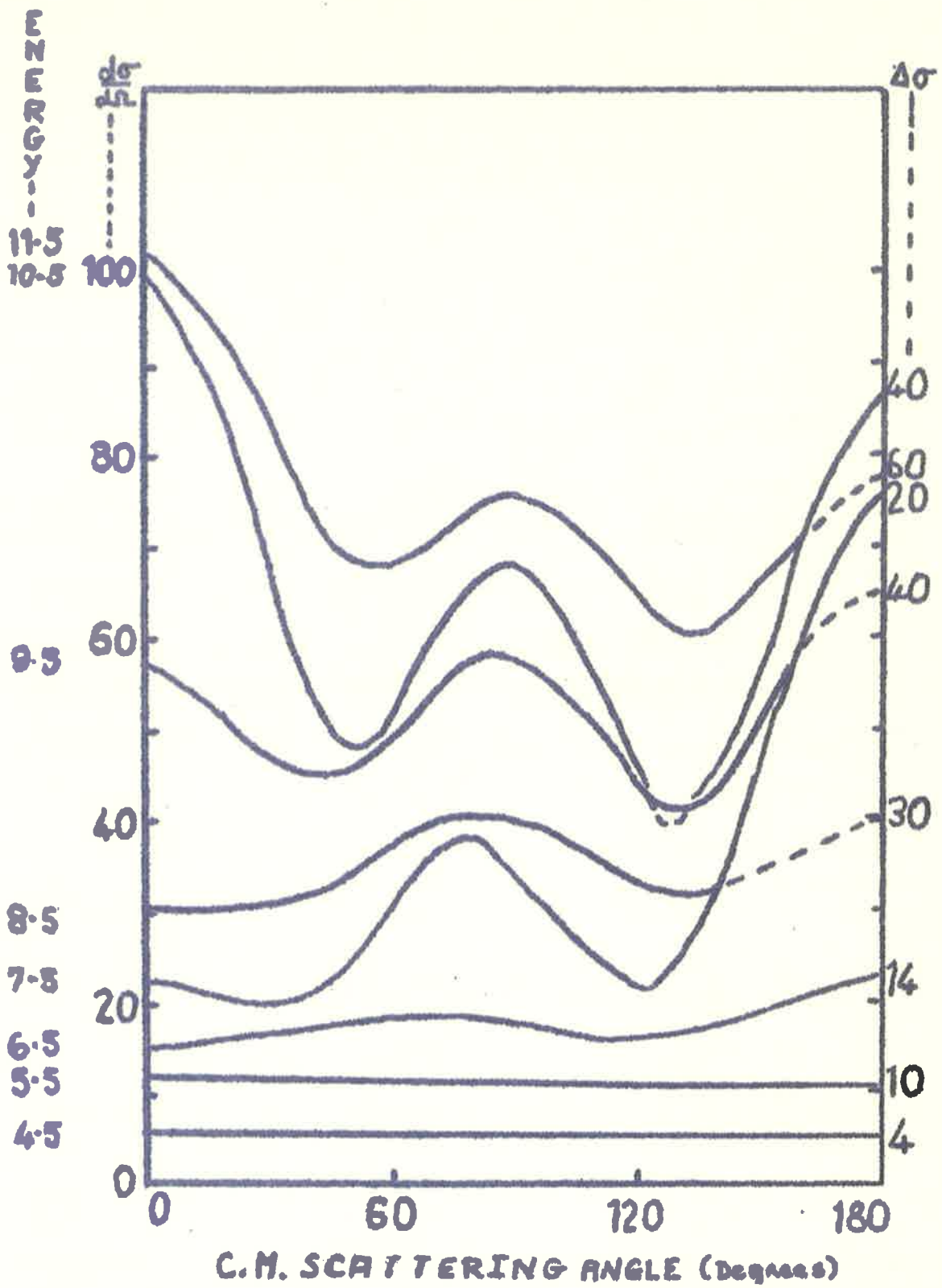
ENERGY
11·5
10·5
9·5
8·5
7·5
6·5
5·5
4·5
dσ/dΩ
100
80
60
40
20
0
Δσ
40
60
20
40
30
14
10
4
0
60
120
180
C.M. SCATTERING ANGLE (Degrees)

parameters. This has not yet been done for the following reasons. First, the results reported above indicate that a surface weighted formalism is necessary. Since spin orbit potentials should give some surface weighting effects, these must be included. This is strengthened by the fact that the peaks in the energy variation of the extreme angle cross-sections are very sensitive to the central potentials. Second, the calculations of Agodi et al[*22,23] have shown that the angular distributions for the $Si^{28}(n,p)Al^{28}$ reaction are strongly affected by the exchange character of a realistic two-body interaction. In particular, the extreme angle cross-sections are most affected. Consequently the extension of the analysis mentioned before has been suspended in favour of one using a more realistic finite range two-body force with exchange, and, if the computing facilities and economics permit with the code adjusted to include spin-orbit potentials in the optical model wave function calculation.

Nevertheless, the surface weighting calculations show large deviations from the volume interaction calculations. The corrections due to the above two points may not be able to account for these deviations. The discussion of this effect is reported in the next section.

Finally, in this section the effect of the foci in producing forward peaks for cases where L is even, and

non-zero, is shown in Figure 15. This figure shows the results of volume interaction (continuous lines) and surface weighted (broken lines) calculations for the inelastic scattering of 10MeV (left diagram) and 20MeV (right diagram) proton on F^{19} for the case where the nucleus is left in its second excited state with a Q value of -.22MeV. The angular momentum transfer quantum number in this reaction is 2 and the parameters used were those of table 4 for the L=1 reaction. The curves are arbitrarily normalized, and in this case only the shapes are significant. The weighting parameters used were f=0 $R_f=R_N$, where R_N is the Saxon well radius.

In the 10MeV case, the surface result has more structure than in the volume case, and has small forward cross-section, whereas the forward cross-section is peaked in the volume case. This can be understood from the fact that the foci are centred more in the nuclear interior, and the phase of the internal contributing regions results in constructive interference. In the 20MeV case, the two calculations exhibit extreme angle peaking with the same amplitude ratios of forward to backward peaks. However, this may be just coincidental for this energy.

FIGURE 15

Angular Distributions of 10MeV (left) and 20MeV (right) protons in the reaction $F^{19}(p,p')F^{19*}$ to the second excited level with a Q-value of 0.2MeV. This is an L=2 reaction.

Parameters are given in Table 4.

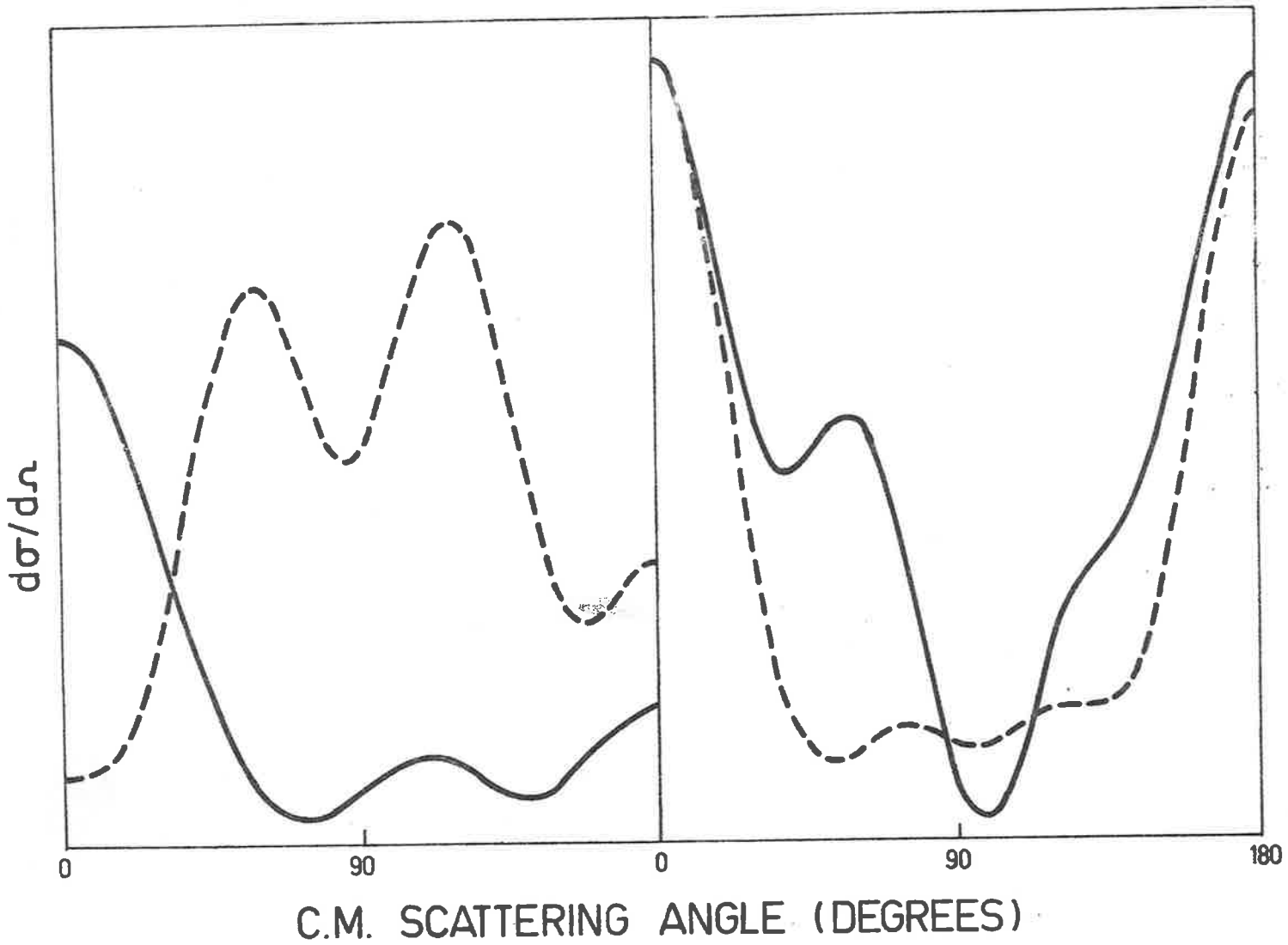
dσ/dΩ
0
90
0
90
180
C.M. SCATTERING ANGLE (DEGREES)

4.2 THE REACTION MECHANISM AND THE NUCLEAR INTERIOR

In the preceding section and in Chapter 3, the optical model effects on angular distributions were discussed, and the effect of reasonable variations of the parameters noted. In particular the importance of the foci in extreme angle scattering was emphasized.

Hence, if the reaction mechanism is density dependent, then its effect must be more outstanding than those considered in the earlier discussions. More fully, the angular distribution for a surface weighted calculation, or one in which the contribution from the nuclear interior (defined as all $r<R_f$) is weighted by the value $f(0 \leq f \leq 1)$, must exhibit differences from the volume interaction calculation ($f=1$), and these differences must not be produced by realistic parameter variations.

Figures 16 and 17 show the results of the volume and surface ($f=o$, $R_f=R_N$) calculations for the reactions and parameters as given in Table 4. Large differences are evident. Figures 16 and 17 compare the volume (continuous line) and surface weighted (broken line) calculations for incident energies 5MeV and 10MeV respectively. The characteristics are plotted on a linear scale to emphasize their shapes, and the scales for the surface calculations have been adjusted by means of a factor of the order of 100 to facilitate

TABLE 4

THE PARAMETERS USED IN FIGURES 16 AND 17. THE ENTRANCE AND EXIT CHANNELS ARE DESCRIBED BY THE SAME SET OF PARAMETERS.

$W = 4\text{MeV} \qquad a = .55\text{f} \qquad r_o = 1.2\text{f}$

$R_b = R_N = r_o A^{1/3}\text{f}.$

Reaction	E(MeV)	V(MeV)	L	Q(MeV)
$F^{19}(p,p')F^{19*}$	5	45	1	-.11
	10	55		
$C^{13}(p,n)N^{13}$	5	55	0	-3.005
	10	55		
$I_N^{115}(p,p')I_N^{115*}$	5	45	5	-.34
$Ca^{40}(n,p)K^{40}$	5	45	3,5	-.6

FIGURE 16

Angular distributions for the reactions shown with parameters in Table 4 for 5MeV incident energy nucleons. Volume calculations are shown by the continuous line, surface by the broken line.

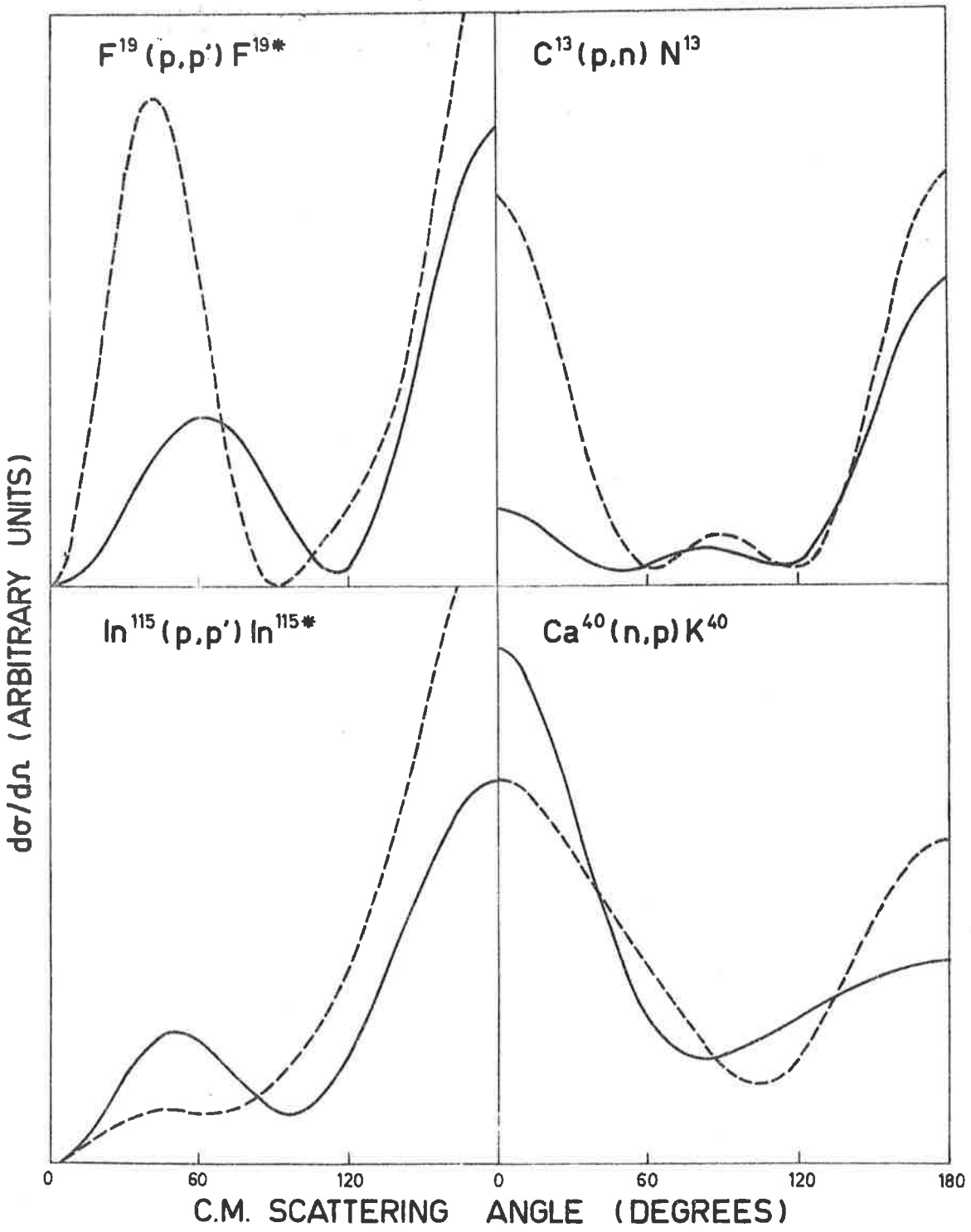
$F^{19}(p,p')F^{19*}$
$C^{13}(p,n)N^{13}$
$In^{115}(p,p')In^{115*}$
$Ca^{40}(n,p)K^{40}$
dσ/dΩ (ARBITRARY UNITS)
0
60
120
0
60
120
180
C.M. SCATTERING ANGLE (DEGREES)

FIGURE 17

Angular distributions for the reactions shown with parameters in Table 4 for 10MeV incident energy nucleons . Volume calculations are shown by the continuous line, surface by the broken line.

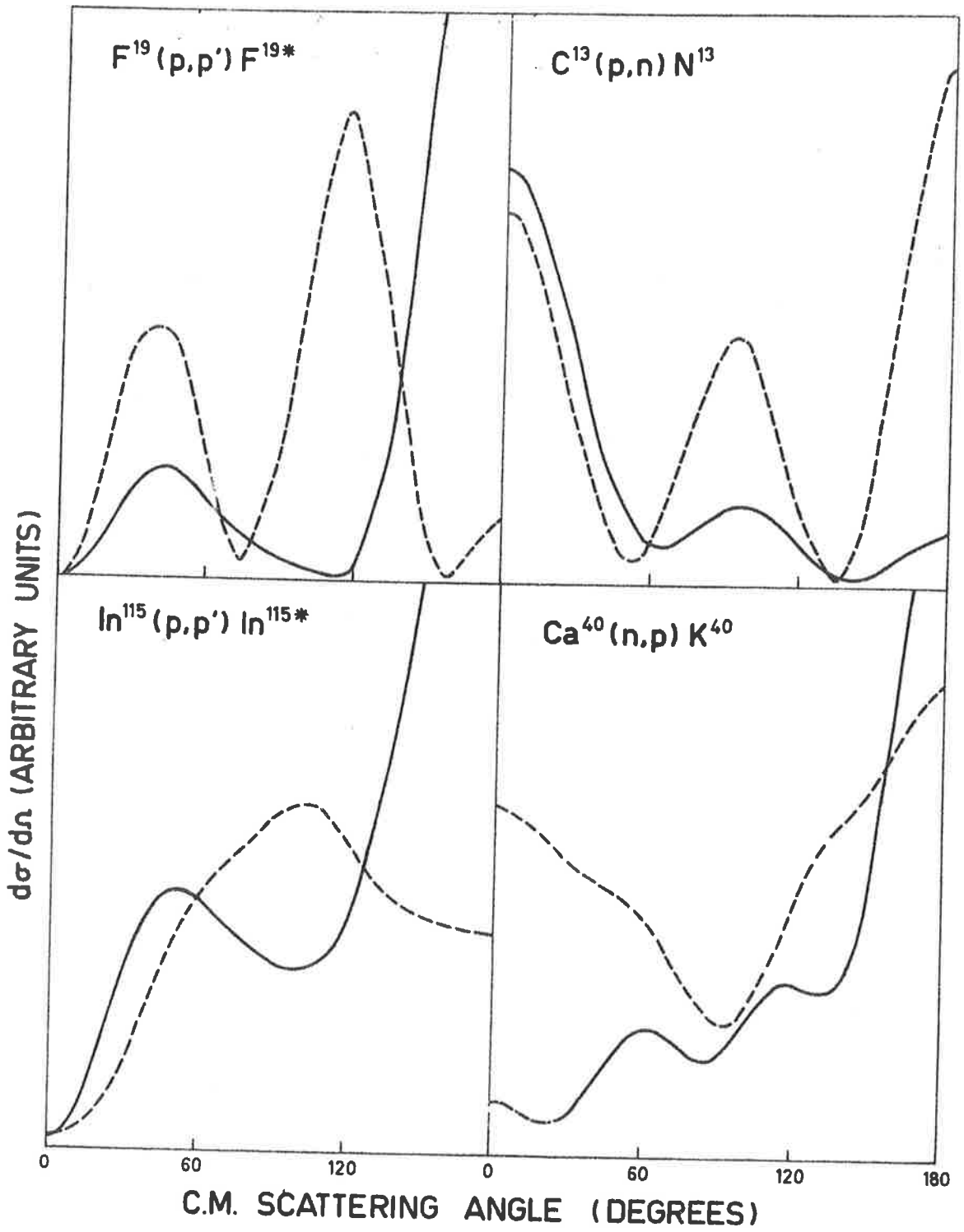
$F^{19}(p,p')F^{19*}$
$C^{13}(p,n)N^{13}$
$In^{115}(p,p')In^{115*}$
$Ca^{40}(n,p)K^{40}$
dσ/dΩ (ARBITRARY UNITS)
0
60
120
0
60
120
180
C.M. SCATTERING ANGLE (DEGREES)

comparisons. In other words, the contribution to the matrix element from the nuclear interior is about 10 times that of the nuclear surface. The 5MeV results of Figure 16 show differences between the volume and surface calculations that could possibly be explained by parameter variations, but this is not the case for the 10MeV results of Figure 17, where far greater structure exists in the surface calculations.

Disregarding the Ca^{40} results, which are complicated considerably by the allowable double angular momentum transfer, the surface calculations resemble the volume calculations, if the latter were compressed to much smaller angles, as are obtained if the average radius is increased. However, the amount of compression needed is far greater than any reasonable variation of the average radius would permit.

(a) Variation of the Optical Model Parameters

Figure 18 shows that realistic variation of the optical model potential V is unlikely to cause the change from surface to volume shape for the F^{19} reaction. This figure shows the angular distributions for the 10MeV incident energy case; volume calculation results are on the left and surface weighted (f=o, $R_f=R_N$) calculations are on the right. The continuous lines show the calculations using V=45MeV, the broken lines, V=55MeV.

FIGURE 18

Angular distributions for 10MeV proton on F^{19} leading to the first excited state. Volume calculations are on the left and surface ($R_f = R_N$, f = o) are on the right. The continuous lines are the results for V = 45MeV and the broken lines are those for V = 55MeV. All other parameters are given in Table 4.

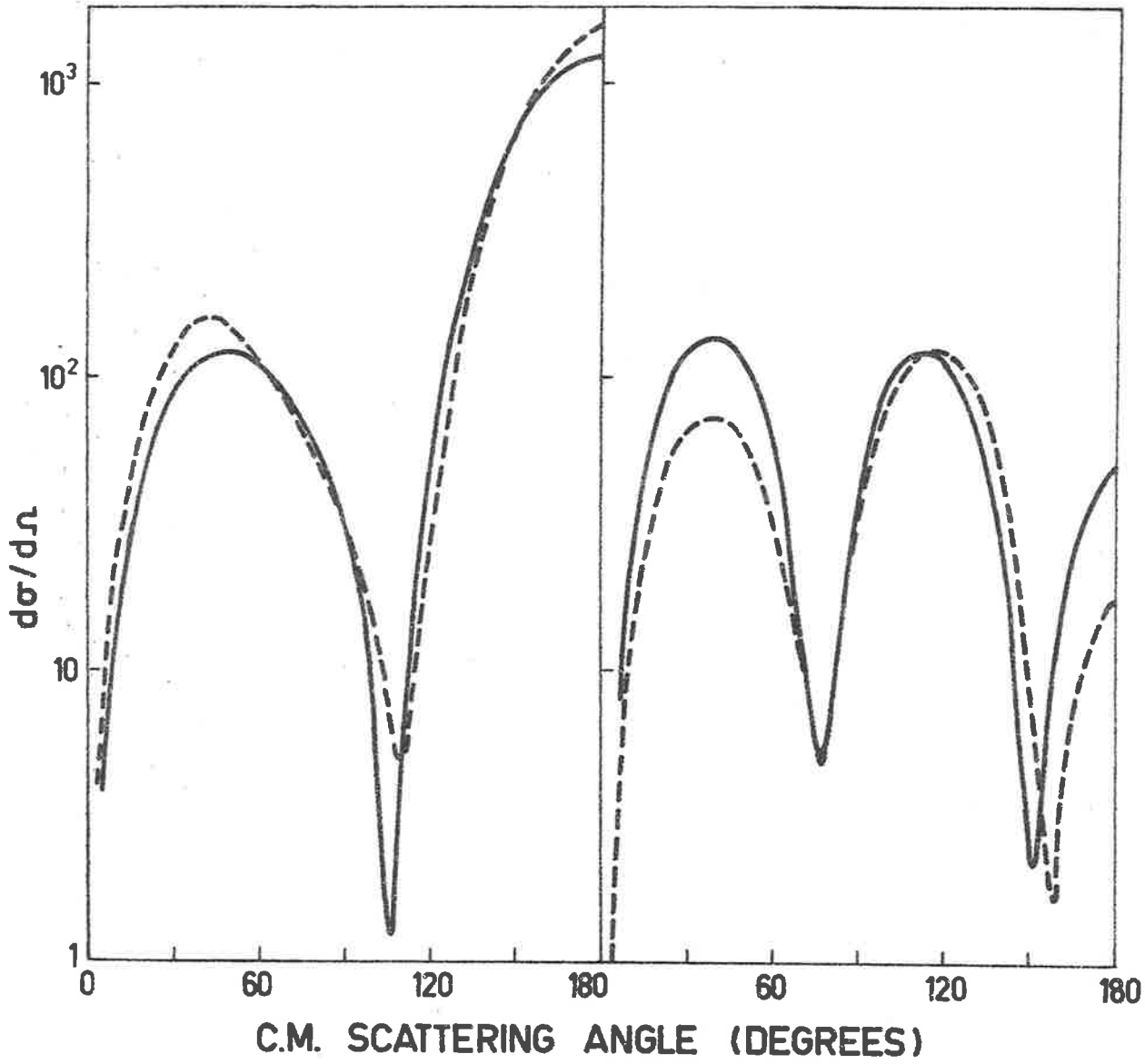
10^3
10^2
10
1
$d\sigma/d\Omega$
0
60
120
180
60
120
180
C.M. SCATTERING ANGLE (DEGREES)

All other parameters are as given in Table 4. The surface calculations are again multiplied by approximately 100, and the scale values are arbitrary, but consistent for the two potentials. These results show that changing the real potential by a large amount has little effect on the volume calculations, but greater effect on the surface calculations. As shown in Section 3.2, increasing the potential by this amount means that the focus in the optical model wave function is centred more in the nuclear interior. The changes in position of the foci are not important for volume calculations because they are spread. In addition, the phase changes associated with the change in potential are small, and more over any effects that phase changes may have are further reduced because of the spread of the foci. However, with the definition of the surface used in this figure, only the tail of the foci enter into the matrix element, so that only slight shift in position of the foci will cause a noticeable change in their contribution. Further, the change in phase in the contributing region is not compensated by the shift in the positions of the foci. This noticeable surface effect could be most significant in producing the energy

variation of the extreme angle peaks, as the phase relationships between the two regions (defined before for backward scattering as the surface and focal regions), could become destructive and then constructive, and thereby produce the start of the second peak. It is the backward scattering cross-section that is most affected by the change in potential. It is reduced by a factor of 3 when the potential is changed from 45MeV to 55MeV. The effect on the forward cross-section is not shown in this case because this reaction, with an angular momentum transfer L=1 and a small Q value, obeys the parity rule[*43] for the parity change case.

We have already noted the effect of increasing the nuclear radius. Of the remaining parameters increase of W decreases the magnitude by a constant amount, and increase of 'a' rotates the angular distribution slightly anti-clockwise. The net result of changing the parameters cannot account for the observed differences between the two types of calculation.

Figure 19 gives the comparison of the change in potential for the L=0 case of 10MeV protons on C^{13} in the reaction $C^{13}(p,n)N^{13}$ Q = -3.005. The parameters other than V are those in Table 4

FIGURE 19

The angular distributions or 10MeV protons on C^{13} for the L=0 reaction $C^{13}(p,n)N^{13}$ with a Q-value of -3.005MeV. The volume calculations are on the left and surface ($R_f = R_N$, f = o) are on the right. The continuous lines are the results for V = 45MeV and the brokes lines for V = 55MeV. All other parameters are as given in Table 4.

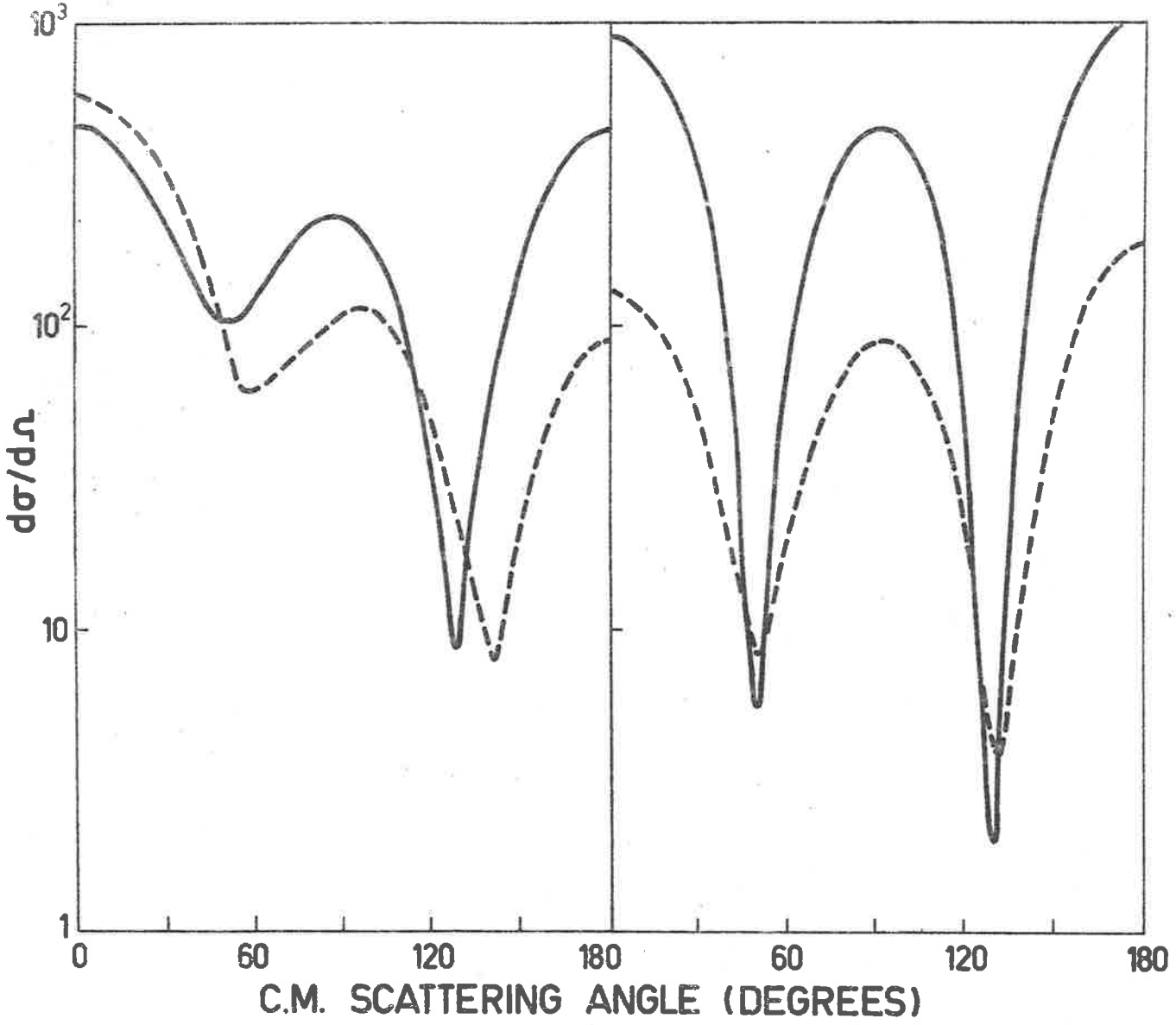
10^3
10^2
10
1
$d\sigma/d\Omega$
0
60
120
180
60
120
180
C.M. SCATTERING ANGLE (DEGREES)

and the diagrams are to be read as for figure 18, except that the surface weight interaction factor is now 1000. This reaction, unlike the F^{19} case, preserves the parity of the nuclei, and so both extreme angle values are strongly dependent on the foci, and are not small. In the volume case, when the potential is increased the backward cross-section is affected more than the forward value, and in the opposite sense.

On the other hand the surface results show a general decrease in the cross-sections, in agreement with the fact that more of the foci are in the non-contributing region of the matrix element when the potential is increased.

(b) Variation of Weight Radius R_f and Weight Value f.

The large differences shown in Section 4.1 (a) result from a stringent definition of the surface weighting. We shall now look at the effect of varying the two parameters, f and R_f, that define the surface and its weight. All calculations in this Chapter, unless otherwise stated, use as a radial weight factor, a step function form -

$$(r) = f \text{ for } r \quad R_f$$

$$= 1 \text{ for } r \quad R_f$$

The first calculation was performed with the optical model parameters (as given in Table 4)

for the 10MeV incident energy reaction $F^{19}(p,p')F^{19*}$ to the first excited level. With the Saxon well radius value of R_f and a weight, f, of 0.5, the resulting angular distribution has a shape indistinguishable from that of the corresponding volume calculation, but with a magnitude reduced by a factor of 4. Hence this is equivalent to a volume calculation with a reduced interaction strength, or a slightly different bound state description. In fact, the form of the angular distribution will be that of the appropriate extreme case with different magnitudes, unless the two regions of nuclear space, defined by our definition of the weighting surface, contribute to the matrix element in the same order of magnitude. That is, there are three categories of results defined by the weight parameters. The first category contains those values of f and R_f which yield angular distributions indistinguishable in shape from that of the complete volume interaction case; the second contains those parameters which give the characteristic pure surface interaction results; the third classification contains the intermediate results. In the first and second categories, as the weight parameters change the magnitudes of the cross-sections decrease in the direction

of the pure surface case.

The intermediate results are shown in Figure 20. The parameters are those of Table 4. The broken curve is the angular distribution for the weight values R_f=1.8f and f=o, andthe continuous line is that for R_f=2.2f and f=0.5. These results show the third peak characteristic of the surface interaction case, but each has a large backward peak which is characteristic of the volume interaction results. Consequently, the intermediate region is observably different from either extreme case.

The angular distributions were also calculated using the Eckart form factor shape for the weight variation with radius. These were found to be indistinguishable from the surface calculation results.

(c) Variation of Energy

We have already seen in Figures 16 and 17 that for an incident energy of 5MeV, the differences between the surface and volume calculations could be explained by a reasonable variation of parameters, but for the 10MeV results the differences are too great to be explained this way.

Figure 21 compares the surface and volume calculations for incident energies 15MeV, 25MeV and 30MeV for the reaction $F^{19}(p,p')F^{19*}$ to the

FIGURE 20

Angular distributions for 10MeV protons on F^{19} exciting it to the first state. The broken line is the result of using R_f = 1.8f and f = o, the continuous line for R_f = 2.2f and f = 0.5. All other parameters are as in Table 4.

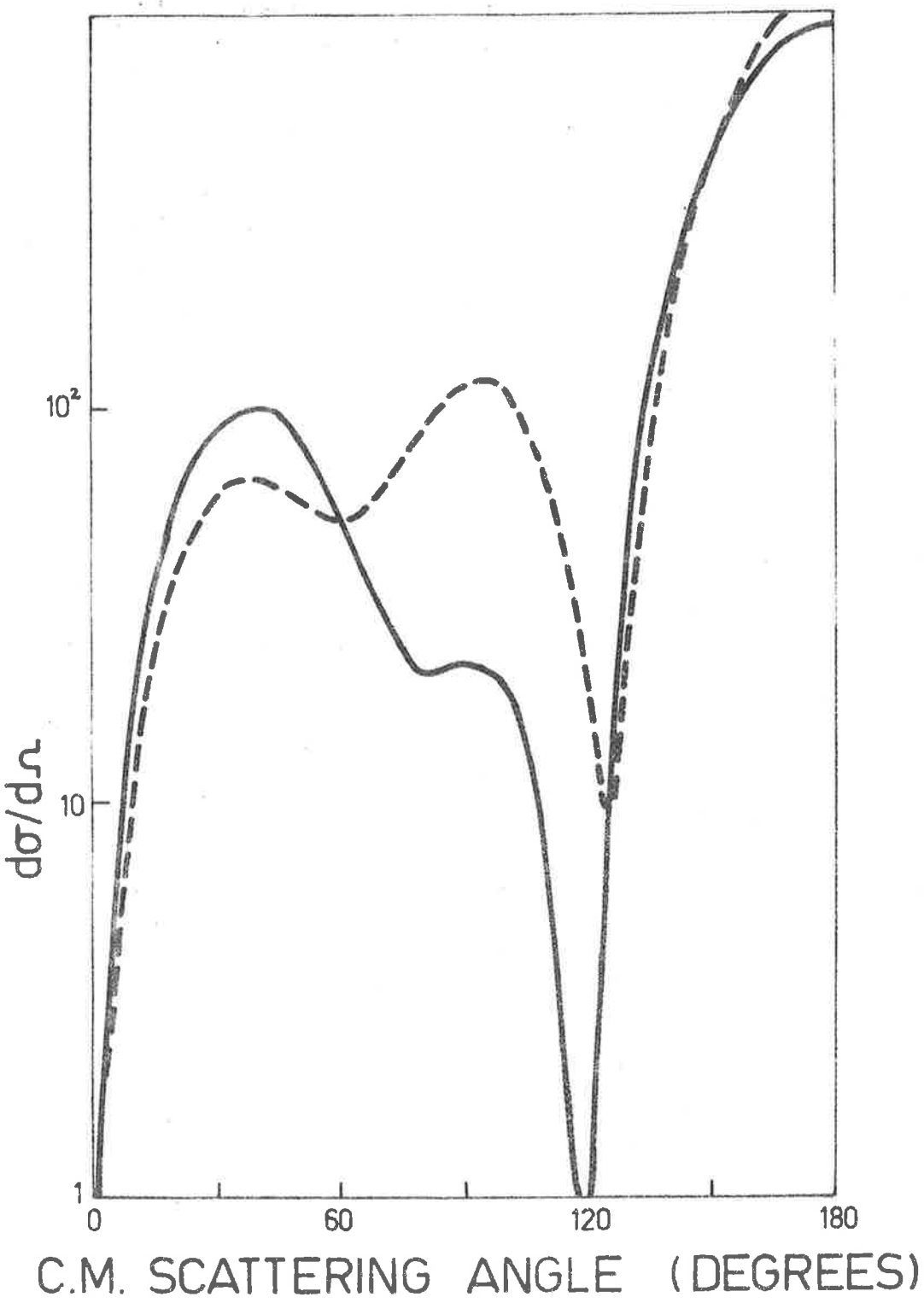
10^2
10
1
$d\sigma/d\Omega$
0
60
120
180
C.M. SCATTERING ANGLE (DEGREES)

first excited level. The volume calculations are shown by the continuous lines, surface calculations by the broken lines. The entrance and exit channel potentials are the same and are V = 55MeV, W = 4MeV, a = 0.55, r_o = 1.2f, and the surface factors are R_f = 3.2f, f = o. The bound states are calculated using an interaction radius of 3.2f, and are described by a 2S Harmonic Oscillator wave function in the entrance channel, and a 1P wave function in the exit channel. The surface cases all contain one more peak in their angular distributions than the corresponding volume calculations. As the incident energy increases, the backward cross-section in the volume calculations show little magnitude change, but the rest of the angular distributions increase, until, at 30MeV, the other peaks in the cross-section have a larger value than the backward scattering angle value. For the surface cases, however, as the energy increases the valleys in the angular distributions are more sharply defined. These energy variation differences between the volume and surface calculations may not be a sensitive test of the reaction mechanism, because the variation of potentials with energy alters the angular distributions. Nevertheless, Figure 21 supports the fact that negligible

FIGURE 21

The angular distributions for 15, 20 and 25 and 30 MeV protons on F^{19} to the first excited state. The continuous lines are the results for volume cases, the broken lines for surface (R_f = 3.2f, f = o) cases. The parameters used are -

$V = V' = 55MeV$ $\quad W = W' = 4MeV$

$a = a' = 0.55f$ $\quad r_o = 1.2f$

$R_b = 3.2f$

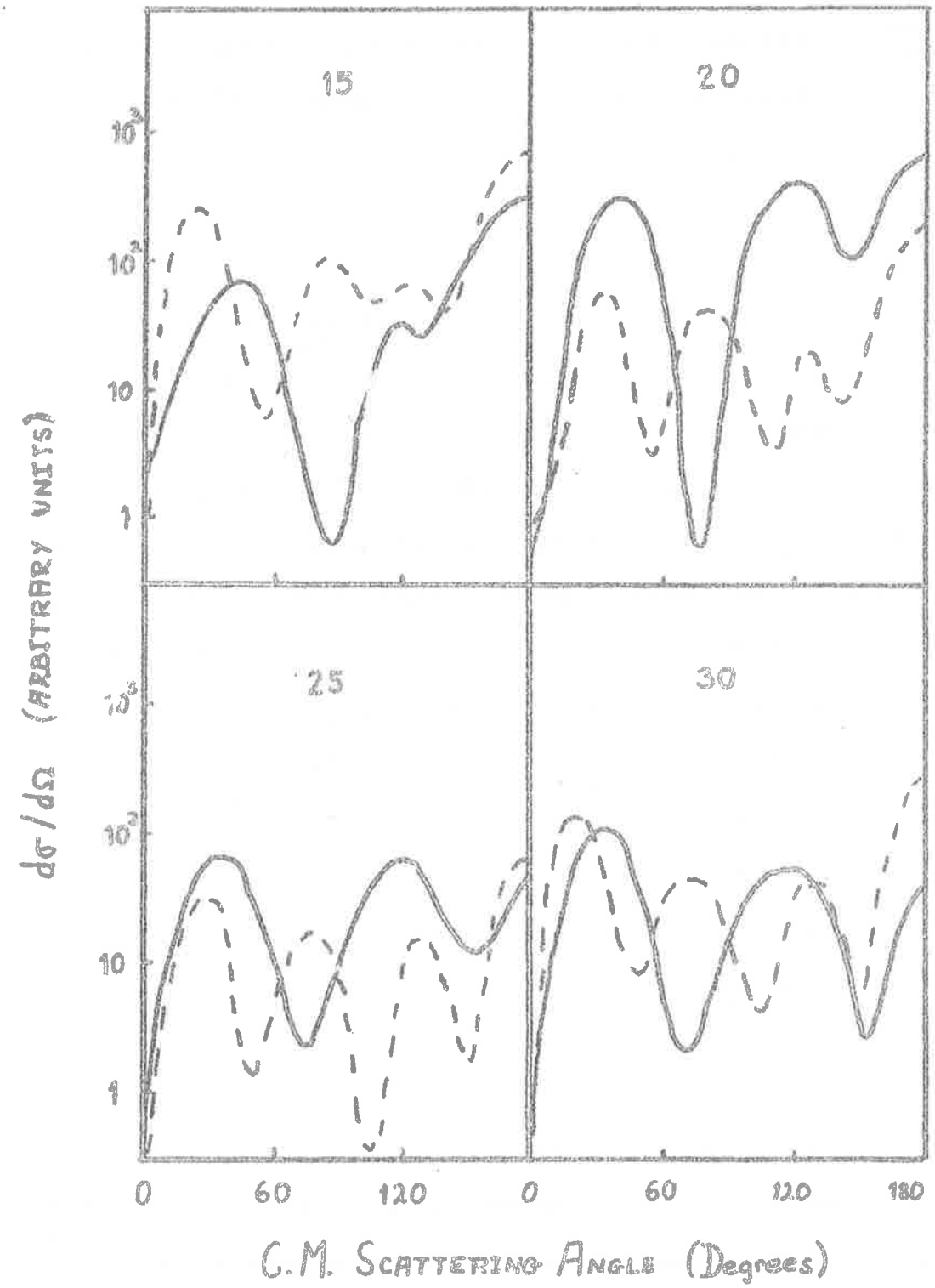
15
20
25
30
10^3
10^2
10
1
0
60
120
180
$d\sigma/d\Omega$ (ARBITRARY UNITS)
C.M. SCATTERING ANGLE (Degrees)

contribution to the matrix element from the nuclear interior will not be due solely to any optical model property. Also, these results, when compared with the 5MeV and 10MeV results, show that the foci contribute more to the surface cases with increase in energy. In fact, these foci are centred well out in the nuclear surface region for these energies. The surface results are normalized by a factor of the order of 100. Figure 22a shows a higher energy case. In this case the incident energy is 60MeV, and the parameters used are V=30MeV, W=15MeV, a=0.55f, r_o=1.2f. Once again surface results are characterized by greater structure than the corresponding volume case. The curves are on a linear scale to emphasize shape, and the surface results are adjusted by a factor of 3. When compared with figure 21, this smaller value of normalization is consistent with the larger attenuation caused by the value of W=15MeV, with the smaller distortion that exists because of the smaller value of V=30MeV, and with the higher incident energy. The absence of a backward peak in either calculation shows that the foci are centred in a region weighted little by the bound state wave functions, and that the phase changes throughout the focal region are

rapid, thereby causing a larger destructive interference than is present in the lower energy cases.

Figure 22b shows the effects of using different potentials in the entrance and exit channels for the reaction $F^{19}(p,p')F^{19*}$ at incident energies of 5MeV and 10MeV. The parameters used are those of Table 5.

It is expected that the 10MeV difference in potentials is excessive for the Q value -0.11MeV in this reaction. However, in spite of this fact, we expect the trend of change in curve shape with a more realistic variation of potential to have the same form. The most important feature of these results is that the parity rule, most evident in Figures 16 to 21, while not as obvious as in the previous figures, is still obeyed, in that the derivatives still have the correct sign. Further, the surface and volume calculation differences are not as pronounced as in the equipotential calculations, but for the 10MeV results they are still quite evident.

4.3 FINITE RANGE EFFECTS

From the previous Sections, it can be seen that, using a zero-range approximation for a single particle

FIGURE 22a

The angular distributions for the reaction $F^{19}(p,p')F^{19*}$ to the first excited level.

These 60 MeV incident energy results used parameters -

$V = V' = 30MeV$ $W = W' = 15MeV$

$a = a' = 0.55f$ $r_o = 1.2f$

$R_b = 3\ 2f$

The continuous lines show the volume interaction results, the broken lines the surface cases.

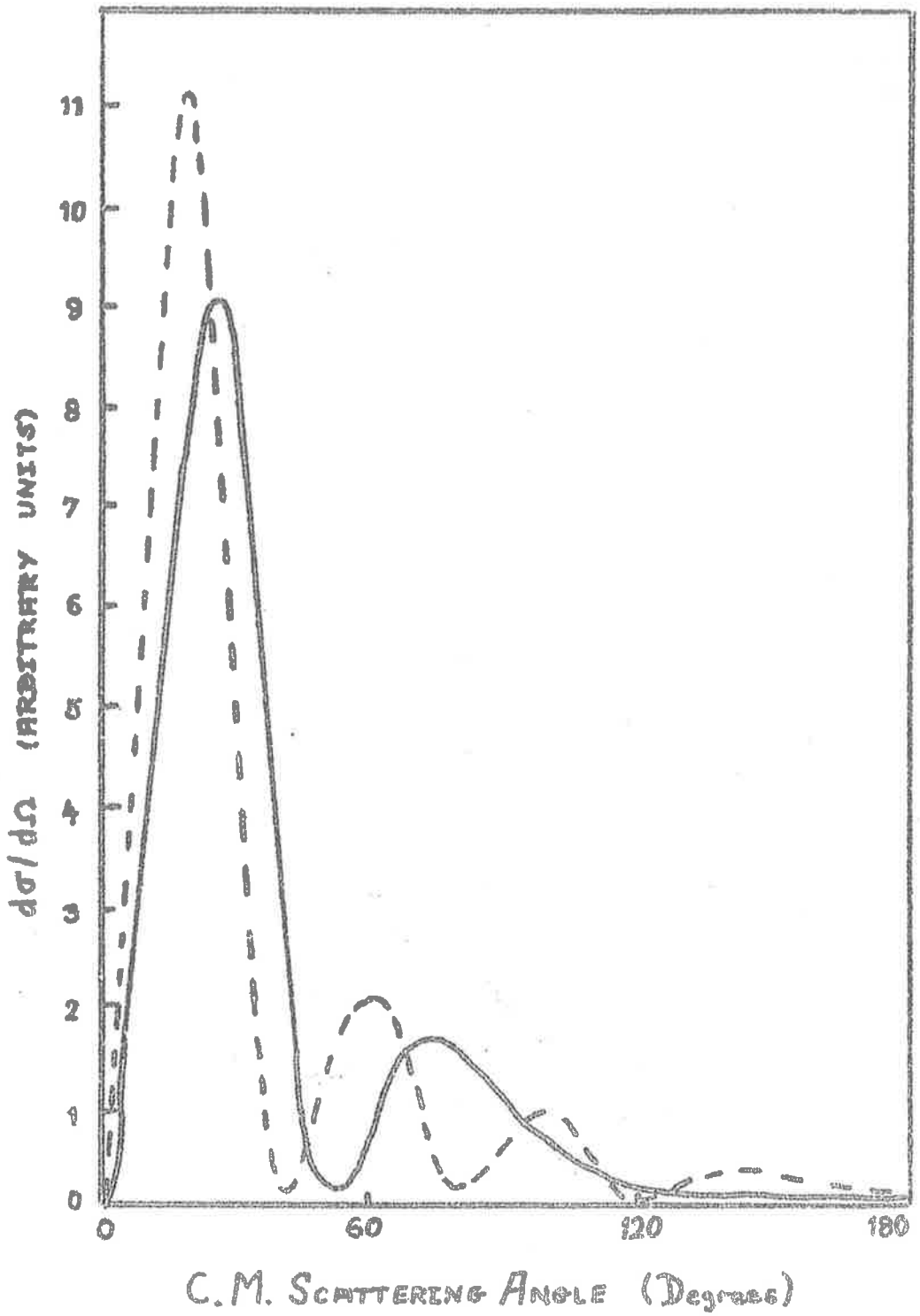
dσ/dΩ (ARBITRARY UNITS)
0
1
2
3
4
5
6
7
8
9
10
11
0
60
120
180
C. M. SCATTERING ANGLE (Degrees)

FIGURE 22b

The angular distributions for 5MeV and 10MeV protons on F^{19} to the first excited level. These show the effects of different potentials in the entrance and exit channels. The parameters are those in Table 5 and the volume calculations are shown by the continuous lines, the surface results by the broken lines. The 5MeV results are on the left.

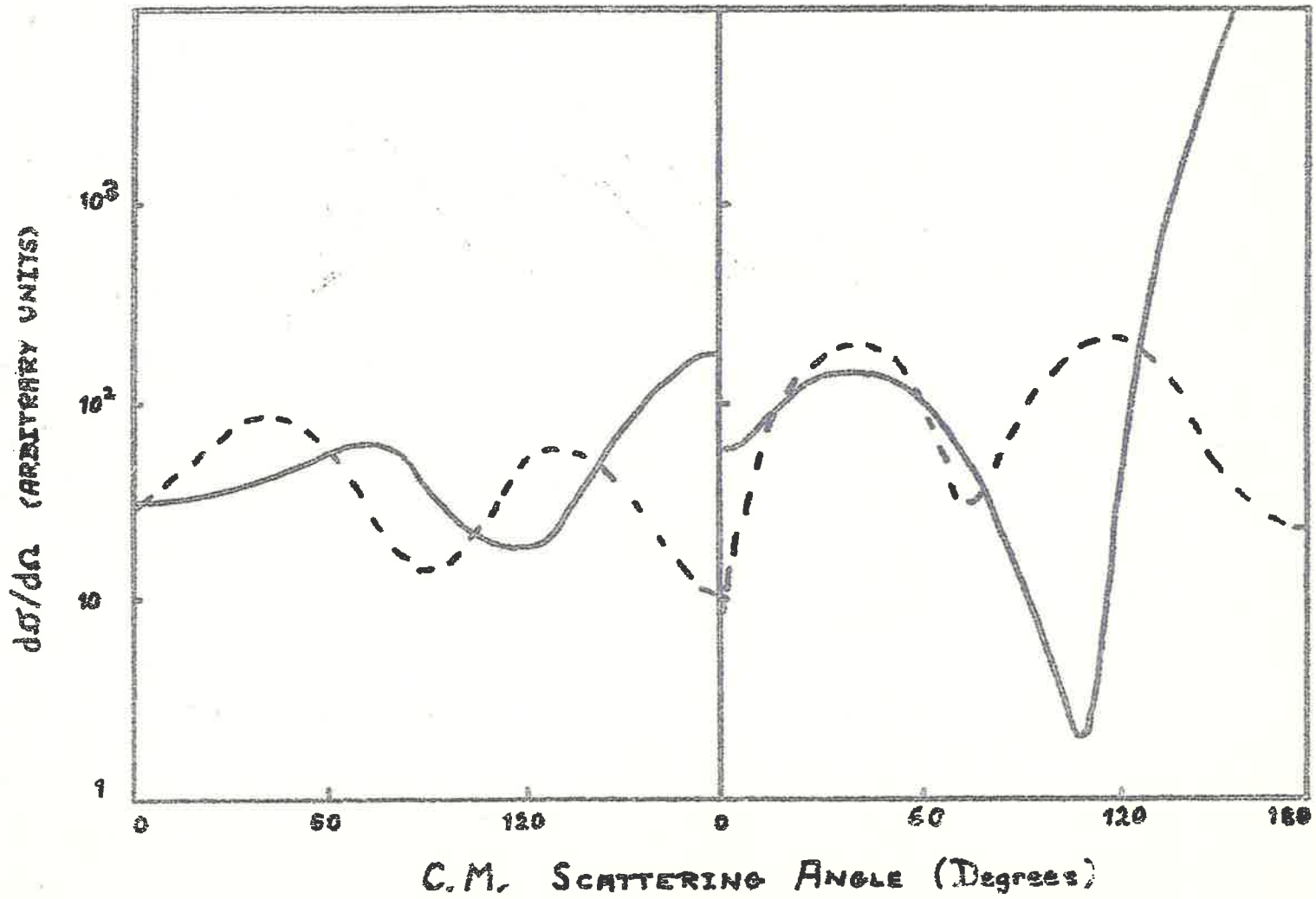
dσ/dΩ (ARBITRARY UNITS)
10²
10
1
0
60
120
0
60
120
180
C.M. SCATTERING ANGLE (Degrees)

TABLE 5

PARAMETERS FOR THE 5MeV AND 10MeV RESULTS OF FIGURE 22 (PRIMES DENOTE EXIT CHANNEL)

E(MeV)	V(MeV)	V'(MeV)
5	55	45
10	55	45

$W = W' = 4MeV$ $a = a' = .55f$ $r_o = 1.2f$

$R_f = 3.2f$ $f = o.$

excitation, the optical model effects of phase averaging, absorption and focussing often do not cause the nuclear interior to give an insignificant contribution to the angular distributions.

However, the inclusion of a finite range force may be expected to amplify the optical model effects and cause a greater reduction in the contribution from the nuclear interior*[42]. In fact, it may be that this reduction is large enough to remove the significant differences between the total volume and surface calculations. That the finite-range force has a noticeable effect on angular distributions is well known*[22,23]. That this should be so can be seen from Figure 23. In this diagram a comparison is made between the bound state coordinate dependent part of the radial integrals for the zero-range (continuous line) and the finite range Yukawa force with $\mu = 0.87 f^{-1}$ (broken line).

These curves show the product of the nuclear wave functions $\Psi(r)$ for the F^{19} reaction to the first excited state using radial harmonic oscillator wave functions, $R_{nl}(r)$, where the partial matrix elements have the following form -

$$I_{ll'L} = \int r^2 dr \, f_{l'}(k'r) \, f_l(kr) \, \Psi(r)$$

For the zero-range case $\mathcal{F}(r) = R_{11}(r)R_{20}(r)$ and for the finite range case $\mathcal{F}(r') = \int r^2 \, dr \, R_{11}(r)R_{20}(r) \, \mathcal{V}_1(|\underline{r}'-\underline{r}|)$. These curves have been arbitrarily normalized to allow for an easier comparison. It can be clearly seen that the finite range emphasises the nuclear surface region far more than the zero-range case not only in relative magnitude but also in radial spread.

We describe this partially by saying that the finite range causes the average interaction radius to be increased. Hence from purely magnitude grounds we expect that the relative magnitude of the contributions from the low partial wave terms in the matrix element to be much smaller in the finite range case than in the zero-range case. This is the case as can be seen in Figure 24, where the partial matrix elements, the $I_{11'}$ as defined in Figure 9, for the zero-range case of 60MeV protons incident of F^{19} and leading to the first excited state are compared with the finite range values.

However, while the phase averaging effect is amplified because of the change in the magnitude and shape of the bound state term, Figure 25 shows that the significant differences between the volume and surface calculations still exist. These are angular distributions for 10MeV protons F^{19} to the first excited state. The volume calculation is shown by the continuous line, the surface using

FIGURE 23

The bound states weighting amplitudes for the zero-range (continuous line) and finite range Yukawa (broken line) forces. The quantum numbers are $n = 1$, $l = 1$ and $N' = 2$, $l' = 0$ with $L = 1$. (The primes denote final state quantities).

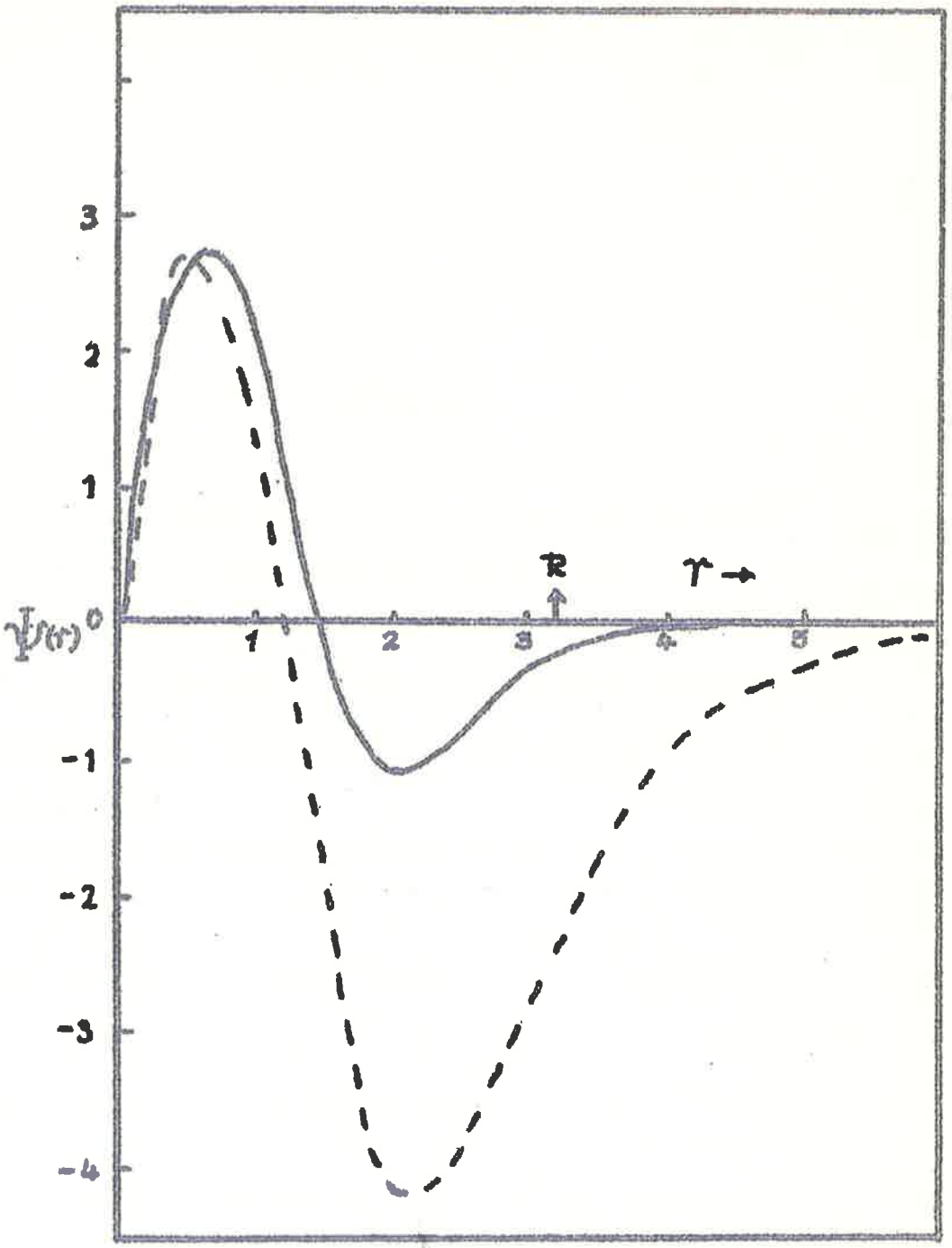
3
2
1
R
r →
ψ(r) 0
1
2
3
4
5
-1
-2
-3
-4

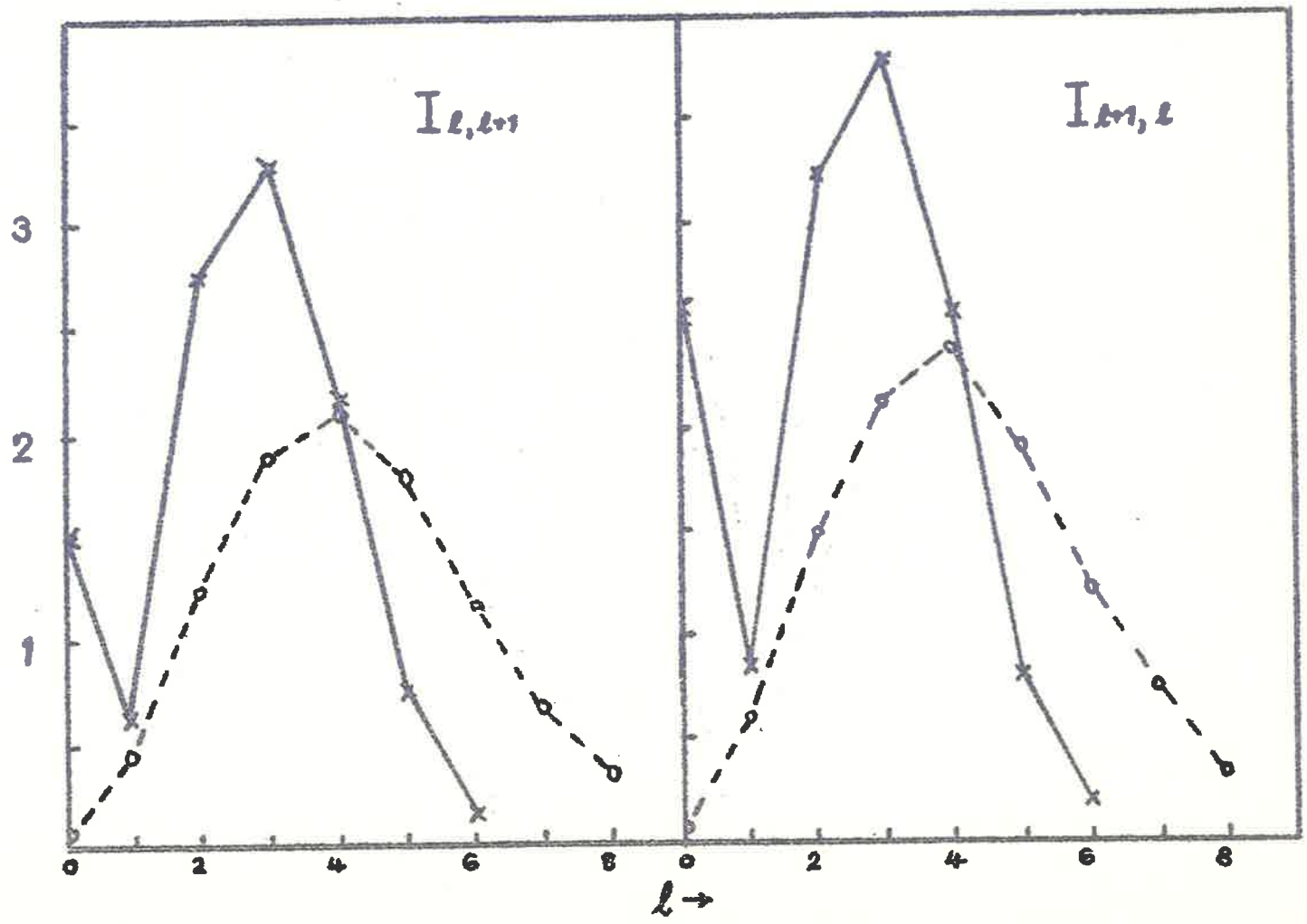
$I_{\ell,\ell+1}$
$I_{\ell+1,\ell}$
3
2
1
0
2
4
6
8
$\ell \rightarrow$

FIGURE 25

The angular distributions for 10MeV protons on F^{19} exciting the first level. The volume calculation is shown by the continuous line while the broken and dotted lines respectively show the surface cases $R_f = 3.2f$, $f = o$, and $R_f = 1.8f$, $f = o$. All curves use the parameters V = 55MeV, W = 4MeV, a = 0.55f and $r_o = 1.2f$. The surface calculation with $R_f = 3.2f$ is normalised by a factor of 100.

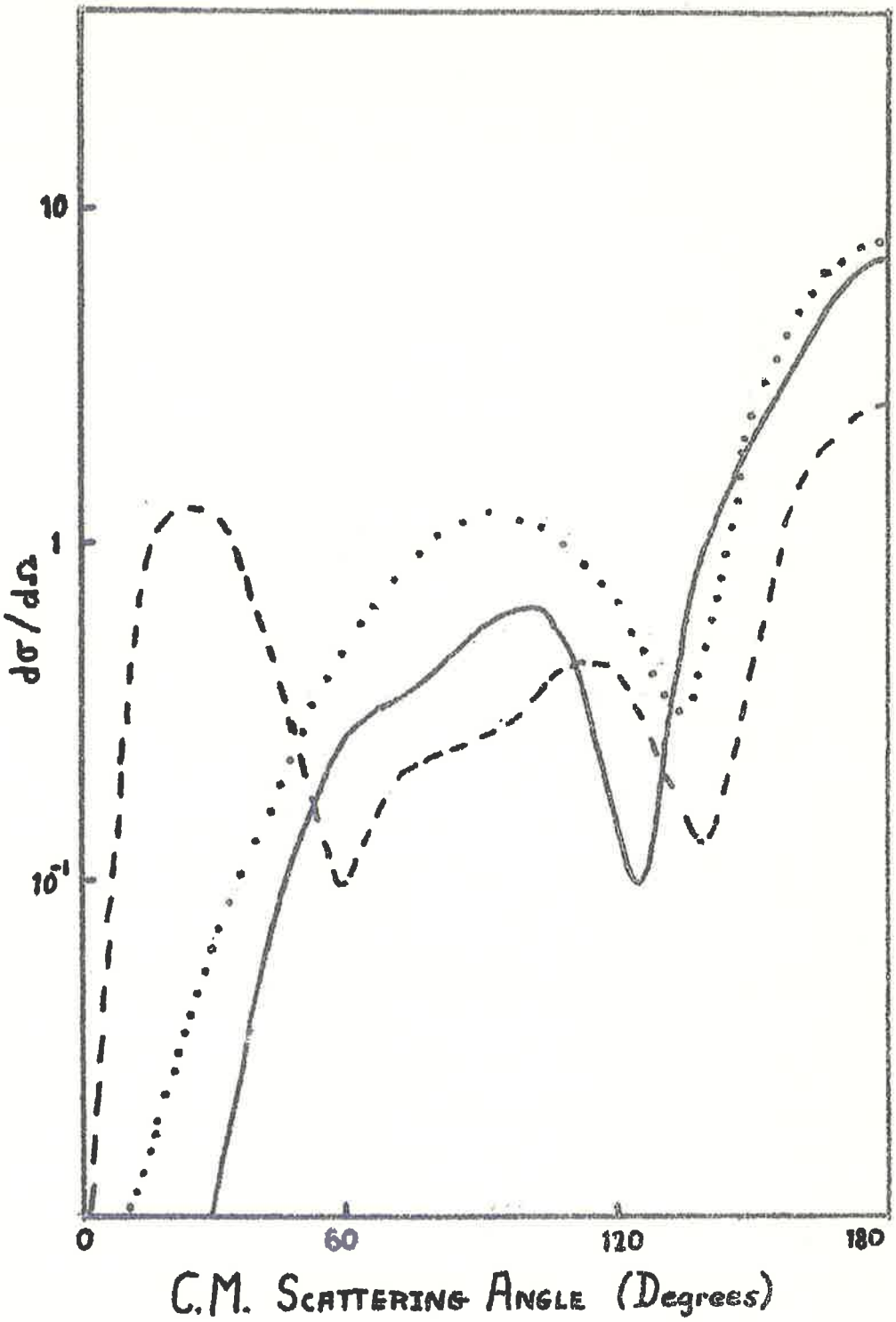
10
1
10⁻¹
dσ/dΩ
0
60
120
180
C.M. Scattering Angle (Degrees)

R_f = 3.2f, f = 0 by the broken line, and the middle case R_f = 1.8f, f = 0 by the dotted line. The parameters used for all these curves were V = 55MeV, W = 4MeV, a = 0.55f, r_o = 1.2f, R_b = 3.2f. The surface case, R_f = 3.2f, is normalised by a factor of 100.

As for the zero-range cross-sections the two extreme calculations show the characteristic difference of one more peak in the surface angular distribution. However, the third case, R_f = 1.8f, shows that the nuclear centre does not have asmuch influence in these finite range results since the differences between this calculation and the pure volume case are far less evident in both magnitude and shape than in the corresponding zero-range cases. In fact the region out to r = 1.8f in the finite range results seems only to affect the slope of the forward cross-section and the relative magnitude of the peak to the backward cross-section value, both of which could probably be produced by a variation of the parameters. Nevertheless, the differences between the two extreme cases cannot be overcome by parameter variation.

Hence while the finite range force reduces the results discussed in the zero-range calculations, it does not appear to invalidate them.

4.4 THE REACTION $Y^{89}(p,p')Y^{89*}$ (Q = -0.915MeV)

The results shown in the previous sections of this chapter consider reactions that are expected to be single particle transitions, but use pure j-j coupling shell model wave functions for the initial and final bound states in the calculation of the matrix elements. While this description is not the best, expecially for F^{19} which is essentially a three body problem, if one considers only particles, the states used are expected to be predominant over other possible configurations and so we expect the angular distribution shapes to be meaningful but not the absolute magnitudes. In any event, these have permitted us to investigate the effects on angular distributions of the properties of the optical model representations of the unbound particles.

However, the ground and first excited states of Y^{89} are well described in this simple theory as not only does the j-j coupling model predict the correct spins, parities and energy separation*[45,46] but also expects an M4 γ-ray transition whose calculated rate*[46] agrees well with the experimental value of 16 secs. Consequently, we expect both the shapes and magnitudes shown in the following diagrams to be meaningful at least to within the limitations imposed by the neglect of spin-orbit coupling in the optical models and the exchange effect which, as seen in Chapter 2, also includes the antisymmetry.

Figure 26 shows the surface (broken lines) and volume (continuous lines) calculations for a zero-range (left and finite range Yukawa (right) interaction for the inelastic scattering of 10MeV protons from Y^{89} leading to the first excited 9/2+ state. The Q-value of the reaction is 0.915MeV and the bottom diagrams are the results of calculations using V=40MeV and other parameters as given for the top curves which use V=50MeV. The other parameters used are as shown in the Figure 26 caption and there is a weight factor of 100 multiplying the magnitude of the surface calculations.

As with the calculations on lighter nuclei, there are noticeable differences between the volume and surface weighted calculations and, although it is not evident for the 10MeV results of Figure 26, the surface calculations exhibit more structure than the corresponding volume results.

In the volume calculations, the delta function interaction results show little difference when the real part of the distorting potential is changed by 10MeV. This is also the case for the Yukawa interaction volume calculations because the structural differences that can be seen at scattering angles less than about 70° have small magnitude, less than 1.0% of the value of the backward peak.

FIGURE 26

The angular distributions of 10MeV protons on Y^{89} leading to the first excited state.

The delta-function results are on the left and the Yukawa finite range with $\mu = 0.87f^{-1}$ are on the right.

Surface results are shown by the broken lines and volume results by the continuous line.

The parameters used were:-

$V = V' = 50MeV$

$W = W' = 10MeV$

$a = a' = 0.6f$

$r_o = 1.2f$

$R_b = 5.4f$

$R_f = 5.4f$ and $f=0$

The bottom curves are the results for calculations using $V=V' = 40MeV$ with all other parameters unchanged.

These results both are normalized using V_o, the two-body interaction strength, = 100MeV.

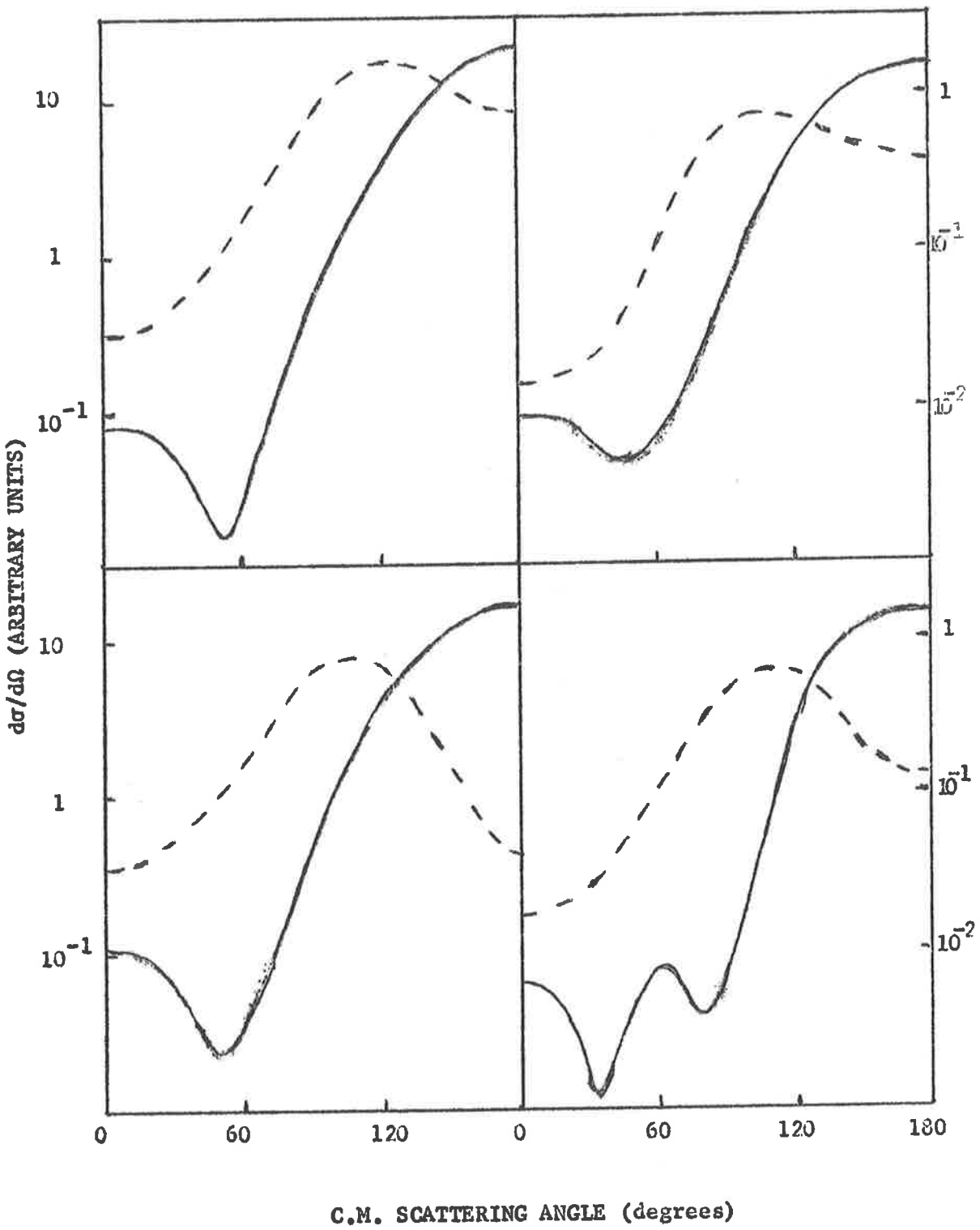
10
1
10^{-1}
1
10^{-1}
10^{-2}
10
1
10^{-1}
1
10^{-1}
10^{-2}
0
60
120
0
60
120
180
dσ/dΩ (ARBITRARY UNITS)
C.M. SCATTERING ANGLE (degrees)

However, most important is the fact that there seems to be a breakdown of the parity rule although the cross-section slope is essentially flat in the range 0^{o} - 10^{o} scattering angle. This effect will be shown to persist for higher incident energies for lower values of V which one may expect to be applicable from the analyses of elastic scattering on heavy nuclei.

The surface calculations show three significant facts when compared with the volume results. First, the shapes of the angular distributions are very different from the volume results so that any such effect should be experimentally observable. Second, large effects are noticed in the magnitude of the backward cross-sections as the potential V changes. Third, and possibly most significantly, the parity rule is always obeyed.

The 20 and 30 MeV incident energy results shown in the following figures indicate similar trends as those of Figure 26, except, as was seen in the earlier discussions, that more structure is evident at higher energies. Figure 27 is a plot of the partial matrix elements for various l and l' combinations in the delta-function results. This shows little phase averaging for the cases where l and l' differ by three to five and begins to indicate this effect only in the $|l-l'| = 1$ cases. This can be understood as in the first four cases the low l (or low l') terms involve a surface l' (or l respectively) in the overlaps.

FIGURE 27

The partial matrix elements for M=0, $m_j = \frac{1}{2}$, in the L=5 $Y^{89}(p,p')Y^{89*}$ reaction for 20MeV incident energy The $I_{\ell\ell'}$ are plotted against ℓ on the top row and against ℓ' on the bottom row.

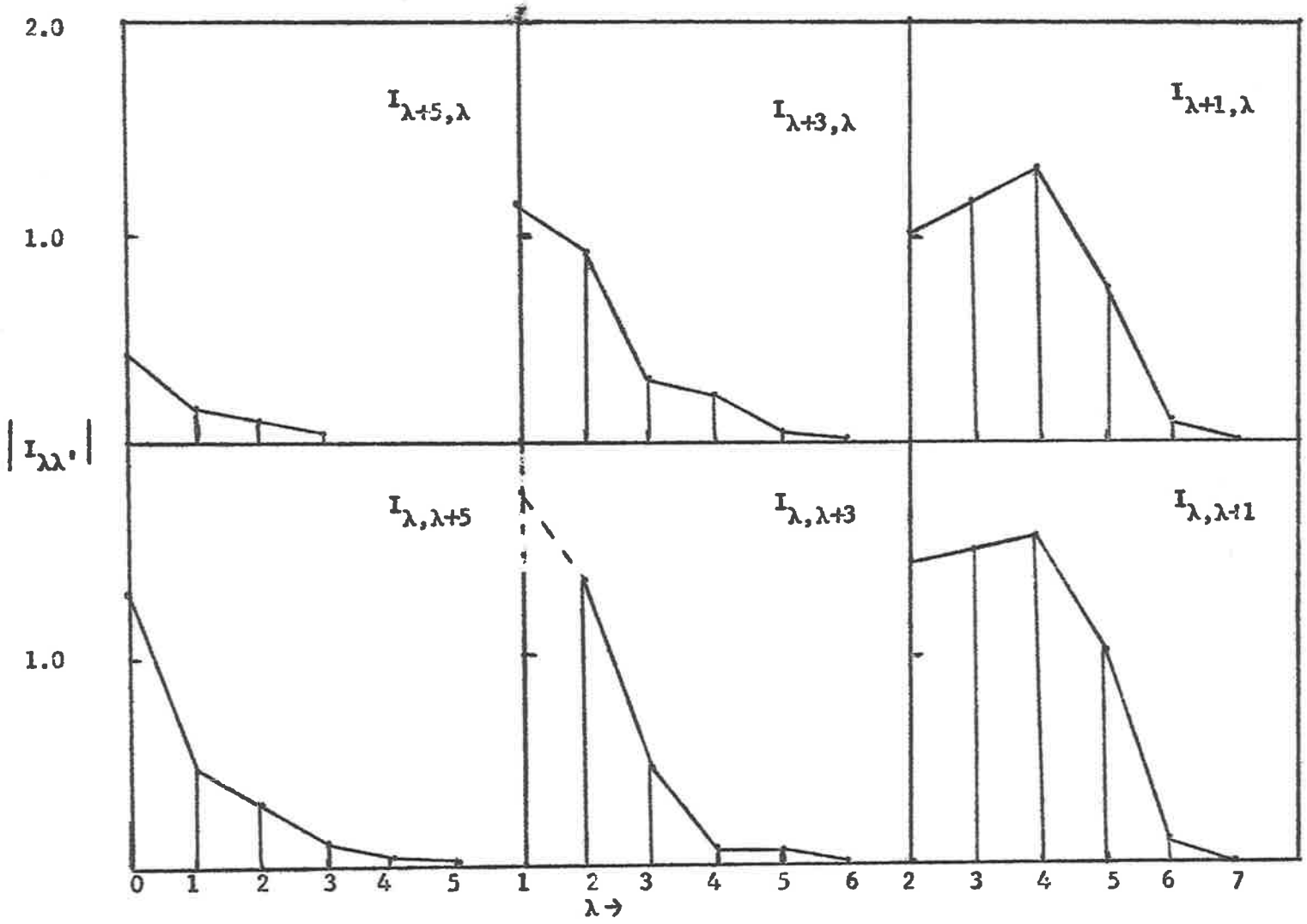
2.0
1.0
$|I_{\lambda\lambda'}|$
$I_{\lambda+5,\lambda}$
$I_{\lambda+3,\lambda}$
$I_{\lambda+1,\lambda}$
$I_{\lambda,\lambda+5}$
$I_{\lambda,\lambda+3}$
$I_{\lambda,\lambda+1}$
1.0
0 1 2 3 4 5
1 2 3 4 5 6
2 3 4 5 6 7
$\lambda \rightarrow$

However Figure 28 is a plot of $J_{\ell'}$ against ℓ' where

$$\mathcal{M} = \sum_{\ell' M} J_{\ell'} Y^*_{\ell', M}(\Omega_{sc})$$

for this case of M=0, $m_j = \frac{1}{2}$ and the phase averaging effect can be seen more easily. This is produced by the partial cancellation of the $I_{\ell, \ell+p}$ and $I_{\ell+p, \ell}$ where p is 3 or 5 for any scattering angle but more so for $\theta_{sc} = 0^\circ$ and 180° where the $Y_{\ell,0}(\theta) = (\pm)^\ell \left[\frac{(2\ell+1)}{4\pi}\right]^{\frac{1}{2}}$ respectively, make these matrix elements comparable in magnitude. Their phases are always nearly 180° apart so that cancellation occurs.

However while phase averaging still exists even for large momentum transfer and the phase cancellation of the $I_{\ell\ell'}$ is more important, there are quantitative differences between the volume and surface results for 20 and 30MeV incident energy protons on Y^{89} using the zero range interaction as shown in the top left and right diagrams of Figure 29 respectively.

The 20 and 30 MeV volume results for the Yukawa interaction are shown on the bottom diagrams of Figure 29.

Finally figures 30 and 31 have the results for 20MeV incident energy protons with a variation of the weighting value and radius.

In Figure 29 it can be seen that the structural differences between the volume and surface calculations persists with increase in energy with an overall increase

FIGURE 28

The total matrix element term $J_{\ell'}$ given in the text plotted against ℓ'. The crosses are the delta function interaction results and the circles are the Yukawa results for 20MeV incident energy protons on Y^{89} with the parameters:-

$V = V' = 45\text{MeV}$

$W = W' \ 10\text{MeV}$

$a = a' = 0.55\text{f}$

$r_o = 1.2\text{f}$

$R_b = 5.4\text{f}$

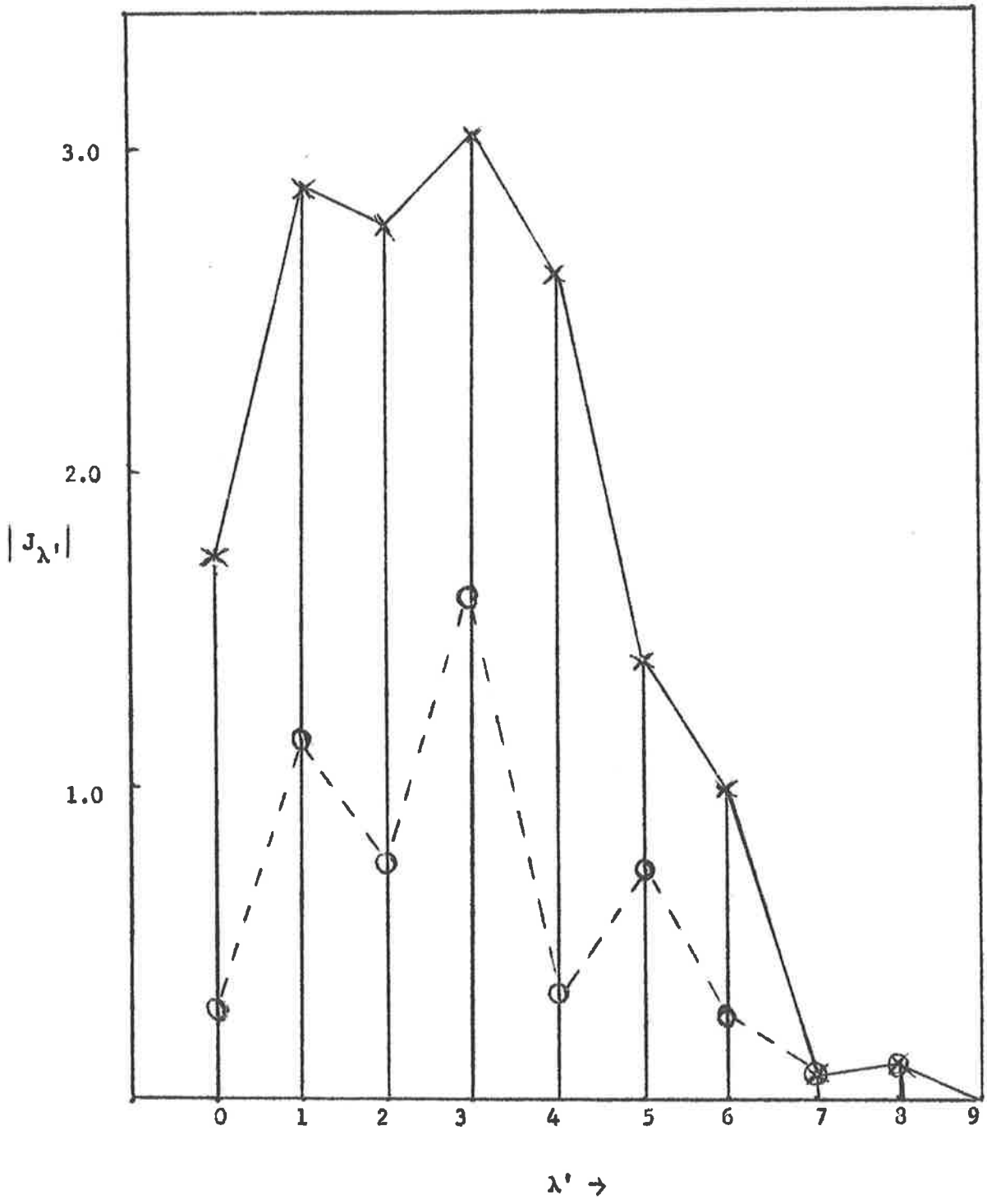
3.0
2.0
1.0
$|J_{\lambda'}|$
0
1
2
3
4
5
6
7
8
9
$\lambda' \rightarrow$

FIGURE 29

The angular distributions for 20MeV (left) and 30MeV (right) protons on Y^{89} leading to the first excited state. The delta function results (top diagrams) show the volume (continuous) and surface weighted (broken lines) and the finite range results use a range $\mu = 0.87f^{-1}$.

The parameters used are:

$V = V' = 50MeV$

$W = W' = 10MeV$

$a = a' = 0.6MeV$

$r_o = 1.2f$

$R_b = 5.4f$

$R_f = 5.4f$

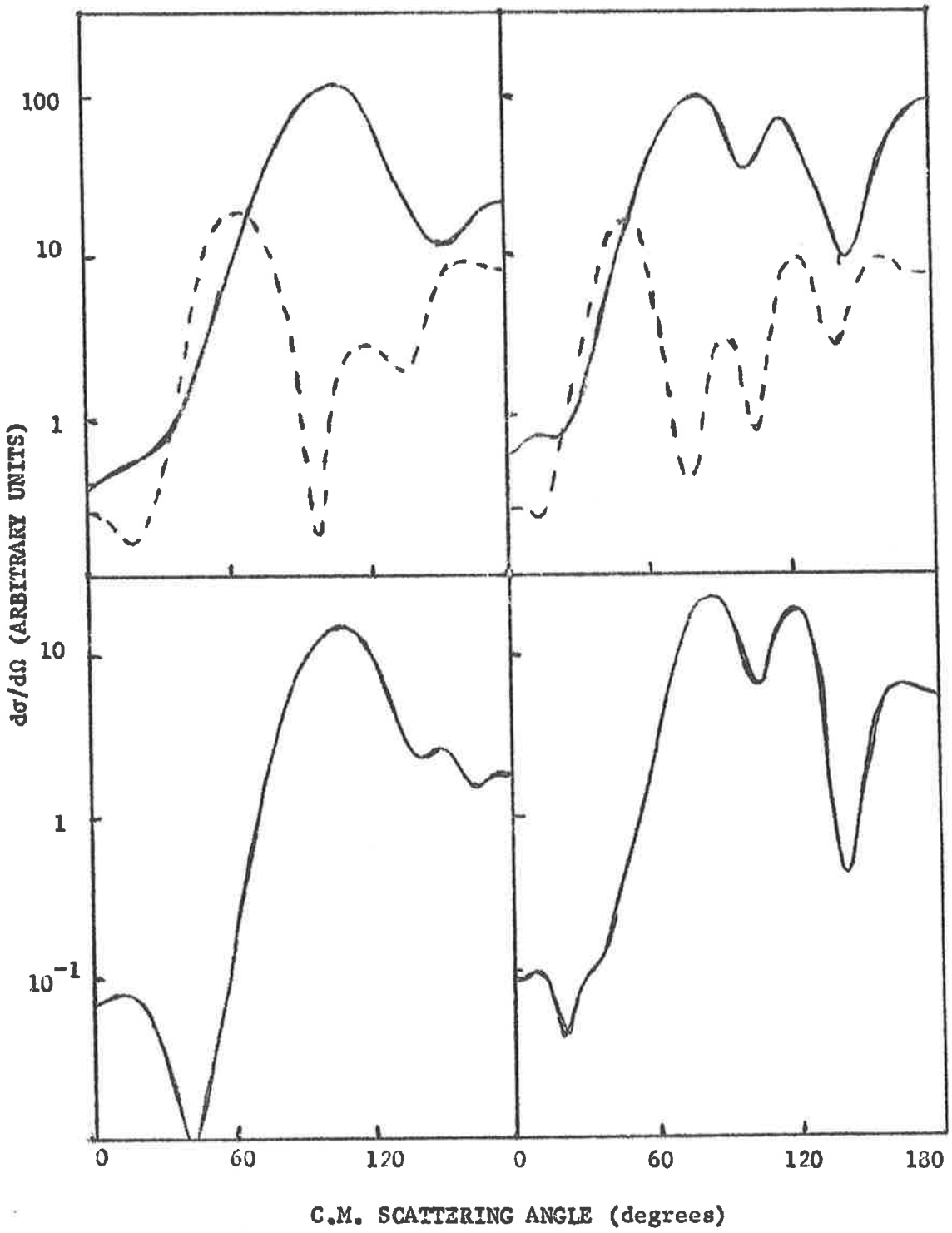
100
10
1
10
1
10^{-1}
$d\sigma/d\Omega$ (ARBITRARY UNITS)
0
60
120
0
60
120
180
C.M. SCATTERING ANGLE (degrees)

in structure as energy increases. Once again there is a scale factor of 100 between the surface and volume magnitudes and the parity rule is barely discernable for the volume results which is now also the case for the surface calculations.

As with the previous calculations the finite range results show more structure than the zero range ones but still not enough to produce the differences between the volume and surface theories. Most striking however is the fact that the finite range results are smaller in magnitude than the corresponding delta function results as energy increases. For example the ratios of the major peaks in the zero and finite range volume calculations are about 10 as to 1 and the ratio is about 4:3 in the surface calculations at 10MeV. Also, as energy increases, the differences in angular distributions for different potentials increase for the volume calculations especially in the value of the backward scattering angle, but although differences in shape appear in the surface calculations, the variation in the backward cross-section value is much less than that for the 10MeV case shown in Figure 26.

Figure 30 contains the results for 20MeV protons on Y^{89} again exciting the nucleus to the first excited level. These use a delta function interaction and use the parameters, $V=V_{s}=40$MeV, $W=W_{s}=10$MeV, $a=a_{s}=0.6$f, $r_{o}=1.2$f and $R_{int} = 5.4$f.

FIGURE 30

The angular distributions for 20 MeV protons on Y^{89} to the first excited state via a delta function interaction. The continuous line is the result for a pure volume calculation. The bottom broken line is the result for a single calculation using $R_f = 5.4f$ and $f = 0.0$.

The top broken line is the result using $R_f = 3.8f$ and $f = 0.5$ and the dotted line is that using $R_f = 3.8f$ and $f = 0.0$.

The other parameters are as given in the text and the magnitudes shown are not scaled as in previous diagrams.

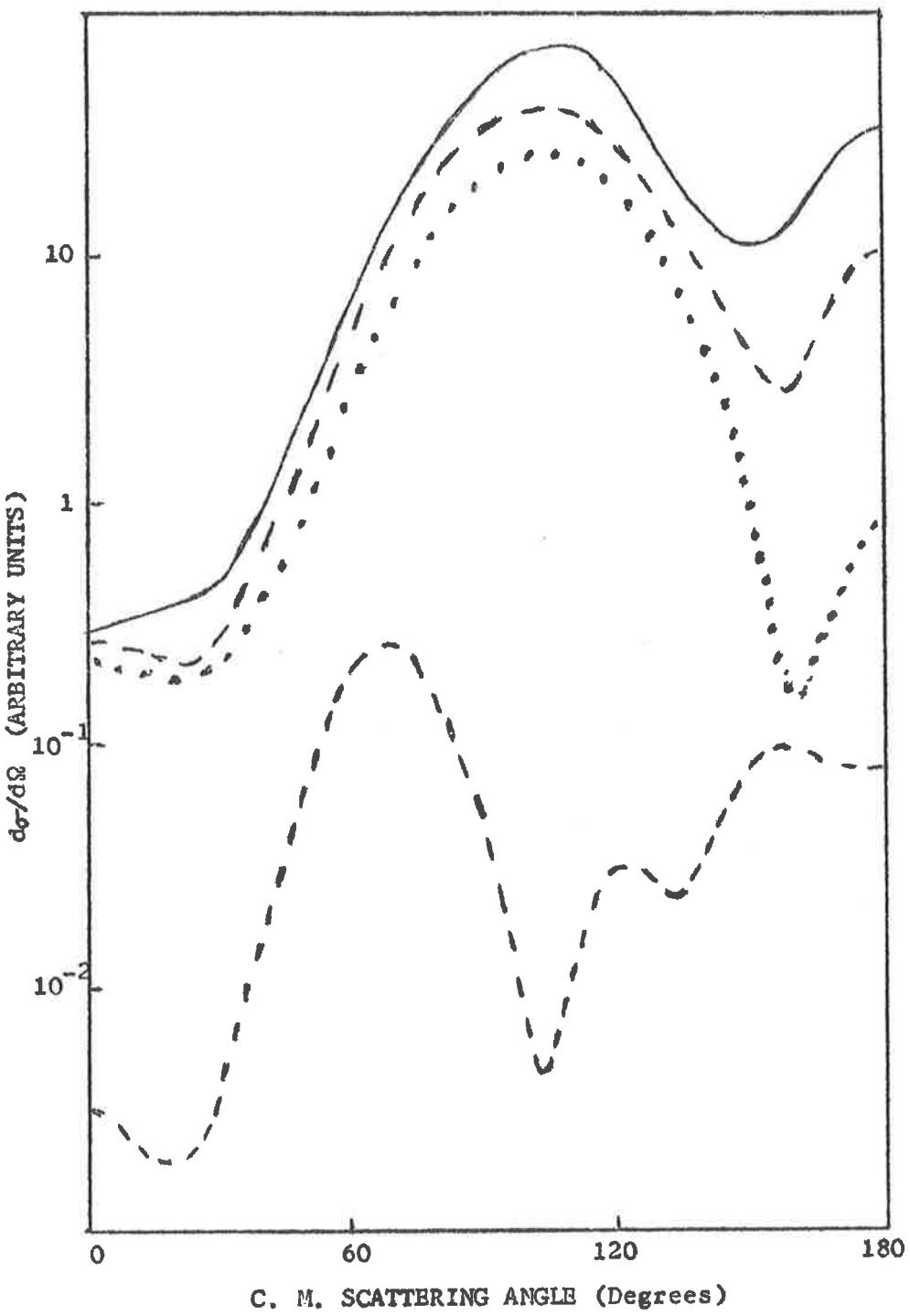
10
1
10^{-1}
10^{-2}
$d\sigma/d\Omega$ (ARBITRARY UNITS)
0
60
120
180
C. M. SCATTERING ANGLE (Degrees)

As shown in Figure 29, there are large differences between the volume and extreme surface (R_f = 5.4f, f = 0.0) results. However, if the cut off radius is reduced to R_f = 3.8f then irrespective of the value of the weighting, no evidence of the surface results appear. Consequently the interior of the nucleus as defined by this radius has no effect on the angular distribution for a volume reaction other than on the relative magnitudes of the backward peaks.

But this is expected because, as we have seen from the earlier sections, the foci of the optical model wave functions extend well into the nuclear interior and are critical in forming the backward peaking.

Finally, Figure 31 shows the 20 MeV results for a different surface weighting using a radius R_f = 4.4f and weighting the central region by 1/2 (continuous line) and by zero (the broken line).

These angular distributions are similar in structure to the surface results of Figure 29 in that peaks and minima occur at the same angles but differ not only in absolute magnitude but also in the relative heights of the peaks within the cross-sections. Figure 30 shows the curves for the intermediate band defined earlier. Also, as expected from the extreme cases, the parity rule is not clearly evident because the large angular momentum transfer involved in this reaction as well

FIGURE 31

The angular distributions for 20 MeV protons on Y^{89} leading to the first excited state. The continuous line is the result using a weight radius R_f = 4.4f and weight of 1/2, whereas the broken line weights the same region by zero.

Parameters used:-

$V = V = 40$ MeV

$W = W = 10$ MeV

$a = a = 0.6f$

$r_o = 1.2f$

$R_b = 5.4f$

$\mu = 0.87f^{-1}$

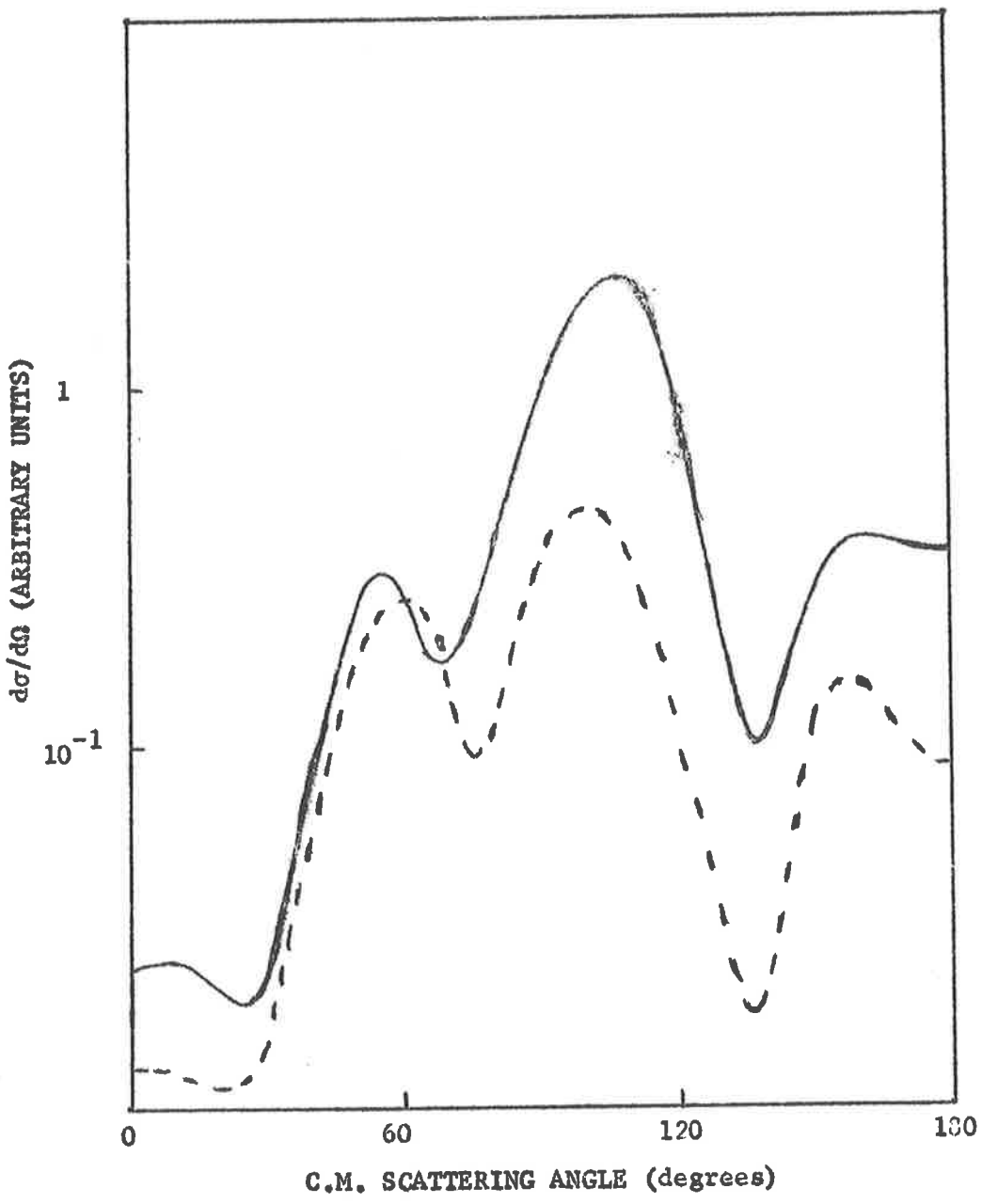
dσ/dΩ (ARBITRARY UNITS)
1
10^-1
0
60
120
180
C.M. SCATTERING ANGLE (degrees)

as the larger Q-value cause small deviations in the parity rule condition

Hence the conclusions drawn from the earlier calculations on F^{19} and C^{13} apply equally well in the heavier nuclei cases. Furthermore as discussed earlier we expect this Y^{89} reaction to be well described by the model we have used, save perhaps for the inclusion of the exchange character of the interaction, and therefore antisymmetrization of the wave functions, and the spin-orbit coupling in the optical model wave functions.

At present two things are being done in regard to this reaction. First, the experiments are being performed by the group at Davis, and second we are performing the final debugging of the extended version of the code described in the thesis which removes many time consuming operations and includes the space exchange term. This is being made as an intermediate step towards the complete D.W.B.A. code which will use a more realistic bound state description for other reactions as well as including the spin-orbit coupling and full exchange character in the two-body interaction.

CHAPTER 5 CONCLUSIONS

We have seen that the angular distributions for direct reactions via a two-body interaction mechanism are strongly influenced by the optical model effects of phase averaging and focussing. In particular, the extreme angle peaking can be qualitatively understood from the overlap of the foci in the optical model wave functions and the parity rule holds even for a realistic finite range form of the two-body interaction.

However the analysis of the results for the $C^{13}(p,n)N^{13}$ reaction to the ground state showed that the pure volume calculations were most inadequate in explaining the direct reaction features of the experimental results, namely the general energy variation of the backward cross-sections and the angular distributions that changed little in shape over an energy range of an MeV or so. But this situation was greatly improved through the introduction of a density dependence for the effective two-body force in nuclear matter by surface weighting, as, not only did this give the double peak in the energy variation of the backward cross-section but also the angular distribution shapes were far closer to the experimental results.

Of course, one may expect reduction of the nuclear interior contribution on two other grounds. First, the success of the non-local optical model potential in

reproducing elastic scattering indicates a correcting effect. As was shown by Satchler*[42] in the Padua conference, this potential causes a reduction of the nuclear wave functions in the nuclear interior by about 15% from the values generated by the local potential. However, we have seen that to produce the surface results, one needs a central weight far in excess of this. Second, the optical model can only be strictly believed beyond the matching boundary and by good extrapolation back to the nuclear surface region. Hence the significance of the internal wave function may be suspect. However, as shown in Section 3.2 the internal values of the wave functions for nucleons, especially in the heavier nuclei, has small and fairly constant value and there is an almost plane wave appearance about the phases. Now for the cases considered the bound state descriptions have small values in this region so that one can expect little contribution from the region well inside the nucleus in any event. However, it was also seen that the focus, which is formed by those partial waves arising from the nuclear surface and therefore from the region most critical in describing elastic scattering, extends into the nuclear interior. Hence we expect the nuclear interior to have contribution unless there exists some density dependence of the two-body force in nuclear matter.

The analysis of the reaction $F^{19}(p,p')F^{19*}$ to the first excited level, with a Q-value of -.11MeV and an angular momentum transfer L=1, has shown that there are significant differences between the volume interaction and the surface weighted calculations, and that there is a large range of surface weight parameters which give intermediate results. Hence it should be possible to experimentally observe a density dependence of the reaction mechanism.

This is in agreement with the evidence from doublet splitting*27 that the strength of the two-body force in shell model calculations decreases with increasing nucleon density, as one could expect in view of the Pauli Principle, and also to some extent with the recent experimental material of Clegg*44.

The most striking difference between the surface weighted and volume calculations in this reaction is the greater structure (more peaks) associated with the surface values. This difference persists over a large range of energies and is therefore more general than the distinction implied by the focus property of the backward peaks.

The appearance of a peak in the angular distributions at about 90° for incident energies between 10MeV and 20MeV seems to be a critical test of the surface weighting assumption. The inclusion of a spin-orbit potential (which accentuates the surface contribution)

into the optical model calculations, and also the inclusion of a more realistic two-body force, or of a different shape of the density dependence of the two-body interaction, is not expected to change this qualitative conclusion. Although the results of Agodi et al*[22,23] for the reaction $Si^{28}(n,p)Al^{28}$ have shown that an exchange character in the two-body interaction has a significant effect on the angular distributions, mainly on the extreme angle parts, it is not expected to dominate contribution from the nuclear interior, and hence surface and volume calculations should still exhibit differences.

The persistence of the differences between volume and surface calculations at high energies shows that no purely optical model effect, such as phase averaging, focussing or total internal reflection, makes the interior non-contributing. Therefore, we are tempted to conclude that any experimental evidence of surface weighting in a two-body reaction is caused by a density dependence of the reaction mechanism.

Further, the finite range form for the two-body interaction emphasises the nuclear surface more than the corresponding zero-range interaction, not only by spreading the effective bound states product but also by amplifying the phase averaging effect. However, despite this amplification, the phase averaging effect still does not remove all contribution from the nuclear

interior and the differences between the surface and volume calculations persist. Hence the general conclusions derived from the zero-range calculations remain.

As noted earlier, the absolute magnitudes of the cross-sections for a given reaction are not expected to be correct because of the bound state description used. However, this is not the case for the results for the inelastic scattering from Y^{89}. In this nucleus the j-j coupling shell model can be believed at least for the ground and first excited states and so should be a means of investigating the reaction mechanism.

We have seen from the first analysis of this reaction that the surface weighted and volume calculations exhibit differences in both zero and finite range results that are in keeping with the results derived from the lighter nuclei calculations namely that extra peaks appear in the surface calculations. Further this reaction involves a large angular momentum transfer and has a Q-value of nearly an MeV which we found to be limiting the parity rule effect. However, this apparent loss, or at least reduction, of the parity rule may be changed by the inclusion of the exchange properties of the interaction, so that further investigation of this has been left till the more complete code is developed.

LIBRARY OF THE UNIVERSITY OF ADELAIDE

APPENDIX

This Appendix describes the construction and calculation procedure of the direct interaction code used to find the results reported in this thesis. It is divided into four parts as listed:-

A. Description of Code

B. Results of a Typical Data Deck

C. Glossary of Symbols

D. Listing of Code

The code SCAT4 of Melkanoff, Saxon, Cantor and Nodvik has been used as the basis of our code. In SCAT4, the optical model wave functions and the elastic scattering results are calculated. Consequently, in the sections of this Appendix outlining routines of SCAT4, only a general outline is given along with changes that have been made.

Total Flow Chart

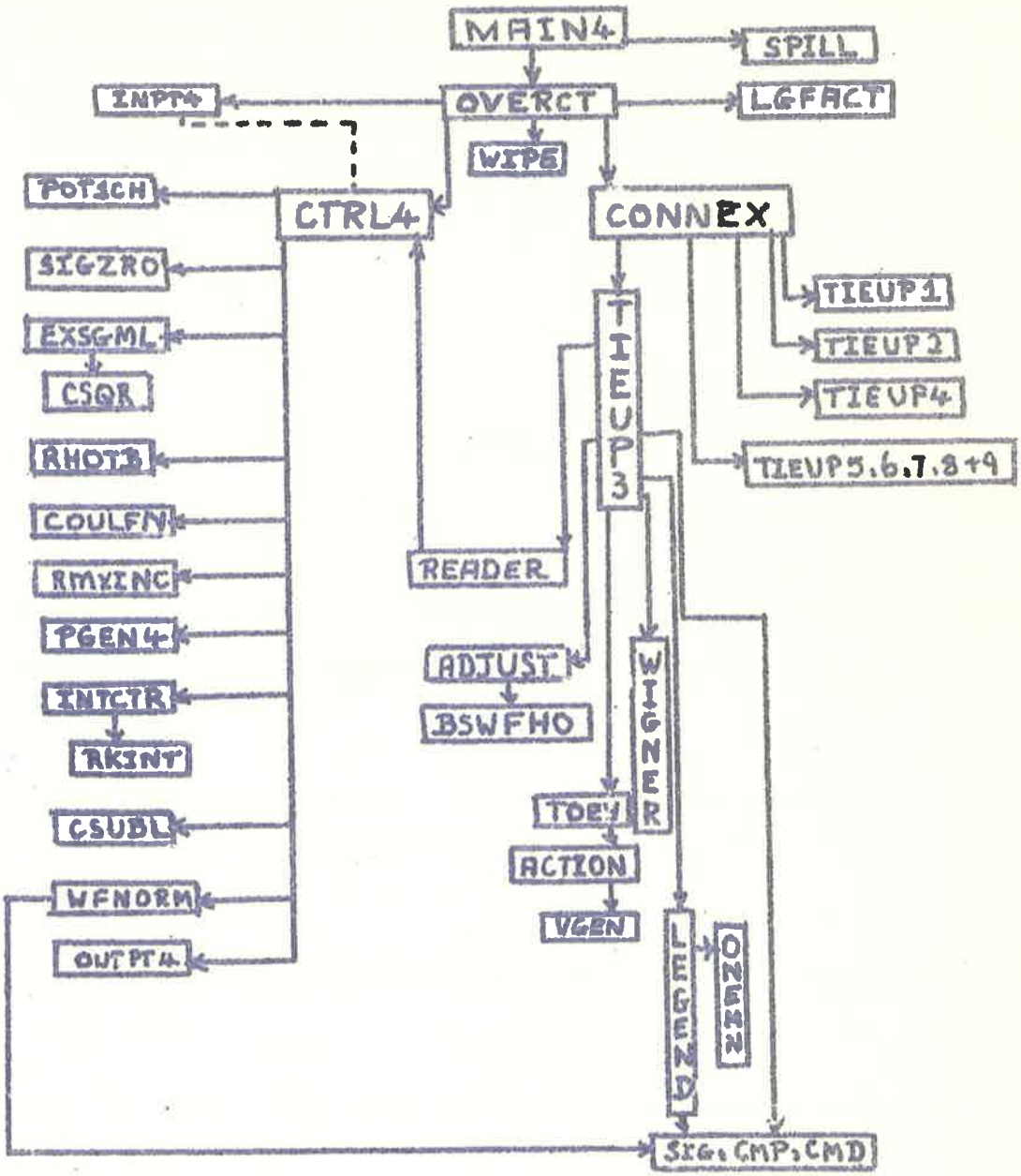

A. DESCRIPTION OF CODE

MAIN4

This routine is the commencement point of the calculation. When all variations and/or changes have been carried out and answers printed, the computation returns to this routine and the programme is terminated.

It calls the FAP routine SPILL (JSPILL,ISPILL,0.0,0.0) and this sets up a system by which underflow and/or overflow in any section of the code can be identified.

Then four test numbers are defined EPS1,EPS2,EPS3 and EPS4.

The first six cards of data (identification) are read, an instruction to the machine operators printed out on line, and the main directive routine OVERCT is called.

The program is then terminated.

NOTE - EPS1 and EPS2 are later used as the real and imaginary parts of the Yukawa interaction, but are always redefined before any further optical model wave function is calculated.

Data Used

NUMRUN(I),I=1,5

NUMRUN(1) = day

NUMRUN(2) = month

NUMRUN(3) = year

NUMRUN(4) = 0

NUMRUN(5) = 0 - This must be so for an ordered label of run numbers.

NUMPRG = 20 - gives print out of partial matrix elements.

Dimension and Common Requisites

JSPILL

ISPILL

EPS1 EPS2 EPS3 EPS4

NUMRUN(5)

NUMPRG

Statements require 85 locations in which to work.

OVERCT

This routine controls the pattern of the calculation and is divided into two parts:-

(a) Calls the routines that generate the incident particle wave function, the final wave function and the computation that uses these wave functions.

(b) Has control over parameter variation.

Has control over energy (of unbound particles) variation.

Has control over surface/volume calculation.

The calculations will be performed in the order of section (b) viz, for a given type of calculation (surface/volume) and given energy, all variations of parameters are performed.

The general pattern of OVERCT is as follows:-

(1) Calls LGFACT - this generates all log n! for n up to 50 (except (n = 0)).

(2) Calls INPT4 - this reads in all relevant incident particle data necessary to form the incident particle optical model wave function.

KSUPER is then set as 2 so that INPT4 is then side-stepped in the variations which follow.

NOTE - KSUPER is used to transfer LT, the angular momentum transfer, in the differential cross-section calculation to generate the two body interaction. It is reset to 2 after this use.

(3) Parameter variation is set up as follows:-

V/W, Real/Imaginary parts of central potential varied by amounts DV/DW, NVMAX/NWMAX times.

VS/WS, Real/Imaginary parts of spin orbit potential varied by amounts DVS/DWS, NVSMAX/NWSMAX times.

A - surface thickness parameter varied by amounts DA, NAMAX times.

(4) Calls CTRL4 which generates the normalised optical model wave functions for the incident particle. Then all incident particle data is set aside into temporary storage so that we can set the final particle data into the working storage locations. These temporary locations are not in common or dimension as they are only used in this routine.

(5) The final wave function is calculated and the differential cross-section is formed by calling CØNNEX. If we are performing the first run of parameters these are set into storage so that we can recalculate the same parameter variations for a different energy or type of calculation, starting with the first values that were defined by the input data.
We also change the value of RG so that subroutine READER will not attempt to read in data after the very first calculation has been performed. However, the value of RG only sidesteps cards that read in data in READER, hence, all energy dependent quantities for the final particle are calculated for every run.
This is not so for the incident particle quantities, as INPT4 is completely sidestepped. Consequently, energy dependent incident particle data are recalculated in this routine for every energy variation and many energy dependent final state quantities do not need to be allocated temporary

storage for the parameter variation.

NOTE - Using RG in this way prohibits the use of a Gaussian shaped central well, i.e. KTRL(1) must never be 1.

(6) The final particle data is reset into its temporary locations and the incident particle data is replaced into the working locations. Further, all relevent quantities originally calculated in INPT4 are recalculated here. Following this, the subroutine WIPE, which resets the matrix element locations to zero values, is called and the parameter variation loops are closed.

(7) The energy variation is now performed. In this section the lab. energy of the incident particle is changed by a positive amount, DELAB. The final particle lab. energy is redefined so that the Q-value of the reaction is unchanged.

NOTE - READER reads in the Q-value and calculates the final particle's lab. energy, but the Q-value (QVAL) is not in common storage.

The incident particle energy-dependent quantities are redefined and cross-sections calculated until the value ELAB of the incident particle exceeds the input quantity EFIN. However, the first values of energy used are kept in temporary storage, so that the energy (and parameter) variations will all be reperformed if calculations with differently weighted central regions are required.

(8) Finally, this routine permits repetition of the above variations, weighting the central region of integration (out to a radius value RADWC) by an amount $(WF)^2$. This is done in the

calculation of the bound state radial wave functions with each wave function weighted by WF for all radii less than or equal to RADWC. The central weighting calculations will be performed ISP1 times, each run using a weight value reduced by ISP3 percent of the initial weight value from the value of WF used in the previous run. The calculations are concluded by returning to MAIN4, if ISP1 variations have been performed or the value of WF has become negative.

NOTE (i) This does not accept a single surface run unless ISP3 = 0 because, if not, the WF will always be zero and we can never exit from the weighting loop.

NOTE (ii) The single location RENMZ(100) is used to transfer the first used lab. energy of the incident particle to other subroutines.

Data Used - Nil

Dimension and Common Requisites

KSUPER

NV	NW	NVS	NWS	NA	
NVMAX	NVMAX	NVSMAX	NWXMAX	NAMAX	
TV	TW	TVS	TWS	TA	
V	W	VS	WS	A	
DV	DW	DVS	DWS	DA	
KTRL(13)					
RHØIN(NMAX)	NMAX	FKAY	ECM	LMAXM	ISP1
FMI	ELAB	LMAX	NMAXP	RG	ISP3
FMB	RENMZ(100)	BG	CØ2	DELAB	ISPILL
ZZ	RC	RO	FIP	FMU	ETA

EFIN JSPILL RHØBN RHØBC DRHØIN(NMAXP)

Statements require 716 locations in which to work.

Flow of OVERCT

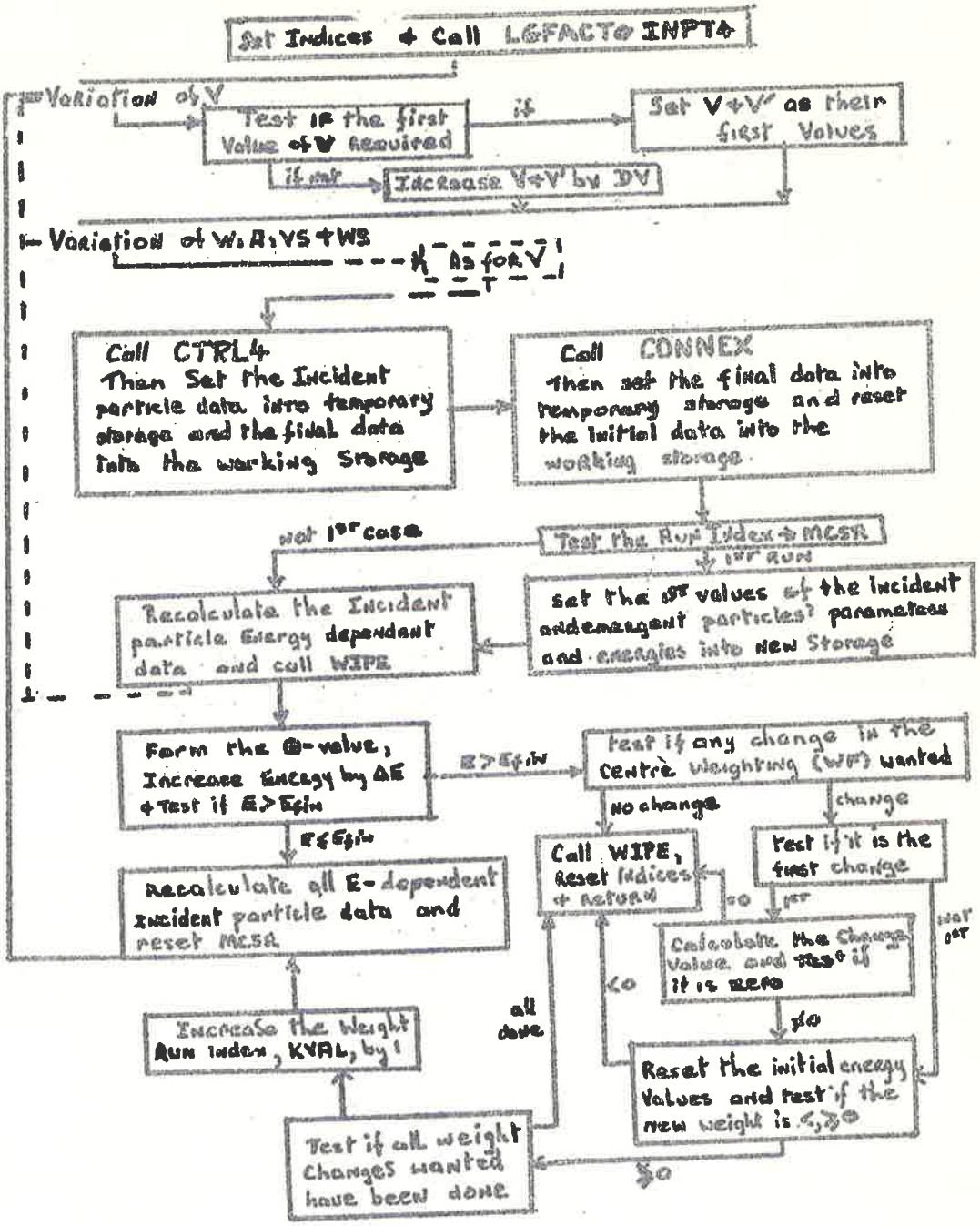

CTRL4

This controls the order of the operations which generate an optical model wave function normalised to the extent that each partial wave function is matched to a linear combination of coulomb or bessel functions for a proton or neutron respectively. This matching occurs at a boundary, RHØMAX, sufficiently far removed from the nucleus so that the non-coulomb part of the potential is negligible.

The run number identification is changed by 1 every time CTRL4 is called. This means it will be increased by two for each differential cross-section calculation. The run number is therefore decreased by one for each cross-section print out so that identification is in integer order.

Data Used - Nil

Dimension and Common Requisites

KSUPER

NUMRUN(5)

KTRL(13)

Statements require 92 locations in which to work.

INPT4

This routine inputs all basic data necessary for the evaluation of the initial particle optical model partial wave functions. It is used only once in the matrix element code as it stands at present, i.e. once for a given target and projectile. We can still vary energy, parameters and weight some central region in some way as well as eliminating the central region contribution alltogether, without needing a new set of input data.

Data Used

KTRL(13)

FMI	FMB	ELAB	ZZ	RC	V	W
A	RO	VS	WS	RG	BG	
DV	DW	DA	DVS	DWS	DBG	
NVMAX	NWMAX	NAMAX	NVSMAX	NWSMAX	NBGMAX	
DELAB	EFIN					
ISP1	ISP2	ISP3	ISP4			
NMAX						
RHØIN(NMAX)		DRHØIN(NMAXP)		NMAXP = NMAX - 1		
LMAXM						

Dimension and Common Requisites

All the above data and -

TV	TW	TA	TVS	TWS	TBG	
FMU	ECM	FKAY	RHØBN	RHØBC	RHØBNG	ETA
IIN(LMAX)						
LMAX						
NMAXP						

Statements require 346 locations in which to work.

PØT1CH

This routine checks the values of LMAX, the number of partial waves specified by data, and RHØMAX, the boundary at which the wave functions are to be matched, so that -

(1) All partial waves sensibly affected by the potential are included in the calculation.

(2) The non-coulomb part of potential is negligible at this boundary.

Both these checks, one of them or neither of them, are performed depending on the input value of KTRL(13).

KTRL(13) = 1 Routine checks both ρ max and lmax

2 Routine checks only ρ max

3 Routine checks only lmax

4 Routine is sidestepped altogether

The form of this routine is just as is specified in the code SCAT4. The checks used depend on what type of potentialis to be used (but, now we cannot use the Gaussian form).

Briefly, this routine operates in the following way:-

(1) Find the maximum values of all potentials to be used.

(2) If KTRL(1) = 0 $\rightarrow$ Saxon Well potential

using S = ρ max

P = lmax

C = Vmax

D = Wmax

X = VSmax

Y = WSmax

Check max by:- $[C^2+D^2]^{1/2} / \{E_{CM}[1+\exp((S-\bar{\rho}_N)/ha)]\} \leq \varepsilon_4$

Check lmax by the above test with p in place of s, and also by:-

$$[X^2+Y^2] / \{E_{CM}[1+\exp((P-\bar{\rho}_N)/ka)]\} \leq \varepsilon_4$$

KTRL(1) = 2 → Square Well

check ρmax by, ρmax $\geqslant \bar{\rho}$N - the RHØ corresponding to the nuclear surface

lmax by lmax $\geqslant \bar{\rho}_N + 3$

If any condition is not met, then a print-out to this effect occurs, and the tests are reapplied with the values of ρmax and/or lmax increased by $\Delta\rho_{last}$ and 1 respectively.

For a more explicit discussion of routines like this, that are developed from SCAT4, the reader is referred to the write up of SCAT4 by MELKANOFF et al.

NOTE - If a square well is used, the surface thickness should not be taken as zero. It does not enter the calculation except in an irrelevant way, but in this it will cause an overflow if taken as zero.

Data Used - Nil

Dimension and Common Requisites

IKTRL

FKAYA

FKAYB

Statements require 636 locations in which to work.

SIGZRØ

This isthe SCAT4 routine that generates the coulomb phase shifts for 1 = 0, 1, from the following expressions:-

If $$\alpha = \{ \tan^{-1}\eta + \tan^{-1}(\eta/2) + \tan^{-1}(\eta/3) \}$$

$$\beta = \left[1 - \frac{(\eta^2-48)}{30(\eta^2+16)^2} + \frac{(\eta^4-160\eta^2+1280)}{105(\eta^2+16)^4} \right]$$

η = coulomb parameter

Then

$$\sigma_0 = \arg\Gamma(1+i\eta)$$

$$= -\eta + \tfrac{\eta}{2}\log_e(\eta^2+16) + \tfrac{7}{2}\tan^{-1}(\eta/4) - \alpha - \beta\eta/12(\eta^2+16)$$

and

$$\sigma_1 = \sigma_0 + \tan^{-1}\eta$$

All other σ_l can be calculated with these.

Data Used - Nil

Dimension and Common Requisites

SIGMA0

SIGMA1

Statements require 204 locations in which to work.

EXSGML

This routine is used to calculate $e^{i\sigma_\ell}$. In this, the subroutine CSQR(A,B,C,D), which finds the $\sqrt{(A+iB)} = C+iD$ is applied to the SCAT4 calculation of $e^{2i\sigma_\ell}$ in its real and imaginary parts.

Data Used - Nil

Dimension and Common Requisites

EXSGMR(L) EXSGMI(L) L=1,LMAX

Statement requires 190 locations in which to work.

RHØTB

This is the SCAT4 routine that generates the table of points $\rho_i = kr_i$ at each of which the solutions of the Schroedinger equation for the inelastic Scattering problem will be calculated.

It also forms a table of spacings between these points and can vary the last spacing of the table so that any uneven (in spaces) ρ max can be reached.

The table is constructed from the basic set of values read in INPT4.

e.g. the case of NMAX = 3.

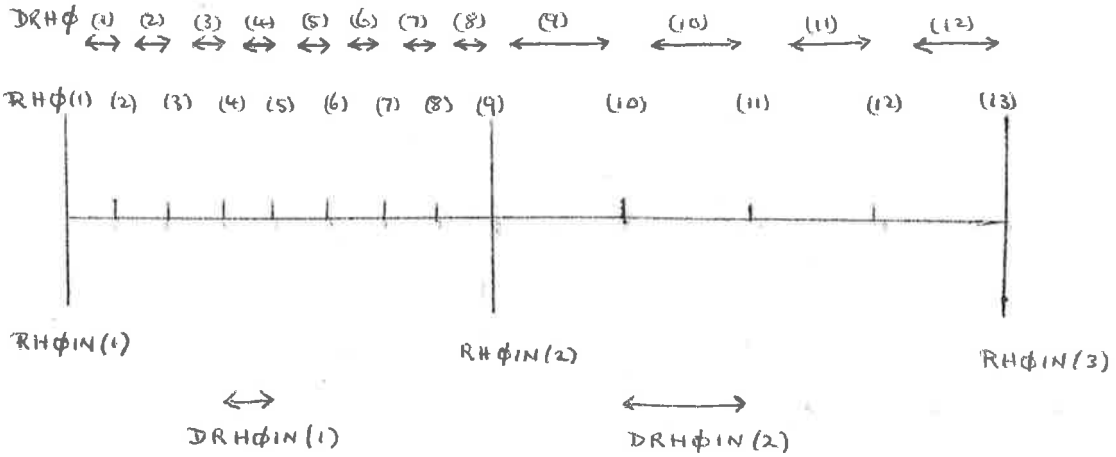

Data Used - Nil

Dimension and Common Requisites

RHØ(I) I=1,IIAST

DRHØ(I) I=1,IIAST-1

RHØIN(J) J=1,NMAX

DRHØIN(J) J=1,NMAXP

IIAST NMAXP RHØMAX NMAX DRHØL

Special Notes

The first value of ρ (RHØ(1)) will not be the first stored point corresponding to first stored value of wave functions (see RKINT).

Statements require 165 locations in which to work.

CØULFN

This is a sub-routine from SCAT4 in which are calculated the regular and irregular coulomb wave functions and their derivatives, for all l values needed (by PØTICH), at the boundary $\rho = \rho$ max. These will be used to normalize the solutions of the Schroedinger equation.

A brief outline of the basic steps in this routine follows:-

The first calculations for large ρ and l=0 and 1, are the assymptotic forms of the coulomb functions:-

$$F_{0,1} = Sin\left[Re(\phi_{0,1})\right] \exp\left[-\mathcal{I}m(\phi_{0,1})\right]$$

$$G_{0,1} = Cos\left[Re(\phi_{0,1})\right] \exp\left[-\mathcal{I}m(\phi_{0,1})\right]$$

Where -

$$\phi_0 = \rho - \eta \log_e(2\rho) + \sigma_0 + \sum_{k=2}^{\infty} \frac{\alpha_k}{(1-k)\rho^{k-1}}$$

$$\phi_1 = \rho - \eta \log_e(2\rho) + \sigma_1 - \pi/2 + \sum_{k=2}^{\infty} \frac{\beta_k}{(1-k)\rho^{k-1}}$$

and if -

$$\alpha_1 = \eta = X_1$$

$$\alpha_2 = \eta^2/2 + i\eta = X_2$$

for the α series

and -

$$\beta_1 = \eta = X_1$$

$$\beta_2 = -1 - \eta^2/2 + i\eta/2 = X_2$$

for the β series, these series are found from the recurrence relation

$$X_k = -\frac{1}{2} \sum_{m=1}^{k-1} X_m X_{k-m} - i(k-1) X_{k-1}/2$$

These assymptotic values are then used to give an accuracy check on the recurrence relations for the coulomb functions.

The irregular functions $G_1(\rho max)$ can be computed by the forward recursion -

$$G_{l+1} = (2l+1)\ \frac{[\eta + (l(l+1)/\rho_{max})]G_l - (l+1)\sqrt{l^2+\eta^2}\,G_{l-1}}{l\sqrt{(l+1)^2+\eta^2}}$$

The regular functions must be computed by a backward recursion having a formula as for G_1 above.

Then when an accurate set of $G_1(\rho\,max)$ has been found the derivatives are formed via:-

$$X_l' = \frac{[\eta + (l+1)^2/\rho_{max}]\,X_l - \sqrt{\eta^2+(l+1)^2}\,X_{l-1}}{l+1}$$

The computation is as follows:-

(a) Calculate the α and β series and if:-

$$U_k = \alpha_k / [(k-1)\,\rho_{max}^{k-1}]$$

then the following tests are performed:-

Test 1

$$[Re\,(U_{N+1})]^2 + [Im\,(U_{N+1})]^2 = |U_{N+1}|^2 > |U_N|^2$$

Test 2

The contributions of both the real and imaginary terms eventually must give negligible changes in Φ_0, Φ_1 .

Test 3

The series must not diverge too quickly.

Test 4

The series must not converge too slowly. (i.e. that the series do not need more than 48 terms).

(b) Form the assymptotic quantities, and check that the Wronskian ω satisfies:-

$$| \omega - \sqrt{1+\eta^2} | = | F_0 G_1 - F_1 G_0 - \sqrt{1+\eta^2} | \leqslant \varepsilon_1$$

(c) Perform a backward recursion to get the regular coulomb functions F_ℓ and check if:-

$S = F_\ell$ found by the n^{th} recursion

$T = F_\ell$ found by the $(n+1)^{th}$ recursion

$$|S/T - 1| \leqslant \varepsilon_2$$

(d) Perform the forward recursion giving the irregular functions G_ℓ and check if:-

$$| F_\ell G_{\ell+1} - F_{\ell+1} G_\ell - (\ell+1)\sqrt{\eta^2 + (\ell+1)^2} | \leqslant \varepsilon_3$$

(e) Calculate the derivatives of these functions, F_ℓ', G_ℓ'.

Data Used - Nil

Dimension and Common Requisites

IKTRL	ETA2	L	DRHØL	
AR(75)	AI(75)	FBAR(J) J up to LMAX+40		
F(L)	G(L)	FP(L)	GP(L)	L=1,1MAX

Statements require 1135 locations in which to work.

RMXINC

This sub-routine, as in SCAT4, enables us to increase the table of ρ and $\Delta\rho$ if the value of ρ max had been increased to give the correct generation of the coulomb functions. Any increase is done by increments of $\Delta\rho$(ILAST) until the modified value of ρmax is reached.

Statements require 36 locations in which to work.

PGEN4

This is a SCAT4 routine that calculates and stores the required values of the potentials at all the tabled points ρ_i, and at all midpoints of the ρ_i. Actually it generates the 1-independent sections of the various potentials, and stores them in the following locations:-

UCRB(I), UCIB(I) and UCRM(I), UCIM(I)	Real and imaginary parts of 1-independent section of the central potential at points ρ_i and $(\rho_i + \frac{\Delta\rho_i}{2})$.
USRB(I), USIB(I) and USRM(I), USIM(I)	As above for the spin-orbit potential.
FFCR(I), FFCI(I) and FFCRM(I), FFCIM(I)	Real and imaginary parts of the form factor used on the central potential at the same points as above.
FFSR(I), FFSI(I) and FFSRM(I), FFSIM(I)	As for FFCR etc. for the spin-orbit form factor.

Now it is here that KTRL(1) operates and chooses what form of potential will represent the nucleus. Furthermore, although in SCAT4 there is a facility for having a wide range of shapes of the nuclear surface, we have eliminated this, leaving only the standard Saxon form-factor.

Data Used - Nil

Dimension and Common Requisites

UCRB(I)	USRB(I)	UCRM(I)	USRM(I)	FCR(I)	FFSR(I)
FFCRM(I)	UCIB(I)	USIB(I)	UCIM(I)	USIM(I)	FFCI(I)
FFSI(I)	FFCIM(I)	FFSRM(I)	FFSIM(I)		I=1,1LAST

RHØM

Special Note

At present KTRLS(7).....(12) all must be zero, otherwise the program stops.

Statements require 715 locations in which to work.

INTCTR

This sub-routine controls the flow pattern of computation over the routine RKINT. It sets up the initial data necessary to perform the integration of the Schroedinger equation, and, on completion of the integration for a given partial wave, it stores the value of the wave function and its derivative at the boundary ρ max. These are used later to normalize all the values of this wave function at the different ρi . It is at this point that the spin-orbit potential is omitted, i.e. we store only the $\underset{\sim}{s}.\underset{\sim}{l} = 1$ function and use Vs = Ws = 0.0.

Data Used - Nil

Dimension and Common Requisites

IFIRST	XC1	XCP1	YC1	YCP1	X1(L)	X1P(L)
	XD1	XDP1	YD1	YDP1	Y1(L)	Y1P(L)

Statements require 84 locations in which to work.

RKINT

This is the sub-routine that performs a Runge-Kutta integration procedure on the Schroedinger equation. We have only modified the SCAT4 version so that all wave functions at points ρ_i are stored and their corresponding values of ρ have the same index number. Also the SCAT4 version has a renormalization procedure that prohibits overflow in the machine. If any such process occurs we store its value along with the value of ρ_i at which it occurred.

NOTE - The renormalization procedure is such that there must always be at least one point used (because, later, we have DØ I = 1, NEND, therefore, NEND $\geq$ 1). So, if no renormalization occurs, we define NEND = 1

RØE(1) = 2* max

RENMZ(1) = 1.0.

NOTE - the points ρ_i corresponding to the stored wave functions are now stored in RØSP(I).

Data Used - Nil

Dimension and Common Requisites

ISP1	RENMZ(J)	J=1,NEND	RØE(J)
RØSP(I)	XCS(I,L)	YCS(I,L)	
I=1, IEND	L=1,LMAX		

Statements require 871 locations in which to work.

CSUBL

The sub-routine generates the matching coefficients c_1, needed in the normalization of the wave function values calculated in RKINT. The c_1 are found from -

$$\frac{\Psi_\ell'}{\Psi_\ell} = \left. \frac{F_\ell' + C_\ell [G_\ell' + i F_\ell']}{F_\ell + C_\ell [G_\ell + i F_\ell]} \right|_{\text{at } \rho = \rho_{max}}$$

where Ψ_ℓ, Ψ_ℓ' are the boundary values of the wave functions X1(L), Y1(L), X1P(L), Y1P(L) stored in INTCTR, the F_ℓ, G_ℓ, F_ℓ', G_ℓ' are coulomb functions and the primes denote differentiation with respect to ρ, i.e. at some point, far enough removed from the nucleus so that the coulomb field alone influences a particle, the wave function describing this particle is a linear combination of the regular and irregular coulomb functions.

This logarithmic matching is obviously independent of the normalization of the solutions of the Schroedinger equations.

Data Used - Nil

Dimension and Common Requisites

CR1(L) CI1(L) L = 1,LMAX

Statements require 261 locations in which to work.

WFNØRM

This sub-routine normalizes the stored wave functions. In fact, this routine only normalizes the radial part of the complete partial wave expression:-

$$\Phi = \Sigma_l [4\pi(2l+1)]^{1/2} i^l e^{i\sigma_l} f_l(\rho) Y_{l,0}(\Omega)$$

The integration in RKINT calculates $\chi_l(\rho) = A\rho f_l(\rho)$. Hence here we want to calculate $\chi_l(\rho)/A\rho$. Defining the renormalization procedure values by R (i.e., from the overflow prevention section in RKINT), this normalization is:-

$$f_l(\rho_j) = \prod_{i \text{ w.r.to } j} R_i \left[\frac{F_l + C_l [G_l + i F_l]}{\chi_l} \right]_{\rho=\rho_{max}} \frac{\chi_l(\rho_j)}{\rho_j}$$

Where $\prod$ means that, whenever the point at which a renormalization occurred in RKINT, ρ_i , is greater than ρ_j , the wave function is further modified by this renormalization value, R_i .

Data Used - Nil

Dimension and Common Requisites

All as before

Statements require 378 locations in which to work.

FLOW of WFNORM

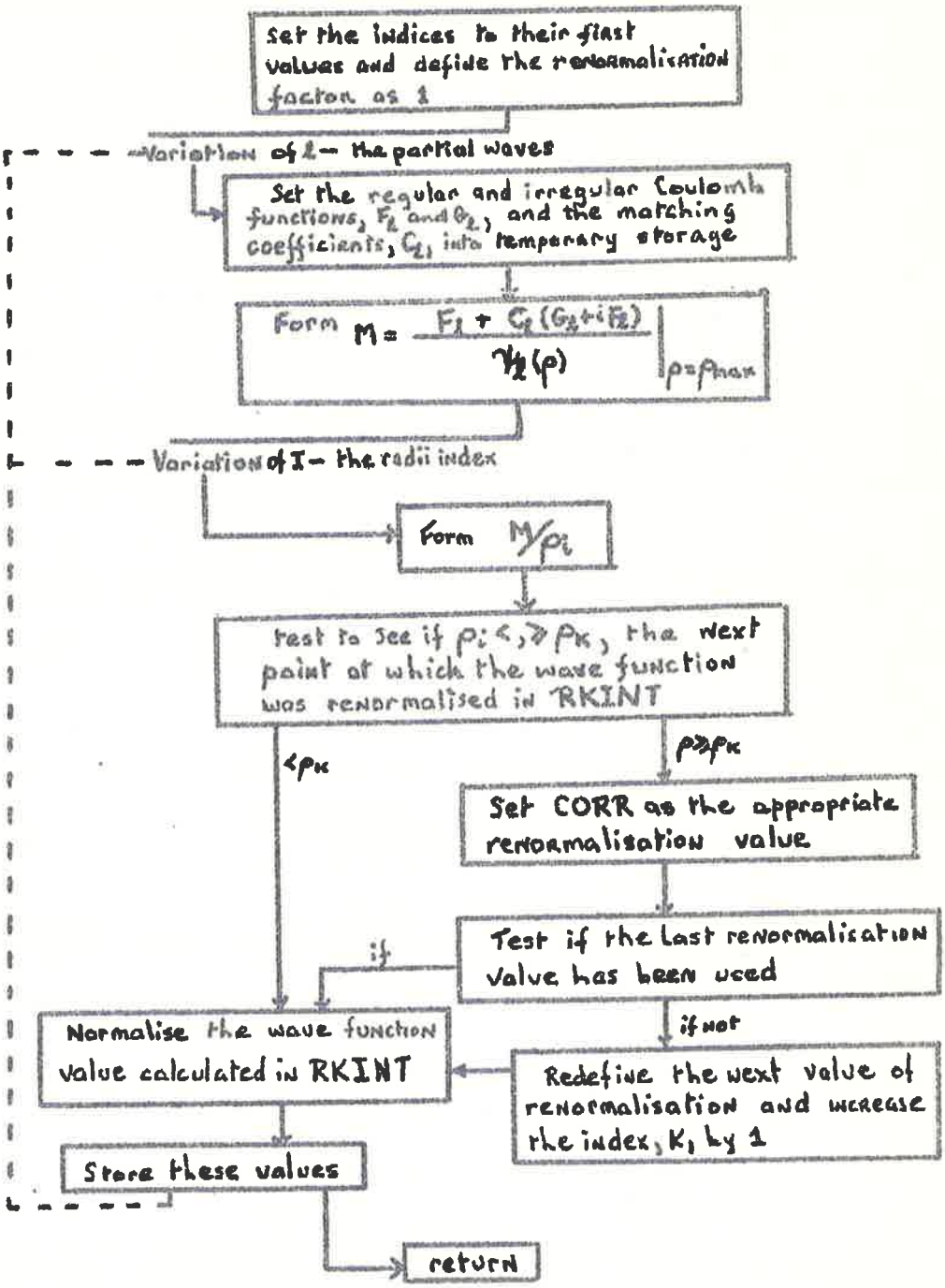

OUTPT4

This sub-routine prints out the data relevant to each optical model wave function calculation. This is dependent on whether KTRL(2) = 1 or not. If KTRL(2) = 1, then a print out occurs. Furthermore, it prints out appropriate headings for the different data and keeps NUMRUN(5) increasing only by 1 for each complete cross-section calculation.

Statements require 308 locations in which to work.

LGFACT

This sub-routine is first called in ØVERCT and generates the logarithms of all factorials from n = 1 to 51.

e.g. $FG(3) = \log_e 3! = \log_e 6 = 1.7918$

Log n! is used so that any possible multiplication or division of a set of factorials will not cause overflow at any stage. This is especially so in generating Clebsch-Gordan coefficients.

NOTE - We cannot use 0! To overcome this the following expression is used:-

$\log n! = \log (n+1)! - \log (n+1)$

Data Used - Nil

Dimension and Common Requisites

FG(51)

Statements require 42 locations in which to work.

SPILL (JSPILL, ISPILL, 0.0.0.0)

This sub-routine is a FAP section operative throughout the program and pinpoints the location in the machine at which underflow or overflow occurs. If underflow occurs, this routine shows where and replaces the small quantity by zero and allows the program to continue (See SCAT4).

Statements require 53 locations in which to work.

CSQR(E6, E7, E8, E9)

This evaluates -

(E6+iE7) = E8+iE9

This is done by forming the modulus and phase φ of the complex number.

Statements require 161 locations in which to work.

ØNEMN(NN, ZP)

This evaluates $(-)^{NN}$ for NN a positive or negative integer.

Statements require 73 locations in which to work.

SIG(NN, II, JJ)

This evaluates $(i)^{NN}$ for NN a positive or negative integer.

NOTE - This routine outputs the real or imaginary sign coefficient in FIXED PØINT form.

Statements require 134 locations in which to work.

CMP(AU, B, C, D, RL, UR)

This computes the complex product -

RL + iUR = (AU + iB) (C + iD)

hence

RL = AU*C - B*D

UR = B*C + AU*D

Statements require 59 locations in which to work.

CMD(A1, B, C, D, RL, UR)

This computes the complex division -

$$RL + iUR = \frac{A1 + iB}{C+iD}$$

hence

$RL = (A1*C + B*D)/(C^2 + D^2)$

$UR = (B*C - A1*D)/(C^2 + D^2)$

Statements require 70 locations in which to work.

CØNNEX

CØNNEX is the routine that controls what calculation is to be done. It does this by reading in a set of control numbers KCØNT(I) I=1,9 if RG $<$20.0. (For the parameter or energy variations or the varied weight calculations, ØVERCT will put RG $>$20.0 thereby sidestepping this input reading).

The subroutine then tests these numbers in the order I=1 up to 9. If any of them are one, e.g. say for I=J KCØNT(J) = 1, then the corresponding TIEUP will be called, e.g.

TIEUP"J" where "J" is an integer.

KCØNT(1) = 1 - form $|\psi_\ell|\, e^{i\delta_\ell}$ for the incident particle (call TIEUP1).

KCØNT(3) = 1 - form $\eta(m_j, \theta)$ (call TIEUP3)

KCØNT(4) = 1 - form $d\sigma(\theta)/d\Omega$ (call TIEUP4)

Data Used

KCØNT(I) I = 1,9

Dimension and Common Requisites

KCØNT(9)

Statements require 127 locations in which to work.

TIEUP1

This sub-routine is called if KCØNT(1)=1, and prints out the incident particle wave function in the form $|\psi_\ell| e^{i\phi_\ell}$ (ϕ_ℓ referred between $\pm\pi$) where -

$$|\psi_\ell| = (2\ell+1)\,|f_\ell(\rho)|$$

(partial normalised) as from WFNØRM.

These values are printed out in blocks of 4, e.g.

RHØ	MØD	PHS	L=0	MØD	PHS	L=1	MØD	PHS	L=2	MØD	PHS	L=3
(1)	x	x		x	x		x	x		x	x	
(2)	x	x		x	x		x	x		x	x	
etc.	etc.			etc.			etc.			etc.		

Also if KCØNT(9) > 5, the potential well shape that has been used, is printed out.

Statements require 673 locations in which to work.

TIEUP2

This performs no calculation and is present if any incident particle quantity (e.g. elastic scattering) is to be coded.

TIEUP3

This is the routine that computes the matrix element for an inelastic scattering process by a direct reaction mechanism using distorted unbound particle wave functions, i.e. we compute

$$\eta = \langle \psi_f \phi_f | V_{int} | \psi_i \phi_i \rangle$$

which by using a partial wave expansion in the unbound particles wave functions is -

$$\eta(m_j, \theta_{sc}) = \sum_{\ell\ell'}' (4\pi)^{3/2} i^{\ell-\ell'} \exp i[\sigma_\ell + \sigma_{\ell'}] \quad (2\ell+1)$$

$$\times \left[\frac{(2j+1)}{(2j'+1)(2\ell'+1)}\right]^{1/2} \sum_{L}' (2L+1) \mathcal{R}_{\ell L \ell'} \quad C^{-\frac{1}{2}\ 0\ -\frac{1}{2}}_{j\ L\ j'}$$

$$\times C^{0\ 0\ 0}_{\ell\ L\ \ell'} \sum_{M}' C^{0\ -M\ -M}_{\ell\ L\ \ell'} \quad C^{m_j\ M\ m_{j'}}_{j\ L\ j'} \quad Y^{*}_{\ell',M}(\theta_{sc})$$

where σ_ℓ, $\sigma_{\ell'}$ are the coulomb phase shifts.

$\mathcal{R}_{\ell L \ell'}$ = Radial integral

$$= \int_0^\infty r_1^2 dr_1 \int_0^\infty r_2^2 dr_2 \; f_\ell(\rho_1) \, f_{\ell'}(\rho_1) \, R_{np}(r_2) \, R_{n'p'}(r_2) \, V_L(r_1, r_2)$$

where $f_\ell(\rho)$, $f_{\ell'}(\rho)$ are the partially normalized optical model functions and R_{np}, $R_{n'p'}$ the bound state wave functions, n, n′, p, p′ being the initial and final state prime and orbital angular momentum quantum numbers. $V_L(r_1, r_2)$ is the two body interaction.

$C^{m_1\ m_2\ m_3}_{j_1\ j_2\ j_3}$ = Clebsch-Gordan coefficients

$Y_J^{M_J}(\theta)$ = Normalised spherical harmonic.

As yet we have not included the exchange operator, which in effect puts in the antisymmetry of the wave functions. This extension will be included when we also consider spin-orbit coupling in the optical model.

NOTE - The matrix element above is only dependent on the scattering angle θ_{sc} and m_j - the initial bound state projection quantum number. The final state projection quantum number is not a variable in this case because of the Sum rule in the coefficient $C_{jLj}^{m_j.Mm'_j}$, i.e. m'_j is fixed for each m_j and M by $m_j+M=m_j$. This also effects the formation of the differential cross-section (see TIEUP4).

Before this routine is used, the initial unbound particle wave functions, and all quantities relevant to this, must have been calculated.

The routine then follows this pattern:-

(1) Store the following in new locations:-

(a) The Incident particle wave function for all l and $\rho_j = kr_j$

(b) The Coulomb phases, $e^{i\sigma_l}$, for all l.

(c) The Values of l_{max} and k_i.

These are placed in the locations XCST(I,L), YCST(I,L) RSGML(L), USGML(L), LIP, FIP respectively.

(2) Call READER. This inputs the final particle data (for the first calculation of all variations to be performed in one data deck). Then it calculates the energy dependent quantities and recalls CTRL4 to generate the final particle optical wave functions. This routine inputs the scattering angles and

redefines the basic ρ values by $\rho_i' = \frac{k_f}{k_i}\rho_i$ - which allows the final particle wave functions to be calculated at the same radii, r, as were the initial particle wave functions.

(3) Call ADJUST - This redefines the indexing of the stores wave functions so that even spacing in r is achieved. It also defines a table of these radii and finally calculates the bound state wave functions and their products at these radii.

(4) The matrix element computation is then begun and summation of 1, 1′ initiated. The 1,1′ dependent terms are formed

$$TERI = (2l+1)\left[\frac{(2j+1)}{(2j'+1)(2l'+1)}\right]^{1/2}$$

and puts $e^{i\sigma_l}, e^{i\sigma_{l'}}, i^{l-l'}$ into temporary storage.

Then if 1 and 1′ both are greater than 4, the routine checks whether $(21+1)|f_l|^2 + (21'+1)|f_{l'}|^2 \lesssim SN\emptyset 1$ at the nuclear surface (f_l - optical model wave functions, SNØ1 is a small test number read in from data). If this is the case, a print out occurs and the 11′ term is not calculated further and the next 11′ calculation begins.

Then the products of the two optical model wave functions and of the two bound states are found.

(5) The summation of angular momentum transfer, L, is begun, and selection rules are tested. They are:-

$$1+1+L \equiv \text{even}$$

$$|j-L| \lesssim j' \lesssim j+L$$

$$p+p+L \equiv \text{even}$$

$$|1-L| \lesssim 1' \lesssim 1+L$$

If these are not satisfied, the calculation of the next term contribution to the Summation is begun.

If they are all obeyed, the 1,1′ and L dependent part of the matrix element is formed, the integral having been performed in TØEY with KSUPER used to transfer the angular momentum values and reset to the value 2 after the integral had been calculated.

$$R + iU = (4\pi)^{3/2}\, i^{l-l'} \exp[i(\sigma_l + \sigma_{l'})]\ \text{TERI}$$

$$\times (2L+1)\, R_{lLl'}\, C^{000}_{lLl'}\, C^{-\frac{1}{2}0-\frac{1}{2}}_{j_L j_{j'}}$$

(6) Then the summation over the projection numbers of the angular momentum transfer is performed, and includes the variation of m_j- the initial bound state (projection) quantum number, and θ_{sc}- the Scattering angles.

The matrix element $\eta(m_j, \theta_{sc})$ is then stored in the locations.

WFMØD(M,J), PHASE(M,J) -[Real and Imaginary parts of η]

In this section we also have the facility to print out the $I_{11'LM}$ for all m_j- where $I_{11'LM}$ are the contributions to $\eta(m_j, \theta_{sc})$ for each m_j without the spherical harmonic $Y^{M\,*}_{1'}(\theta)$.

This will be done if the value of NUMPRG specified in data is greater than 10.

Data Used - Nil

Dimension and Common Requisites

LMAX	FKAY	HØJF	LW1	MW1	CIEB
LIP	FIP	HØJI	LW2	MW2	WØMR

IEND	SNØ1	RHØBN	LW3	IW	SØMI
MEND	LX	YLMI	EXSGRM(L)	RHØ(I)	
DTHETA	MX	RSGML(L)	EXSGMI(L)	THETA(J)	
RTHETA	YLMR	USGML(L)	ULRN(I)	THETAD(J)	
XCST(I,L)	XCS(I,L)	UCRB(I)	WFMØD(MS,J)		
YCST(I,L)	YCS(I,L)	UCIB(I)	PHASE(MS,J)		

NOTE - The locations of WFMØD and PHASE are not reset to zero before or after the matrix elements are calculated - this is done in subroutine WIPE which is called in routine ØVERCT. Statements require 1154 locations in which to work.

NOTE - The $I_{11'LM}$ print out is in the form e.g. for $I_{o11}{}^{M}$ for $F^{19}(1p_{\frac{1}{2}})$

				$(m_j=-\frac{1}{2})$		$(m_j=\frac{1}{2})$	
1	2	2	+1	.119	.00137	.890	.517
1	2	2	0	.0841	.000968	-.08412	- .0000968
1	2	2	-1	.0841	.000968	-.119	- .00137

i.e.

$\ell+1$	$\ell'+1$	L+1	M	a + ib	c + id

But when a selection rule is violated as is the case in above for M=-1 $m_j=-\frac{1}{2}$ ($m_j+M=-3/2$ and $|m_j'| \leq \frac{1}{2}$) the partial matrix element values of the preceding case is printed out again.

Hence when using these one must also keep in mind the selection rules on η viz. $1' \geq |M|$

$$m_j + M = m_j' \text{ and } |m_j'| \leq j'$$

FLOW of TIEUP3

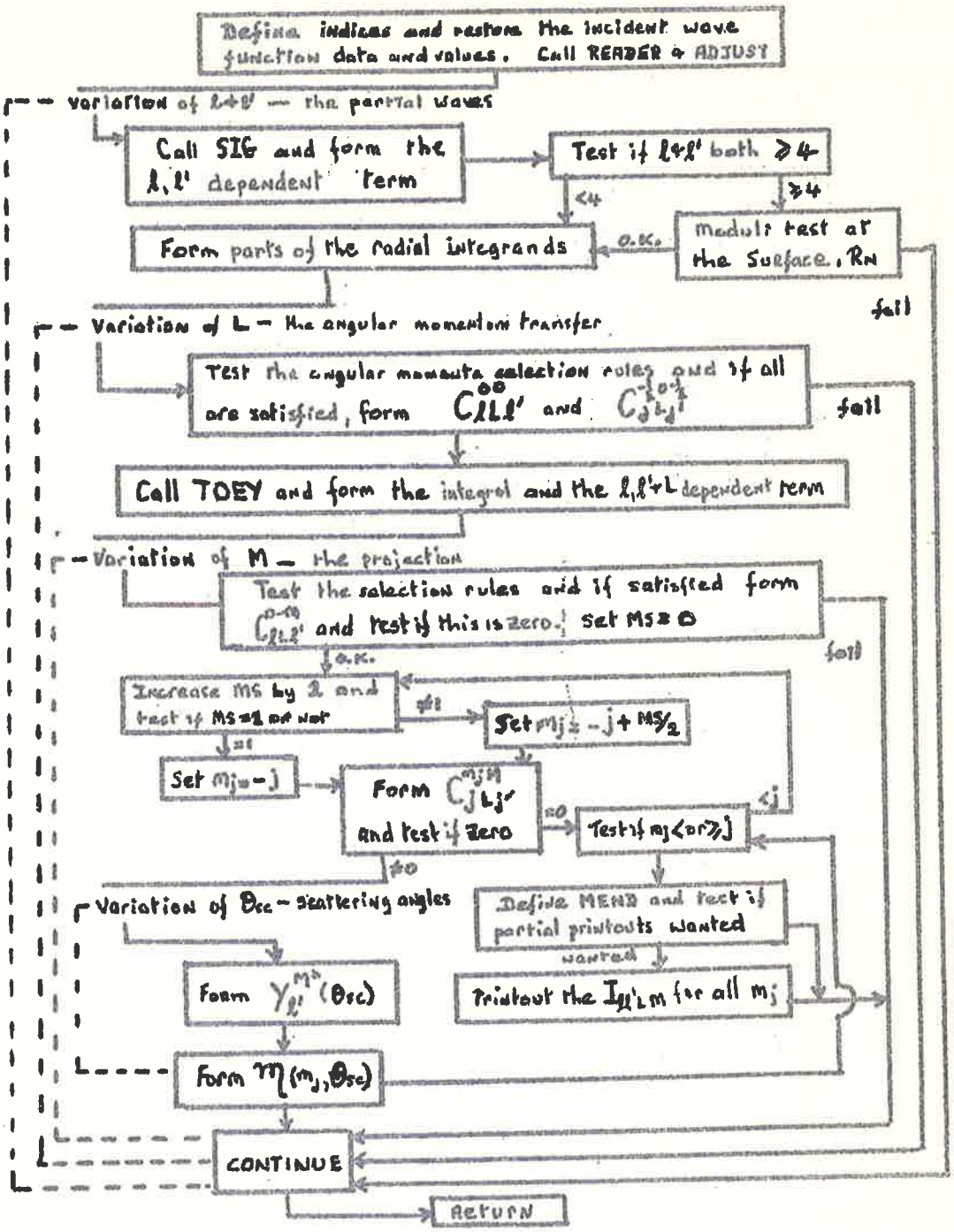

TIEUP4

This generates the differential cross-section from the stored values (complex) of the matrix elements $\eta(m_j, \theta_{sc})$ via

$$\frac{d\sigma(\theta_{cc})}{d\Omega} = \frac{k_f}{k_i}\left[\frac{\mu}{2\pi\hbar^2}\right]^2 \sum_{ave}^{1} |\eta(m_j, \theta_{cc})|^2 \times 10 \quad \text{mbs/ster-Rad.}$$

$\sum_{ave}^{1} = \frac{1}{2j+1}\sum_{m_j m_j'}^{1}$

i.e. effectively a summation over projection quantum numbers of the residual target nucleon (effectively, as $m_j' = M + m_j$) and an average of projections of initial target nucleon.

The interaction strength V_o has been removed from and so the actual calculated expression is

$$\frac{d\sigma}{d\Omega} = \frac{k_f}{k_i} \frac{\mu^2 V_o^2}{6764.44} \frac{1}{2j+1} \sum_{m_j}^{1} |\eta(m_j, \theta_{sc})|^2$$

Data Used - Nil

Dimension and Common Requisites

TBDPØT

SPECIAL NOTE

This routine prints out the answers in form

Angle	Cross-Section	Arb. Normalized
A1	B1	1.0
A2	B2	B2/B1 if B1 > 1.0
		1.0 if B1 < 1.0

The print out may include an angular distribution normalized to 1.0 at $\theta = 0$ (or 1st angle) as well as results calculated by the code, but only if the cross-section for the first angle considered is greater than 1.0. If this is not the case 1.0 is printed for all angles, e.g. if the parity rule holds, $\sigma(0)$ may be 10^{-9} or smaller, then one possibly may

overflow the machine by dividing by this number.

Statements require 284 locations in which to work.

TIEUP5, 6, 7, 8 and 9

TIEUP5 to 9 are "dummy" routines; they perform no calculation as yet.

READER

This is the counterpart of INPT4 for the final state data. However, it has important differences from INPT4. The pattern of this routine is as follows:-

(1) Tests the value RG - for the first (absolute) calculation of any specific reaction, all relevant data is read in. This is so if the input value of RG from INPT4 is less than 20.0. All subsequent calculations, e.g. parameter, energy, surface calculations, use RG $>$ 20.0 - this is from ØVERCT.

(2) If data is to be read, there are again differences from INPT4, e.g.

   (a) RG, BG, DV, DW ..... DBG, RHØIN(I), DRHØIN(I) are not input data here.

   (b) The Q-value of the reaction is read, instead of E_{lab} in INPT4.

(3) All energy dependent values are always calculated in this routine. Hence, ØVERCT only needs to construct the initial particle energy dependent quantities for variation runs. However, ØVERCT changes energy and potentials for final particle.

(4) Although the basic $\rho' = k_f r$ values are not read, the table of ρ_j' for the final state is calculated by this routine so that both the initial and final wave functions are evaluated at the same points τ_j .

This is done by constructing

$$\rho_j' = \frac{k_f}{k_i} \rho_j$$

(5) If KTRL(5) = 1 and RG $<$ 20.0, the scattering angles are read in. Also, this routine inputs -

(a) the bound state quantum numbers;

(b) the interior weighting factor ($\sqrt{f}$) and its change radius;

(c) the test number to terminate partial wave contributions to the matrix element;

(d) the bound state interaction radius;

(e) the interaction strength.

(6) Finally, CTRL4 is called using KSUPER = 2 and this generates the final particle optical model wave function.

Data Used

KTRL(I) I = 1,13 KTRL(5)=1 for scattering angles

FMI RC A

FMB V VS

QUAL W WS

ZZ R_o

LMAXM

JMAX THETAD(JMAX)

LPI LPF NHI NHF

HØJI HØJF

RADWC WF

SNØ1 RHØBS TBDPØT

Dimension and Common Requisites

Above data and FMU, ECM, FKAY, RHØBN, RHØBC, ETA, RHØ(I), DRHØ(I), NMAX, FIP, RG, LMAXM, IIN(J), THETA(JMAX)

NOTE

(1) Lab Energy is calculated from Q value by -

$$E_{lab}^{final} = E_{lab}^{Initial} + Q \frac{m+M}{M}$$

the $E_{lab}^{Initial}$ is carried over by RENMZ(100), i.e.

RENMZ(100) = $E_{lab}^{Initial}$ - from ØVERCT

(2) Scattering angles THETAD(J) are read in degrees - then this routine immediately forms the THETA(J) - these angles in radians.

(3) LPI, LPF, NHI, NHF, HØJI, HØJF - p,p′, n,n′, j,j′ - are the initial and final quantum numbers of the bound states (p is the orbital angular momentum).

RADWC is the change radius, inside of which each bound state is weighted by WF, hence the nuclear interior will be weighted by $(WF)^2$.

SNØ1 is the number in the test -

$$\left[(2l+1)\,|f_l(\bar{p}_N)|^2 + (2l'+1)\,|f_{l'}(\bar{p}_N)|^2\right] \leq SN\phi 1 \quad \text{for } l, l' \text{ both} \geq 4$$

The terms with both 1 and 1′ greater than 4, satisfying this relation, do not contribute. RHØBS is the interaction radius of Harmonic Oscillator functions used in

$$\nu = \frac{2[2(n-1)+\phi] + 3}{R_{int}^2}$$

TBDPØT is the interaction strength V_0 in

$$V(|\underline{r}_1 - \underline{r}_2|) = V_0\, f(|\underline{r}_1 - \underline{r}_2|)$$

Statements require 412 locations in which to work.

FLOW of READER

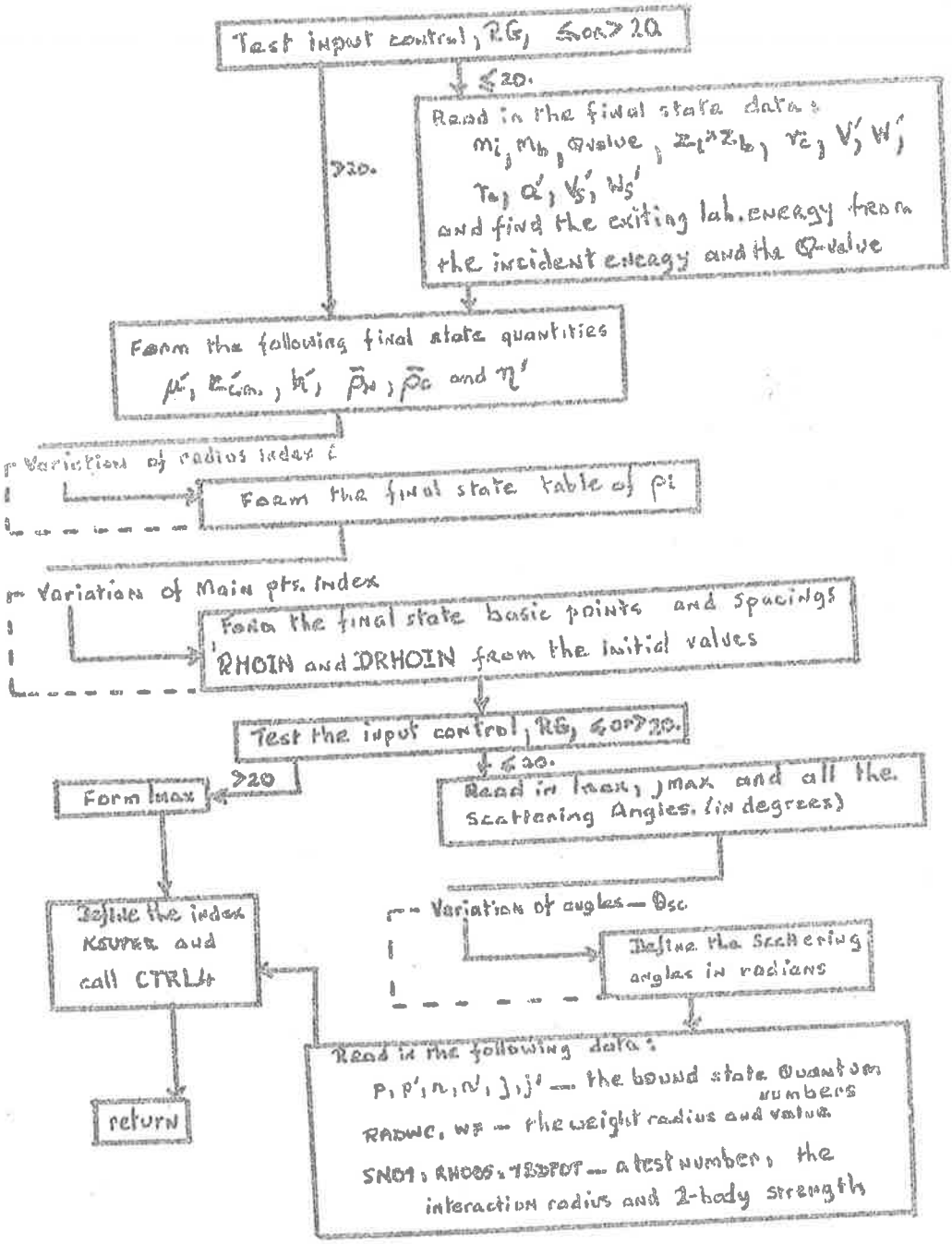

ADJUST

This does three things:-

(a) It creates a new table of ρ_i so that all points are equally spaced (there may be the exception that $\rho_1 \to \rho_2$ has not the same separation as $\rho_i \to \rho_{i+1}$, $i > 1$. It also relabels the wave functions so that they correspond in index number to this new set of ρ_i .

(b) It forms a table of r_i, the radii, from these ρ_i .

(c) It calls BSWFHØ twice to generate the incident and final bound state wave functions, using the appropriate quantum numbers input from READER.

These functions are stored in locations FFSRM(I) and FFSIM(I).

(d) Finally, the product of these two are placed in locations ULRN(I) which are to be used in the case of a δ-function interaction (ISP2 <5 in TØEY).

Furthermore, this routine ensures that we have in all an odd number of points, evenly spaced, so that a Simpsons Rule integration can be performed. However, from RHØTB, the original spacing arrangement must be such that spacings increase in size from range to range, and each range's spacing is a multiple of every preceding one. This can be more readily seen from the examples of all looping in ADJUST as shown below.

The sumbols used are:-

RØSP(1) - the first storage point (≡ RHØ(2) from routine RHØTB if a volume calculation is used).

IND - index number referring to table of ρ before adjustment.

NP - index number referring to table of ρ after adjustment.

MZ - index number referring to table of ρ at which spacing value changes.

MC - index number referring to the number of spaces in each range that must be missed to get even spacing of ρ_i.

LR - index number referring to value of IND at which the next ρ is to be stored to give even spacing of ρ_i.

KA - number of points in the first region (0→RHØIN(1)).

KB - number of points in the first region (0→RHØIN(1)) that have the same length ($\Sigma_1^i \Delta\rho_i$) as the last region spacing ($\Delta\rho$(LAST)).

KC - the number of points in the first region (0→RHØIN(1)) remaining after all KB sets possible have been formed.

KUP - is the index count that gives the value of the second value of ρ to be kept. This is because the first space may not be separated from ρ_2 with the even spacing that separates all other pairs of points ρ_i.

Part 1

Statement 6000

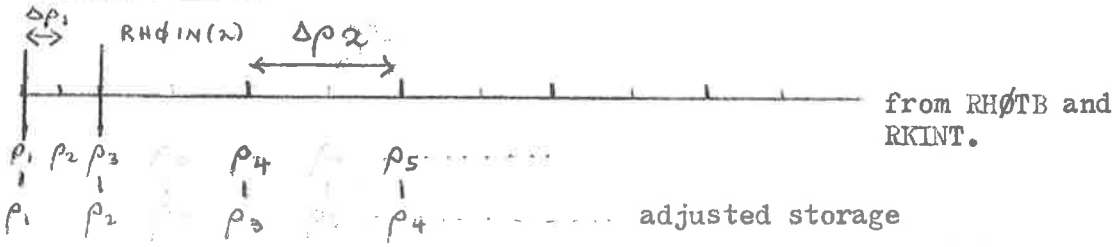

Here KA=3, therefore KB=0 (as $4x\ \Delta\rho_1 > \Delta\rho_2$) MC=4

KC=3, thus ρ_1=RØSP(1) ρ_2=RØSP(3)and as shown

Part 2

(a) Statement 6010

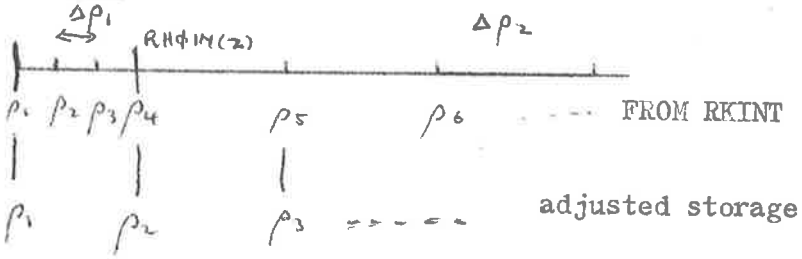

Here MC=4 KA=4, therefore KB=1 KC=0

Thus ρ_1=RØSP(1) ρ_4=RØSP(4) ρ_5=RØSP(5)

(b) Statement 6011

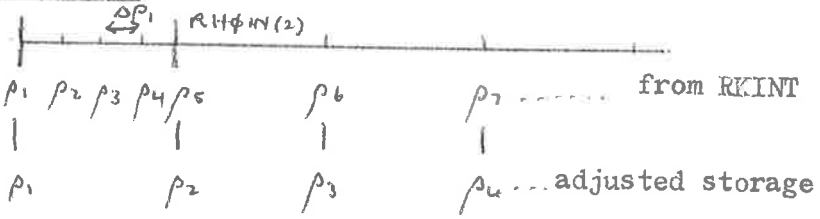

Here MC=4 KA=5, therefore KB=1 KC=1

Thus ρ_1=RØSP(1) ρ_5=RØSP(5) ρ_6=RØSP(6)

(c) Statement 6012

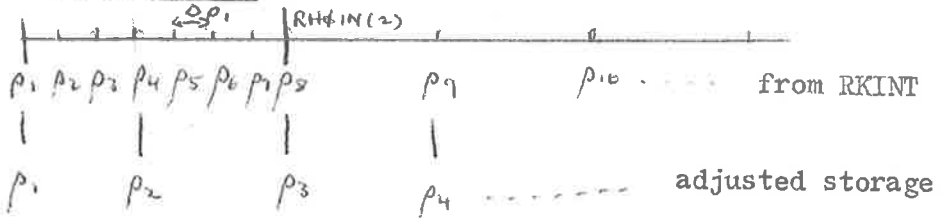

Here MC=4 KA=7, therefore KB=1 KC=3

Data Used - Nil

Dimension and Common Requisites

RADS(I)	LHØ	LMAX
RHØ(I)	NHØ	LIP
DRHØIN(I)	LPI	NMAX
XCS(I,L)	LPF	NMAXP
XCST(I,L)	NHI	FKAY

YCS(I,L)	NHF
YCST(I,L)	ULRN(I)
FFSRM(I)	IEND
FFSIM(I)	DRHØL

Statements require 616 locations in which to work.

FLOW of ADJUST

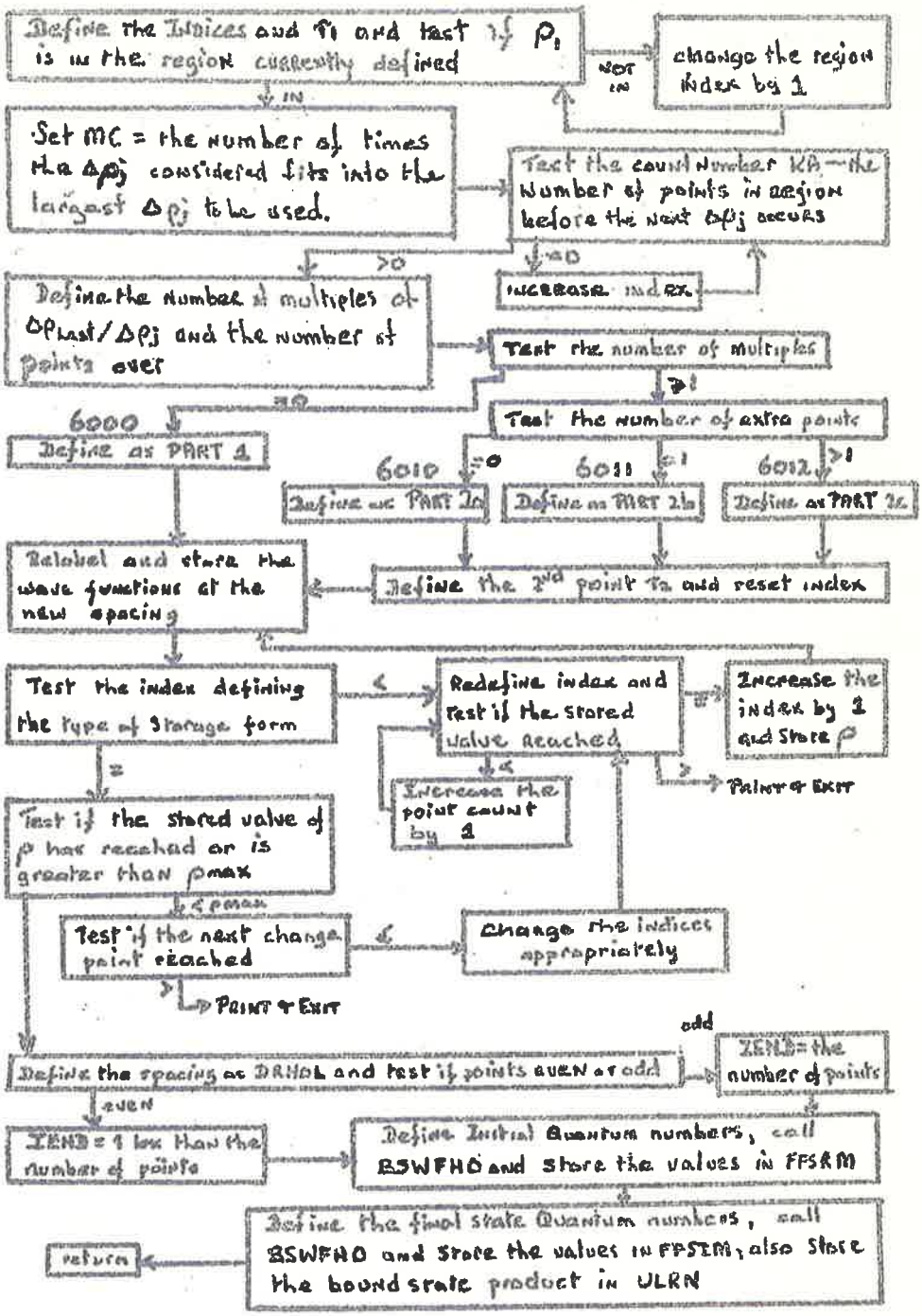

BSWFHØ

This generates the radial Harmonic Oscillator wave functions for any l-(angular-momentum value) with n-("principal quantum number) taking the values 1, 2 or 3. Also, we are able to generate the n=4 l=0 function. The routine computes -

$$R_{nl}(r) = \left[\frac{2^{2(l-n+2)}\,(2l+2n-1)!}{\sqrt{\pi}\,(n-1)!\,(l+n-1)!}\right]^{\frac{1}{2}}\left[\frac{l!}{(2l+1)!}\right]\nu^{3/4}e^{-\nu r^2/2}$$

$$\times\left[\sqrt{\nu}\,r\right]^{l}\sum_{k=0}^{n-1}\binom{n-1}{k}(-)^{k}\frac{(2l+1)!!}{(2l+2k+1)!!}\,(2\nu r^2)^{k}$$

where

$$\nu = \frac{2[2(n-1)+l]+3}{R_{int}^{2}}$$

Rint = RHØBS - input data from READER (following Glendenning, we use Rint = Saxon Well radius)

$\binom{a}{b}$ = binomial coefficient

s!! = 1, 3, 5 .....s if s is odd.

To operate this routine the calling code must define, prior to calling BSWFHØ,

LHØ = l + 1

NHØ = n

RADS(I), I = 1, IEND - the set of points at which the $R_{nl}(r_i)$ is to be calculated.

IEND - the total number of points at which the R_{nl} is to be calculated.

FG(N) - a set of log(n!) for n as large as will be required.

RADWC - the value of the radius out to which the function

is to be weighted by WF.

WF - the weight number modifying the $R_{n\ell}$ for all r_i up to the value RADWC

RHØBS - the interaction radius to be used in the calculation of ν .

The harmonic oscillator values at all r_i are put into the set of locations defined by ULRN(I).

A simplification used is that we treat 1=0 separately for any n=1, 2, 3 or 4.

Statements require 550 locations in which to work.

FLOW of BSWFHO

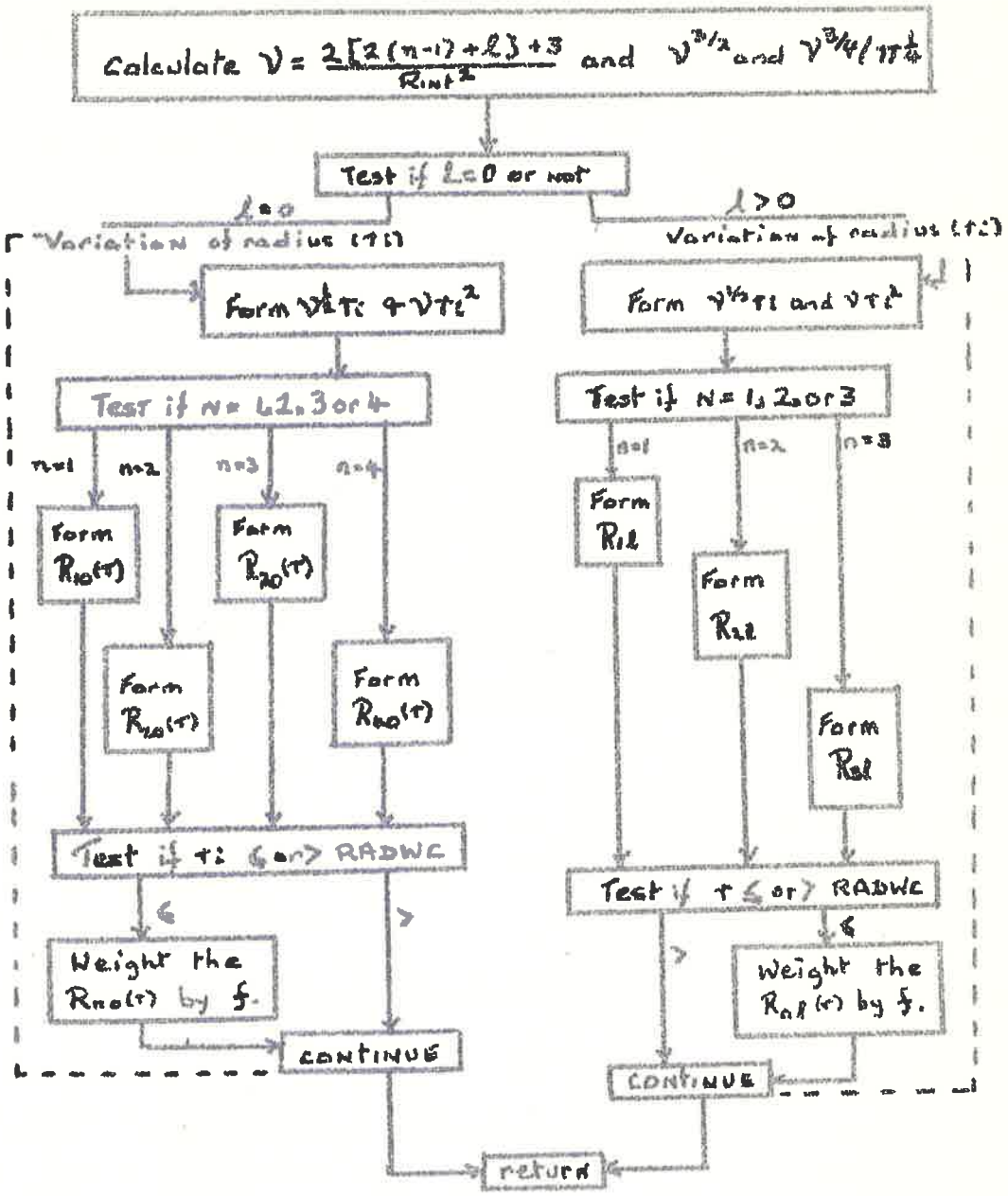

TØEY

This subroutine performs the r_1 integration (by Simpson's Rule) of the integral -

$$R_{\ell\ell' L} = \int dr_1 r_1^2 f_\ell(kr_1) f_{\ell'}(k'r_1) \int dr_2 r_2^2 R_{np}(r_2) R_{n'p'}(r_2) V_L(|\underline{r}_1 - \underline{r}_2|)$$

where $V_L(|\underline{r}_1 - \underline{r}_2|)$ = Yukawa radial function if ISP2 $\geqslant 5$, or it forms complete integral when $V_L(|\underline{r}_1 - \underline{r}_2|) = \frac{\delta(r_1 - r_2)}{r_1^2}$ if ISP2 < 5.

It first defines $r_i^2 f_\ell f_{\ell'}$ for a given point of the integration grid for which the product $f_\ell f_{\ell'}$ has previously been stored in the locations UCRB and UCIB. The value of the index of the grid point r_i is put into the location IKTRL, this allows the Yukawa function to be calculated at the correct r_i value. Then the routine tests ISP2 to see what type of interaction we require.

If ISP2 < 5, a δ-function interaction is used and then this subroutine performs the complete integration using ULRN(I) for the product of the two bound state wave functions.

If ISP2 $\geqslant 5$, a Yukawa interaction is used and the r_2 integration, by Simpson's Rule, is performed in Subroutine ACTIØN.

The total integral $R_{\ell L \ell'}$ is evaluated and its values are put in the locations SØMR and SØMI.

The location DRHØL contains the value of the spacing between successive points of integration.

Data Used - Nil

Dimension and Common Requisites

SØMR	DRHØL	YLMR	ULRN(I)	UCRB(I)	UCIB(I)
SØMI	IEND	YLMI	ISP2	IKTRL	RADS(I)

NOTE - This shows that the products $f_\ell(kr_i) f_{\ell'}(k'r_i)$ and $R_{np}(r_i) R_{n'p'}(r_i)$ must be stored in the locations UCRB(I), UCIB(I) and ULRN(I) respectively at each point in the table of RADS(I) prior to calling this routine. Statements require 125 locations in which to work.

FLOW of TOEY

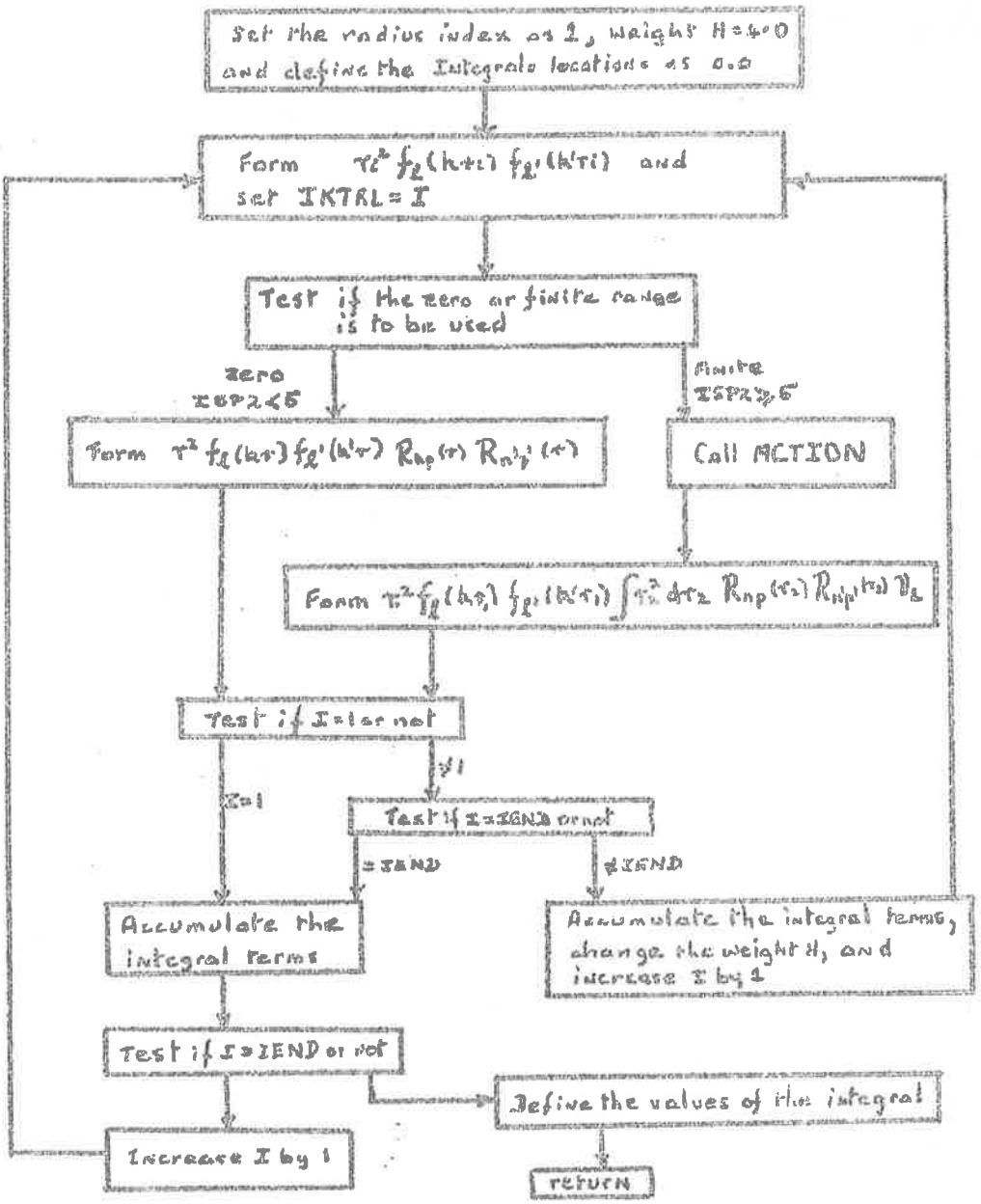
Set the radius index as 1, weight H=4.0 and define the Integrals locations as 0.0
Form $r_i^2 f_\ell(kr_i) f_{\ell'}(k'r_i)$ and set IKTRL=I
Test if the zero or finite range is to be used
zero
$I \le P2 < 6$
finite
$I \le P2 \ge 6$
Form $r^2 f_\ell(kr) f_{\ell'}(k'r) R_{np}(r) R_{n'l'}(r)$
Call ACTION
Form $r_2^2 f_\ell(kr_2) f_{\ell'}(k'r_2) \int r_1^2 dr_1 R_{np}(r_1) R_{n'l'}(r_1) V_1$
Test if I=1 or not
I=1
≠1
Test if I=IEND or not
=IEND
≠IEND
Accumulate the integral terms
Accumulate the integral terms, change the weight H, and increase I by 1
Test if I=IEND or not
Define the values of the integral
Increase I by 1
RETURN

ACTIØN

This subroutine performs the r_2 integration for each given value of r_1 . This is used only is ISP2 $\geq$ 5, i.e. we want to use a Yukawa interaction form. The integration is done via Simpson's Rule with the appropriate radial values of the Yukawa potential being generated in the routine VGEN and carried to this subroutine by EPS1 and EPS2.

Now because EPS1 and EPS2 are test number locations, we first set these test numbers into temporary storage STØR1 and STØR2 and replace them in EPS1 and EPS2 after the Yukawa values have been used.

The integral's values are put into the locations YLMR and YLMI.

The two r_2 dependent wave functions must have previously been stored in the locations FFSRM(I) and FFSIM(I).

Data Used - Nil

Dimension and Common Requisites

FFSRM(I)	RADS(I)	EPS2	YLMI	IEND
FFSIM(I)	EPS1	YLMR	DRHØL	

Statements require 211 locations in which to work.

VGEN

This routine generates the radial part of the Yukawa potential between the points r_1 and r_2 for a given angular momentum transfer L. This is calculated from the expression obtained by the multipole expansion -

$$\frac{\exp[-\mu|r_1-r_2|]}{\mu|r_1-r_2|} = \sum_{L=0}^{\infty}\sum_{m=-L}^{+L} j_L(i\mu r_<)\, h_L^{(1)}(i\mu r_>)\, Y_L^M(\Omega_1)\, Y_L^{M*}(\Omega_2)$$

where μ = finite range parameter

$r_<, r_>$ are respectively smaller and larger values of r_1 and r_2 respectively.

The $h_L^{(1)}(i\mu r)$ is calculated from:

$$h_L(i\mu r) = -(-i)^L \sum_{k=0}^{L} \alpha_k \frac{e^{-\mu r}}{\mu r}$$

where $$\alpha_{k+1} = \alpha_k \frac{(L-k)(L+k+1)}{2(k+1)\mu r}, \quad \alpha_0 = 1.0$$

and $$j_L(i\mu r) = (i)^L (\mu r)^L \sum_{k=0}^{\infty} \beta_k$$

where

$$\beta_{k+1} = \beta_k (\mu r)^2 / 2(k+1)(2L+2k+3), \quad \beta_0 = \frac{1}{(2L+1)!!}$$

Before this routine is used, the calling code must -

(1) Define the finite range parameter value as DBG. This value is set in from data.

(2) Define KSUPER = L+1.

(3) Define a table of RADS(I) = r_i for I=1, IEND.

(4) Define IKTRL as the index i corresponding to the point r_1.

(5) Define ILAST as the index i corresponding to the point r_2.

Data Used - Nil

Dimension and Common Requisites

DBG IKTRL RADS(I) EPS2

KSUPER ILAST EPS1

Statements require 547 locations in which to work.

FLOW of VGEN

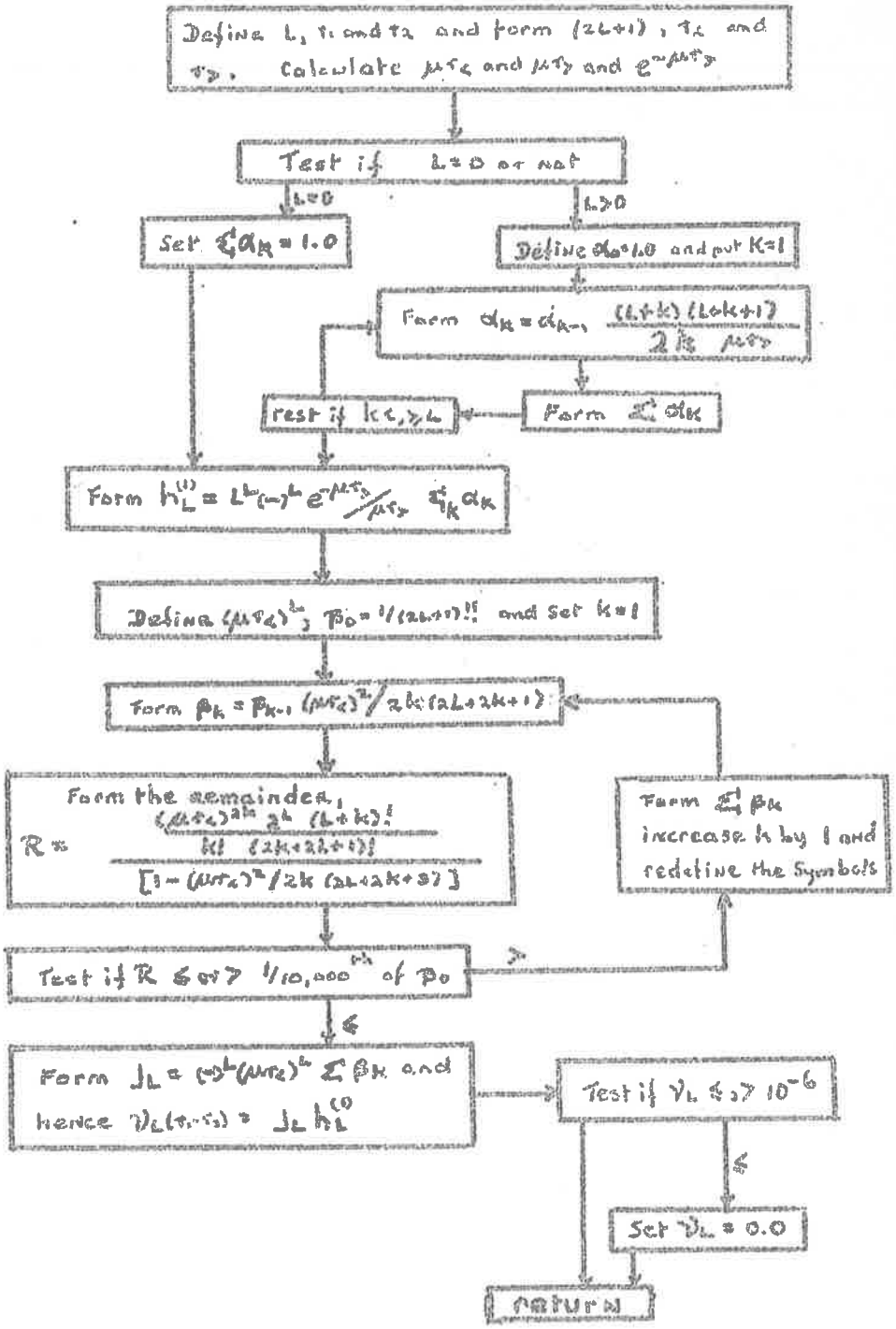
Define L, r1 and r2 and form (2L+1), τL and τ>. Calculate μr< and μr> and e^-μr>
Test if L=0 or not
L=0
L>0
Set Σ aK = 1.0
Define a0=1.0 and put K=1
Form aK = aK-1 (L+K)(L+K+1) / 2K μr>
Test if K<, >L
Form Σ aK
Form h(1)L = L^L (-)^L e^-μr> / μr> Σ K aK
Define (μr<)^L, P0 = 1/(2L+1)!! and set K=1
Form PK = PK-1 (μr<)^2 / 2K(2L+2K+1)
Form the remainder, R = (μr<)^2K 2^K (L+K)! / K! (2K+2L+1)! / [1-(μr<)^2 / 2K(2L+2K+3)]
Form Σ PK increase K by 1 and redefine the Symbols
Test if R ≤ or > 1/10,000th of P0
>
≤
Form JL = (-)^L (μr<)^L Σ PK and hence VL(r1,r2) = JL h(1)L
Test if VL ≤, > 10^-6
≤
Set VL = 0.0
return

WIGNER

This computes $C^{m_1 m_2}_{j_1 j_2 j}$, the Clebsch-Gordan coefficients, via -

$$C^{m_1 m_2 m}_{j_1 j_2 j} = \left[\frac{(j_1+j-j_2)!(j-j_1+j_2)!(j_1+j_2-j)!(j+m)!(j-m)!(2j+1)}{(j+j_1+j_2+1)!(j_2-m_2)!(j_2+m_2)!(j_1-m_1)!(j_1+m_1)!} \right]^{\frac{1}{2}}$$

$$\times \sum_k \frac{(-)^{k+j_2+m_2}\,(j+j_2+m_1-k)!(j_1-m_1+k)!}{k!\,(j-j_1+j_2-k)!\,(j+m-k)!\,(k+j_1-j_2-m)!}$$

for j, j_1, j_2 integers, or two of them half-intergers.

To use this subroutine, the calling routine must define prior to calling WIGNER.

(1) A table of FG(N) - log (N!).

(2) Have a routine ØNEMN(N,S) which evaluates $(-)^N$=S (for N positive or negative).

(3) Set IW<2 for integer j's or> 2 for half integer values of two of the j's.

(4) Set LW1 = j_1 for integer case, or $2j_1$ for half integer case
LW2 = j_2 for integer case, or $2j_2$ for half integer case
LW3 = j for integer case, or 2j for half integer case

(5) Set MW1 = j_1+1-m_1
MW2 = j_2+1-m_2 for both cases

The answer is put in the location CLEB

NOTE - This always uses n! = EXPF [log(n+1)! - log (n+1)]
= EXPF [FG(N+1) - log (n+1)]

which permits 0! to be defined.

These coefficients have selection rules

$$m_1+m_2 = M$$

$$|j_1 - j_2| \leq j \leq j_1 + j_2$$

and these rules are built into this code. If they are not satisfied,

the coefficient is taken as zero. The $\sum_{k}^{}$ is restricted to those values of k for which none of the arguments of the factorials, shown under $\sum_{}^{}$ above, is negative.

Examples

To evaluate $C\begin{matrix}-3-1-2\\3\,4\,4\end{matrix}$ IW=1 LW1=1 LW2=3 LW3=4 MW1=7 MW2=4

$C\begin{matrix}-\frac{1}{2}\;1\frac{1}{2}\\\frac{1}{2}\;2\;\frac{3}{2}\end{matrix}$ IW=5 LW1+1 LW2=4 LW3=6 MW1=2 MW2=2

Data Used - Nil

Dimension and Common Requisites

CLEB	MW1
LW1	MW2
LW2	IW
LW3	FG(N)

Statements require 1245 locations in which to work.

FLOW of WIGNER → $C^{\alpha\beta\gamma}_{abc}$

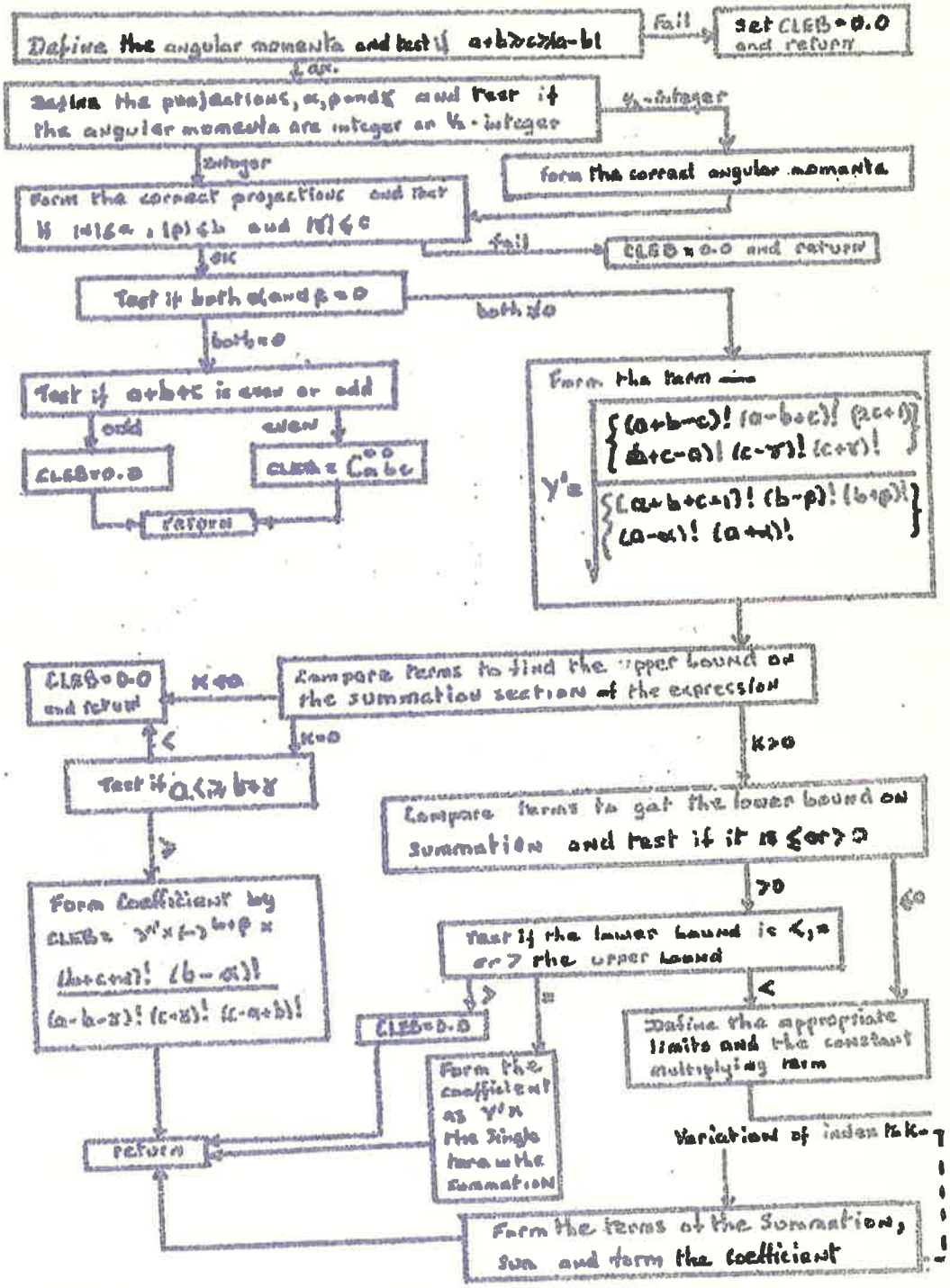

LEGEND

This calculates the Spherical Harmonics via -

$$Y_L^M(\theta,\phi) = \left[\frac{(2L+1)\,(L-|m|)!}{4\pi\,(L+|m|)!}\right]^{\frac{1}{2}} P_L^{|m|}(\cos\theta)\, e^{iM\phi}$$

The $P_L^{|m|}(\cos\theta)$ (Legendre functions) are generated by their recurrence formula.

As for subroutine WIGNER, to use this routine, the calling code must have previously defined -

(1) A table of FG(N) - log(N!) for all N needed.

(2) LX - true value of angular momentum L

MX - L+1-M

PHI - ϕ in degrees

RPHI - ϕ in radians

DTHETA - θ in degrees

RTHETA - θ in radians

The spherical harmonic values are placed in locations YLMR and YLMI.

Examples

Y_3^2 (60°, 30°)	Y_4^{-1} (0°, 10°)
LX = 3	LX = 4
MX = 2	MX = 6
DTHETA = 60.0	DTHETA = 0.0
RTHETA = 1.0472	RTHETA = 0.0
PHI = 30.0	PHI = 10.0
RPHI = .5236	RPHI = 0.1745
CALL LEGEND	CALL LEGEND

Terminology

Y_{ℓ}^{ℓ} - use LX = ℓ mx = ℓ

$Y_{\ell}^{-\ell}$ - use LX = ℓ mx = 2ℓ+1

Data Used - Nil

Dimension and Common Requisites

YLMR	PHI	DTHETA	LX	FG(N)
YLMI	RTHETA	RPHI	MX	

Statements require 795 locations in which to work.

FLOW of LEGEND

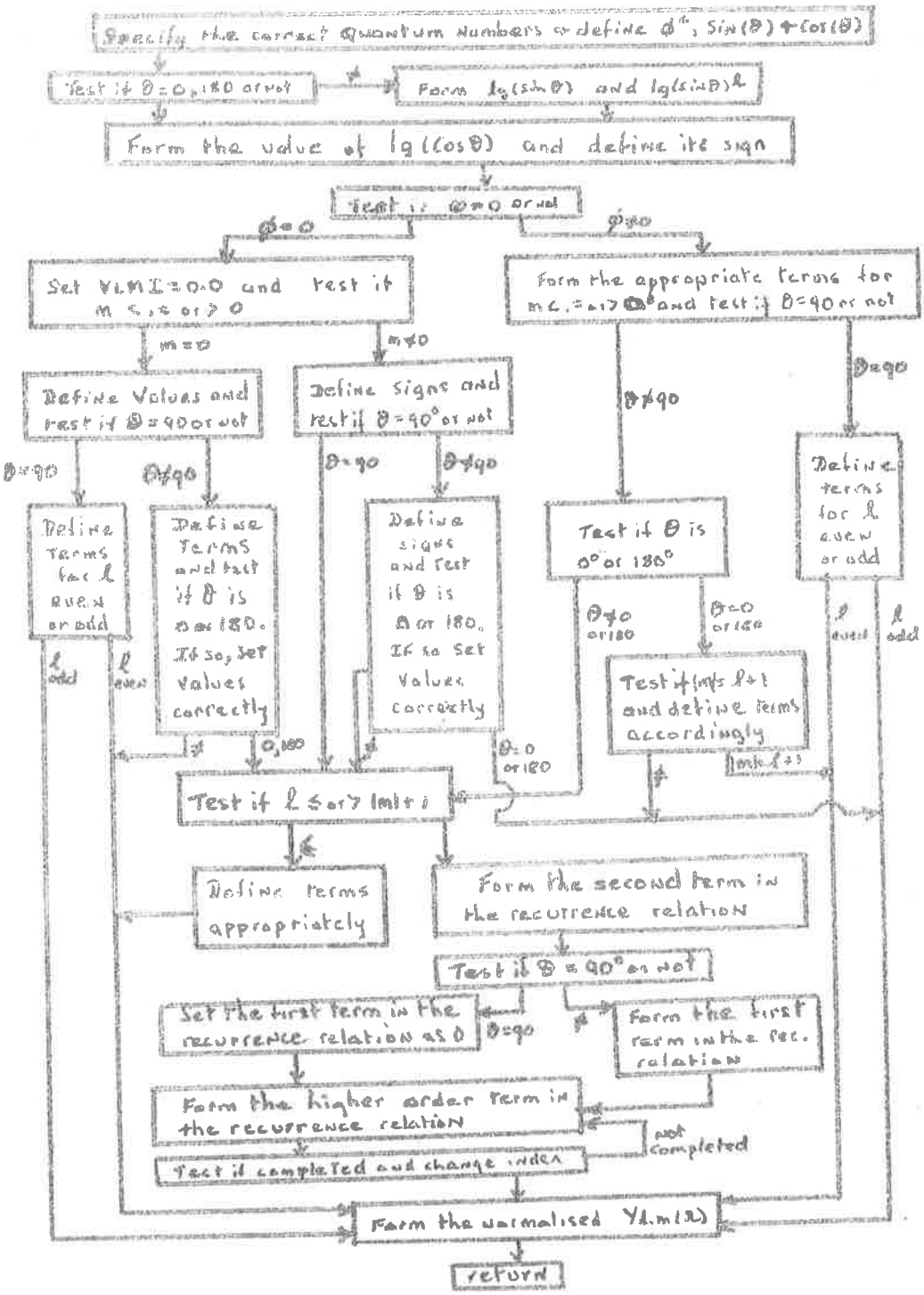

WIPE

This routine is used to clear the matrix element storage locations WFMØD(m,J) and PHASE(m,J), after any cross-section has been evaluated and printed onto the output tape and before the next calculation is performed.

Statements require 36 locations in which to work.

B. RESULTS OF A TYPICAL DATA DECK

The typical data should perform 8 calculations; 2 energies 10 and 20 MeV; two potentials 55 and 51 MeV for real well depth, and each of these four cases are calculated for central region weighted by 1.0 and 0.0, the so called volume/surface calculations.

Each calculation is identified by a run number and the date.

(1) The Data Deck and Its Description

This contains 131 cards either in format I5 or E15.9. For simplicity all numbers without decimals read as in I5 all with as in E15.9.

22 4 1963	Date
1	- Dummy
0	- Run identification start value - 1
100	- NUMPRG $>$ 10 and so partial matrix elements will be printed out.
0	- (KTRL(1) = 0 $\rightarrow$ Saxon Well used.
1	- (KTRL(2) = 1 $\rightarrow$ ØUTPT4 will be used.
0	
0	
0	
0	
0	- KTRL(I) I = 1,13
0	
0	
0	

0

0

1 - (KTRL(13) = 1 Both ρ max and lmax will be checked

1.0 - m_i

19.0 - M_b

10.0 - E_{lab} (incident)

9.0 - $Z_i \times Z_B$

1.2 - R_c

55.0 - V

4.0 - W

1.2 - R_o

0.55 - a

0.0 - V_s

0.0 - W_s

0.0 - R_g

0.0 - B_g

-4.0 - Δ V

0.0 - Δ W

0.0 - Δ A

0.0 - Δ VS

0.0 - Δ WS

0.0 - μ

2 - Number of V's to be used

1 - Number of W's to be used

1 - Number of A's to be used

1 - Number of V_s's to be used

1 - Number of W_s's to be used

1 - Number of B_g's to be used

10.0 - ΔE_{lab}

20.0 - E_{lab} (last value of incident energy to be used)

2 - Number of times weight factor is to be varied

1 - Test whether a δ -function or a finite range interaction is to be used. A δ -function is used in this case.

100 - Percentage of first weight factor that is to be subtracted for subsequent values.

1 - Dummy.

3 - Number of basic points $k_i r$

0.625 -)
0.5 -) The basic points.
10.0 -)

0.625 -)
0.25 -) The spacings between the basic points.

7 - $l_{max}+1$

0

0

1

1 -) KCØNT(J) J=1,9.
0 -)

KCØNT(3)=1 → TIEUP3 used → matrix elements.

KCØNT(4)=1 → TIEUP4 used → $d\sigma/d\Omega$

KCØNT(7)=1 → TIEUP7 used → on-line print out to operator on completion of each run.

0

1

0

0

=

0

1

0

0

1 -) KTRL(I), I=1,13. KTRL(5)=1 Scattering angles
) will be used in final state
0 -) data.

0

0

0

0

0

0

1

=

1.0 - m_i

19.0 - M

-0.11 - Qvalue

9.0 - $Z_i \times Z_b$

1.2 - R_c

55.0 - V

4.0 - W

1.2 - R_o

0.55 - a

0.0 - V_s

0.0 - W_s

7 - $1'_{max}-1$

28 - Number of angles to be used.

0.0	10.0	60.0	100.0	110.0	160.0
2.0	20.0	70.0	102.0	120.0	170.0
4.0	30.0	80.0	105.0	130.0	180.0
6.0	40.0	90.0	106.0	140.0	
8.0	50.0	95.0	108.0	150.0	

The 28 Scattering Angles

1 -) p

0 -) Bound State Quantum numbers p'

1 -) n=prime p=orbital n

2 -) n'

=

0.5 -)

) j_i and j_f

0.5 -)

3.202 -)

) "Rc.off" and initial weight value.

1.0 -)

0.001 - Test number.

3.202 - "Rint"

100.0 - Two body potential strength.

(2) The Results

Because KTRL(2)=1 in both the incident and the emergent particles' data, each angular distribution is preceded by at least 16 lines of output of data values. Then, because NUMPRG $>$ 10, the partial matrix elements $I_{11'_{LM}}$ are printed

The print out takes the form

$\ell+1$, $\ell'+1$, L+1, M, $I_{11'LM}$ for $m_j=-j$, $I_{11'LM}$ for $m_j=-j+1$ .....

The $I_{11'LM}$ are printed in real and imaginary parts.

If $j > 3/2$ then the print out is of the form:-

$\ell+1$ $\ell'+1$ L+1 M $Im_j=-j$ $Im_j=-j+1$ $Im_j=-j+2$ $Im_j=-j+3$

$Im_j=-j+4$ $Im_j=-j+5$ etc.

Further, all selection rules must be remembered and used in conjunction with these results, as zeros are not shown, e.g. for F^{19} run:-

L	LP	LT	M	$(m_j=-\frac{1}{2})$	$(m_j=\frac{1}{2})$					
1	2	2	1	1.5-.14	.89	.51	(A*)	0.0	0.0	0.0	0.0
1	2	2	0	1.1-.10(B*)	etc.						
1	2	2	-1	1.1-.10	etc.						
2	1	2	0	-1.8 .16	etc.						

(A*) for the first line as $j \geq |(m+m_j)|$ $j' = \frac{1}{2}$.

$m+m_j = \frac{1}{2}$ and 3/2 not valid

(B*) for the third line $j' = \frac{1}{2}$ and $m+m_j = -1-\frac{1}{2} = -3/2$ is not allowed

So, the $I_{1,2,2,-1}$ for $m_j=-\frac{1}{2}$ is zero. This is shown by the fact that it has the I value immediately above it.

The angular distributions. Exponent is superscript.

$1.4 \times 10^{-3} = 1.4^{3}$

Run No Angle	1	2	3	4	5	6	7	8
0.0	1.40^{3}	8.22^{4}	5.17^{6}	5.22^{5}	3.29^{6}	3.15^{6}	5.99^{6}	3.38^{6}
2.0	1.03^{3}	7.13^{3}	3.87^{2}	4.61^{2}	5.22^{5}	6.64^{5}	7.44^{4}	7.90^{4}
4.0	3.68^{2}	2.59^{2}	1.54^{1}	1.83^{1}	1.98^{4}	2.55^{4}	2.92^{3}	3.11^{3}
6.0	8.02^{2}	5.67^{2}	3.42^{1}	4.06^{1}	4.35^{4}	5.63^{4}	6.40^{3}	6.83^{3}
8.0	1.40^{1}	9.89^{2}	5.97^{1}	7.10^{1}	7.59^{4}	9.82^{4}	1.10^{2}	1.17^{2}
10.0	2.13^{1}	1.51^{1}	9.12^{1}	1.09	1.16^{3}	1.50^{3}	1.65^{2}	1.75^{2}
20.0	7.30^{1}	5.22^{1}	3.04	3.62	3.89^{3}	5.05^{3}	4.55^{2}	4.88^{2}
30.0	1.27	9.18^{1}	5.01	5.96	6.46^{3}	8.43^{3}	5.18^{2}	5.63^{2}
40.0	1.55	1.15	5.65	6.69	7.32^{3}	9.54^{3}	2.85^{2}	3.25^{2}
50.0	1.46	1.14	4.68	5.46	5.99^{3}	7.72^{3}	3.77^{3}	6.29^{3}
60.0	1.12	9.45^{1}	2.67	3.04	3.31^{3}	4.14^{3}	4.44^{3}	4.64^{3}
70.0	7.31^{1}	6.89^{1}	7.50^{1}	8.04^{1}	1.02^{3}	1.18^{3}	2.42^{2}	2.21^{2}
80.0	4.64^{1}	4.65^{1}	1.08^{2}	2.55^{2}	8.87^{4}	9.65^{4}	3.51^{2}	3.27^{2}
90.0	3.13^{1}	2.78^{1}	1.11	1.23	3.62^{3}	4.06^{3}	2.43^{2}	2.45^{2}
95.0	2.47^{1}	1.90^{1}	2.26	2.41	5.80^{3}	6.43^{3}	1.50^{2}	1.72^{2}
100.0	1.74^{1}	1.09^{1}	3.62	3.75	8.16^{3}	8.89^{3}	7.26^{3}	1.09^{2}
102.0	1.44^{1}	8.09^{2}	4.17	4.28	9.07^{3}	9.82^{3}	5.19^{3}	9.22^{3}
105.0	9.96^{2}	4.95^{2}	4.95	5.02	1.03^{2}	1.11^{2}	3.41^{3}	7.63^{3}
106.0	8.63^{2}	4.26^{2}	5.20	5.24	1.07^{2}	1.14^{2}	3.18^{3}	7.36^{3}
108.0	6.36^{2}	3.62^{2}	5.64	5.65	1.14^{2}	1.21^{2}	3.23^{3}	7.16^{3}
110.0	4.86^{2}	4.15^{2}	6.01	5.99	1.20^{2}	1.26^{2}	3.88^{3}	7.36^{3}
120.0	2.23^{1}	3.54^{1}	6.58	6.45	1.26^{2}	1.28^{2}	1.09^{2}	9.94^{3}
130.0	1.23	1.44	5.06	5.07	9.59^{3}	9.35^{3}	1.02^{2}	6.11^{3}
140.0	3.52	3.59	3.21	3.50	4.79^{3}	4.55^{3}	2.05^{3}	2.37^{3}

Run No / Angle	1	2	3	4	5	6	7	8
150.0	7.07	6.65	3.59	3.91	1.13[3]	1.14[3]	1.38[2]	2.62[2]
160.0	11.09	9.97	7.00	6.87	1.99[4]	4.56[4]	6.54[2]	9.17[2]
170.0	14.32	12.58	11.39	10.59	1.13[3]	1.49[3]	1.34[1]	1.69[1]
180.0	15.56	13.57	13.39	12.28	1.81[3]	2.18[3]	1.66[1]	2.06[1]
E	10	10	20	20	10	10	20	20
V	55	51	55	51	55	51	55	51
Weight	1.0	1.0	1.0	1.0	0.0	0.0	0.0	0.0

C. GLOSSARY AND DESCRIPTION OF SYMBOLIC VARIABLES APPEARING IN COMMON AND DIMENSION STATEMENTS

FORTRAN SYMBOL	MATH. SYMBOL	DESCRIPTION	REFERENCE
A	a	Value of the ROUNDING PARAMETER appearing in optical model potential.	(ØVERCT)
AR(I),AI(I)	$Re(a_i)$, $Im(a_i)$	Real and Imaginary parts of the terms of the auxillary series used to calculate assymptotically the coulomb functions	(CØULFN)
BG		If it is input as zero, this keeps a count of the total number of runs performed.	(ØVERCT)
CØ2	(1) m_i+MTarget or m_f+M Residual	Sum of masses of - incident and target or emergent and residual	(ØVERCT)
	(2)	As a term used in generating the matching coefficients	(CSUBL)

FORTRAN SYMBOL	MATH. SYMBOL	DESCRIPTION	REFERENCE
CR1(L), CI1(L) L=1, LMAX	$Re(C_\ell), Im(C_\ell)$	Real and Imaginary parts of matching coefficients for all ℓ's.	(CUBL)
CR2(L), CI2(L) L=1, LMAX		Dummy variables.	
CLEB	$C^{m_1\ m_2}_{j_1\ j_2\ j}$	The value of the Clebsch-Gordan coefficient.	(SIGNER)
DV,DW,DVS, DWS,DA		Amounts by which V,W,VS, WS and A must be incremented for succeeding runs.	(ØVERCT)
DBG	μ	The width parameter in the Yukawa interaction	(VGEN)
DRHØIN(I) I=1, NMAXP		Intervals between points in different ranges at which integration is to be performed.	(RHØTB)
DELAB	ΔE_{lab}	Lab. Energy increments in energy variation	(ØVERCT)
DRHØ(I) I=1, ILAST	$\Delta\rho_i$	Interval for numerical integration.	(RHØTB)

FORTRAN SYMBOL		MATH. SYMBOL	DESCRIPTION	REFERENCE
DRHØL	(1)		Value of h st spacing needed to reach Runge-Kutta integration limit	(RHØTB)
	(2)		Spacing of points at which Simpson's Rule integration performed.	(TØEY)
DTHETA		θ_{sc}	Scattering angle in degrees	(TIEUP3)
EPS1	(1)	ε_1	Error Threshold used in coulomb function calculation	(CØULFN)
	(2)		Real part of interaction potential for given points r_1, r_2 angular momentum transfer L.	(VGEN)
EPS2	(1)	ε_2	Error threshold used in coulomb function calcula tion.	(CØULFN)
	(2)		Imaginary part of inter-action potential.	(VGEN)
EPS3		ε_3	Error threshold used in coulomb function calcula tion.	(CØULFN)
EPS4		ε_4	Error threshold used in PØT1CH	(PØT1CH)

FORTRAN SYMBOL	MATH. SYMBOL	DESCRIPTION	REFERENCE
ELAB	E_{lab}	Lab. energy of unbound particle.	(ØVERCT)
ECM	E_{cm} or E_{cofm}	Centre of mass energy of unbound particle.	(ØVERCT)
ETA	η	Coulomb parameter	(ØVERCT)
EFIN	E_{lab}^{fin}	Last value of E_{lab} to be used (for incident particle)	(ØVERCT)
EXSGMR(L) EXSGMI(L) L=1, LMAX	$e^{i\sigma_\ell}$	Real and Imaginary parts of the exponential of the coulomb phase shifts.	(EXSGML)
ETA2	η^2	Coulomb Parameter Squared	(EXSGML)
FMI	m_i	Mass number of unbound particle in atomic units.	(ØVERCT)
FMB	$m_B\{M_T \text{ or } M_R\}$	Mass number of Target (or Residual) nucleus	(ØVERCT)
FMU	μ	Reduced mass of unbound particle.	(ØVERCT)

FORTRAN SYMBOL	MATH. SYMBOL	DESCRIPTION	REFERENCE
FKAY,FIP	k',k	Wave number associated with energy of final and initial unbound particle	(INPT4)
FKAYA	k x largest a		(PØT1CH)
FBAR(L) L=1,LMAX	$F_1^{(n)}$	Regular Coulomb functions used in backward recurrence relation to find the correct $F_1(\rho max)$	(CØULFN)
F(L) L=1,LMAX	F_1	Regular Coulomb functions	(CØULFN)
FP(L) L=1,LMAX+1	F_1'	Derivative of the regular Coulomb function	(CØULFN)
FFCR(I) FFCI(I) I=1,ILAST		Real and Imaginary parts of the derivative of the Saxon form factor used in the central potential.	(PGEN4)
FFSR(I) FFSI(I) I=1,ILAST		Real and Imaginary parts of the form factor used on the Spin-Orbit central potential.	(PGEN4)

FORTRAN SYMBOL	MATH. SYMBOL	DESCRIPTION	REFERENCE
FFCRM(I) FFCIM(I) I=1,ILAST		Central form factor at SCAT4 half values of ρ.	(PGEN4)
FFSRM(I) I=1,IIAST	(1)	Spin-Orbit form factor at half values of ρ.	(PGEN4)
	(2)	Storage for the initial bound state).	(BSWFHØ)
FG(N) N=1,51	log(n!)	Logarithm of n!	(LGFACT)
G(L) L=1,LMAX	G_1	Irregular Coulomb functions	(CØULFN)
GP(L) L=1,LMAX+1	G'_1	Derivatives of the irregular Coulomb functions.	(CØULFN)
HØJF,HØJI	j',j	The final and initial bound states total spins (in j-j coupling model for a single extra-core particle),	(TIEUP3)
ISPILL		Underflow indicator in FAP routine, SPILL.	(SPILL)
ISP1		Number of times the centre weight value is to be varied.	(OVERCT)

FORTRAN SYMBOL	MATH. SYMBOL	DESCRIPTION	REFERENCE
ISP2		Test number defining whether a δ-function (ISP2 <5) or Yukawa (ISP2 ≥ 5) interaction is to be used.	(TØEY)
ISP3		Percentage of first weight value that the change in weight is to be.	(ØVERCT)
ISP4		Dummy variable.	(ØVERCT)
IIN(L)L=1,LMAX		Dummy variables defined as one in SCAT4.	(INPT4)
IKTRL	(1)	Temporary storage of KTRL(13)	(CØULFN)
	(2)	Index number for r_i used to generate interaction.	(VGEN)
IEND		Total number of points at which wave functions are stored (for even spacing of points.	(TIEUP3)
ILAST	(1)	Total number of points at which wave functions for the unbound particle are calculated.	(RKINT)

FORTRAN SYMBOL	MATH. SYMBOL	DESCRIPTION	REFERENCE
	(2)	Index number for $\vec{r}_2$ used to generate interaction.	(VGEN)
IFIRST		Index of first value of $\rho = kr$ used.	(INTCTR)
IW		Index number to generate correct Clebsch-Gordan coefficient.	(WIGNER)
JSPILL		Overflow indicator used in FAP routine, SPILL.	(SPILL)
JMAX		Total number of Scattering angles to be used.	(READER)
KTRL(I)		Control numbers to fix the pattern of the calculation of the optical model wave functions.	(INPT4)
KSUPER	(1)	Sidesteps INPT4 being called twice (must = 2 for correct operation).	(CTRL4)
	(2) L+1	Ls used to transfer the value of the angular momentum transfer to the interaction calculation.	(VGEN)

FORTRAN SYMBOL	MATH. SYMBOL	DESCRIPTION	REFERENCE
KCØNT(I) I=1,9		Control numbers that determine what calculations will be performed	(CØNNEX)
LMAXM	l_{max}	Maximum partial wave to be used in the calculation of the wave function.	(ØVERCT)
LMAX,LIP	lmax+1	Total number of partial waves used in final and initial cases.	(ØVERCT)
L	$l+1$	Partial wave number plus one.	(INTCTR)
LPI,LPF	p,p'	Orbital angular momentum quantum numbers of initial and final bound states used.	(BSWFHØ)
LW1,LW2, LW3	j_1, j_2, j	Angular momentum values used in the Clebsch-Gordan coefficients.	(WIGNER)
LX	$l' + l$	Angular momentum used in the Spherical Harmonic.	(LEGEND)
LHØ	$p+l$	Angular momentum (orbital) used to generate the Harmonic Oscillator function.	(BSWFHØ)

FORTRAN SYMBOL	MATH. SYMBOL	DESCRIPTION	REFERENCE
MW1,MW2	j_1-m_1+1 j_2-m_2+1	Projections used in Clebsch-Gordan coefficients.	(WIGNER)
MEND		Total number of initial state projections needed to evaluate $d\sigma/d\Omega$	(TIEUP3)
MX	$1'-M+1$	As used in the Spherical Harmonic.	(LEGEND)
NUMRUN(I) I=1,5		Identification data.	(MAIN4)
NUMPRG		Governs the print out of the partial matrix elements (>10).	(TIEUP3)
NV,NW,NA,NVS NWS		Count of the variations of the parameters V,W,A,VS,WS.	(ØVERCT)
NVMAX, NVSMAX NWMAX, NWSMAX NAMAX		Total number of variations of the parameters V,W,A, VS,WS required.	(ØVERCT)
NMAX		Total number of basic kr input. These specify the various ranges mentioned before in DRHØIN(I)	(ØVERCT)

FORTRAN SYMBOL	MATH. SYMBOL	DESCRIPTION	REFERENCE
NMAXP		NMAX-1	(ØVERCT)
NBGMAX		Dummy variable.	(ØVERCT)
NEND		Total number of points at which renormalization occurred in RKINT.	(RKINT)
NHI,NHF	n,n'	The prime quantum numbers for the initial and final bound states.	(ADJUST)
NHØ	n''	The prime quantum number used in calculating the Harmonic oscillator function.	(BSWFHØ)
PHI	ϕ	The elevation angle used in Spherical Harmonics $Y_L^M(\theta,\phi)$	(IEGEND)
PHASE(MS,J) MS=1,MEND J=1,JMAX	$\mathcal{I}_m[\eta(m_j,\theta_{sc})]$	Imaginary part of the matrix element for an inelastic scattering from a closed shell plus one nucleus in the j-j coupling model.	(TIEUP3)

FORTRAN SYMBOL	MATH. SYMBOL	DESCRIPTION	REFERENCE
QVAL	Q	The Q-value for a reaction. This is not in dimension and common.	(READER)
RENMZ(100)	E_{lab}(initial)	Permanent location for the incident particle lab. energy.	(ØVERCT)
RENMZ(I) I=1,NEND		The renormalization values defined in the Runge-Kutta integration.	(LEGEND)
RTHETA	θ_{sc}^{c}	Scattering angle in radians.	(LEGEND)
RADWC	R_{cut}	Cut off radius for central weighting.	(BSWFHØ)
RADS(I) I=1,IEND	r_i	Table of equally spaced radii.	(ADJUST)
RC	r_c	The Coulomb radius parameter ($R_c = r_c A^{1/3}$)	(ØVERCT)
RO	r_o	The nuclear radius parameter ($R_N = r_o A^{1/3}$)	(ØVERCT)

FORTRAN SYMBOL	MATH. SYMBOL	DESCRIPTION	REFERENCE
RHØIN(I) I=1,NMAX		The basic points kr where spacings DRHØIN(I) change.	(RHØTB)
RHØBN	kR_N	Corresponds to the nuclear radius.	(ØVERCT)
RHØBS	R_{int}	The average interaction radius used in Harmonic oscillator function.	(BSWFHØ)
RHØBC	kR_c	Corresponds to the Coulomb radius.	(ØVERCT)
RG		Input as < 20.0 - this is increased with each run and is used to sidestep repetition of reading data - i.e. allows energy and weight variations.	(ØVERCT)
RSGML(L)	$Re[e^{i\sigma_\ell}]$	Real part of exponential of coulomb phase shifts for the incident particle.	(TIEUP3)
RHØBNG		Dummy variable	

FORTRAN SYMBOL	MATH. SYMBOL	DESCRIPTION	REFERENCE
RHØ(I) I=1,ILAST	ρ_i	Table of kr_i at which optical model wave functions are calculated.	(RHØTB)
RHØMAX	ρ_{max}	The integration limit value.	(RHØTB)
RØE(I)		Values of kr at which renormalization occurs.	(RKINT)
RØSP(I) I=1,IEND		Values of kr at which wave function stored.	(RKINT)
SIGMA0 SIGMA1	σ_0, σ_1	Coulomb phase shifts for $l = 0, 1$	(SIGZRØ)
SNØ1		A test number to restrict the number of partial wave contributions to the matrix elements.	(TIEUP3)
SØMR,SØMI		Real and Imaginary parts of the radial integral in the matrix elements.	(TØEY)
TV,TW,TA, TVS,TWS		Initial values of the parameters V,W,A,TVS,TWS.	(INPT4)

FORTRAN SYMBOL	MATH. SYMBOL	DESCRIPTION	REFERENCE
THETAD(J) J=1,JMAX	θ_{sc}^{o}	Scattering angles input in degrees.	(READER)
THETA(J) J=1,JMAX	θ_{sc}^{c}	Scattering angles in radians.	(READER)
TBDPØT	V_o	Strength of the two-body interaction used.	(TIEUP4)
UCRB(I) UCIB(I) I=1,(ILAST or IEND)	(1)	Real and imaginary parts of the 1-independent part of the central nuclear potential at each value of ρ_i.	(PGEN4)
	(2)	Real and imaginary parts of (TØEY) r dependent wave function product in the matrix elements.	
USRM(I),UCIM(I) I=1,ILAST		Real and imaginary parts of the 1-independent central potential at half values of ρ.	(PGEN4)
USRB(I), USIB(I) I=1,ILAST		Real and imaginary parts of the spin-orbit nuclear potential at the tabled values of ρ.	(PGEN4)

FORTRAN SYMBOL	MATH. SYMBOL	DESCRIPTION	REFERENCE
USRM(I) USIM(I) I=1,ILAST		Real and imaginary parts of the spin-orbit nuclear potential at the half values of ρ	(PGEN4)
USGML(L) L=1,LMAX	$\mathrm{Im}[e^{i\sigma_l}]$	Imaginary part of the incident particle's coulomb phase shifts.	(TIEUP3)
ULRN(I) I=1,IEND	(1)	Storage locations of the Harmonic oscillator wave function at all points	(BSWFHØ)
	(2)	Product of two bound state wave functions.	(BSWFHØ)
V	V	Real part of the central potential well depth.	(ØVERCT)
VS	V_s	Real part of the spin-orbit nuclear potential well depth.	(ØVERCT)
W	W	Imaginary part of the central potential well depth.	(ØVERCT)
WS	W_s	Imaginary part of the spin-orbit nuclear potential well depth.	(ØVERCT)

FORTRAN SYMBOL	MATH. SYMBOL	DESCRIPTION	REFERENCE
WFMØD(MS,J) MS=1,MEND J=1,JMAX	$\mathcal{R}e[m(m_j,\theta_{sc})]$	Real part of the matrix element for m_j and θ_{sc}.	(TIEUP3)
WF	W_f	Weight factor in each bound state wave function.	(BSWFHØ)
XC1,XCP1	$f_\ell^+(\rho)$, $f_\ell^{+\prime}(\rho)$	Real part of the unnormalized radial wave function and its derivative for spin up case.	(INTCTR)
XD1,XDP1	$f_\ell^-(\rho)$ $f_\ell^{-\prime}(\rho)$	Real part of wave function for spin down.	(INTCTR)
X1(L), X1P(L) L=1,LMAX	$f_\ell^+(\rho_{max})$ $f_\ell^{+\prime}(\rho_{max})$	Real part of the unnormalized spin up radial wave function and its derivative at the boundary.	(INTCTR)
XCS(I,L) XCST(I,L) I=1,IEND L=1,LMAX	$f_{\ell'}(\rho_i)$ $f_\ell(\rho_i)$	Real parts of the normalized radial wave equations for the final and initial unbound particles.	(WFNØRM)

FORTRAN SYMBOL	MATH. SYMBOL	DESCRIPTION	REFERENCE
YC1,YCP1		Imaginary part of the unnormalized radial wave function and its derivative for spin up case.	(INTCTR)
YD1,YDP1		Imaginary part of the spin down wave function and its derivative.	(INTCTR)
Y1(L), Y1P(L) L=1,LMAX		Imaginary part of the unnormalized spin up radial wave function and its derivative at the boundary.	(INTCTR)
YCS(I,L) YCST(I,L) I=1,IEND L=1,LMAX		Imaginary parts of the normalized radial wave functions for the final and initial unbound particles.	(WFNØRM)
YLMR,YLMI	(1) $Y_{\ell'}^{M}(\theta_{sc},\phi)$	Real and Imaginary parts of the spherical harmonic.	(LEGEND)
	(2)	Real and imaginary parts of the r_2 integral in the matrix elements.	(ACTIØN)

FORTRAN SYMBOL	MATH. SYMBOL	DESCRIPTION	REFERENCE
ZZ	$Z_i * Z_T$	Product of the charges of the unbound particle and the target (or residual) nucleus.	(INPUT4)

*C5 2001 K A AMOS UNIV OF ADELAIDE

CODE FOR ANGULAR DISTRIBUTIONS FOR INELASTIC SCATTERING OF NUCLEONS BY A DIRECT REACTION TWO-BODY COLLISION MECHANISM. THE INTERACTION CAN BE EITHER OF ZERO OR FINITE RANGE (YUKAWA).

JANUARY 1964

```
C       THE COMMON AND DIMENSION STATEMENTS
        COMMONA,AR,AI,
       1BG,
       2CR1,CI1,CR2,CI2,CLEB,
       3DA,DV,DW,DVS,DWS,DBG,DELAB,DTHETA,DRHO,DRHOIN,DRHOL,
       4ECM,ELAB,EFIN,EPS1,EPS2,EPS3,EPS4,ETA,ETA2,EXSGMR,EXSGMI,
       5F,FP,FBAR,FG,FIP,FMI,FMB,FMU,FKAYA,FKAYB,FKAY,FFCR,FFCI,FFSR,FFSI,
       6FFCRM,FFCIM,FFSRM,FFSIM,
       7G,GP,
       8HOJI,HOJF,
       9ISPILL,IFIRST,IIN,ILAST,IKTRL,ISP1,ISP2,ISP3,ISP4,IEND,IW
        COMMONJSPILL,JMAX,
       1KTRL,KSUPER,KCONT,
       2LMAX,L,LMAXM,LIP,LW1,LW2,LW3,LX,LHO,LPI,LPF,
       3MEND,MX,MW1,MW2,
       4NUMPRG,NUMRUN,NMAX,NMAXP,NVMAX,NWMAX,NAMAX,NVSMAX,NWSMAX,NBGMAX,
       5NV,NW,NA,NVS,NWS,NBG,NHO,NEND,NHI,NHF,
       6PHASE,PHI,
       7RHOBC,RHOBN,RHOBNG,RO,RC,RG,RHOMAX,RHO,RHOM,RHOIN,RSGML,RADS,
       8RTHETA,RADWC,RENMZ,ROE,ROSP,
       9SOMR,SOMI,SIGMA0,SIGMA1
        COMMONTV,TW,TA,TVS,TWS,TBG,THETAD,THETA,
       1UCRB,UCIB,USRB,USIB,UCRM,UCIM,USRM,USIM,USGML,ULRN,
       2V,VS,
       3W,WS,WFMOD,WF,
       4X1,X2,X1P,X2P,XC1,XCP1,XD1,XDP1,XCS,XCST,XDS,
       5Y1,Y2,Y1P,Y2P,YC1,YCP1,YD1,YDP1,YCS,YCST,YLMR,YLMI,YDS,
       6ZZ
        COMMONSNO1,RHOBS,TBDPOT
        DIMENSIONAR(75),AI(75),
       1CR1(21),CI1(21),
       2DRHO(100),DRHOIN(100),
       3EXSGMR(21),EXSGMI(21),
       4F(22),FP(21),FFCR(100),FFCI(100),FFSR(100),FFSI(100),FFCRM(100),
       5FFCIM(100),FFSRM(100),FFSIM(100),FG(101),FBAR(70),
       6G(22),GP(21),
       7IIN(21),
       8KTRL(13),KCONT(20),
       9NUMRUN(5)
        DIMENSIONRSGML(21),
       1RHO(100),RHOIN(100),RADS(100),RENMZ(100),ROE(100),ROSP(100),
       2THETA(75),THETAD(75),
       3UCRB(100),UCIB(100),USRB(100),USIB(100),UCRM(100),UCIM(100),
       4USRM(100),USIM(100),USGML(21),ULRN(100),
       5X1(21),X1P(21),XCS(100,16),XCST(100,16),
       6Y1(21),Y1P(21),YCS(100,16),YCST(100,16)
        DIMENSIONWFMOD(11,75),PHASE(11,75)
```

```
C       MAIN ROUTINE   INEL SCAT
        CALL SPILL(JSPILL,ISPILL,0.,0.)                                    00-
        EPS1= 0.00001                                                      00-
        EPS2= 0.00001                                                      00-
        EPS3= 0.00001                                                      00-
        EPS4=0.001                                                         00-
        READINPUTTAPE2,10,(NUMRUN(I),I=1,5)
        READINPUTTAPE2,10,NUMPRG
   10   FORMAT(I5)                                                         00-
        PRINT21
    21  FORMAT(100H TERMINATE PROGRAM IF ANY HOLLERITH   REPEAT HOLLERITH
       1FIELD PRINTED MORE THAN 20 TIMES REPETITIVELY)
        CALLOVERCT
    78  CALLEXIT
        END
```

```
      SUBROUTINEOVERCT
      KVAL=0
      MCSR=1
      KSUPER=1
      CALLLGFACT
   93 CALLINPT4
      KSUPER=2
      AA1=RHOIN(1)
      AA2=RHOIN(2)
      AA3=RHOIN(3)
      AA4=RHOIN(4)
      BB1=DRHOIN(1)
      BB2=DRHOIN(2)
      BB3=DRHOIN(3)
      UGB=RHOMAX
    9 DO20NV=1,NVMAX
      IF(NV-1)102,101,102
  101 V=TV
      V2D=TV2
      GOTO103
  102 V=V+DV
      V2D=V2D+DV
  103 DO20NW=1,NWMAX
      IF(NW-1)105,104,105
  104 W=TW
      W2D=TW2
      GOTO109
  105 W=W+DW
      W2D=W2D+DW
  109 DO20NA=1,NAMAX
      IF(NA-1)111,110,111
  110 A=TA
      A2D=TA2
      GOTO112
  111 A=A+DA
      A2D=A2D+DA
  112 DO20NVS=1,NVSMAX
      IF(NVS-1)114,113,114
  113 VS=TVS
      VS2D=TVS2
      GOTO115
  114 VS=VS+DVS
      VS2D=VS2D+DVS
  115 DO20NWS=1,NWSMAX
      IF(NWS-1)117,116,117
  116 WS=TWS
      WS2D=TWS2
      GOTO118
  117 WS=WS+DWS
      WS2D=WS2D+DWS
  118 KSUPER=2
      RHOIN(1)=AA1
      RHOIN(2)=AA2
      RHOIN(3)=AA3
      RHOIN(4)=AA4
      DRHOIN(1)=BB1
      DRHOIN(2)=BB2
      DRHOIN(3)=BB3
      RHOMAX=UGB
```

```
      CALLCTRL4
      WRITEOUTPUTTAPE3,1515,(RHOIN(I),DRHOIN(I),I=1,3),RHOIN(NMAX),RHOMA
     1X
 1515 FORMAT(1H /1H ,1P8E13.4/1H )
      NO101=KTRL(1)
      NO201=KTRL(2)
      NO301=KTRL(3)
      NO401=KTRL(4)
      NO501=KTRL(5)
      NO601=KTRL(6)
      NO701=KTRL(7)
      NO801=KTRL(8)
      NO901=KTRL(9)
      NO1001=KTRL(10)
      NO1101=KTRL(11)
      NO1201=KTRL(12)
      NO1301=KTRL(13)
      FMI1T=FMI
      FMB1T=FMB
      ELAB1T=ELAB
      RENMZ(100)=ELAB1T
      RENMZ(99)=FMB/(FMI+FMB)
      ZZ1T=ZZ
      RC1T=RC
      V1T=V
      W1T=W
      A1T=A
      RO1T=RO
      VS1T=VS
      WS1T=WS
      LMAXM1=LMAXM
      FMI=FMI2D
      FMB=FMB2D
      ELAB=ELAB2D
      ZZ=ZZ2D
      RC=RC2D
      V=V2D
      W=W2D
      RO=RO2D
      A=A2D
      VS=VS2D
      WS=WS2D
      LMAXM=LMAXM2
      KTRL(1)=NO102
      KTRL(2)=NO202
      KTRL(3)=NO302
      KTRL(4)=NO402
      KTRL(5)=NO502
      KTRL(6)=NO602
      KTRL(7)=NO702
      KTRL(8)=NO802
      KTRL(9)=NO902
      KTRL(10)=NO1002
      KTRL(11)=NO1102
      KTRL(12)=NO1202
      KTRL(13)=NO1302
      CALLCONNEX
      WRITEOUTPUTTAPE3,1515,(RHOIN(I),DRHOIN(I),I=1,3),RHOIN(NMAX),RHOMA
     1X
```

```
      CALLWIPE
      BG=BG+1.0
      FMI2D=FMI
      FMB2D=FMB
      RENMZ(98)=FMB/(FMI+FMB)
      ELAB2D=ELAB
      ZZ2D=ZZ
      RC2D=RC
      V2D=V
      W2D=W
      RO2D=RO
      A2D=A
      VS2D=VS
      WS2D=WS
      LMAXM2=LMAXM
      NO1O2=KTRL(1)
      NO2O2=KTRL(2)
      NO3O2=KTRL(3)
      NO4O2=KTRL(4)
      NO5O2=KTRL(5)
      NO6O2=KTRL(6)
      NO7O2=KTRL(7)
      NO8O2=KTRL(8)
      NO9O2=KTRL(9)
      NO1OO2=KTRL(10)
      NO11O2=KTRL(11)
      NO12O2=KTRL(12)
      NO13O2=KTRL(13)
      KTRL(1)=NO1O1
      KTRL(2)=NO2O1
      KTRL(3)=NO3O1
      KTRL(4)=NO4O1
      KTRL(5)=NO5O1
      KTRL(6)=NO6O1
      KTRL(7)=NO7O1
      KTRL(8)=NO8O1
      KTRL(9)=NO9O1
      KTRL(10)=NO1OO1
      KTRL(11)=NO11O1
      KTRL(12)=NO12O1
      KTRL(13)=NO13O1
      FMI=FMI1T
      FMB=FMB1T
      ELAB=ELAB1T
      ZZ=ZZ1T
      RC=RC1T
      V=V1T
      W=W1T
      RO=RO1T
      A=A1T
      VS=VS1T
      WS=WS1T
      LMAXM=LMAXM1
      MCSR=NUMRUN(5)
      IF(MCSR-1)241,241,242
  241 TV2=V2D
      TW2=W2D
      TA2=A2D
      TVS2=VS2D
```

```
      TWS2=WS2D
      MCSR=10
      E1=ELAB
      E2=ELAB2D
  242 CONTINUE
      CO2=FMI+FMB
      FMU=(FMI*FMB)/CO2
      ECM=ELAB*(FMB/CO2)
      FKAY=0.2195376*SQRTF(FMU*ECM)
      T=FKAY*(FMB**0.333333333)
      RHOBN=T*RO
      RHOBC=T*RC
      ETA=0.15805086*ZZ*SQRTF(FMI/ELAB)
      LMAX=LMAXM+1
      RG=RG+50.0
   20 CONTINUE
      QOM=RENMZ(99)*ELAB-RENMZ(98)*ELAB2D
      ELAB=ELAB+DELAB
      IF(DELAB)889,210,889
  889 IF(ELAB-EFIN)200,200,210
  200 ELAB2D=(RENMZ(99)*ELAB-QOM)/RENMZ(98)
      ECM=ELAB*FMB/(FMB+FMI)
      FKAY=0.2195376*SQRTF(FMU*ECM)
      T=FKAY*(FMB**0.333333333)
      RHOBN=T*RO
      RHOBC=T*RC
      ETA=0.15805086*ZZ*SQRTF(FMI/ELAB)
      GOTO9
  210 IF(ISP3)201,201,260
  260 KVAL=KVAL+1
      IF(KVAL-1)261,261,262
  261 RTV=WF
      PC=ISP3/100
      DEL=1.0-SQRTF(1.0-PC)
      DELWF=DEL*RTV
      IF(DELWF)868,901,868
  868 CONTINUE
  262 WF=WF-DELWF
      MCSR=1
      ELAB=E1
      ELAB2D=E2
      IF(WF)901,200,263
  263 IF(KVAL-ISP1)200,200,901
  901 ISP4=5000
      KVAL=0
      CALLWIPE
  201 IF(ISPILL)651,652,651
  651 PRINT653,ISPILL
  653 FORMAT(14H UNDERFLOW AT I5,10H IN OVERCT)
  652 IF(JSPILL)654,656,654
  654 PRINT655,JSPILL
  655 FORMAT(13H OVERFLOW AT I5,10H IN OVERCT)
      CALL EXIT
  656 RETURN
      END
```

```
      SUBROUTINE INPT4                                                  02-
      IF DIVIDE CHECK 100,110                                           02-
  100 PRINT101
  101 FORMAT(59H DIVIDE CHECK TRIGGER FOUND ON AT START OF INPT4 SUBROUT 02-
     1INE)                                                              02-
      CALLEXIT
  110 ISPILL=0                                                          02-
      JSPILL=0                                                          02-
      READINPUTTAPE2,10,KTRL(1)
      IF (KTRL(1)-100) 150,151,151                                      02-
  151 CALL EXIT                                                         02-
  150 READINPUTTAPE2,10,(KTRL(I),I=2,13)
   10 FORMAT (I5)                                                       02-
      READINPUTTAPE2,12,FMI,FMB,ELAB,ZZ,RC,V,W,RO,A,VS,WS,RG,BG,
     1DV,DW,DA,DVS,DWS,DBG                                              02-
      READINPUTTAPE2,10,NVMAX,NWMAX,NAMAX,NVSMAX,NWSMAX,NBGMAX
      READINPUTTAPE2,12,DELAB,EFIN
      READINPUTTAPE2,10,ISP1,ISP2,ISP3,ISP4
   12 FORMAT (E15.9)                                                    02-
      TV= V                                                             02-
      TW=W                                                              02-
      TA=A                                                              02-
      TVS=VS                                                            02-
      TWS=WS                                                            02-
      TBG=BG                                                            02-
      READINPUTTAPE2,10,NMAX
      NMAXP=NMAX-1                                                      02-
      READINPUTTAPE2,12,(RHOIN(I),I=1,NMAX),(DRHOIN(I),I=1,NMAXP)
      CO2=FMI+FMB                                                       02-
      FMU=(FMI*FMB)/CO2                                                 02-
      ECM=ELAB*(FMB/CO2)                                                02-
      FKAY= .2195376*SQRTF(FMU*ECM)                                     02-
      T=FKAY*(FMB**.333333333)                                          02-
      RHOBN= T*RO                                                       02-
      RHOBNG=T*RG                                                       02-
      RMA=PMA*RHOBN                                                     02-
      RMB=PMB*RHOBN                                                     02-
      RHOBC= T*RC                                                       02-
      ETA= .15805086*ZZ*SQRTF(FMI/ELAB)                                 02-
      IF DIVIDE CHECK 200,47                                            02-
  200 PRINT201
  201 FORMAT(43H INPUT DIVISOR WAS ZERO IN INPT4 SUBROUTINE)            02-
      CALLEXIT
   47 READINPUTTAPE2,10,LMAXM
      LMAX=LMAXM+1                                                      02-
      DO 147 J=1,LMAX                                                   02-
  147 IIN(J)=1                                                          02-
      IF (KTRL(5)) 48,50,48                                             02-
   48 READINPUTTAPE2,10,JMAX
      READINPUTTAPE2,12,(THETAD(I),I=1,JMAX)
      DO 49 I=1,JMAX                                                    02-
   49 THETA(I)= 0.01745329252*THETAD(I)                                 02-
   50 CONTINUE
  207 IF(ISPILL)202,204,202                                             02-
  202 PRINT203,ISPILL
  203 FORMAT(23H UNDERFLOW OCCURRED AT I5,20H IN INPT4 SUBROUTINE)      02-
  204 IF(JSPILL)205,210,205                                             02-
  205 PRINT206,JSPILL
  206 FORMAT(22H OVERFLOW OCCURRED AT I5,20H IN INPT4 SUBROUTINE)       02-
```

```
      CALLEXIT
210   RETURN
      END
```

```
      SUBROUTINECTRL4
      IFDIVIDECHECK111,112
  111 PRINT222
  222 FORMAT(59H DIVIDE CHECK TRIGGER F3UND ON IN START OF CTRL4 SUBROUT
     1INE)
      CALLEXIT
  112 GOTO(20,30,40),KSUPER
   20 CALLINPT4
   30 CALLPOTICH
      CALLSIGZRO
      CALLEXSGML
   40 NUMRUN(5)=NUMRUN(5)+1
      CALLRHOTB
      CALLCOULFN
      CALLRMXINC
      CALLPGEN4
      CALLINTCTR
      CALLCSUBL
      CALLWFNORM
      IF(KTRL(2))33,100,33
   33 CALLOUTPT4
  100 RETURN
      END
```

```
      SUBROUTINE POT1CH                                                 03·
      IF DIVIDE CHECK 30,31                                             03·
   30 PRINT130
  130 FORMAT (60H DIVIDE CHECK TRIGGER FOUND ON AT START OF POT1CH SUBRO 03·
     1UTINE)                                                            03·
      CALLEXIT
   31 ISPILL=0                                                          03·
      JSPILL=0                                                          03·
      IKTRL=KTRL(13)                                                    03·
      NMAX=NMAX                                                         03·
      NMAXP= NMAX-1                                                     03·
      AMAX=NAMAX-1                                                      03·
      TTA=MAX1F(A,((AMAX*DA)+A))                                        03·
      VMAX=NVMAX-1                                                      03·
      TTV=MAX1F(V,((VMAX*DV)+V))                                        03·
      WMAX=NWMAX-1                                                      03·
      TTW=MAX1F(W,((WMAX*DW)+W))                                        03·
      VSMAX=NVSMAX-1                                                    03·
      TTVS=MAX1F(VS,((VSMAX*DVS)+VS))                                   03·
      WSMAX=NWSMAX-1                                                    03·
      TTWS=MAX1F(WS,((WSMAX*DWS)+WS))                                   03·
      BGMAX=NBGMAX-1                                                    03·
      TTBG=MAX1F(BG,((BGMAX*DBG)+BG))                                   03·
      FKAYA=FKAY*TTA                                                    03·
      FKAYB=FKAY*TTBG                                                   03·
      T2=SQRTF(TTV**2+TTW**2)/ECM                                       03·
      T7=TTV/ECM                                                        03·
      T8=TTW/ECM                                                        03·
      IF DIVIDE CHECK 60,61                                             03·
   60 PRINT160
  160 FORMAT(26H ECM IS ZERO IN POT1CH SUB)                             03·
      CALLEXIT
   61 GO TO (3,3,111,15),IKTRL                                          03·
    3 IF(KTRL(1)-2) 24,25,24                                            03·
   25 IF(RHOIN(NMAX)-RHOBN) 10,10,8                                     03·
   24 T1=1./(1.+EXPF((RHOIN(NMAX)-RHOBN)/FKAYA))                        03·
      IF DIVIDE CHECK 50,28                                             03·
   50 PRINT150
  150 FORMAT(28H FKAYA IS ZERO IN POT1CH SUB)                           03·
      CALLEXIT
   28 IF(KTRL(1)-1) 40,41,40                                            03·
   40 T3= T2*T1                                                         03·
      GO TO 43                                                          03·
   41 T3=T7*T1                                                          03·
   43 IF(T3-EPS4) 42,42,10                                              03·
   10 PRINT100,RHOIN(NMAX),DRHOIN(NMAXP)
  100 FORMAT(13H RHOIN(NMAX)=E16.9,2H+ E16.9,46H RHOIN(NMAX) IS TOO SMAL 03·
     1L IN NUCLEAR POTENTIAL)                                           03·
      RHOIN(NMAX)= RHOIN(NMAX)+DRHOIN(NMAXP)                            03·
      GO TO 3                                                           03·
   42 IF(KTRL(1)-1) 3,6,8                                               03·
    6 T11= EXPF(-((RHOIN(NMAX)-RHOBNG)/FKAYB)**2)                       03·
      IF((T8*T11)-EPS4) 8,8,7                                           03·
    7 PRINT103,RHOIN(NMAX),DRHOIN(NMAXP)
  103 FORMAT(13H RHOIN(NMAX)=E16.9,2H+ E16.9,46H RHOIN(NMAX) IS TOO SMAL 03·
     1L IN NUCLEAR POTENTIAL)                                           03·
      RHOIN(NMAX)= RHOIN(NMAX)+DRHOIN(NMAXP)                            03·
      GO TO 6                                                           03·
    8 GO TO(111,15),IKTRL                                               03·
```

```
111   FLMAX=LMAXM                                                          03-
      IF(KTRL(1)-2) 29,300,29                                              03-
300   IF(FLMAX-(RHOBN+3.)) 12,12,15                                        03-
29    T4=1./(1.+EXPF((FLMAX-RHOBN)/FKAYA))                                 03-
      IF(KTRL(1)-1) 33,32,33                                               03-
33    T5= T2*T4                                                            03-
      GO TO 310                                                            03-
32    T5=T7*T4                                                             03-
310   IF(T5-EPS4)13,13,12                                                  03-
  12  PRINT101,LMAXM
 101  FORMAT (7H LMAXM=I5,3H +1,45H LMAXM TOO SMALL BECAUSE OF CENTRAL P   03-
     1OTENTIAL)                                                            03-
      LMAX= LMAX+1                                                         03-
      LMAXM= LMAXM+1                                                       03-
      IIN(LMAX)=1                                                          03-
      GO TO 111                                                            03-
13    IF(KTRL(1)-1) 17,19,17                                               03-
19    T4=EXPF(-((FLMAX-RHOBNG)/FKAYB)**2)                                  03-
      IF((T8*T4)-EPS4) 17,17,20                                            03-
  20  PRINT200,LMAXM
200   FORMAT (7H LMAXM=I5,3H +1,45H LMAXM TOO SMALL BECAUSE OF CENTRAL P   03-
     1OTENTIAL)                                                            03-
      LMAX=LMAX+1                                                          03-
      LMAXM=LMAXM+1                                                        03-
      IIN(LMAX)=1                                                          03-
      GO TO 19                                                             03-
17    T2=SQRTF(TTVS**2+TTWS**2)/ECM                                        03-
18    FLMAX=LMAXM                                                          03-
      T4=1./(1.+EXPF((FLMAX-RHOBN)/FKAYA))                                 03-
38    T6=2.*T2*T4*(FKAY**2)                                                03-
      IF(T6-EPS4) 15,15,14                                                 03-
  14  PRINT102,LMAXM
 102   FORMAT (7H LMAXM=I5,3H +1,48H LMAXM TOO SMALL BECAUSE OF SPIN ORB   03-
     1IT POTENTIAL)                                                        03-
      LMAX= LMAX+1                                                         03-
      LMAXM= LMAXM+1                                                       03-
      IIN(LMAX)=1                                                          03-
      GO TO 13                                                             03-
15    IF(ISPILL)202,204,202                                                03-
 202  PRINT203,ISPILL
 203  FORMAT(23H UNDERFLOW OCCURRED AT I5,14H IN POT1CH SUB)                03-
204   IF(JSPILL)205,210,205                                                03-
 205  PRINT206,ISPILL
 206  FORMAT(22H OVERFLOW OCCURRED AT I5,14H IN POT1CH SUB)                 03-
      CALLEXIT
210   RETURN                                                               03-
      END
```

```
      SUBROUTINE SIGZRO                                                 05
      IF DIVIDE CHECK 5,6                                               05
    5 PRINT105
  105 FORMAT (60H DIVIDE CHECK TRIGGER FOUND ON AT START OF SIGZRO SUBRO 05
     1UTINE)                                                            05
      CALLEXIT
    6 ISPILL=0                                                          05
      JSPILL=0                                                          05
      SIGMA0=-(ETA/(12.*(ETA**2+16.)))*(1.+(ETA**2-48.)/(30.*((ETA**2+16 05
     1.)**2))+(ETA**4-160.*(ETA**2)+1280.)/(((16.+ETA**2)**4)*105.))    05
      SIGMA0=SIGMA0-ETA+(ETA/2.)*LOGF(ETA**2+16.)+((7./2.)*ATANF(ETA/4.) 05
     1)-(ATANF(ETA)+ATANF(ETA/2.)+ATANF(ETA/3.))                        05
      SIGMA1=SIGMA0+ATANF(ETA)                                          05
   15 IF (ISPILL) 30,31,30                                              05
   30 PRINT130,ISPILL
  130 FORMAT (23H UNDERFLOW OCCURRED AT I6,21H IN SIGZRO SUBROUTINE)    05
   31 IF (JSPILL) 32,11,32                                              05
   32 PRINT132,JSPILL
  132 FORMAT (22H OVERFLOW OCCURRED AT I6,21H IN SIGZRO SUBROUTINE)     05
      CALLEXIT
   11 RETURN                                                            05
      END
```

```
      SUBROUTINE EXSGML                                                 07-
      IF DIVIDE CHECK 10,11                                             07-
   10 PRINT110
  110 FORMAT (60H DIVIDE CHECK TRIGGER FOUND ON AT START OF EXSGML SUBRO 07-
     1UTINE)                                                            07-
      CALLEXIT
   11 ISPILL=0                                                          07-
      JSPILL=0                                                          07-
    1 FL=0.                                                             07-
      EXSGMR(1)=COSF(2.0*SIGMA0)                                        07-
      EXSGMI(1)=SINF(2.0*SIGMA0)                                        07-
      ETA2=ETA**2                                                       07-
      ETA2A=2.0*ETA                                                     07-
      DO 20 L=2,LMAX                                                    07-
      FL=FL+1.0                                                         07-
      TER0=FL**2                                                        07-
      TER1=TER0+ETA2                                                    07-
      TER2=(TER0-ETA2)/TER1                                             07-
      TER3=(ETA2A*FL)/TER1                                              07-
      IF DIVIDE CHECK 12,13                                             07-
   12 PRINT112,L
  112 FORMAT (44H DIVISOR IS ZERO IN EXSGML SUBROUTINE FOR L=I3)        07-
      CALLEXIT
   13 EXSGMR(L)=(TER2*EXSGMR(L-1))-(TER3*EXSGMI(L-1))                   07-
   20 EXSGMI(L)=(TER2*EXSGMI(L-1))+(TER3*EXSGMR(L-1))                   07-
      DO666L=1,LMAX
      PG=EXSGMR(L)
      PH=EXSGMI(L)
      CALLCSQR(PG,PH,AC,AD)
      EXSGMR(L)=AC
  666 EXSGMI(L)=AD
      IF (ISPILL) 14,15,14                                              07-
   14 PRINT114,ISPILL
  114 FORMAT(23H UNDERFLOW OCCURRED AT I6,21H IN EXSGML SUBROUTINE)     07-
   15 IF (JSPILL) 16,17,16                                              07-
   16 PRINT116,JSPILL
  116 FORMAT(22H OVERFLOW OCCURRED AT I6,21H IN EXSGML SUBROUTINE)      07-
      CALLEXIT
   17 RETURN                                                            07-
      END
```

```
      SUBROUTINE RHOTB                                                  08
      DRHO(1)=DRHOIN(1)                                                 08
      RHO(1)=RHOIN(1)                                                   08
      N=1                                                               08
      I=1                                                               08
   20 RHO(I+1)=RHO(I)+DRHOIN(N)                                         08
      IF (RHO(I+1)-RHOIN(NMAX))30,50,70                                 08
   30 IF(ABSF(RHO(I+1)-RHOIN(N+1))-.5*DRHOIN(N)) 35,35,40               08
   35    N=XMINOF(N+1,NMAX-1)                                           08
   40 DRHO(I+1)=DRHOIN(N)                                               08
      I=I+1                                                             08
      GO TO 20                                                          08
   50 ILAST=I+1                                                         08
   60 RHO(ILAST)=RHOIN(NMAX)                                            08
      DRHO(ILAST-1)=RHO(ILAST)-RHO(ILAST-1)                             08
      RHOMAX=RHOIN(NMAX)                                                08
      DRHOL=DRHOIN(NMAX-1)                                              08
      IF(ISPILL) 80,81,80                                               08
   80 PRINT180,ISPILL
  180 FORMAT(23H UNDERFLOW OCCURRED AT I6,21H IN RHOTB  SUBROUTINE)     08
   81 IF(JSPILL)82,83,82                                                08
   82 PRINT182,JSPILL
  182 FORMAT(22H OVERFLOW OCCURRED AT I6,21H IN RHOTB  SUBROUTINE)      08
      CALLEXIT
   83 RETURN                                                            08
   70 IF((RHO(I+1)-RHOIN(NMAX))-.5*DRHOIN(N))50,50,75                   08
   75 ILAST=I                                                           08
      GO TO 60                                                          08
      END
```

```
      SUBROUTINE COULFN                                                 09-
      IF DIVIDE CHECK 50,51                                             09-
   50 PRINT150
  150 FORMAT (60H DIVIDE CHECK TRIGGER FOUND ON AT START OF COULFN SUBRO 09-
     1UTINE)                                                            09-
      CALLEXIT
   51 ISPILL=0                                                          09-
      JSPILL=0                                                          09-
      IKTRL=KTRL(13)                                                    09-
      LMAX=LMAXM+1                                                      09-
      ETA2=ETA**2                                                       09-
      SQ=SQRTF(1.+ETA2)                                                 09-
    1 IJ=1                                                              09-
      AR(1)=-ETA                                                        09-
      AI(1)=0.                                                          09-
      AR(2)=-.5*ETA2                                                    09-
      AI(2)=.5*ETA                                                      09-
    2 SI=0.                                                             09-
      SR=0.                                                             09-
      PR= RHOMAX                                                        09-
      DO 10  K=2,49                                                     09-
      T= PR*FLOATF(1-K)                                                 09-
      TR=AR(K)/T                                                        09-
      TI=AI(K)/T                                                        09-
      IF DIVIDE CHECK 52,53                                             09-
   52 PRINT152
  152 FORMAT(57H DIVISOR T IS ZERO IN FIRST DIVISION OF COULFN SUBROUTIN 09-
     1E)                                                                09-
      CALLEXIT
   53 SQN=TR**2+TI**2                                                   09-
      IF(K-2) 4,4,3                                                     09-
    3 IF(SQN-SQO) 4,4,11                                                09-
    4 TR=SR+TR                                                          09-
      TI=SI+TI                                                          09-
      IF(TR-SR) 6,5,6                                                   09-
    5 IF(TI-SI) 6,13,6                                                  09-
    6 SR=TR                                                             09-
      SI=TI                                                             09-
      AR(K+1)=0.                                                        09-
      AI(K+1)=0.                                                        09-
      KP=K/2                                                            09-
      DO 7 M=1,KP                                                       09-
      KM=K+1-M                                                          09-
      AR(K+1)=AR(K+1)-AR(M)*AR(KM)+AI(M)*AI(KM)                         09-
    7 AI(K+1)=AI(K+1)-AI(KM)*AR(M)-AI(M)*AR(KM)                         09-
      IF(K-2*KP) 8,9,8                                                  09-
    8 AR(K+1)=AR(K+1)-.5*(AR(KP+1)**2-AI(KP+1)**2)                      09-
      AI(K+1)=AI(K+1)-AR(KP+1)*AI(KP+1)                                 09-
    9 FK=.5*FLOATF(K)                                                   09-
      AI(K+1)=AI(K+1)-FK*AR(K)                                          09-
      AR(K+1)=AR(K+1)+FK*AI(K)                                          09-
      PR= PR*RHOMAX                                                     09-
   10 SQO=SQN                                                           09-
      GO TO 101                                                         09-
   11 T=SR**2+SI**2                                                     09-
      IF(T) 105,105,12                                                  09-
   12 IF(ABSF(SQO/T)-EPS3) 13,13,106                                    09-
   13 GO TO (14,15),IJ                                                  09-
   14 PAR=RHOMAX-ETA*LOGF(2.*RHOMAX)                                    09-
```

```
      PHIOR=PAR+SIGMA0+SR                                                09-
      PHIOI=SI                                                           09-
      AR(2)=-1.+AR(2)                                                    09-
      IJ=2                                                               09-
      GO TO 2                                                            09-
   15 PHI1R=PAR+SIGMA1-1.570796325+SR                                    09-
      PHI1I=SI                                                           09-
   25 T1=EXPF(-PHIOI)                                                    09-
      T2=EXPF(-PHI1I)                                                    09-
      G(1)=T1*COSF(PHIOR)                                                09-
      G(2)=T2*COSF(PHI1R)                                                09-
      F1=T1*SINF(PHIOR)                                                  09-
      F2=T2*SINF(PHI1R)                                                  09-
      IF(ABSF(F1*G(2)-F2*G(1)-1./SQ)-EPS1)  31,31,102                    09-
   31 IDEC=11                                                            09-
   32 I=LMAX+IDEC                                                        09-
      FBAR(I)=.1                                                         09-
      FBAR(I+1)=0.                                                       09-
      LIMIT=LMAXM+IDEC                                                   09-
      FL=LMAX+11                                                         09-
      T1=SQRTF((FL+1.)**2+ETA2)                                          09-
      IF(JSPILL) 139,133,139                                             09-
  139 PRINT1390,JSPILL
 1390 FORMAT(23H OVERFLOW2 OCCURRED AT I6,21H IN COULFN SUBROUTINE)      09-
      CALLEXIT
  133 DO 33 I=1,LIMIT                                                    09-
      L=LMAX+IDEC-I                                                      09-
      FL=L                                                               09-
      T2=SQRTF(FL**2+ETA2)                                               09-
      FBAR(L)=((2.*FL+1.)*(ETA+FL*(FL+1.)/RHOMAX)*FBAR(L+1)-FL*T1*FBAR(L 09-
     1+2))/((FL+1.)*T2)                                                  09-
      IF DIVIDE CHECK 54,600                                             09-
   54 PRINT154
  154 FORMAT(56H DIVISOR IS ZERO IN SECOND DIVISION OF COULFN SUBROUTINE 09-
     1)                                                                  09-
      CALLEXIT
  600 IF(JSPILL) 601,33,601                                              09-
  601 PRINT1601,JSPILL
 1601 FORMAT(22H OVERFLOW OCCURRED AT I6,21H IN COULFN SUBROUTINE,24H MU 09-
     1LTIPLY FBAR(I) BY 0.1)                                             09-
      K=LMAX+IDEC                                                        09-
      FBAR(K)=FBAR(K)*0.1                                                09-
      JSPILL=0                                                           09-
      GO TO 133                                                          09-
   33 T1=T2                                                              09-
      ALPHA=1./((FBAR(1)*G(2)-FBAR(2)*G(1))*SQ)                          09-
      IF DIVIDE CHECK 55,43                                              09-
   55 PRINT155
  155 FORMAT (55H DIVISOR IS ZERO IN THIRD DIVISION OF COULFN SUBROUTINE 09-
     1)                                                                  09-
      CALLEXIT
   43 LMAXP=LMAX+1                                                       09-
      DO 34 I=1,LMAXP                                                    09-
   34 FBAR(I)=ALPHA*FBAR(I)                                              09-
      IF(IDEC-11) 371,35,371                                             09-
  371 IF(ABSF(F1/FBAR(1)-1.)-EPS2) 37,37,35                              09-
   35 DO 36 I=1,LMAXP                                                    09-
   36 F(I)=FBAR(I)                                                       09-
      IDEC=IDEC+5                                                        09-
```

```
      IF (IDEC-40) 32,32,103                                              09·
   37 DO 38 I=1,LMAXP                                                     09·
      IF(ABSF(F(I)/FBAR(I)-1.)-EPS2) 44,44,35                             09·
   44 IF DIVIDE CHECK 56,38                                               09·
   56 PRINT156,L,I
  156 FORMAT(74H DIVISOR FBAR(I)-1. IS ZERO IN FOURTH DIVISION OF COULFN  09·
     1 SUBROUTINE FOR L=I3,7H AND I=I3)                                   09·
      CALLEXIT
   38 CONTINUE                                                            09·
      DO 381 I=1,LMAXP                                                    09·
  381 F(I)=FBAR(I)                                                        09·
  382 T1=SQ                                                               09·
      DO 40 L=1,LMAX                                                      09·
      FL=L                                                                09·
      T2=SQRTF((FL+1.)**2+ETA2)                                           09·
      G(L+2)=((2.*FL+1.)*(ETA+FL*(FL+1.)/RHOMAX)*G(L+1)-(FL+1.)*T1*G(L))  09·
     1/(FL*T2)                                                            09·
      TS=FL/T1                                                            09·
      IF DIVIDE CHECK 57,45                                               09·
   57 PRINT157
  157 FORMAT(58H DIVISOR T1 IS ZERO IN FIFTH DIVISION OF COULFN SUBROUTI  09·
     1NE)                                                                 09·
      CALLEXIT
   45 IF(ABSF(F(L)*G(L+1)-F(L+1)*G(L)-TS)-EPS1) 40,40,104                 09·
   40 T1=T2                                                               09·
   41 DO 42 L=1,LMAX                                                      09·
      FL=L                                                                09·
      T=FL**2                                                             09·
      T1=T/RHOMAX+ETA                                                     09·
      IF DIVIDE CHECK 58,46                                               09·
   58 PRINT158
  158 FORMAT (62H DIVISOR RHOMAX IS ZERO IN SIXTH DIVISION OF COULFN SUB  09·
     1ROUTINE)                                                            09·
      CALLEXIT
   46 T2=SQRTF(1+ETA2)                                                    09·
      FP(L)=(T1*F(L)-T2*F(L+1))/FL                                        09·
   42 GP(L)=(T1*G(L)-T2*G(L+1))/FL                                        09·
      IF DIVIDE CHECK 59,47                                               09·
   59 PRINT159
  159 FORMAT(60H DIVISOR FL IS ZERO IN SEVENTH DIVISION OF COULFN SUBROU  09·
     1TINE)                                                               09·
      CALLEXIT
   47 IF(ISPILL) 60,61,60                                                 09·
   60 PRINT160,ISPILL
  160 FORMAT(23H UNDERFLOW OCCURRED AT I6,21H IN COULFN SUBROUTINE)       09·
   61 IF(JSPILL) 62,63,62                                                 09·
   62 PRINT162,JSPILL
  162 FORMAT(22H OVERFLOW OCCURRED AT I6,21H IN COULFN SUBROUTINE)        09·
      CALLEXIT
   63 RETURN                                                              09·
  101 PRINT121,RHOMAX,DRHOL
      GO TO (110,110,109,109),IKTRL                                       09·
  109 PRINT114
      GO TO 13                                                            09·
  102 PRINT122,RHOMAX,DRHOL
      GO TO(110,110,111,111),IKTRL                                        09·
  111 PRINT114
      GO TO 31                                                            09·
  103 PRINT123,RHOMAX,DRHOL
```

```
      GO TO (110,110,112,112),IKTRL                                     09-
  112 PRINT114
      GO TO 382                                                         09-
  104 PRINT124,RHOMAX,DRHOL,L
      GO TO (110,110,113,113),IKTRL                                     09-
  113 PRINT114
      GO TO 40                                                          09-
  105 PRINT125,RHOMAX,DRHOL
      GO TO (110,110,115,115),IKTRL                                     09-
  115 PRINT114
      GO TO 12                                                          09-
  106 PRINT126,RHOMAX,DRHOL
      GO TO (110,110,116,116),IKTRL                                     09-
  116 PRINT114
      GO TO 13                                                          09-
  110 RHOMAX=RHOMAX+DRHOL                                               09-
      GO TO 1                                                           09-
  121  FORMAT(18H INCREASE RHO MAX=E11.4,2H+ E11.4,35H A OR B SERIES CONV 09-
     1ERGES TOO SLOWLY)                                                 09-
  122 FORMAT(18H INCREASE RHO MAX=E11.4,2H+ E11.4,22H BAD INITIAL WRONSK 09-
     1IAN)                                                              09-
  123  FORMAT(18H INCREASE RHO MAX=E11.4,2H+ E11.4,24H L TOO LARGE IN FBA 09-
     1R (L))                                                            09-
  124  FORMAT(18H INCREASE RHO MAX=E11.4,2H+ E11.4,21H BAD WRONSKIAN FOR  09-
     1L=I3)                                                             09-
  125  FORMAT(67H SERIES IN PHI0 OR PHI1 IS ZERO, CHECK DATA, IF OK INCRE 09-
     1ASE RHOMAX=E11.4,2H+ E11.4)                                       09-
  126  FORMAT(52H A OR B SERIES DIVERGES TOO QUICKLY INCREASE RHOMAX=E11. 09-
     14,2H+ E11.4)                                                      09-
  114  FORMAT(42H RHOMAX INCREASE NOT PERMITTED BY KTRL(13))             09-
      END
```

```
      SUBROUTINE RMXINC                                                 10-
3     IF (RHOMAX-RHO(ILAST)) 1,2,1                                      10-
1     ILAST=ILAST+1                                                     10-
      RHO(ILAST)=RHO(ILAST-1)+DRHOL                                     10-
      DRHO(ILAST-1)=DRHOL                                               10-
      GO TO 3                                                           10-
2     RETURN                                                            10-
      END
```

```
      SUBROUTINE PGEN4                                                  11-
      IF DIVIDE CHECK 60,61                                             11-
   60 PRINT160
  160 FORMAT (59H DIVIDE CHECK TRIGGER FOUND ON AT START OF PGEN4 SUBROU 11-
     1TINE)                                                             11-
      CALLEXIT
   61 ISPILL=0                                                          11-
      JSPILL=0                                                          11-
      IF(KTRL(1)) 3,4,3                                                 11-
    3 KTRL(7)=0                                                         11-
      KTRL(8)=0                                                         11-
      KTRL(9)=0                                                         11-
      KTRL(10)=0                                                        11-
    4 T1=V/ECM                                                          11-
      T2=W/ECM                                                          11-
      T10=VS/ECM                                                        11-
      T11=WS/ECM                                                        11-
      T12=FKAY*BG                                                       11-
      T3=2.*FKAY/A                                                      11-
      IF DIVIDE CHECK 62,65                                             11-
   62 PRINT162
  162 FORMAT (65H DIVISORS ECM OR A WERE WRONGLY INPUT AS ZERO IN PGEN4  11-
     1SUBROUTINE)                                                       11-
      CALLEXIT
   65 T4=T10*T3                                                         11-
      T5=T11*T3                                                         11-
      T6=FKAY*A                                                         11-
      T7=ETA/RHOBC                                                      11-
      IF DIVIDE CHECK 63,64                                             11-
   63 PRINT163
  163 FORMAT(61H DIVISOR RHOBC IS ZERO IN SECOND DIVISION OF PGEN4 SUBRO 11-
     1UTINE)                                                            11-
      CALLEXIT
   64 T8=RHOBC**2                                                       11-
      T9=ETA*2.                                                         11-
      I=1                                                               11-
   40 EX=EXPF((RHO(I)-RHOBN)/T6)                                        11-
      IF DIVIDE CHECK 80,66                                             11-
   80 PRINT165
  165 FORMAT (58H QUANTITY T6 IS ZERO IN THIRD DIVISION OF PGEN4 SUBROUT 11-
     1INE)                                                              11-
      CALLEXIT
   66 K=1                                                               11-
   41 IF(I-1) 42,43,42                                                  11-
   42 IF(DRHO(I)-DRHO(I-1)) 43,44,43                                    11-
   43 HDRHO=DRHO(I)*.5                                                  11-
      DEX=EXPF(HDRHO/T6)                                                11-
   44 IF(KTRL(1)-2)53,52,53                                             11-
   52 IF(RHO(I)-RHOBN) 54,55,55                                         11-
   54 S1=1.0                                                            11-
      GO TO 68                                                          11-
   55 S1=0.0                                                            11-
      GO TO 68                                                          11-
   53 S1=1./(1.+EX)                                                     11-
      IF DIVIDE CHECK 67,68                                             11-
   67 PRINT167
  167 FORMAT(60H DIVISOR 1.+EX IS ZERO IN FOURTH DIVISION OF PGEN4 SUBRO 11-
     1UTINE)                                                            11-
      CALLEXIT
```

```
 68   S2=EX*(S1**2)                                                    11-
      S4=S2/RHO(I)                                                     11-
      IF DIVIDE CHECK 69,70                                            11-
  69  PRINT169,I
 169  FORMAT(58H DIVISOR RHO IS ZERO IN FIFTH DIVISION OF PGEN4 SUBROUTI 11-
     1NE)                                                              11-
      CALLEXIT
  70  IF (RHO(I)-RHOBC) 9,9,10                                         11-
  9   S3=T7*(3.-(RHO(I)**2)/T8)                                        11-
      GO TO 11                                                         11-
  10  S3=T9/RHO(I)                                                     11-
 11   IF (KTRL(7)) 350,300,350                                         11-
 300  UCRB(I)=-1.-T1*S1+S3                                             11-
      FFCR(I)=S1                                                       11-
 301  IF (KTRL(8)) 355,302,355                                         11-
 302  IF(KTRL(1)-1) 309,308,309                                        11-
 308  S1=EXPF(-((RHO(I)-RHOBNG)/T12)**2)                               11-
      IF DIVIDE CHECK 82,309                                           11-
  82  PRINT182
 182  FORMAT(22H BG IS ZERO IN PGEN SR)                                11-
      CALLEXIT
 309  UCIB(I)=-T2*S1                                                   11-
      FFCI(I)=S1                                                       11-
 303  IF (KTRL(9)) 360,304,360                                         11-
 304  USRB(I)=T4*S4                                                    11-
      FFSR(I)=S4                                                       11-
 305  IF (KTRL(11)) 501,500,501                                        11-
 500  IF (KTRL(10))365,306,365                                         11-
 306  USIB(I)=T5*S4                                                    11-
      FFSI(I)=S4                                                       11-
 307  IF (I-ILAST) 50,200,200                                          11-
 50   I=I+1                                                            11-
      EX=EX*DEX                                                        11-
      RHOM=RHO(I-1)+HDRHO                                              11-
      IF(KTRL(1)-2) 153,152,153                                        11-
 152  IF(RHOM-RHOBN)34,35,35                                           11-
 34   S1=1.0                                                           11-
      GO TO 72                                                         11-
 35   S1=0.0                                                           11-
      GO TO 72                                                         11-
 153  S1=1./(1.+EX)                                                   11-
      IF DIVIDE CHECK 71,72                                            11-
  71  PRINT171
 171  FORMAT(54H DIVISOR IS ZERO IN SIXTH DIVISION OF PGEN4 SUBROUTINE) 11-
      CALLEXIT
  72  S2=EX*(S1**2)                                                    11-
      S4=S2/RHOM                                                       11-
      IF DIVIDE CHECK 73,74                                            11-
  73  PRINT173
 173  FORMAT (62H QUANTITY RHOM IS ZERO IN SEVENTH DIVISION OF PGEN4 SUB 11-
     1ROUTINE)                                                         11-
      CALLEXIT
  74  IF(RHOM-RHOBC) 21,21,22                                          11-
  21  S3=T7*(3.-(RHOM**2)/T8)                                          11-
      GO TO 23                                                         11-
  22  S3=T9/RHOM                                                       11-
  23  IF (KTRL(7))1350,1300,1350                                       11-
1300  UCRM(I-1)=-1.-T1*S1+S3                                           11-
      FFCRM(I-1)=S1                                                    11-
```

```
1301 IF (KTRL(8)) 1355,1302,1355                                        11
1302 IF(KTRL(1)-1) 1309,1308,1309                                       11
1308 S1=EXPF(-((RHOM-RHOBNG)/T12)**2)                                   11
1309 UCIM(I-1)=-T2*S1                                                   11
     FFCIM(I-1)=S1                                                      11
1303 IF (KTRL(9)) 1360,1304,1360                                        11
1304 USRM(I-1)=T4*S4                                                    11
     FFSRM(I-1)=S4                                                      11
1305 IF (KTRL(11)) 1501,1500,1501                                       11
1500 IF (KTRL(10))1365,1306,1365                                        11
1306 USIM(I-1)=T5*S4                                                    11
     FFSIM(I-1)=S4                                                      11
1307 IF (K-10) 24,40,40                                                 11
 350 NOJ=350
     KK=7
     GOTO778
 355 NOJ=355
     KK=8
     GOTO778
 360 NOJ=360
     KK=9
     GOTO778
 501 NOJ=501
     KK=11
     GOTO778
 365 NOJ=365
     KK=10
     GOTO778
 778 PRINT777,KK,NOJ
     PRINT779
 777 FORMAT(18H  ERROR   KTRL NO=I3,32H NOT ZERO IN STATEMENT NUMBER =
    1I4)
 779 FORMAT(34H  CHECK  DATA  LISTING   KTRL POSN)
     CALLEXIT
1350 NOJ=1350
     KK=7
     GOTO778
1355 NOJ=1355
     KK=8
     GOTO778
1360 NOJ=9
     KK=9
     GOTO778
1501 NOJ=1501
     KK=11
     GOTO778
1365 NOJ=1365
     KK=10
     GOTO778
  24 K=K+1                                                              11
     EX=EX*DEX                                                          11
     GO TO 42                                                           11
 200 IF(ISPILL) 75,76,75                                                11
  75 PRINT175,ISPILL
 175 FORMAT(23H UNDERFLOW OCCURRED AT I6,20H IN PGEN4 SUBROUTINE)       11
  76 IF (JSPILL) 77,51,77                                               11
  77 PRINT177,JSPILL
 177 FORMAT(22H OVERFLOW OCCURRED AT I6,20H IN PGEN4 SUBROUTINE)        11
     CALLEXIT
```

```
   51  RETURN                                                        11-
       END
```

```
      SUBROUTINE INTCTR                                                 12-
      DO1 L=1,LMAX                                                      12-
      IFIRST=IIN(L)                                                     12-
      T=RHO(IFIRST)**(L-1)                                              12-
      XC1=T*RHO(IFIRST)                                                 12-
      XD1=XC1                                                           12-
      FL=L                                                              12-
      XCP1=FL*T                                                         12-
      XDP1=XCP1                                                         12-
      YC1=0.                                                            12-
      YD1=0.                                                            12-
      YCP1=0.                                                           12-
      YDP1=0.                                                           12-
      CALL RKINT                                                        12-
      X1(L)=XC1                                                         12-
      Y1(L)=YC1                                                         12-
      X1P(L)=XCP1                                                       12-
      Y1P(L)=YCP1                                                       12-
    1 CONTINUE
      RETURN                                                            12-
      END
```

```
      SUBROUTINE RKINT
      IF DIVIDE CHECK 10,11                                              13
   10 PRINT110,L,I
  110 FORMAT(66H DIVIDE CHECK TRIGGER FOUND ON AT START OF RKINT SUBROUT  13
     1INE FOR L=I3,7H AND I=I3)                                          13
      CALLEXIT
   11 ISPILL=0                                                           13
      JSPILL=0                                                           13
      INDEX=0
      IND=1
      INDRE=1
    1 FL=L-1                                                             13
      F2L=-1.-FL                                                         13
      F3L=FL*(FL+1.)                                                     13
      TB=UCRB(IFIRST)+F3L/(RHO(IFIRST)**2)                               13
      IF DIVIDE CHECK 12,13                                              13
   12 PRINT112,L,I
  112 FORMAT(76H DIVISOR RHO(IFIRST)**2 IS ZERO IN FIRST DIVISION OF RKI  13
     1NT SUBROUTINE FOR L=I3,7H AND I=I3)                                13
      CALLEXIT
   13 PCB=TB+USRB(IFIRST)*FL
      PDB=TB+USRB(IFIRST)*F2L
      QCB=UCIB(IFIRST)+USIB(IFIRST)*FL
      QDB=UCIB(IFIRST)+USIB(IFIRST)*F2L
      IK=ILAST-1                                                         13
      DO66I=IFIRST,IK
    2 HDRHO=.5*DRHO(I)                                                   13
      DRHO2=(DRHO(I)**2)*.5                                              13
      RHOM=RHO(I)+HDRHO                                                  13
      TM=UCRM(I)+F3L/(RHOM**2)                                           13
      IF DIVIDE CHECK 14,15                                              13
   14 PRINT114,L,I
  114 FORMAT(70H DIVISOR RHOM**2 IS ZERO IN SECOND DIVISION OF RKINT SUB  13
     1ROUTINE FOR L=I3,7H AND I=I3)                                      13
      CALLEXIT
   15 PCM=TM+USRM(I)*FL
      PDM=TM+USRM(I)*F2L
      QCM=UCIM(I)+USIM(I)*FL
      QDM=UCIM(I)+USIM(I)*F2L
      XCPP1=PCB*XC1-QCB*YC1                                              13
      YCPP1=QCB*XC1+PCB*YC1                                              13
      XDPP1=PDB*XD1-QDB*YD1                                              13
      YDPP1=QDB*XD1+PDB*YD1                                              13
      XC2=XC1+XCP1*HDRHO                                                 13
      YC2=YC1+YCP1*HDRHO                                                 13
      XD2=XD1+XDP1*HDRHO                                                 13
      YD2=YD1+YDP1*HDRHO                                                 13
      XCPP2=PCM*XC2-QCM*YC2                                              13
      YCPP2=QCM*XC2+PCM*YC2                                              13
      XDPP2=PDM*XD2-QDM*YD2                                              13
      YDPP2=QDM*XD2+PDM*YD2                                              13
      DRHO4=.5*DRHO2                                                     13
      SDRHO=.33333333*HDRHO                                              13
      XC3=XC2+XCPP1*DRHO4                                                13
      YC3=YC2+YCPP1*DRHO4                                                13
      XD3=XD2+XDPP1*DRHO4                                                13
      YD3=YD2+YDPP1*DRHO4                                                13
      XCPP3=PCM*XC3-QCM*YC3                                              13
      YCPP3=QCM*XC3+PCM*YC3                                              13
```

```
      XDPP3=PDM*XD3-QDM*YD3                                              13-
      YDPP3=QDM*XD3+PDM*YD3                                              13-
      XC4=XC2+XCPP2*DRHO2+XCP1*HDRHO                                     13-
      YC4=YC2+YCPP2*DRHO2+YCP1*HDRHO                                     13-
      XD4=XD2+XDPP2*DRHO2+XDP1*HDRHO                                     13-
      YD4=YD2+YDPP2*DRHO2+YDP1*HDRHO                                     13-
      TB=UCRB(I+1)+F3L/(RHO(I+1)**2)                                     13-
      IF DIVIDE CHECK 16,17                                              13-
   16 PRINT116,L,I
  116 FORMAT(74H DIVISOR RHO(I+1)**2 IS ZERO IN THIRD DIVISION FOR RKINT  13-
     1 SUBROUTINE FOR L=I3,7H AND I=I3)                                  13-
      CALLEXIT
   17 PCB=TB+USRB(I+1)*FL
      PDB=TB+USRB(I+1)*F2L
      QCB=UCIB(I+1)+USIB(I+1)*FL
      QDB=UCIB(I+1)+USIB(I+1)*F2L
      XCPP4=PCB*XC4-QCB*YC4                                              13-
      YCPP4=QCB*XC4+PCB*YC4                                              13-
      XDPP4=PDB*XD4-QDB*YD4                                              13-
      YDPP4=QDB*XD4+PDB*YD4                                              13-
      SXC=XCPP2+XCPP3                                                    13-
      SYC=YCPP2+YCPP3                                                    13-
      SXD=XDPP2+XDPP3                                                    13-
      SYD=YDPP2+YDPP3                                                    13-
      TXC=SXC+XCPP1                                                      13-
      TYC=SYC+YCPP1                                                      13-
      TXD=SXD+XDPP1                                                      13-
      TYD=SYD+YDPP1                                                      13-
      TXC1=XC1+DRHO(I)*(XCP1+SDRHO*TXC)                                  13-
      TYC1=YC1+DRHO(I)*(YCP1+SDRHO*TYC)                                  13-
      TXD1=XD1+DRHO(I)*(XDP1+SDRHO*TXD)                                  13-
      TYD1=YD1+DRHO(I)*(YDP1+SDRHO*TYD)                                  13-
      TXCP1=XCP1+SDRHO*(TXC+SXC+XCPP4)                                   13-
      TYCP1=YCP1+SDRHO*(TYC+SYC+YCPP4)                                   13-
      TXDP1=XDP1+SDRHO*(TXD+SXD+XDPP4)                                   13-
      TYDP1=YDP1+SDRHO*(TYD+SYD+YDPP4)                                   13-
      IF (JSPILL) 20,21,20                                               13-
   20 RENMZ(INDRE)=MAX1F(ABSF(XC1),ABSF(YC1),ABSF(XCP1),ABSF(YCP1),ABSF(
     1XD1),ABSF(YD1),ABSF(XDP1),ABSF(YDP1))
      RUE(INDRE)=RHO(I)
      RENORM=RENMZ(INDRE)
      INDRE=INDRE+1
      XC1=XC1/RENORM                                                     13-
      YC1=YC1/RENORM                                                     13-
      XCP1=XCP1/RENORM                                                   13-
      YCP1=YCP1/RENORM                                                   13-
      XD1=XD1/RENORM                                                     13-
      YD1=YD1/RENORM                                                     13-
      XDP1=XDP1/RENORM                                                   13-
      YDP1=YDP1/RENORM                                                   13-
      PRINT200,RENORM,L,RHO(I)
  200 FORMAT(24H RENORMALIZATION FACTOR=E16.9,22H IN RKINT FOR CODED L=I  13-
     13,9H AND RHO=E16.9)                                                13-
      JSPILL=0                                                           13-
      GO TO2                                                             13-
   21 XC1=TXC1                                                           13-
      YC1=TYC1                                                           13-
      XD1=TXD1                                                           13-
      YD1=TYD1                                                           13-
```

```
      XCP1=TXCP1                                                        13-
      YCP1=TYCP1                                                        13-
      XDP1=TXDP1                                                        13-
      YDP1=TYDP1                                                        13-
      INDEX=INDEX+1
      IF(INDEX-ISP)66,71,71
   71 XCS(IND,L)=XC1
      YCS(IND,L)=YC1
      ROSP(IND)=RHO(I+1)
      IND=IND+1
   66 CONTINUE
      ROE(INDRE)=2.0*RHOMAX
      NEND=INDRE
      IEND=IND-1
      IF (ISPILL) 30,31,30                                              13-
   30 PRINT130,ISPILL,L,I
  130 FORMAT(23H UNDERFLOW OCCURRED AT I6,27H IN RKINT SUBROUTINE FOR L=  13-
     1I3,7H AND I=I3)                                                   13-
   31 IF (JSPILL) 32,4,32                                               13-
   32 PRINT132,JSPILL,L,I
  132 FORMAT(22H OVERFLOW OCCURRED AT I6,27H IN RKINT SUBROUTINE FOR L=I  13-
     13,7H AND I=I3)                                                    13-
      CALLEXIT
    4 RETURN                                                            13-
      END
```

```
      SUBROUTINE CSUBL                                                  14-0
      IF DIVIDE CHECK 50,51                                             14-0
   50 PRINT150
  150 FORMAT (50H DIVIDE CHECK TRIGGER FOUND ON AT START OF CSUBL SUBROU 14-0
     1TINE)                                                             14-0
      CALLEXIT
   51 ISPILL=0                                                          14-0
      JSPILL=0                                                          14-0
      DO 40 L=1,LMAX                                                    14-0
      XNORM1=MAX1F(ABSF(X1(L)),ABSF(Y1(L)),ABSF(X1P(L)),ABSF(Y1P(L)))   14-0
      TX1L=X1(L)/XNORM1                                                 14-0
      TY1L=Y1(L)/XNORM1                                                 14-0
      TX1PL=X1P(L)/XNORM1                                               14-0
      TY1PL=Y1P(L)/XNORM1                                               14-0
      FNORM=MAX1F(F(L),G(L),FP(L),GP(L))                                14-0
      TFL=F(L)/FNORM                                                    14-0
      TGL=G(L)/FNORM                                                    14-0
      TFPL=FP(L)/FNORM                                                  14-0
      TGPL=GP(L)/FNORM                                                  14-0
      CO1=TFL*TY1PL-TFPL*TY1L                                           14-0
      CO2=TFPL*TX1L-TFL*TX1PL                                           14-0
      CO3=TY1L*TGPL-TY1PL*TGL+TX1L*TFPL-TX1PL*TFL                       14-0
      CO4=TX1PL*TGL-TX1L*TGPL+TY1L*TFPL-TY1PL*TFL                       14-0
      CO7=1.0/(CO3**2+CO4**2)                                           14-0
      IF DIVIDE CHECK 52,53                                             14-0
   52 PRINT152
  152 FORMAT(54H DIVISOR IS ZERO IN FIRST DIVISION OF CSUBL SUBROUTINE) 14-0
      CALLEXIT
   53 CR1(L)=(CO1*CO3+CO2*CO4)*CO7                                      14-0
      CI1(L)=(CO2*CO3-CO1*CO4)*CO7                                      14-0
   40 CONTINUE
      IF (ISPILL) 56,57,56                                              14-0
   56 PRINT156,ISPILL,L
  156 FORMAT (23H UNDERFLOW OCCURRED AT I6,27H IN CSUBL SUBROUTINE FOR L 14-0
     1=I3)                                                              14-0
   57 IF (JSPILL) 58,59,58                                              14-0
   58 PRINT158,JSPILL,L
  158 FORMAT (22H OVERFLOW OCCURRED AT I6,27H IN CSUBL SUBROUTINE FOR L= 14-0
     1I3)                                                               14-0
      CALLEXIT
   59 RETURN                                                            14-0
      END
```

```
      SUBROUTINE WFNORM
      IFDIVIDECHECK333,334
  333 PRINT300
  300 FORMAT(60H DIVIDE CHECK TRIGGER FOUND ON AT START OF WFNORM SUBROU
     1TINE)
      CALLEXIT
  334 ISPILL=0
      JSPILL=0
      KK=1
      CORR=1.0
      DO100IL=1,LMAX
      GM1=CR1(IL)
      HM1=CI1(IL)
      QQQ=F(IL)
      PPP=G(IL)
      CALLCMP(GM1,HM1,PPP,QQQ,RR1,SS1)
      TT1=RR1+QQQ
      AZR=X1(IL)
      AZI=Y1(IL)
      CALLCMD(TT1,SS1,AZR,AZI,R1,U1)
      IFDIVIDECHECK666,667
  666 PRINT1666,TT1,SS1,AZR,AZI,IL
 1666 FORMAT(53H DIV CH TRIGGER ON IN WFNORM AT FIRST CMD FOR VALUES 1P4
     1E13.4,8H WHEN L=I3)
  667 AGR=R1
      AGI=U1
      IF(ISPILL)441,442,441
  441 PRINT443,ISPILL,IL,GM1,HM1,QQQ,PPP,RR1,SS1,TT1,AZR,AZI,AGR,AGI
  443 FORMAT(1H ,I5,I3,11F10.5)
  442 CONTINUE
      DO100IND=1,IEND
      R1=AGR/ROSP(IND)
      U1=AGI/ROSP(IND)
      IFDIVIDECHECK668,669
  668 PRINT1668,IND
 1668 FORMAT(37H DIV CH ON IN WFNORM FOR ROSP WHEN I=I4)
  669 IF(ROSP(IND)-ROE(KK))90,50,50
   50 CORR=RENMZ(KK)
      IF(KK-NEND)51,51,90
   51 RENMZ(KK+1)=RENMZ(KK+1)*RENMZ(KK)
      KK=KK+1
   90 EG1=CORR*R1
      EG2=CORR*U1
      EG3=XCS(IND,IL)
      EG4=YCS(IND,IL)
    5 CALL CMP(EG1,EG2,EG3,EG4,EG5,EG6)
    7 XCS(IND,IL)=EG5
      YCS(IND,IL)=EG6
      IF(ISPILL)481,482,481
  481 PRINT483,ISPILL,IL,IND,R1,U1,ROSP(IND),AGR,AGI,KK,ROE(KK),CORR,NEN
     1D,RENMZ(KK)
      PRINT484,EG1,EG2,EG3,EG4,EG5,EG6
  483 FORMAT(1H ,I5,2I3,5F10.5,I3,2F10.5,I3,F10.5)
  484 FORMAT(1H ,1P6E14.5)
  482 CONTINUE
  100 CONTINUE
      IF(ISPILL)651,652,651
  651 PRINT653,ISPILL
  653 FORMAT(14H UNDERFLOW AT I5,10H IN WFNORM)
```

```
652 IF(JSPILL)654,656,654
654 PRINT655,JSPILL
655 FORMAT(13H OVERFLOW AT I5,10H IN WFNORM)
    CALLEXIT
656 RETURN
    END
```

```
      SUBROUTINE OUTPT4
      IF(KTRL(5)-1)73,74,73
   74 NUMRUN(5)=NUMRUN(5)-1
      WRITEOUTPUTTAPE3,75
   75 FORMAT(1H /1H /1H /25H BASIC DATA   FINAL STATE)
      GOTO79
   73 CONTINUE
      WRITEOUTPUTTAPE3,4321,NUMRUN(5),(NUMRUN(I),I=1,3)
 4321 FORMAT(1H /1H /8H RUN NO=I5,11H         ON I2,1H I2,1H I4)
      WRITEOUTPUTTAPE3,76
   76 FORMAT(1H /1H /27H BASIC DATA   INITIAL STATE)
   79 WRITEOUTPUTTAPE3,22,(KTRL(I),I=1,13),ISP1,ISP2,ISP3,ISP4
   22 FORMAT(1H /7H KTRLS=13I3,6H ISPS=4I3)
      WRITEOUTPUTTAPE3,24,LMAX,NMAX,JMAX,NHI,LPI,HOJI,NHF,LPF,HOJF
   24 FORMAT(6H LMAX=I2,7H  NMAX=I2,7H  JMAX=I2,10X,24H BD STATES   INIT
     1IAL  N=I2,4H  L=I2,4H  J=F4.2,4X,10H FINAL  N=I2,4H  L=I2,4H  J=F4.
     2.2)
      WRITEOUTPUTTAPE3,26,FMI,FMB,FMU,ZZ,ELAB,DELAB,EFIN,ECM,V,W,A,VS,WS
     1,RC,RO,RHOBN,RHOBC,RHOMAX,RHOBS,RADWC,WF,ROSP(1),SNO1,FKAY,ETA,RG,
     2BG,TBDPOT
   26 FORMAT(1H /12H MASSES  MI=F4.2,4H MB=F5.2,4H MU=F5.2,4H ZZ=F6.2,25
     1X,16H ENERGIES   LAB=F5.2,7H DEL E=F5.2,6H EFIN=F5.2,5H ECM=F5.2/1
     2H /22H MODEL PARAMETERS   V=F5.2,3H W=F5.2,3H A=F5.3,4H VS=F4.1,4H
     3 WS=F4.2,4H RC=F4.2,4H RO=F4.2/1H /21H POSN VALUES   RHOBN=F6.3,6H
     4 RHOC=F6.3,8H RHOMAX=F6.3,7H RHOBS=F6.3,7H RADWC=F6.3,4H WF=F6.3,9
     5H 1ST RHO=F6.3/1H /19H OTHER DATA   TEST=F5.4,3H K=F6.4,5H ETA=F6.
     64,6H   RG=F6.2,4H BG=F4.2,14H    INT POTNL=F7.2)
      WRITEOUTPUTTAPE3,34,DV,DW,DVS,DWS,DA,DBG
   34 FORMAT(1H /17H INCREMENTS   DV=F6.2,5H  DW=F5.2,6H  DVS=F5.2,6H  DWS
     1WS=F5.2,5H  DA=F5.2,9H    BETA=F6.3/1H /1H )
      RETURN
      END
```

```
      SUBROUTINELGFACT
      FG(1)=0.0
      DO100KZ=1,50
      AKZ=KZ+1
  100 FG(KZ+1)=FG(KZ)+LOGF(AKZ)
      RETURN
      END
```

```
*        FAP                                                          22-0
         COUNT    43                                                  22-0
*SPILL   SUBROUTINE                                                   22-0
         ENTRY    SPILL                                               22-0
 SPILL   STZ*     1,4          STORE ZERO IN JSPILL                   22-0
         STZ*     2,4            STORE ZERO IN ISPILL                 22-0
         STZ      0             STORE ZERO IN LOCATION 00000          22-0
         CAL      1,4                                                 22-0
         STA      AA41               SET ADDRESS AA41,                22-0
         STA      AA36                 AA36 TO JSPILL                 22-0
         CAL      2,4                    SET ADDRESS AA31             22-0
         STA      AA31                   TO ISPILL                    22-0
         CLA*     3,4                      SET COMMON STORAGE         22-0
         STO      AA45                                                22-0
         CLA*     4,4                      SET COMMON STORAGE         22-0
         STO      AA46                                                22-0
         CAL      AA47             PLACE TRANSFER                     22-0
         SLW      8              INSTRUCTION IN LOCATION 8            22-0
         TRA      5,4                    EXIT TO MAIN PROGRAM         22-0
 AA16    LDI      0            ENTRY IN CASE OF OVER-OR UNDERFLOW     22-0
         LFT      4            TEST FOR OVERFLOW                      22-0
         TRA      AA36       TRANSFER IN CASE OF OVERFLOW             22-0
         LFT      16                                                  22-0
         TRA      AA24                 TRANSFER IN CASE OF UNDERFLOW  22-0
         TRA*     0                  TRANSFER TO MAIN PROGRAM, NO UFLOW 22-0
 AA24    LNT      1                    TEST FOR UNDERFLOW            22-0
         TRA*     0                UNDERFLOW IN AC ONLY              22-0
         CAL      0              PLACE LOCATION AT WHICH             22-0
         SUB      AA35           UNDERFLOW OCCURRED IN AC            22-0
         LLS      18           SHIFT LEFT 18                         22-0
 AA31    STD      AA31       STORE IN ISPILL                         22-0
         CLA      AA46       SET AC, MQ WITH                         22-0
         LDQ      AA46               SPECIFIED CONSTANTS             22-0
         TRA*     0                EXIT TO MAIN PROGRAM              22-0
 AA35    HTR      1                  CONSTANT                        22-0
 AA36    CLA      AA36                 TEST IF JSPILL ZERO           22-0
         TNZ      AA42           TRANSFER IN CASE JSPILL NON-ZERO    22-0
         CAL      0            PLACE LOCATION AT WHICH OVERFLOW OCCURRED 22-0
         SUB      AA35                   IN AC                       22-0
         LLS      18                   SHIFT LEFT 18                 22-0
 AA41    STD      AA41               STORE IN JSPILL                 22-0
 AA42    CLA      AA45             SET AC,MQ WITH SPECIFIED CONSTANTS 22-0
         LDQ      AA45                                                22-0
         TRA*     0                    EXIT TO MAIN PROGRAM           22-0
 AA45    HTR      0                    COMMON STORAGE                 22-0
 AA46    HTR      0                    COMMON STORAGE                 22-0
 AA47    TRA      AA16           INSTRUCTION TO BE INSERTED AT LOC.  8 22-0
         END                                                          22-0
```

```
      SUBROUTINEONEMN(NN,ZP)
      IF(NN)16,17,17
   16 NX=-NN
      NN=NX
   17 CONTINUE
      IF(NN-(NN/2)*2)3,4,5
    3 PRINT30,NN
      CALLEXIT
    4 ZP=1.0
      GOTO50
    5 ZP=-1.0
   50 RETURN
   30 FORMAT(45H INCORRECT LOOPING IN SUBROUTINE SIGN FOR NN=I5)
      END
```

```
      SUBROUTINECSQR(E6,E7,E8,E9)
      R=MAX1F(ABSF(E6),ABSF(E7))
      S=MIN1F(ABSF(E6),ABSF(E7))
      T=SQRTF(0.5*(ABSF(E6)+R*SQRTF(1.0+(S/R)**2)))
      IF(E6)33,32,32
   32 E8=T
      E9=E7/(2.0*E8)
      IFDIVIDE CHECK61,62
   61 PRINT161,E6,E7
  161 FORMAT(27H E8 IS ZERO IN CSQR FOR E6=E13.4,8H AND E7=E13.4)
      CALLEXIT
   62 GOTO100
   33 E9=SIGNF(T,E7)
      E8=E7/(2.0*E9)
      IFDIVIDECHECK63,100
   63 PRINT163,E6,E7
  163 FORMAT(27H E9 IS ZERO IN CSQR FOR E6=E13.4,8H AND E7=E13.4)
      CALLEXIT
  100 RETURN
      END
```

```
SUBROUTINECMP(AU,B,C,D,RL,UR)
QN1=AU
QN2=B
QN3=C
QN4=D
RL=QN1*QN3-QN2*QN4
UR=QN1*QN4+QN2*QN3
RETURN
END
```

```
SUBROUTINECMD(A1,B,C,D,RL,UR)
QM1=A1
QM2=B
QM3=C
QM4=D
QU=QM3**2+QM4**2
RL=(QM1*QM3+QM2*QM4)/QU
UR=(QM2*QM3-QM1*QM4)/QU
RETURN
END
```

```
      SUBROUTINESIG(NN,II,JJ)
      IF(NN)81,82,82
   81 N7=NN/2
      IF(NN-N7*2)83,82,83
   83 N8=N7/2
      IF(N7-N8*2)85,84,85
   84 II=0
      JJ=-1
      GOTO100
   85 II=0
      JJ=1
      GOTO100
   82 N10=NN/2
      IF(NN-N10*2)3,4,3
    3 II=0
      N11=N10/2
      IF(N10-N11*2)31,32,31
   31 JJ=-1
      GOTO100
   32 JJ=+1
      GOTO100
    4 JJ=0
      N11=N10/2
      IF(N10-N11*2)41,42,41
   41 II=-1
      GOTO100
   42 II=+1
  100 RETURN
      END
```

```
      SUBROUTINECONNEX
      IFDIVIDECHECK333,334
  333 PRINT300
  300 FORMAT(60H DIVIDE CHECK TRIGGER FOUND ON AT START OF CONNEX SUBROU
     UTINE)
      CALLEXIT
  334 ISPILL=0
      JSPILL=0
      IF(RG-20.0)111,112,112
  111 READINPUTTAPE2,10,(KCONT(I),I=1,9)
   10 FORMAT(I5)
  112 CONTINUE
      IF(KCONT(1)-1)11,12,11
   12 CALLTIEUP1
   11 IF(KCONT(2)-1)13,14,13
   14 CALLTIEUP2
   13 IF(KCONT(3)-1)15,16,15
   16 CALLTIEUP3
   15 IF(KCONT(4)-1)17,18,17
   18 CALLTIEUP4
   17 IF(KCONT(5)-1)19,20,19
   20 CALLTIEUP5
   19 IF(KCONT(6)-1)21,22,21
   22 CALLTIEUP6
   21 IF(KCONT(7)-1)23,24,23
   24 CALLTIEUP7
   23 IF(KCONT(8)-1)25,26,25
   26 CALLTIEUP8
   25 IF(KCONT(9)-1)27,28,27
   28 CALLTIEUP9
   27 RETURN
      END
```

```
      SUBROUTINE TIEUP1
      WRITEOUTPUTTAPE3,77
   77 FORMAT(17H TIEUP1 PRINTOUTS)
      LFUD=0
      I=1
      IF(KCONT(9)-5)31,31,32
   31 WRITEOUTPUTTAPE3,131
  131 FORMAT(14H INCIDENT PART/112H     RHO                    MOD PHS L=0
     1              MOD PHS 6=1                    MOD PHS L=2                    MO
     2D PHS L=3)
      GOTO100
   32 WRITEOUTPUTTAPE3,132
  132 FORMAT(11H FINAL PART/60H       RHO        MOD L=0      PHS L=0      M
     1OD L=1       PHS L=1)
  100 RPT=ROSP(I)
  550 IF(I-1)444,444,443
  443 IF(KCONT(9)-5)444,444,445
  445 IF(RPT-10.0)444,151,151
  444 L1=LFUD+1
      L2=L1+1
      L3=L1+2
      L4=L1+3
      ARGR=XCS(I,L1)
      ARGI=YCS(I,L1)
      BRGR=XCS(I,L2)
      BRGI=YCS(I,L2)
      CRGR=XCS(I,L3)
      CRGI=YCS(I,L3)
      DRGR=XCS(I,L4)
      DRGI=YCS(I,L4)
      S1=(2*L1-1)
      S2=(2*L2-1)
      S3=(2*L3-1)
      S4=(2*L4-1)
      POD1=S1*SQRTF(ARGR*ARGR+ARGI*ARGI)
      PHS1=ATANF(ARGI/ARGR)
      POD2=S2*SQRTF(BRGR*BRGR+BRGI*BRGI)
      PHS2=ATANF(BRGI/BRGR)
      POD3=S3*SQRTF(CRGR*CRGR+CRGI*CRGI)
      PHS3=ATANF(CRGI/CRGR)
      POD4=S4*SQRTF(DRGR*DRGR+DRGI*DRGI)
      PHS4=ATANF(DRGI/DRGR)
      IF(KCONT(9)-5)887,888,888
  888 WRITEOUTPUTTAPE3,1888,RPT,POD1,PHS1,POD2,PHS2,POD3,PHS3
 1888 FORMAT(1H 1P7E13.4)
      GOTO484
  887 CONTINUE
      WRITEOUTPUTTAPE3,461,RPT,POD1,PHS1,POD2,PHS2,POD3,PHS3,POD4,PHS4
  461 FORMAT(1H 1P9E13.4)
  483 I=I+1
  485 IF(ROSP(I)-RHOIN(2))483,484,484
  484 IF(KCONT(9)-5)486,487,487
  486 IF(IEND-I)551,551,100
  487 I=I+4
      GOTO100
  551 IF(LFUD-2)1550,1551,1551
 1550 I=1
      LFUD=L4
      WRITEOUTPUTTAPE3,1573
```

```
1573 FORMAT(112H      RHO                    MOD PHS L=4                    MOD PH
    1S L=5                  MOD PHS L=6                  MOD PHS L=7)
     GOTO100
1551 WRITEOUTPUTTAPE3,607
 607 FORMAT(56H      RHO          SUBT          RPOT          UPOT          UCRB
    1)
     I=1
 556 RPT=ROSP(I)
 201 UPOT=UCIB(I+1)*ECM
     IF(RPT-RHOBC)80,80,81
  80 SUBT=ETA/RHOBC*(3.0-RPT*RPT/RHOBC/RHOBC)
     GOTO82
  81 SUBT=2.0*ETA/RHOBC
  82 IFDIVIDECHECK991,992
 991 WRITEOUTPUTTAPE3,1991,RHOBC,I
1991 FORMAT(34H DIVIDE CHECK IN TIEUP1 FOR RHOBC=1PE12.4,3H I=I3)
 992 RPOT=ECM*(UCRB(I+1)+1.0-SUBT)
     WRITEOUTPUTTAPE3,10,RPT,SUBT,RPOT,UPOT,UCRB(I+1)
  10 FORMAT(1H 1P5E12.4)
     I=I+5
     IF(I-21)556,556,151
 151 RETURN
     END
```

```
      SUBROUTINETIEUP2
      KSUPER=1
      RETURN
      END
```

```
      SUBRCUTINETIEUP3
      IFDIVIDECHECK3,4
    3 PRINT990
  990 FORMAT(60H DIVIDE CHECK TRIGGER FOUND ON AT START OF TIEUP3 SUBRO
     1TINE)
      CALLEXIT
    4 ISPILL=0
      JSPILL=0
      IT=1
      NT=0
      DO5IL=1,LMAX
      RSGML(IL)=EXSGMR(IL)
      USGML(IL)=EXSGMI(IL)
      DO5IND=1,IEND
      XCST(IND,IL)=XCS(IND,IL)
    5 YCST(IND,IL)=YCS(IND,IL)
      LIP=LMAX
      FIP=FKAY
      CALLREADER
      CALLADJUST
      DO600IL=1,LIP
      DO500L=1,LMAX
      NS=IL-L
      CALLSIG(NS,N1,N2)
      R1=N1
      U1=N2
      R2=EXSGMR(L)
      U2=EXSGMI(L)
      R3=RSGML(IL)
      U3=USGML(IL)
      AIL=IL-1
      AL=L-1
      TERM1=(2.0*AIL+1.0)*SQRTF((2.0*HOJI+1.0)/(2.0*HOJF+1.0)/(2.0*AL+1
     10))
      IF(IL-5)99,99,532
  532 IF(L-5)99,99,533
  533 IK=1
  113 IF(RHO(IK)-RHOBN)111,112,112
  111 IK=IK+1
      GOTO113
  112 RT=XCS(IK,IL)
      UT=YCS(IK,IL)
      RU=XCST(IK,L)
      UU=YCST(IK,L)
      PT1=RT*RT+UT*UT
      PT2=RU*RU+UU*UU
      AP1=2*IL-1
      AP2=2*L-1
      SSS=AP1*PT1+AP2*PT2
      IF(SSS-SNO1)114,115,115
  115 GOTO99
  114 IT=IT+1
      IF(IT-15)1114,1114,500
 1114 WRITEOUTPUTTAPE3,2222,RHO(IK),XCS(IK,IL),YCS(IK,IL),XCST(IK,L),YC
     1T(IK,L),IL,L
 2222 FORMAT(47H INTEGRAND TEST IN TIEUP3 SAVES REDUNDANCY WHEN/5H RHO=
     112.4,13H INITIAL FNS 1PE12.4,1H 1PE12.4,11H FINAL FNS 1P2E12.4,1)
     2 CASE OF L=I5,9H FINAL L=I5)
      GOTO500
   99 DO287IPT=1,IEND
      AN1=XCS(IPT,L)
```

```
      AC1=YCS(IPT,L)
      BN1=XCST(IPT,IL)
      BC1=YCST(IPT,IL)
      CALLCMP(AN1,AC1,BN1,BC1,AN2,AC2)
      UCRB(IPT)=AN2
  287 UCIB(IPT)=AC2
      LT1=XABSF(L-IL)+1
      LT2=L+IL-1
      DC386LT=LT1,LT2
      INT=LT+L+IL-3
      IF(INT-(INT/2)*2)6,7,8
    6 KKK=6
      PRINT991,KKK,LT
  991 FORMAT(28H LOOPING FAILURE IN TEST AT I3,15H FOR VALUE LT =I5)
      CALLEXIT
    7 AL1=LT-1
      M1=1
      ATS=ABSF(HCJI-AL1)
      ATT=HCJI+AL1
      IF(HCJF-ATS+0.1)8,463,463
  463 IF(HCJF-ATT-0.1)464,464,8
  464 TERM2=2*LT-1
      M2=1
      IKON=LPI+LPF+LT-1
      IF(IKON-(IKON/2)*2)8,3333,8
 3333 LW1=IL-1
      M3=1
      LW2=LT-1
      LW3=L-1
      MW1=IL
      MW2=LT
      IW=0
      CALLWIGNER
      TERM3=CLEB
      IW=5
      LW1=2.0*HCJI+0.1
      LW2=2*(LT-1)
      LW3=2.0*HCJF+0.1
      MW1=HCJI+1.6
      MW2=LT
      CALLWIGNER
      TERM4=CLEB
      IF(TERM4)9,8,9
    9 CALLCMP(R1,U1,R3,U3,R,U)
      M4=1
      LPXT=KSUPER
      KSUPER=LT
      CALLTOEY
      KSUPER=LPXT
      CALLCMP(R,U,R2,U2,R,U)
      CALLCMP(R,U,SCMR,SCMI,R,U)
      TERM=TERM1*TERM2*TERM3*TERM4
      R=R*TERM*44.546624
      U=U*TERM*44.546624
      MT1=2*LT-1
      DC387MT=1,MT1
      MTR=LT-MT
      MMT=XABSF(MTR)+1
      IF(MMT-L)937,937,80
  937 MS=0
      M5=1
```

```
      Iw=0
      Lw1=IL-1
      Lw2=LT-1
      Lw3=L-1
      Mw1=IL
      Mw2=2*LT-MT
      CALLWIGNER
      IF(CLEB)401,80,401
 401  TERM5=CLEB
      M6=1
      Iw=5
      LW1=2.0*HOJI+0.01
      Lw2=2*LT-2
      Lw3=2.0*HOJF+0.01
 406  MS=MS+1
      M7=0
      IF(MS-1)403,403,404
 403  AMU=-HOJI
      GOTO405
 404  AMU=AMU+1.0
 405  Mw1=HOJI+1.0-AMU
      Mw2=MT
      CALLWIGNER
      IF(CLEB)411,81,411
 411  ADD1=CLEB
      IF(NUMPRG-10)8765,8765,8764
8764  F(MS)=ADD1*TERM5*R
      G(MS)=ADD1*TERM5*U
      AWR=-HOJI
8765  CONTINUE
      M7=1
      GOTO412
  81  IF(AMU-HOJI+0.01)406,407,407
 407  MEND=MS
      IF(NUMPRG-10)8763,8763,8762
8762  IF(JCT-1)8761,8761,8769
8761  JCT=10
      WRITEOUTPUTTAPE3,7759,MEND,AWR,HOJI
7759  FORMAT(1H /1H /50H PARTIAL MATRIX ELEMENTS    NO ANGLE PART    MJ
     1OFI3,16H VALUES    FROM F5.2,4H TO F5.2/10H L LP LT M)
8769  IF(MEND-4)8749,8748,8748
8749  MFT=MEND+1
      DO7730MC=MFT,4
      F(MC)=0.0
7730  G(MC)=0.0
8748  WRITEOUTPUTTAPE3,7742,IL,L,LT,MTR,(F(I),G(I),I=1,4)
7742  FORMAT(1H ,3I2,I3,4X,1P2E13.5,4X,1P2E13.5,4X,1P2E13.5,4X,1P2E13.5)
      IC=1
8900  IF(MEND-4*IC)8763,8763,8728
8728  IC=IC+1
      IF(MEND-4*IC)8727,8725,8725
8727  NFT=4*IC
      MFT=MEND+1
      DO8723MC=MFT,NFT
      F(MC)=0.0
8723  G(MC)=0.0
8725  LSD=4*(IC-1)+1
      NOT=4*IC
      WRITEOUTPUTTAPE3,8717,(F(I),G(I),I=LSD,NOT)
8717  FORMAT(1H ,13X,1P2E13.5,4X,1P2E13.5,4X,1P2E13.5,4X,1P2E13.5)
      GOTO8900
```

```
8763 CONTINUE
     GOTO80
 412 DO200J=1,JMAX
     DTHETA=THETAD(J)
     RTHETA=THETA(J)
     LX=L-1
     MX=L-MTR
     S=-1.0
     CALLLEGEND
     PT5=ADD1*TERM5*YLMR
     PT6=ADD1*TERM5*YLMI*S
     CALLCMP(R,U,PT5,PT6,ADD2,ADD3)
     WFMOD(MS,J)=WFMOD(MS,J)+ADD2
 200 PHASE(MS,J)=PHASE(MS,J)+ADD3
     GOTO81
  80 CONTINUE
 387 CONTINUE
   8 CONTINUE
 386 CONTINUE
 500 CONTINUE
 600 CONTINUE
     KSUPER=1
     IF(ISPILL)711,713,711
 711 PRINT712,ISPILL
 712 FORMAT(14H UNDERFLOW AT I5,10H IN TIEUP3)
 713 IF(JSPILL)714,716,714
 714 PRINT715,JSPILL
 715 FORMAT(13H OVERFLOW AT I5,10H IN TIEUP3)
     CALLEXIT
 716 RETURN
     END
```

```
      SUBROUTINETIEUP4
C     TO EVALUATE ANG DISTRIB UIA GLENDENNING
      IFDIVIDECHECK171,172
  171 PRINT173
  173 FORMAT(49H DIVIDE CHECK TRIGGR  FOUND ON AT START OF TIEUP4)
      CALLEXIT
  172 ISPILL=0
      JSPILL=0
      AS1=0.0
      WRITEOUTPUTTAPE3,65
      WRITEOUTPUTTAPE3,193
  193 FORMAT(43H RESULTS ANGLE       XSECTN          ARB NORM)
   65 FORMAT(35H ANGULAR DISTRIBUTION NO SPIN ORBIT)
      A3=FMB+FMI
      TER=FKAY/FIP/6764.44/(2.0*HOJI+1.0)*TBDPOT*TBDPOT*FMB*FMB/A3/A3
      IFDIVIDECHECK271,272
  271 PRINT273,FIP,HOJI
  273 FORMAT(29H DIVIDE CHECK PERHAPS OF FIP,1PE10.2,9H OR HOJI=1PE10.2)
      CALLEXIT
  272 CONTINUE
      DO50J=1,JMAX
      DO40M=1,MEND
      T1=WFMOD(M,J)
      T2=PHASE(M,J)
   40 AS1=AS1+T1*T1+T2*T2
      ANSW=AS1*TER
      AS1=0.0
      IF(J-1)41,41,42
   41 XOR=ANSW
      ARB=1.0
      GOTO46
   42 PTS=ABSF(XOR)
      IF(PTS-1.0)421,442,442
  421 JJK=JJK+1
      IF(JJK-1)424,424,425
  424 WRITEOUTPUTTAPE3,431
  431 FORMAT(33H ARB NORM AT ZERO LESS THAN UNITY)
  425 ARB=1.0
      GOTO46
  442 ARB=ANSW/XOR
   46 WRITEOUTPUTTAPE3,67,THETAD(J),ANSW,ARB
      IFDIVIDECHECK371,372
  371 PRINT373,XOR,THETAD(J)
  373 FORMAT(22H DIVIDE CHECK FOR XOR=1PE12.2,9H WHEN ANG1PE14.2/30H LOO
     1PING SHOULD NOT ALLOW THIS)
      CALLEXIT
  372 CONTINUE
   50 CONTINUE
   67 FORMAT(1H ,1PE14.4,2X,1P2E15.5)
      IF(ISPILL)691,692,691
  691 PRINT697,ISPILL
  697 FORMAT(24H UNDERFLOW IN TIEUP4 AT I4)
  692 IF(JSPILL)693,694,693
  693 PRINT698,JSPILL
  698 FORMAT(23H OVERFLOW IN TIEUP4 AT I4)
      CALLEXIT
  694 RETURN
      END
```

```
      SUBROUTINETIEUP5
      RETURN
      END
      SUBROUTINETIEUP6
      RETURN
      END
      SUBROUTINETIEUP7
      PRINT66,NUMRUN(4)
   66 FORMAT(1H /9H  RUN NO I3,20H  HAS BEEN COMPLETED)
      NUMRUN(4)=NUMRUN(4)+1
      RETURN
      END
      SUBROUTINETIEUP8
      PRINT66,NUMRUN(4)
   66 FORMAT(1H /9H  RUN NO I3,20H  HAS BEEN COMPLETED)
      NUMRUN(4)=NUMRUN(4)+1
      RETURN
      END
      SUBROUTINETIEUP9
      RETURN
      END
```

```
      SUBROUTINEREADER
      IFDIVIDECHECK100,110
  100 PRINT101
  101 FORMAT(60H DIVIDE CHECK TRIGGER FOUND ON AT START OF READER SUBROU
     1TINE)
      CALLEXIT
  110 ISPILL=0
      JSPILL=0
      IF(RG-20.0)150,151,151
  150 CONTINUE
      READINPUTTAPE2,10,(KTRL(I),I=1,13)
   10 FORMAT(I5)
      READINPUTTAPE2,12,FMI,FMB,QVAL,ZZ,RC,V,W,RO,A,VS,WS
      ELAB=(RENMZ(99)*RENMZ(100)+QVAL)*(FMI+FMB)/FMB
   12 FORMAT(E15.9)
  151 CONTINUE
      CO2=FMI+FMB
      FMU=FMI*FMB/CO2
      ECM=ELAB*FMB/CO2
      FKAY=0.2195376*SQRTF(FMU*ECM)
      T=FKAY*(FMB**0.3333333333)
      RHOBN=T*RC
      RHOBNG=T*RG
      RHOBC=T*RC
      ETA=0.15805086*ZZ*SQRTF(FMI/ELAB)
      IFDIVIDECHECK200,47
  200 PRINT201
  201 FORMAT(44H INPUT DIVISOR WAS ZERO IN READER SUBROUTINE)
      CALLEXIT
   47 DO71IT=1,IEND
      RHO(IT)=RHO(IT)*FKAY/FIP
   71 DRHO(IT)=DRHO(IT)*FKAY/FIP
      DO639NC=1,NMAXP
      RHOIN(NC)=RHOIN(NC)*FKAY/FIP
  639 DRHOIN(NC)=DRHOIN(NC)*FKAY/FIP
      RHOIN(NMAX)=RHOIN(NMAX)*FKAY/FIP
      IFDIVIDECHECK777,778
  777 PRINT779
  779 FORMAT(33H DIV CH TRIG ON IN READER FOR FIP)
      CALLEXIT
  778 IF(RG-20.0)153,154,154
  153 READINPUTTAPE2,10,LMAXM
  154 CONTINUE
      LMAX=LMAXM+1
      DO147J=1,LMAX
  147 IIN(J)=1
      IF(RG-20.0)156,157,157
  156 CONTINUE
      READINPUTTAPE2,10,JMAX
      READINPUTTAPE2,12,(THETAD(J),J=1,JMAX)
      DO49J=1,JMAX
   49 THETA(J)=0.01745329252*THETAD(J)
      READINPUTTAPE2,10,LPI,LPF,NHI,NHF
      READINPUTTAPE2,12,HOJI,HOJF
      READINPUTTAPE2,12,RADWC,WF
      READINPUTTAPE2,12,SNO1,RHOBS,TBDPOT
  157 CONTINUE
      KSUPER=2
      CALLCTRL4
```

```
207 IF(ISPILL)202,204,202
202 PRINT203,ISPILL
203 FORMAT(23H UNDERFLOW OCCURRED AT I5,21H IN READER SUBROUTINE)
204 IF(JSPILL)205,210,205
205 PRINT206,JSPILL
206 FORMAT(22H OVERFLOW OCCURRED AT I5,21H IN READER SUBROUTINE)
    CALLEXIT
210 RETURN
    END
```

```
      SUBROUTINEADJUST
      IFDIVIDECHECK3,4
    3 PRINT900
  900 FORMAT(60H DIVIDE CHECK TRIGGER FOUND ON AT START OF ADJUST SUBROU
     1TINE)
      IME=19
      CALLREDEF
    4 NP=1
      IND=1
      MZ=1
 5772 RHO(1)=ROSP(1)
      RADS(1)=ROSP(1)/FKAY
      IFDIVIDECHECK777,778
  777 PRINT779
  779 FORMAT(37H DIV CHECK TRIG ON IN ADJUST FOR FKAY)
      IME=19
      CALLREDEF
  778 SPACE=DRHOIN(NMAXP)
      JTH=2
  403 ADS=RHOIN(JTH)-0.001
      IF(ROSP(1)-ADS)401,402,402
  402 JTH=JTH+1
      GOTO403
  401 MZ=JTH-1
    9 MC=SPACE/DRHOIN(MZ)+0.001
      IFDIVIDECHECK788,789
  788 PRINT790,MZ
  790 FORMAT(33H DIV CH TRIG ON IN ADJUST FOR MZ=I4)
      IME=19
      CALLREDEF
  789 LR=MC
      RVAL=RHOIN(MZ+1)-0.001
      KA=1
  940 IF(RVAL-ROSP(KA))938,938,939
  939 KA=KA+1
      GOTO940
  938 KB=KA/MC
      KC=KA-KB*MC
      IF(KB)6001,6000,6001
 6000 RHO(2)=RHOIN(MZ+1)
      RADS(2)=RHO(2)/FKAY
      NP=2
      IND=KA
      KLP=2
      MZ=MZ+1
      MC=SPACE/DRHOIN(MZ)+0.001
      LR=KA+MC
      GOTO941
 6001 IF(KC-1)6010,6011,6012
 6010 RHO(2)=ROSP(LR)
      IND=LR
      LR=LR+MC
      NP=2
      GOTO7000
 6011 LR=LR+1
      RHO(2)=ROSP(LR)
      IND=LR
      LR=LR+MC
      NP=2
      GOTO7000
 6012 RHO(2)=ROSP(KC)
```

```
      LR=LR+KC
      NP=2
      IND=KC
 7000 RADS(2)=RHO(2)/FKAY
      KUP=1
      GOTO941
   51 IF(ROSP(IND)-ROSP(LR))5,6,70
    5 IND=IND+1
      GOTO51
   70 PRINT170,ROSP(IND),LR,ROSP(LR)
  170 FORMAT(31H REDUCTION FAILED FOR ROSP (I)=E13.4,26H WHEN STORE PT
     1AS FOR LC=I4,5H RHO=E13.4)
      IME=19
      CALLREDEF
    6 NP=NP+1
      RHO(NP)=ROSP(IND)
  941 RADS(NP)=RHO(NP)/FKAY
      DO345L=1,LMAX
      XCS(NP,L)=XCS(IND,L)
  345 YCS(NP,L)=YCS(IND,L)
      DO346LI=1,LIP
      XCST(NP,LI)=XCST(IND,LI)
  346 YCST(NP,LI)=YCST(IND,LI)
      IF(KUP-2)1100,1100,1111
 1100 KUP=5
      GOTO51
 1111 QQQ=RHOIN(NMAX)-0.001
      IF(RHO(NP)-QQQ)95,72,72
   95 TEST=RHOIN(MZ+1)
      IRO=ROSP(IND)*1000.0
      ICH=TEST*1000.0
      IF(IRO-ICH)91,92,93
   93 PRINT193,RHO(IND),TEST,NP,IND,MZ,MC,LR,(RHO(I),I=1,NP),SPACE,QQQ
     1DRHOIN(I),I=1,MZ),(RHOIN(I),I=1,MZ)
  193 FORMAT(26H STORAGE FAILURE FOR RHO =E13.4,15H AND CHANGE PT E13.
     15H NOS=5I3/5H PTS=10F9.5)
      IME=19
      CALLREDEF
   91 LR=LR+MC
      IND=IND+1
      GOTO51
   92 MC=SPACE/DRHOIN(MZ+1)
      IFDIVIDECHECK793,794
  793 PRINT795,MZ
  795 FORMAT(33H DIV CH TRIG ON IN ADJUST FOR MZ=I4)
      IME=19
      CALLREDEF
  794 MZ=MZ+1
      LR=IND+MC
      GOTO51
   72 DRHOL=SPACE/FKAY
      IFDIVIDECHECK8817,8818
 8817 PRINT8819,FKAY
      WRITEOUTPUTTAPE3,8819,FKAY
 8819 FORMAT(1H /22H DIV CHK IN ADJUST  K=E13.4)
      CALLREDEF
 8818 CONTINUE
      IF(NP-(NP/2)*2)81,82,81
   82 IEND=NP-1
      GOTO83
   81 IEND=NP
```

```
   83 LHO=LPI+1
      NHO=NHI
      CALLBSWFHO
      DO31I=1,IEND
   31 FFSRM(I)=ULRN(I)
      LHO=LPF+1
      NHO=NHF
      CALLBSWFHO
      DO32I=1,IEND
      FFSIM(I)=ULRN(I)
      ULRN(I)=FFSRM(I)*FFSIM(I)
   32 CONTINUE
 2817 CONTINUE
      IF(ISPILL)813,814,813
  813 PRINT815,ISPILL
  815 FORMAT(24H UNDERFLOW IN ADJUST AT I5)
  814 IF(JSPILL)816,817,816
  816 PRINT818,JSPILL
  818 FORMAT(23H OVERFLOW IN ADJUST AT I5)
      IME=19
      CALLREDEF
  817 RETURN
      END
```

```
      SUBROUTINEBSWFHO
      IFDIVIDECHECK50,51
   50 PRINT150
  150 FORMAT(60H DIVIDE CHECK TRIGGER FOUND ON AT START OF BSWFHO SUBROU
     UTINE)
      CALLEXIT
   51 ISPILL=0
      JSPILL=0
      ALP=2*(2*(NHO-1)+(LHO-1))+3
      ALP=ALP/RHOBS/RHOBS
      SALP=SQRTF(ALP)
      ALP3H=SALP*ALP
      ALPTQ=SQRTF(ALP3H)*0.75112574
      IF(LHO-2)1,2,2
    1 DO9I=1,IEND
      Q=SALP*RADS(I)
      Q2=Q*Q
      GOTO(3,4,5,6),NHO
    3 Y=2.0*ALPTQ*EXPF(-0.5*Q2)
      GOTO100
    4 Y=2.4494898*ALPTQ*(1.0-2.0*Q2/3.0)*EXPF(-0.5*Q2)
      GOTO100
    5 Q4=Q2*Q2
      Y=2.7386128*ALPTQ*(1.0-4.0*Q2/3.0+4.0*Q4/15.0)*EXPF(-0.5*Q2)
      GOTO100
    6 Q4=Q2*Q2
      Q6=Q4*Q2
      Y=2.9580399*ALPTQ*EXPF(-0.5*Q2)*(1.0-2.0*Q2+0.8*Q4-0.0761905*Q6)
  100 IF(RADS(I)-RADWC)7,7,8
    7 ULRN(I)=WF*Y
      GOTO9
    8 ULRN(I)=Y
    9 CONTINUE
      GOTO30
    2 DO93I=1,IEND
      Q=SALP*RADS(I)
      Q2=Q*Q
      GOTO(21,22,23),NHO
   21 FACTOR=FG(LHO-1)-FG(2*LHO-1)
      HONORM=2.0**(LHO)*EXPF(FACTOR/2.0)
      Y=HONORM*ALPTQ*EXPF(-0.5*Q2)*Q**(LHO-1)
      GOTO90
   22 FACTOR=FG(2*LHO+1)+2.0*FG(LHO-1)-FG(LHO)-2.0*FG(2*LHO-1)
      HONORM=2.0**(LHO-1)*EXPF(FACTOR/2.0)
      Y=HONORM*ALPTQ*EXPF(-0.5*Q2)*Q**(LHO-1)*(1.0-2.*Q2/(2.0*CLHO+1.0))
      GOTO90
   23 FACTOR=FG(2*LHO+3)-FG(LHO+1)+2.0*FG(LHO-1)-2.0*FG(2*LHO-1)
      HONORM=2.0**(LHO-2)*EXPF(FACTOR/2.0)/1.4142135
      Y=HONORM*ALPTQ*EXPF(-0.5*Q2)*Q**(LHO-1)*(1.0-4.0*Q2/(2.0*CLHO+1.0)
     1+4.0*Q2*Q2/(2.0*CLHO+1.0)/(2.0*CLHO+3.0))
   90 IF(RADS(I)-RADWC)91,91,92
   91 ULRN(I)=WF*Y
      GOTO93
   92 ULRN(I)=Y
   93 CONTINUE
  797 WRITEOUTPUTTAPE3,798,NHO,LHO,RHOBS,ALP,SALP,ALP3H,ALPTQ,HONORM,FAC
     1TOR
  798 FORMAT(14H BSWFHO FOR N=I2,3H L=I2,1H ,1P7E15.4)
   30 IF(ISPILL)60,61,60
```

```
 60 PRINT160,ISPILL
160 FORMAT(23H UNDERFLOW OCCURRED AT I6,21H IN BSWFHD SUBROUTINE)
 61 IF(JSPILL)62,63,62
 62 PRINT162,JSPILL
162 FORMAT(23H  OVERFLOW OCCURRED AT I6,21H IN BSWFHD SUBROUTINE)
    CALLEXIT
 63 RETURN
    END
```

```
      SUBROUTINETOEY
      IFDIVIDECHECK3,4
    3 PRINT5
      IME=24
      WRITEOUTPUTTAPE3,5
    5 FORMAT(26H DIVIDE CHECK ON IN   TOEY)
      CALLREDEF
    4 ISPILL=0
      JSPILL=0
      IME=24
      I=1
      ABC=0.0
      DEF=0.0
      H=4.0
  498 TER1=RADS(I)*RADS(I)*LORB(I)
      TEI1=RADS(I)*RADS(I)*LOIB(I)
      IKTRL=I
      IF(ISP2-5)500,550,550
  500 TER1=TER1*ULRN(I)
      TEI1=TEI1*ULRN(I)
      GOTO505
  550 CALLACTION
      CALLCMP(TER1,TEI1,YLMR,YLMI,TER1,TEI1)
      IF(ISPILL)1357,1359,1357
 1357 IF(RENMZ(50)-4.0)1358,1358,1359
 1358 WRITEOUTPUTTAPE3,3579,ISPILL,I,ABC,DEF,TER1,TEI1,RADS(I),ULRN(I),U
     1ORB(I),UOIB(I),YLMR,YLMI,SOMR,SOMI
 3579 FORMAT(22H UNDERFLOW IN TOEY AT I3/7H FOR I=I3,1P6E14.4/1H ,1P6E14
     1.4)
      RENMZ(50)=RENMZ(50)+1.0
 1359 CONTINUE
  505 IF(I-1)504,504,502
  502 IF(I-IEND)503,504,504
  504 ABC=ABC+TER1
      DEF=DEF+TEI1
      IF(I-IEND)510,511,511
  510 I=I+1
      GOTO498
  503 ABC=ABC+H*TER1
      DEF=DEF+H*TEI1
      AGT=ABSF(TER1)
      BGT=ABSF(TEI1)
      CGT=AGT+BGT
      IF(I-30)722,722,723
  723 IF(CGT-1.0E-09)724,724,722
  724 ITL=I
      IF(ITL-2*(ITL/2))511,731,511
  731 H=1.0
      I=I+1
      GOTO498
  722 CONTINUE
      H=6.0-H
      I=I+1
      GOTO498
  511 SOMR=ABC*DRHOL/3.0
      SOMI=DEF*DRHOL/3.0
 2468 IF(JSPILL)3157,4268,3157
 3157 PRINT5317,JSPILL
      WRITEOUTPUTTAPE3,5317,JSPILL
 5317 FORMAT(23H OVERFLOW IN   TOEY AT I5)
      CALLREDEF
```

```
4268 CONTINUE
     RETURN
     END
```

```
      SUBROUTINEACTION
      IFDIVIDECHECK3,4
    3 PRINT5
      WRITEOUTPUTTAPE3,5
    5 FORMAT(26H DIVIDE CHECK ON IN ACTION)
      IME=21
      CALLREDEF
    4 ISPILL=0
      JSPILL=0
      KN=1
      K=1
      STOR1=EPS1
      STOR2=EPS2
      CBA=0.0
      FED=0.0
      H=4.0
  498 OER1=RADS(K)*RADS(K)*FFSRM(K)*FFSIM(K)
      OEI1=0.0
      ILAST=K
      CALLVGEN
      CALLCMP(OER1,OEI1,EPS1,EPS2,OER1,OEI1)
      IF(ISPILL)1357,106,1357
 1357 IF(RENMZ(52)-4.0)105,105,106
  105 WRITEOUTPUTTAPE3,107,ISPILL,K,RADS(K),OER1,OEI1,AGL,BGL,YLMR,YLMI
  107 FORMAT(24H UNDERFLOW IN ACTION AT I3,I5,1P7E13.4)
      RENMZ(52)=RENMZ(52)+1.0
  106 CONTINUE
      KN=KN+1
      IF(K-1)504,504,502
  502 IF(K-IEND)503,504,504
  504 CBA=CBA+OER1
      FED=FED+OEI1
      IF(K-IEND)510,511,511
  510 K=K+1
      GOTO498
  503 CBA=CBA+H*OER1
      FED=FED+H*OEI1
      AGT=ABSF(OER1)
      BGT=ABSF(OEI1)
      CGT=AGT+BGT
      IF(K-20)722,722,723
  723 IF(CGT-1.0E-09)724,724,722
  724 ITL=K
      IF(ITL-2*(ITL/2))511,731,511
  731 H=1.0
      K=K+1
      GOTO498
  722 CONTINUE
      H=6.0-H
      K=K+1
      GOTO498
  511 YLMR=CBA*DRHOL/3.0
      YLMI=FED*DRHOL/3.0
      EPS1=STOR1
      EPS2=STOR2
 2468 IF(JSPILL)3157,4268,3157
 3157 PRINT5317,JSPILL
      WRITEOUTPUTTAPE3,5317,JSPILL
 5317 FORMAT(23H OVERFLOW IN ACTION AT I5)
      IME=21
      CALLREDEF
```

```
4268 CONTINUE
     RETURN
     END
```

```
      SUBROUTINEVGEN
C     YUKAWA POTENTIAL FORM
      IFDIVIDECHECK3,4
    3 PRINT31
      WRITEOUTPUTTAPE3,31
   31 FORMAT(33H DIVIDE CHECK ON AT START OF VGEN)
      IME=22
      CALLREDEF
    4 ISPILL=0
      JSPILL=0
      LM=KSUPER-1
      EG=LM
      R1=RADS(IKTRL)
      R2=RADS(ILAST)
      TER1=2*LM+1
      LG=2*LM+1
      IF(R1-R2)5,6,6
    5 RU=R2
      RL=R1
      GOTO7
    6 RU=R1
      RL=R2
    7 AU=RU*DBG
      AD=RL*DBG
      ARG=-AU
      TEX=EXPF(ARG)
      IF(LM)9,10,11
    9 WRITEOUTPUTTAPE3,91,LM,KSUPER
   91 FORMAT(25H TRANSFER INCORRECT   LM=I2,8H KSUPER=I3)
      IME=22
      CALLREDEF
   10 TSM=1.0
      GOTO20
   11 KL=1
      AL=1.0
      TST=AL
   15 AKL=KL
      AL2=AL*(EG+AKL)*(EG-AKL+1.0)/AKL/2.0/AU
      TSM=TST+AL2
      IF(KL-LM)12,20,20
   12 KL=KL+1
      TST=TSM
      AL=AL2
      GOTO15
   20 FK=TSM*TEX/AU
      CALLSIG(LM,LR,LU)
      A3=LR
      A4=LU
      CALLCMD(FK,0.0,A3,A4,RH,UH)
      HKR=-RH
      HKU=-UH
      SATM=AD**EG
      ES=EG*LOGF(2.0)+FG(LM+1)-FG(LG+1)-LOGF(EG+1.0)+LOGF(TER1+1.0)
      BL=EXPF(ES)
      TS4=BL
      XSM=BL
      KP=1
   56 AKP=KP
      BL2=BL*AD*AD/2.0/AKP/(2.0*EG+2.0*AKP+1.0)
      XSUM=XSM+BL2
      REM1=1.0-AD*AD/2.0/(AKP+1.0)/(2.0*EG+2.0*AKP+3.0)
```

```
      I13=2*KP+2*LM+1
      I14=KP+LM
      RL2=(2.0*AKP)*LOGF(AC)-AKP*LOGF(2.0)-FG(KP+1)+LOGF(AKP+1.0)-FG(I13
     1)+FG(I14)+(AKP+EG)*LOGF(2.0)
      REM2=EXPF(RL2)
      REM=REM2/REM1
      TIP=ABSF(REM/TS4)
      IF(TIP-0.0001)63,63,64
   64 KP=KP+1
      BL=BL2
      XSM=XSUM
      GOTO56
   63 A8=LR
      A9=LU
      CALLCNEMN(LM,B9)
      X8=B9*A8
      X9=B9*A9
      C8=XSUM
      XSUM=C8*SATM
      CALLCMD(XSUM,0.0,X8,X9,PN,PI)
      BESR=PN
      BESI=PI
      CALLCMP(BESR,BESI,HKR,HKU,APP,AQQ)
      EPS1=APP
      EPS2=AQQ
      IF(ISPILL)221,8899,221
  221 IF(RENMZ(53)-4.0)8888,8888,8899
 8888 WRITEOUTPUTTAPE3,8890,ISPILL,R1,R2,KSUPER,LM,DBG,AU,AD,TEX,TSM,FK,
     1HKR,HKU,SATM,ES,BL,BL2,XSUM,REM1,REM2,RL2,REM,TIP,BESR,BESI,APP,AQ
     2Q,EPS1,EPS2
 8890 FORMAT(22H UNDERFLOW IN VGEN AT I3,2F8.4,2I3,1P6E13.4/1H ,1P9E14.4
     1/1H ,1P9E14.4)
      RENMZ(53)=RENMZ(53)+1.0
 8899 CONTINUE
      TAA=ABSF(EPS1)
      TBB=ABSF(EPS2)
      IF(TAA-1.0E-06)101,101,102
  101 EPS1=0.0
  102 IF(TBB-1.0E-06)103,103,104
  103 EPS2=0.0
  104 CONTINUE
  222 IF(JSPILL)223,224,223
  223 PRINT550,JSPILL
      WRITEOUTPUTTAPE3,550,JSPILL
  550 FORMAT(13H OVERFLOW AT I5,8H IN VGEN)
      IME=22
      CALLREDEF
  224 RETURN
      END
```

```
      SUBROUTINEWIGNER
      IFDIVIDE CHECK988,989
  988 PRINT990
  990 FORMAT(60H DIVIDE CHECK TRIGGER FOUND ON AT START OF WIGNER SUBROU
     1TINE)
      CALLEXIT
  989 ISPILL=0
      JSPILL=0
      AJ=LW1
      AK=LW2
      AL=LW3
      AL2=ABSF(AJ-AK)
      AL3=AJ+AK
      IF(AL2-AL-0.5)1,1,29
    1 IF(AL3-AL+0.5)29,2,2
    2 AM=MW1
      AN=MW2
      IF(IW-2)3,3,4
    4 AL=AL/2.0
      AJ=AJ/2.0
      AK=AK/2.0
    3 AM=AJ+1.0-AM
      AN=AK+1.0-AN
      AAM=ABSF(AM)
      AAN=ABSF(AN)
      FM=AM+AN
      AFM=ABSF(FM)
      IF(AFM-AL-0.5)6,6,29
    6 IF(AAM-AJ-0.5)7,7,29
    7 IF(AAN-AK-0.5)8,8,29
    8 IF(AM)201,202,201
  202 IF(AN)201,203,201
  201 GOTO100
  203 JT=AJ+AK+AL
      JTH=JT/2
      IF(JT-JTH*2)204,205,204
  204 CLEB=0.0
      GOTO30
  205 I1=JT-2*LW1
      I1H=I1/2
      I2=JT-2*LW2
      I2H=I2/2
      I3=JT-2*LW3
      I3H=I3/2
      AI1=I1
      AI2=I2
      AI3=I3
      AI1H=I1H
      AI2H=I2H
      AI3H=I3H
      AJT=JT
      Y=FG(I1+1)+FG(I2+1)+FG(I3+1)-FG(JT)
      Y=(Y+LOGF((2.0*AL+1.0)/(AI1+1.0)/(AI2+1.0)/(AI3+1.0)/(AJT+1.0)))/2
     1.0
      Y=Y+FG(JTH)-FG(I1H+1)-FG(I2H+1)-FG(I3H+1)
      Y=Y+LOGF((AI1H+1.0)*(AI2H+1.0)*(AI3H+1.0))
      I6=(LW1+LW2-LW3)/2
      CALLONEMN(I6,X5)
      CLEB=X5*EXPF(Y)
```

```
      GOTO30
  100 I1=AL+AJ+0.1-AK
      AI1=I1
      I2=AL-AJ+AK+0.1
      AI2=I2
      I3=AJ+AK-AL+0.1
      AI3=I3
      I4=AL-FM+0.1
      AI4=I4
      I5=AL+FM+0.1
      AI5=I5
      I6=AL+AJ+AK+1.1
      AI6=I6
      I7=AJ-AM+0.1
      AI7=I7
      I8=AJ+AM+0.1
      AI8=I8
      I9=AK-AN+0.1
      AI9=I9
      I10=AK+AN+0.1
      AI10=I10
    9 Y=FG(I1+1)+FG(I2+1)+FG(I3+1)+FG(I4+1)+FG(I5+1)-FG(I6+1)-FG(I8+1)-F
     1G(I7+1)-FG(I9+1)-FG(I10+1)
      Y=Y+LOGF((2.0*AL+1.0)*(AI6+1.0)*(AI7+1.0)*(AI8+1.0)*(AI9+1.0)*(AI1
     10+1.0)/(AI1+1.0)/(AI2+1.0)/(AI3+1.0)/(AI4+1.0)/(AI5+1.0))
      Y=Y/2.0
      I11=AK+AL+AM+0.1
      AI11=I11
      NU=XMINOF(I2,I5,I11)
      IF(NU)29,11,12
   11 I15=AJ-AK-FM+0.1
      AI15=I15
      IF(I15)13,14,14
   13 CLEB=0.0
      GOTO30
   14 CALLONEMN(I10,XS)
      YL=FG(I11+1)+FG(I7+1)-FG(I5+1)-FG(I15+1)-FG(I2+1)
      YL=YL+Y+LOGF((AI2+1.0)*(AI5+1.0)*(AI15+1.0)/(AI11+1.0)/(AI7+1.0))
      CLEB=XS*EXPF(YL)
      GOTO30
   12 I15=AJ-AK-FM
      IF(I15)15,16,16
   15 I15=XABSF(I15)
      AI15=I15
      IF(NU-I15)17,18,19
   17 CLEB=0.0
      GOTO30
   18 I16=I10+I15
      CALLONEMN(I16,XS)
      I11=I11-I15
      AI11=I11
      I12=I7+I15
      AI12=I12
      I13=I2-I15
      AI13=I13
      I14=I5-I15
      AI14=I14
      YL=FG(I11+1)+FG(I12+1)-FG(I13+1)-FG(I14+1)-FG(I15+1)
      YL=YL+Y+LOGF((AI13+1.0)*(AI14+1.0)*(AI15+1.0)/(AI11+1.0)/(AI12+1.0
```

```
     1))
      CLEB=XS*EXPF(YL)
      GOTO30
   19 NUMIN=I15+1
      NUMAX=NU
      I16=I10+I15
      CALLONEMN(I16,XS)
      I17=I11-I15
      AI17=I17
      I12=I7+I15
      AI12=I12
      I13=I2-I15
      AI13=I13
      I14=I5-I15
      AI14=I14
      SUML=FG(I17+1)+FG(I12+1)-FG(I13+1)-FG(I14+1)-FG(I15+1)
      SUML=SUML+Y+LOGF((AI13+1.0)*(AI14+1.0)*(AI15+1.0)/(AI17+1.0)/(AI12
     1+1.0))
      SUM=XS*EXPF(SUML)
      I15=-I15
      GOTO20
   16 NUMIN=1
      NUMAX=NU
      CALLONEMN(I10,XS)
      AI15=I15
      SUML=FG(I11+1)+FG(I7+1)-FG(I2+1)-FG(I5+1)-FG(I15+1)
      SUML=SUML+Y+LOGF((AI2+1.)*(AI5+1.)*(AI15+1.)/(AI11+1.)/(AI7+1.))
      SUM=XS*EXPF(SUML)
   20 DO21NU=NUMIN,NUMAX
      I21=I11-NU
      AI21=I21
      I12=I7+NU
      AI12=I12
      I13=I2-NU
      AI13=I13
      I14=I5-NU
      AI14=I14
      I22=NU+I15
      AI22=I22
      I16=I10+NU
      CALLONEMN(I16,XS)
      SUML=FG(I21+1)+FG(I12+1)-FG(I13+1)-FG(I14+1)-FG(I22+1)-FG(NU)
      SUML=SUML+Y+LOGF((AI13+1.0)*(AI14+1.0)*(AI22+1.0)/(AI21+1.0)/(AI12
     1+1.0))
      SUMI=XS*EXPF(SUML)
      SUM=SUM+SUMI
   21 CONTINUE
      CLEB=SUM
      GOTO30
   29 CLEB=0.0
   30 IF(CLEB)730,330,730
  730 ETB=ABSF(CLEB)
      IF(ETB-1.0E-06)782,782,330
  782 CLEB=0.0
  330 IF(ISPILL)60,61,60
   60 PRINT160,ISPILL
  160 FORMAT(23H UNDERFLOW OCCURRED AT I6,21H IN WIGNER SUBROUTINE)
   61 IF(JSPILL)62,63,62
   62 PRINT162,JSPILL
```

```
  162 FORMAT(22H OVERFLOW OCCURRED AT I6,21H IN WIGNER SUBROUTINE)
      CALLEXIT
   63 RETURN
      END
```

```
      SUBROUTINELEGEND
      IFDIVIDECHECK100,110
  100 PRINT101
  101 FORMAT(60H DIVIDE CHECK TRIGGER FOUND ON AT START OF LEGEND SUBROU
     1TINE)
      CALLEXIT
  110 ISPILL=0
      JSPILL=0
      AL=LX
      AM=MX
      AM=AL+1.-AM
      RPHI=0.01745329252*PHI
      CS=COSF(RTHETA)
      SN=SINF(RTHETA)
      IF(SN)988,989,988
  988 CONTINUE
      SNL=LOGF(SN)
      SNLL=AL*SNL
  989 CONTINUE
      IF(90.0-DTHETA)1,2,3
    1 ACS=ABSF(CS)
      CSL=LOGF(ACS)
      SOCS=-1.
      CS=ACS
      GOTO4
    2 CSL=1.
      CS=0.
      SOCS=0.
      GOTO4
    3 CSL=LOGF(CS)
      SOCS=1.
    4 IF(PHI)5,6,7
    5 PRINT102
  102 FORMAT(49H PHI NEGATIVE IN STATEMENT 4 OF LEGEND SUBROUTINE)
      CALLEXIT
    6 U=0.
      IF(AM)8,9,10
    7 IF(AM)27,28,29
    8 AM=ABSF(AM)
      N1=XFIXF(AM)
      CALLONEMN(N1,R)
      GOTO17
    9 N1=0
      IF(SOCS)11,12,13
   10 N1=XFIXF(AM)
      R=1.
      GOTO17
   11 CALLONEMN(LX,R)
      GOTO21
   12 IF(LX-(LX/2)*2)14,15,16
   13 R=1.
      GOTO21
   14 PRINT103
  103 FORMAT(41H  L  INCORRECT IN 12 OF LEGEND SUBROUTINE)
      CALLEXIT
   15 LH=LX/2
      CALLONEMN(LH,R)
      FF=FG(LX)-AL*FG(2)-2.0*FG(LH)
      GOTO58
```

```
   16 FF=0.0
      R=0.
      GOTO59
   17 IF(SOCS)18,19,20
   18 CALLONEMN(LX-N1,Z)
      R=R*Z
      GOTO24
   19 GOTO46
   20 GOTO24
   21 IF(DTHETA)80,23,80
   80 IF(180.0-DTHETA)22,23,22
   22 GOTO46
   23 FF=0.0
      GOTO58
   24 IF(DTHETA)81,26,81
   81 IF(180.0-DTHETA)25,26,25
   25 GOTO46
   26 R=0.
      FF=0.0
      GOTO59
   27 AM=ABSF(AM)
      CP=COSF(AM*RPHI)
      SP=-SINF(AM*RPHI)
      N1=XFIXF(AM)
      CALLONEMN(N1,Z)
      GOTO30
   28 CP=1.
      SP=0.
      N1=0
      Z=1.
      GOTO30
   29 Z=1.
      N1=XFIXF(AM)
      CP=COSF(AM*RPHI)
      SP=SINF(AM*RPHI)
   30 R=Z*CP
      U=Z*SP
      IF(SOCS)31,32,33
   31 MM=XFIXF(AL-AM)
      CALLONEMN(MM,Z)
      R=Z*R
      U=Z*U
      GOTO34
   32 IF(LX-(LX/2)*2)70,71,72
   70 PRINT104
  104 FORMAT(39H L INCORRECT IN 32 OF LEGEND SUBROUTINE)
      CALLEXIT
   71 LH=LX/2
      CALLONEMN(LH,Z)
      FF=FG(LX)-AL*FG(2)-2.0*FG(LH)
      R=Z*R
      U=Z*U
      GOTO58
   72 FF=0.0
      R=0.
      U=0.
      GOTO59
   33 GOTO34
   34 IF(DTHETA)82,36,82
```

```
 82 IF(180.0-DTHETA)35,36,35
 35 GOTO46
 36 IF(LX+1-MX)73,74,73
 73 FF=0.0
    R=0.
    U=0.
    GOTO59
 74 FF=0.0
    GOTO58
 46 IF(LX-N1-1)47,48,49
 47 FF=SNLL+FG(2*LX)-AL*FG(2)-FG(LX)
    GOTO58
 48 IF(SOCS)90,91,90
 90 FF=CSL+FG(2*LX)+SNL*(AL-1.0)-AL*FG(2)-FG(LX)
    GOTO58
 91 FF=1.0
    R=0.0
    U=0.0
    GOTO58
 49 JL=LX
    FIT=SNLL+FG(2*LX)-AL*FG(2)-FG(LX)
    FIT=EXPF(FIT)
    IF(SOCS)92,93,92
 92 FQT=CSL+FG(2*LX)+SNL*(AL-1.0)-AL*FG(2)-FG(LX)
    FQT=EXPF(FQT)
    GOTO94
 93 FQT=0.0
 94 AJL=JL
 50 F3=(2.0*(AJL-1.0)*CS*FQT-SN*FIT)/SN/(AL+AJL-1.0)/(AL-AJL+2.0)
    IFDIVIDECHECK105,106
105 PRINT107
107 FORMAT(52H DIVISOR IS ZERO IN STATEMENT50 OF LEGEND SUBROUTINE)
    CALLEXIT
106 IF(N1+2-JL)51,52,53
 51 AJL=AJL-1.0
    JL=JL-1
    FIT=FQT
    FQT=F3
    GOTO50
 52 FF=F3
    AF=ABSF(FF)
    IF(FF)54,55,56
 54 SOF=-1.
    GOTO57
 55 SOF=0.
    GOTO57
 56 SOF=1.
    GOTO57
 53 PRINT108,JL
108 FORMAT(45H INCORRECT LOOPING IN 50 OF LEGEND SUBROUTINEE15.5)
    CALLEXIT
 57 FF=LOGF(AF)
    R=R*SOF
    U=U*SOF
 58 N2=LX-N1+1
    AN2=N2
    N3=LX+N1
    FF=FF+(LOGF(2.0*AL+1.0)+FG(N2)-LOGF(AN2)-LOGF(4.0*3.14159265)-FG(N
   13))/2.0
```

```
   59 YLMR=R*EXPF(FF)
      YLMI=U*EXPF(FF)
      MG1=ABSF(AM)
      IF(MG1-(MG1/2)*2)8000,8001,8000
 8000 S=-1.0
      YLMR=YLMR*S
      YLMI=YLMI*S
 8001 CONTINUE
      IF(ISPILL)200,201,200
  200 PRINT210,ISPILL
  210 FORMAT(22H UNDERFLOW OCCURRED AT I6,21H IN LEGEND SUBROUTINE)
  201 IF(JSPILL)202,203,202
  202 PRINT220,JSPILL
  220 FORMAT(22H  OVERFLOW OCCURRED AT I6,21H IN LEGEND SUBROUTINE)
      CALLEXIT
  203 RETURN
      END
```

```
      SUBROUTINEWIPE
      IF(ISP4-499)32,31,31
   32 CONTINUE
   31 DO70LG=1,11
      DO70LA=1,75
      WFMOD(LG,LA)=0.0
   70 PHASE(LG,LA)=0.0
      RETURN
      END
```

```
      SUBROUTINEREDEF
      PRINT88
      WRITEOUTPUTTAPE3,89
   88 FORMAT(1H /1H /40H OPERATOR   PLEASE SEND ME THIS PRINTOUT/1H /1H
     1)
   89 FORMAT(1H /13H REDEF CALLED)
      CALLEXIT
      END
```

Reprinted from THE PHYSICAL REVIEW, Vol. 132, No. 5, 2261–2269, 1 December 1961
Printed in U. S. A.

Optical Model in the Interior of the Nucleus. II*

K. A. AMOS† AND I. E. MCCARTHY†
Department of Mathematical Physics, University of Adelaide, Adelaide, South Australia, and Department of Physics, University of California, Davis, California

(Received 26 June 1963; revised manuscript received 9 August 1963)

Factors which influence the relative contribution of the interior and the surface of the nucleus to matrix elements for direct interactions involving nucleons in the entrance and exit channels are studied quantitatively. Purely optical-model effects causing localization of the reaction are phase averaging, which tends to de-emphasize the interior at all energies, and focusing which emphasizes the interior at low energies and the surface at higher energies. It is shown that phase averaging does not make the central contribution negligible at any energy. The foci in the optical-model wave functions have large effects on angular distributions. Density dependence of the two-body force for reactions which proceed by a two-body collision mechanism can be identified from angular distributions and from the energy dependence of backward cross sections which are particularly sensitive to the foci.

1. INTRODUCTION

IN a previous publication[1] (referred to as I) the question was discussed whether it is possible to infer anything about the radial localization of a direct interaction involving nucleons in the initial and final states from the general shape of the angular distributions.

The surface interaction model[2] for the excitation of collective states has had considerable success in predicting experimental results. The validity of the model is discussed particularly by Buck.[2] Direct interactions which proceed by a two-body collision in the nucleus have often been regarded also as surface effects for two main reasons.

The first concerns the optical-model wave functions which are used to represent initial and final states in the distorted-wave Born approximation (DWBA). Simple considerations[3] seem to indicate that the product particle would be likely to be reflected back into the nucleus if it came from the interior region. It was shown in I how a reduction of the interior contribution to the matrix element could arise from the fact that the phase of each partial wave of low-angular momentum is a smoother function of r in a distorted wave than in a plane wave. This effect has been called[4] "phase averaging." It is discussed for α particles by Rost.[4]

The second possible reason for reduction of the interior contribution to the matrix element is that it might be due to the reaction mechanism. For example, the fact that the Pauli principle is expected to inhibit two-body reactions more in dense nuclear matter than in the surface leads to a surface localization. There is evidence from doublet splitting that effective two-body forces in the shell model are density dependent.[5]

It was shown in I that, for low-energy direct interactions, a qualitative difference is to be expected between angular distribution shapes for surface and

* Supported in part by the Australian Institute for Nuclear Science and Engineering and the Australian Atomic Energy Commission.

† Present address: University of California, Davis, California.

[1] I. E. McCarthy, Phys. Rev. **128**, 1237 (1962).

[2] G. R. Satchler in *Proceedings of the International Symposium on Direct Interactions and Nuclear Reaction Mechanisms, Padua 1962* (Gordon and Breach Publishers, Inc., New York, 1963); B. Buck, Phys. Rev. **130**, 712 (1963).

[3] L. R. B. Elton and L. C. Gomes, Phys. Rev. **105**, 1027 (1957).

[4] N. Austern, Ann. Phys. (N. Y.) **15**, 299 (1961); E. Rost, Phys. Rev. **128**, 2708 (1962).

[5] D. C. Peaslee, Phys. Rev. **124**, 839 (1961).

volume reactions, where the reaction mechanism is assumed to be the factor causing localization to the surface region. Localization due to the optical-model wave functions was discussed and two possible effects identified, phase averaging and focusing.

The present work reports detailed calculations of angular distributions in the distorted-wave Born approximation for several representative reactions. The object is to describe more quantitatively the effects identified in I. The main conclusions are that focusing is very important in determining general characteristics of angular distributions, in particular, it can cause large backward peaks; phase averaging while it exists, is not so important; the difference between surface and volume reactions is qualitatively significant.

In Sec. 2, phase averaging is discussed and examined quantitatively in a particular case.

In Sec. 3, four reactions which might be expected to proceed by the two-body collision mechanism are studied. Angular distributions for volume interaction are compared with those for surface interaction defined by completely eliminating the contribution to the matrix element from radii less than $r_0A^{\frac{1}{3}}$, the radius parameter in the Eckart form factor used for the optical-model potential. Large differences in shape and magnitude are found. In some cases, the dependence of the differences on the parameters is discussed so that some idea can be obtained about whether the effects would be expected to be genuine features of the reaction. The effects of different assumptions about surface localization are studied.

In Sec. 4, the backward peaks which are due to focusing in the optical-model wave functions are examined for different energies, different potentials, and different radial-localization factors.

The present calculations are done with a δ-function two-body interaction, since we are interested only in the effects of the optical-model wave functions in general. For realistic fits to experimental data it is probably necessary to have a finite range force with a realistic exchange mixture, but this defect is not expected to invalidate the type of conclusions we draw here.

2. PHASE AVERAGING AND FOCUSING IN DISTORTED WAVES

The differential cross section in the distorted-wave Born approximation for incident and outgoing particles of equal mass is given by

$$d\sigma/d\Omega=\frac{k}{k'}\left(\frac{\mu}{2\pi\hbar^2}\right)^2\frac{1}{2j+1}\sum_m|\sum_{LM}\mathfrak{M}_{mML}|^2, \quad (1)$$

where k and k' are the initial and final particle momenta, μ is the reduced mass of the incident particle, j,m are the angular-momentum quantum numbers of the initial bound state (assuming that only one particle can take part in the reaction) L,M are the angular-momentum transfer and its magnetic quantum number.

$$\mathfrak{M}_{mML}=\sum_{ll'} i^{l-l'}I_{mML,ll'}Y_{l'}{}^{M}(\theta,0), \quad (2)$$

where θ is the scattering angle, l,l' are the angular momenta of the partial waves for the entrance and exit channel optical-model wave functions. Suppressing the quantum numbers m, M, L, the partial matrix elements $I_{ll'}$ are overlap integrals of the form

$$I_{ll'}=\int dr\, r^2 f_l(kr)f_{l'}(k'r)R_{npj}(r)R_{n'p'j'}(r)v(r), \quad (3)$$

where f_l and $f_{l'}$ are radial-wave functions for the entrance and exit channel optical models, R_{npj} and $R_{n'p'j'}$ are radial-wave functions for the initial and final bound states whose principal and angular-momentum quantum numbers are respectively n,p and n',p'. Harmonic-oscillator wave functions of the form given by Glendenning[6] are used in this work. The δ-function approximation to the two-body potential has been used but its strength $v(r)$ is assumed to have a radial dependence.

It was shown in I how, in accordance with the suggestion of Austern,[4] the phases of f_l and $f_{l'}$ fall off with r more smoothly for distorted waves than for undistorted waves, thus resulting in a partial cancellation for small ($\ll kR$ where R is the nuclear radius) values of l because of phase averaging in the region where $R_{np}R_{n'p'}$ is appreciable.

Figure 1 illustrates the phases of f_l for different values of l in the case of 30-MeV neutrons on C^{12} with optical-model parameters $V=40$ MeV, $W=18$ MeV, $r_0=1.2$ F, $a=0.5$ F. It is clear that for $l<4$, which is approximately the surface value, the phase falls off quite smoothly with r, whereas for larger l, the phase curves have almost square corners as they do for plane waves, since the optical potential has little effect on these partial waves.

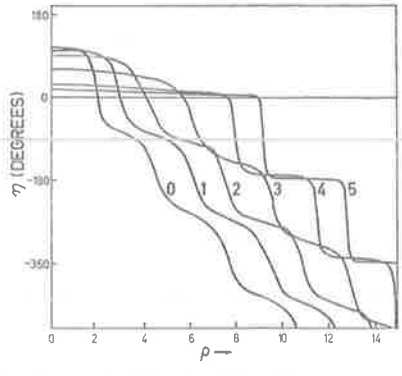

FIG. 1. The phase of $f_l(kr)$, the lth partial wave in the optical-model wave function for the scattering of 30-MeV neutrons from C^{12}, with parameters $V=40$ MeV, $W=8$ MeV, $r=1.2$ F, $a=0.5$ F. The phase is plotted against $\rho=kr$. The curves are labeled by the corresponding value of l.

[6] N. K. Glendenning, Phys. Rev. **114**, 1297 (1959).

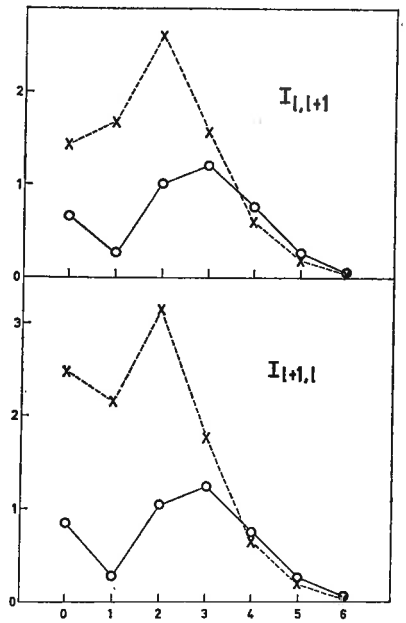

FIG. 2. The overlap integrals $I_{\frac{1}{2}01,ll'}$ and $I_{\frac{1}{2}01,l'l}$ defined in Eq. (3) plotted against l. The permissible values of l' are $l+1$ and $l-1$. The reaction is the inelastic scattering of 60-MeV protons from F^{19} for $L=1$. The circles indicate the values for the distorting potential $V=40$ MeV, $W=8$ MeV, $r_0=1.2$ F, $a=0.5$ F. The crosses indicate the values for distortion by the Coulomb potential but no nuclear potential.

Phase averaging gives a reduction in magnitude of $I_{ll'}$ for small l. It is not a particularly large reduction in the case of nucleons in the entrance and exit channels as can be seen from Fig. 2, where $I_{\frac{1}{2}01,ll'}$ and $I_{\frac{1}{2}01,l'l}$ are plotted against l for the inelastic scattering of 60-MeV protons on F^{19} causing excitation from the $\frac{1}{2}+$ ground state to the $\frac{1}{2}-$ first excited state. The values for fully distorted waves are compared with the values for waves distorted by the Coulomb potential only. $v(r)$ is taken to be constant.

Distortion also produces a phase change in the $I_{ll'}$. It was shown in I how the phase relationships of the partial waves produce focusing in the wave function. For fairly low energies (<30 MeV), as can be seen in Fig. 1, there are differences of up to 90° in the phases of successive partial waves for $l\cong kR$ (excluding the 90° difference arising from the factor i^l) which are capable of roughly reversing the direction of some of the $I_{ll'}$ relative to others so that at a scattering angle of 180°, where the cross section is small in the plane-wave theory due to cancellations among the $I_{ll'}$, it is possible to get reinforcement for distorted waves giving backward peaks. Backward peaks do not appear at high energies when the phase differences between successive partial waves are not large enough to cause significant constructive interference at 180°.

Phase averaging, resulting in a reduction of the magnitude of $I_{ll'}$ for small l,l', is expected to show up in dwBa angular distributions as a reduced dependence of the angular distribution on the center of the nucleus. Focusing, connected with the phases of the $I_{ll'}$ which are very different for successive l,l' in the surface region, large but not very different for successive small l,l' and small for large l,l', is expected to show up in DWBA angular distributions as backward peaking. The backward peaks are dependent on the energy and angular momentum transfer.

3. THE CONTRIBUTION TO THE DWBA FROM THE NUCLEAR INTERIOR

In order to see the effect of completely removing the contribution from the nuclear interior ($r<r_0A^{\frac{1}{3}}$) in different reactions at incident energies of 5 and 10 MeV, angular distributions were calculated using the potentials given in Table I. The potentials were the same in both exit and entrance channels.

The angular distributions for 5 MeV and 10 MeV are plotted in Figs. 3(a) and 3(b). The plots are on a linear scale to emphasize the peaks. The vertical scale is changed arbitrarily from curve to curve in order to facilitate comparison of shapes. In each case, the values of the differential cross section for surface interaction have been multiplied by a factor of about 100. This means that the contribution of the interior to the matrix elements is about 10 times that of the surface with this definition of the surface.

At 5 MeV, although the shapes of the angular distributions for volume and surface interaction are different, the differences are perhaps not so great that they could not be removed by reasonable changes of parameters.

At 10 MeV, systematic differences become obvious. The surface cases show more structure. They are compressed towards small angles as would be expected from the larger average radius, so that where backward peaks occur for volume interaction, they are shifted towards smaller angles for surface interaction and the backward cross section is relatively small. This effect is observed in all the cases except $Ca^{40}(n,p)K^{40}$ which is too complicated to generalize about.

It is interesting to compare odd L cases with even L cases. For this purpose, we will discuss $F^{19}(p,p')F^{19*}$ and $C^{13}(p,n)N^{13}$. Because of the parity rule,[7] the F^{19} case

TABLE I. Potentials used in volume and surface reaction calculations.

Reaction	E (MeV)	V (MeV)	W (MeV)	r_0 (F)	a (F)	L
$F^{19}(p,p')F^{19*}$	5	45	4	1.2	0.55	1
	10	55	4	1.2	0.55	
$C^{13}(p,n)N^{13}$	5	55	4	1.2	0.55	0
	10	55	4	1.2	0.55	
$In^{115}(p,p')In^{115*}$	5	45	4	1.2	0.55	5
	10	45	4	1.2	0.55	
$Ca^{40}(n,p)K^{40}$	5	45	4	1.2	0.55	3, 5
	10	45	4	1.2	0.55	

[7] A. J. Kromminga and I. E. McCarthy, Phys. Rev. Letters 6, 62 (1961).

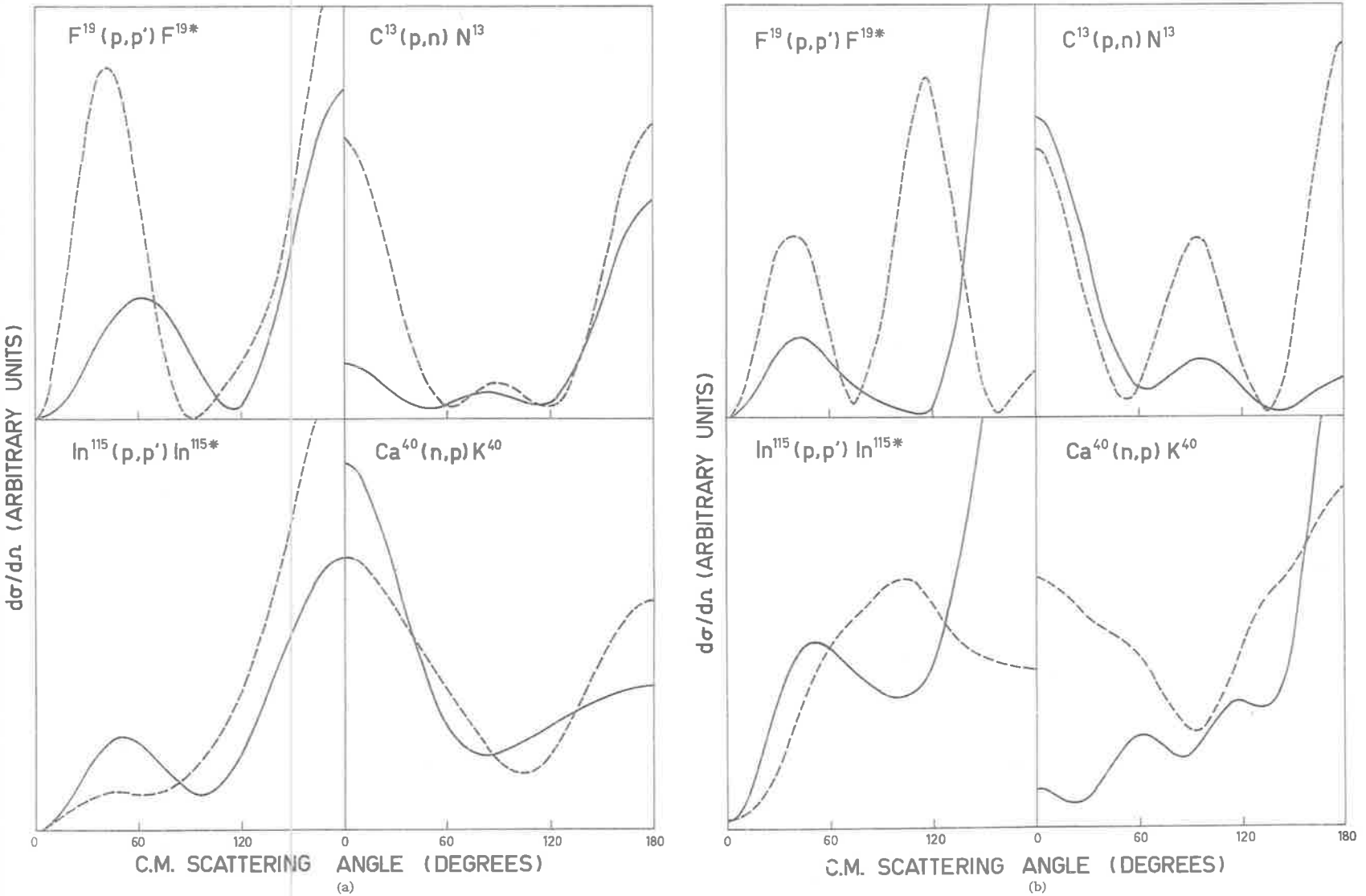

FIG. 3. (a) The angular distributions for 5 MeV and (b) 10 MeV incident energy for the reactions listed in Table I. The continuous line indicates volume interaction, the broken line indicates surface interaction. The vertical scale factors have no significance from one curve to another. The vertical scale is linear.

is constrained to have very small forward cross section. The backward peak is the major qualitative feature that will be discussed.

Figure 4 shows that, for the F^{19} case at 10 MeV, changing the real part of the optical-model potential from 45 to 55 MeV has little effect on the backward peak for volume interaction but decreases it by a factor of 3 for surface interactions without much changing the general shape of the curve. In terms of the focus overlap explanation of backward peaks,[8] this means that the focus is brought a little nearer to the center of the nucleus by the increase in potential and that this has a small relative effect when the whole focus plays a part, but a larger relative effect when we omit the contribution to the matrix element from all but the edge of the focus. This behavior of the foci is illustrated in Fig. 5.

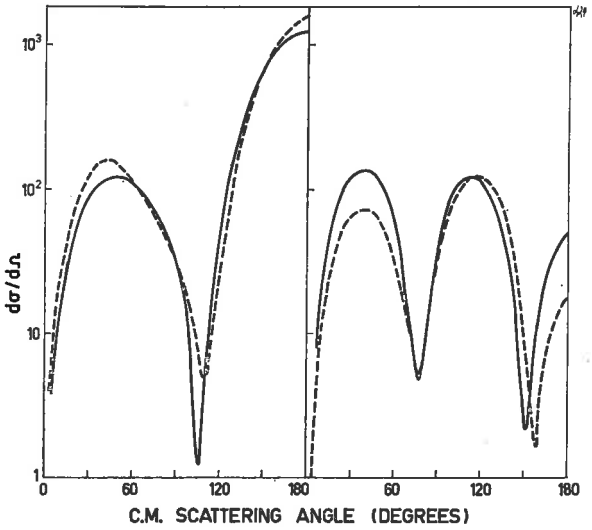

FIG. 4. Angular distributions for the reaction $F^{19}(p,p')F^{19*}$ with $L=1$ at 10 MeV. Volume interaction is on the left, surface interaction on the right. The continuous lines indicate calculations done with $V=45$ MeV. The broken lines are for $V=55$ MeV. Other parameters are those of Table I. The curves on the right have been multiplied by 100. The units on the vertical scale are arbitrary, but consistent from curve to curve.

The other parameters are found to have less effect than V on the shape. Increasing W decreases the magnitude of the cross section by roughly a constant factor. These curves are plotted logarithmically. The scale factors for each volume interaction curve are equal. The scale factors for each surface interaction curve are equal and 100 times those for volume interaction.

Figure 6 shows the C^{13} case at 10 MeV. The surface interaction scale factor is 1000 times the volume interaction scale factor. In this case, where L is even, both forward and backward peaks are strongly dependent on the foci. For volume interaction, increasing the potential from 45 to 55 MeV has a large effect on the backward peak, but not on the forward peak, without qualitatively

[8] I. E. McCarthy and D. L. Pursey, Phys. Rev. 122, 578 (1961).

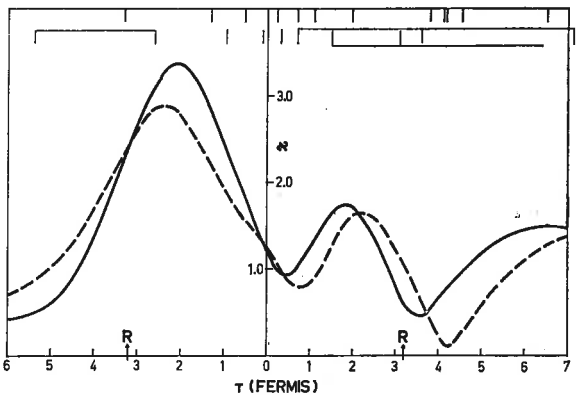

FIG. 5. The magnitude χ and phase of the optical-model wave function for the entrance channel in the cases shown in Fig. 4 calculated on the scattering axis. The broken line is for $V=45$ MeV, the continuous line is for $V=55$ MeV. The top row of marks at the top of the diagram indicates the phase for the broken line. The marks are at intervals of 50°. The bottom row is for the continuous line. Marks representing equal phases are linked.

changing the shape of the angular distribution. For surface interaction, the increase in the potential causes more of the focus to miss the interaction region with a resulting general decrease in cross section. The focal behavior in each channel is shown in Fig. 7.

The greatly reduced magnitude for surface reaction matrix elements is of course due to the fact that only the tail of the bound-state wave function contributes. It is necessary to examine different definitions of surface interaction to see how the cross sections depend on them.

This has been done for the $L=1$ $F^{19}(p,p')F^{19*}$ case. First, the shape of the angular distribution must depend strongly on the reduction factor between central and

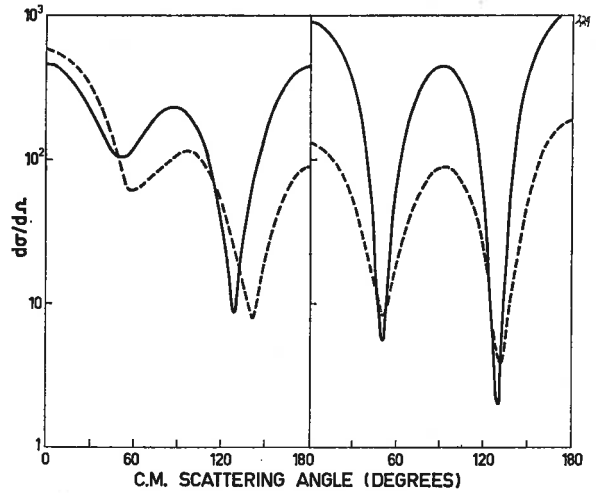

FIG. 6. Angular distributions for the reaction $C^{13}(p,n)N^{13}$ with $L=0$ at 10 MeV. Volume interaction is on the left, surface interaction on the right. The continuous lines are for $V=45$ MeV, the broken lines are for $V=55$ MeV. Other parameters are those of Table I. The curves on the right have been multiplied by 1000. The units on the vertical scale are arbitrary, but consistent from curve to curve.

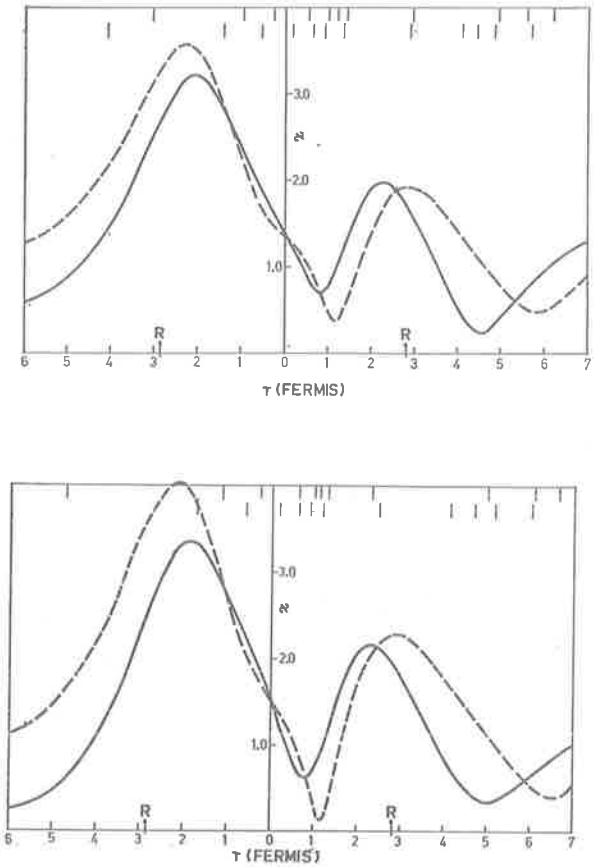

FIG. 7. Magnitudes χ and phases (indicated by marks as for Fig. 5) of the entrance (top) and exit (bottom) channel optical-model wave functions for the cases of Fig. 6. The broken line is for $V=45$ MeV, the continuous line is for $V=55$ MeV.

surface interaction. It is unlikely that reactions would be purely confined to the surface. Calculations have been done with a square-form factor giving the radial dependence of the interaction potential $v(r)$.

$$v(r)=f, \quad r\leqq R_f.$$
$$v(r)=1, \quad r>R_f.$$

The incident energy used was 10 MeV and the parameters were those of Table I. The radius R of the Eckart form factor is about 3.2 F in this case.

For $R_f=R$, $f=0.5$, it was found that the shape of the angular distribution was indistinguishable from that in the case $f=1$ (volume interaction), but the magnitude was reduced by a factor 4. Clearly, this calculation corresponds merely to a volume calculation with a reduced potential $v(r)$ and a slightly different tail. The intermediate cases will have similar shapes to the extreme cases unless the central and surface parts of the overlap integrals are of the same order of magnitude.

When R_f was reduced to 2.2 F, with $f=0$, it was found that the three peaks characteristic of surface interaction remained, but the backward peak was much higher than the first peak, indicating that the interaction region now included a significant amount of the foci.

Figure 8 shows two intermediate cases where the magnitudes of the cross sections are roughly similar. In one case we have larger R_f and larger f than the other. The values used were $R_f=2.2$ F and 1.8 F and $f=0.5$ and 0 respectively. The third peak characteristic of surface interaction is still present in each curve but the backward peaks are large in each case. The magnitudes of the backward peaks are 0.7 of the value for $f=1$.

The angular distribution was also calculated using a form factor $v(r)$ which was the derivative of the Eckart form factor. Three peaks were again observed.

It is fairly clear that in this reaction a tendency to surface weighting is shown by the appearance of a peak at about 90°, which seems to be quite a critical test of the surface weighting assumption. It would perhaps be surprising if refinements to the calculation such as inclusion of spin-orbit coupling in the optical model and a more realistic two-body force would change this qualitative conclusion. Further work is planned on this point. The experiment would be well worth doing.

Surface and volume interaction has also been compared in the F^{19} case at energies up to 60 MeV. It is a

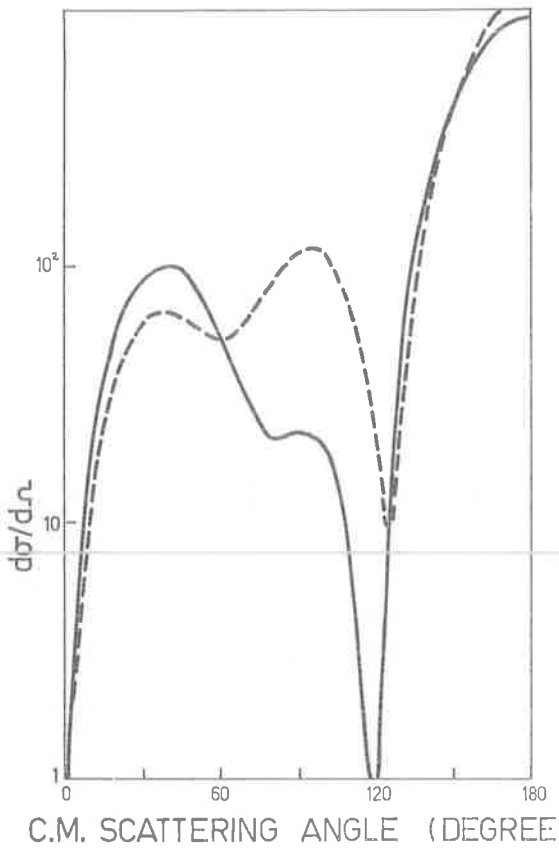

FIG. 8. Angular distributions for the inelastic scattering of 10-MeV protons from F^{19} with $L=1$. The parameters are those of Table I. The continuous line represents the calculation with $R_f=2.2$ F, $f=0.5$, the broken line is for $R_f=1.8$ F, $f=0$.

general rule that there are more peaks in the surface interaction angular distributions than the volume interaction ones. Focusing certainly is not a property of the interior at higher energies, so there is no doubt that the interior contribution to the matrix element is important in determining the angular distribution, independent of focusing. Hence, there is no purely optical-model effect such as phase averaging or total internal reflection that makes the interior contribution unimportant.

The qualitative conclusions that can be drawn from these examples are as follows.

In general, there are significant differences between angular distributions for volume and purely surface interactions. In the case of $L=1$ reactions on light nuclei, the difference is extremely marked, with three peaks in the 10 MeV surface interaction case and only two in the 10 MeV volume interaction case. The general fact that surface interactions have more peaks than volume interactions persists at energies up to at least 60 MeV.

The differences are most marked near 180° in all cases, while they are also important at 0° for parity-preserving reactions. The nature of the differences depends on the real part of the potential, the qualitative dependence being understandable on the picture of focus overlap causing backward peaks. The energy dependence of the backward peaks is different for different potentials as well as for different localization assumptions. In the next section the backward peaks will be examined in more detail in particular cases.

Surface-reaction matrix elements, which include only the tail of the bound-state wave function, are considerably smaller in magnitude than those for volume interaction. The magnitude depends strongly on the exact manner in which the surface interaction is defined.

Intermediate cases between volume and pure surface interaction generally show characteristics of both so that there is hope of identifying them experimentally.

4. FOCUS EFFECTS IN DWBA ANGULAR DISTRIBUTIONS

It has previously been shown[8] how backward peaks can arise in the distorted-wave Born approximation from the fact that, at 180° the foci in the entrance and exit channels overlap. At backward angles the other large parts of the optical-model wave functions, namely the surface parts on the same side of the nucleus as the incident or outgoing particle in the entrance and exit channels, respectively, also overlap, so that two fairly distinct regions of space contribute to the matrix element. Interference between these "surface" and "focus" contributions results in variation of the height of the backward peaks with energy.[9] At forward angles the focus of one wave function overlaps the surface part of the other. The focus is mainly responsible for the forward peaks in parity-preserving reactions with $L>0$. Because of the rather sharp division of the parts of space contributing to the backward matrix element, the backward peaks should depend rather critically on the optical-model properties of the matrix element, which we are considering here, and less on the details of the two-body interaction. The position of the foci, in particular, should be very important.

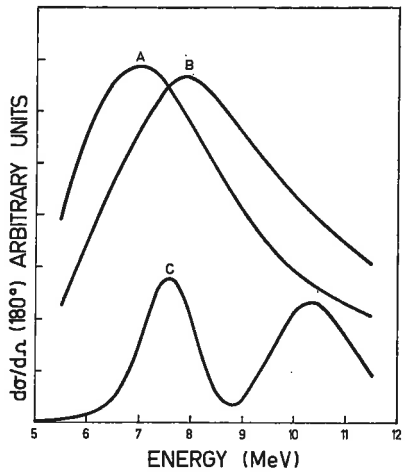

FIG. 9. The differential cross section at 180° for $C^{13}(p,n)N^{13}$ as a function of energy. Curves (A) and (B) are for $V=50$ and 47 MeV, respectively, and $W=6$ MeV, $r_0=1.2$ F, $a=0.55$ F, $R_b=2.3$ F, $f=1$. Curve (C) is for $V=50$ MeV, $W=6$ MeV, $r_0=1.2$ F, $a=0.55$ F, $R_b=2.2$ F, $R_f=2.2$ F, $f=\frac{1}{16}$.

Energy variation of the backward cross section may also be due to the positions of the foci. These are determined by the incident energy and the real parts of the optical-model potentials. Variation of the imaginary parts of the optical-model potentials with energy produces variation of the focal intensities and, hence, variation of the backward cross section.

For low energies and large V, the focus is near the center of the nucleus. As the energy increases or V decreases it moves out to larger radii. Radial variation of the bound-state wave functions therefore produces energy variation of the focal contribution to the matrix element. A semiclassical model of this effect has been calculated by Pearson.[10]

The variation of the backward cross section with energy and potential has been studied for the reaction $C^{13}(p,n)N^{13}$ for which experimental data are available[11] at incident energies between about 3.5 and 13 MeV. The experimental distribution with energy of the backward cross section shows a strong peak at about 6 MeV and possibly a second peak between 8 and 9 MeV. The points are widely scattered due, no doubt, to effects of more or less isolated resonances, but the general trend would be expected to be given by direct interaction theory.

Figure 9 shows the energy variation of the backward

[8] A. J. Kromminga and I. E. McCarthy, Nucl. Phys. 24, 36 (1961).

[9] C. A. Pearson (to be published).

[10] P. Dagley, W. Haeberli, and J. X. Saladin, Nucl. Phys. 24, 353 (1961).

cross section using the following parameters in both entrance and exit channels. $V=50$ MeV, for curves (A) and (C), 47 MeV for curve (B), $W=6$ MeV, $r_0=1.2$ F, $a=0.55$ F. The radius R_b of the $1p$ bound-state wave function used in each channel was 2.3 F for curves (A) and (B), 2.2 F for curve (C). This is unrealistically small. Two different shapes for the radial two-body form factor $v(r)$ were used, namely $f=1$ (volume interaction) for curves A and B, and $f=1/16$, $R_f=2.2$ F. This value of f gives center and surface contributions to the matrix element of the same order of magnitude. Only the shapes of the curves are significant.

The most striking fact about the curves of Fig. 9 is that the energy variation of the backward cross section reflects the shape of the factor

$$R_{npj}(r)R_{n'p'j'}(r)v(r)$$

in the overlap integral for the matrix element. In this case, the same $1p$ harmonic-oscillator wave function was used for both entrance and exit channels. The radial factor has one peak in the $f=1$ case. A peak might be expected to appear in the energy distribution when the focus is situated at the radius of the peak in the wave functions. The peak is at a higher energy for curve (B) than for curve (A). This is contrary to the simple picture because the focus should be at a slightly larger radius for smaller V. However, the situation is complicated by focus-surface interference. The relative phase of the surface and focus contributions changes rapidly with V and energy and the same situation would be expected to arise at lower energy for higher V. The large Q value of -3.005 MeV means also that the entrance and exit channel foci occur at different radii. The magnitude and phase of the entrance channel wave function at 5 and 10 MeV are shown in Fig. 10.

Curve (C) shows that, when the surface is weighted more than the center, the backward cross section increases again as the foci enter the heavily weighted region.

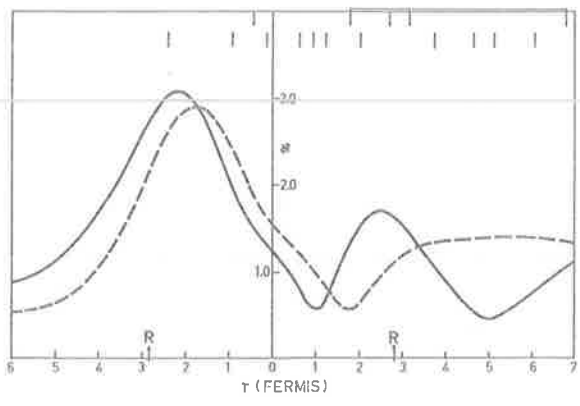

FIG. 10. Magnitudes χ and phases (indicated by marks as for Fig. 5) of the entrance-channel wave functions at 5 MeV (broken line) and 10 MeV (continuous line) on the scattering axis for case A of Fig. 9.

The variation of the optical-model potentials w energy is also a complicating factor. However, t variation should at least be monotonic, so any sign cant tendency to a second peak in the energy variat curve could indicate surface weighting. It was fou that, in this energy region, the increase in W w energy was the most important determining factor the shape of the energy distribution, causing it to di quickly at higher energies.

The effect of the foci in producing forward peaks cases where L is even and greater than zero is illustra in Fig. 11 for the inelastic scattering of protons fr the second excited state of F^{19}. Here $L=2$. The para eters were those of Table I. The curves on the left for 10 MeV, those on the right for 20 MeV incid energy. The shapes only are significant. The solid cur are for $f=1$, the dashed curves for $f=0$, $R_f=R$.

In the 10 MeV case for surface interaction, the fo is in the central region, so the forward cross sectior small. At 20 MeV, the focus is in the surface region. T relative heights of forward and backward peaks are same in this case for surface and volume interactio This may, however, be just an accident at the particu energy.

5. CONCLUSIONS AND DISCUSSIONS OF EXPERIMENTS

Purely optical-model effects such as phase averag do not significantly reduce the contribution of interior of the nucleus to the distorted-wave B approximation matrix elements at any energy. Sign cant differences between surface and volume interact mechanisms persist at high energy and show up angular distributions.

At energies up to about 30 MeV the shapes of angu distributions are greatly affected by the foci in optical-model wave functions. The movement of focus from small to large radii as the energy increa

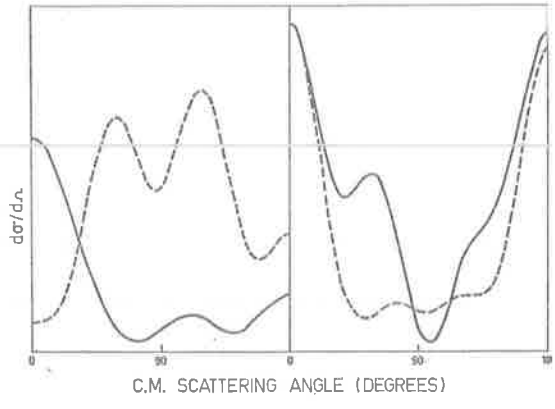

FIG. 11. Angular distribution for the inelastic scattering 10 MeV (left side) and 20 MeV (right side) protons from second excited state of F^{19} with $L=2$. Continuous lines are volume interaction, broken lines are for surface interaction. parameters are $V=55$ MeV, $W=4$ MeV, $r_0=1.2$ F, $A=0.5$ $R_b=R_f=3.2$ F.

should give a sensitive test of the assumption that the surface is more heavily weighted than the center due to the reaction mechanism. The energy dependence of focus effects such as backward peaks should show up any substantial surface weighting.

These general conclusions could be tested by observing the energy dependence of backward cross sections for known collective excitations where the surface weighting assumption is reasonably well established.

It has been shown in Sec. 3 that the magnitude of the cross section is very sensitive to the surface weighting factor. Although the zero-range potential assumption is too crude to expect fits to angular distributions, it is useful to compare the magnitudes of the cross sections with the experimental ones[11] in the case of $C^{13}(p,n)N^{13}$ with different assumptions about surface weighting.

The two-body potential will be written as

$$U(|\mathbf{r}_1-\mathbf{r}_2|)=4\pi\mu^{-3}U_0v(r_1)\delta(|\mathbf{r}_1-\mathbf{r}_2|)$$

in order to compare it with the Yukawa potential (μ is the range parameter set equal to 1.15 F^{-1}). For $f=1$ we find $U_0\approx 60$ MeV, whereas in the extreme case $f=0$, $R_f=R$, a value of $U_0\approx 1000$ MeV must be used. Intermediate cases have intermediate values according to the rough proportionality rules illustrated in Sec. 3. 60 MeV is roughly comparable with the value of U_0 for free nucleon-nucleon scattering.

In this context it is interesting to note that a calculation[12] performed by Agodi and Schiffrer with a realistic potential including finite range and exchange for the reaction $Si^{28}(n,p)Al^{28}$ at 14 MeV required values of U_0 larger by a factor of between two and three than the one determined from the free n-p interaction. Hence, it is clear that there appears to be an effect of nuclear matter on the two-body scattering operator of a large enough magnitude to be observed according to the considerations of Sec. 3 (see particularly the discussion of Fig. 8, where an effect of density dependence on the angular distribution is noticeable when there is a ratio of only 0.7 between the magnitudes of the curves for the surface weighting and volume interaction cases compared with the ratio of 0.1 to 0.5 between U_0^2 for free particles and the value of U_0^2 for the effective potential in $Si^{28}(n,p)Al^{28}$).

A program of future work is planned in which the considerations of the present work will be investigated with an improved model including surface absorption, finite range forces with exchange, and spin-orbit coupling. It is not hoped to fit angular distributions until this is done. The effect of exchange forces in particular on the forward cross section for $Si^{28}(n,p)Al^{28}$ is to improve experimental agreement significantly.[12]

[12] A. Agodi and G. Schiffrer, Nucl. Phys. (to be published); A. Agodi, R. Giordano, and G. Schiffrer, Phys. Letters 4, 253 (1963).

ACKNOWLEDGMENTS

We would like to thank Dr. C. A. Pearson for useful discussions, Dr. J. R. Rook, Dr. P. E. Hodgson, and Dr. B. A. Robson for helping us check our distorted wave code, Dr. A. Agodi and Dr. G. Schiffrer for prepublication information, and the staff of the Adelaide University Computing Center and Weapons Research Establishment, S. A. Salisbury, for cooperation with computing problems.

REFERENCES

*1 G.E. BROWN Proc. Int. Conf. on Nuclear Structure, Kingston 1960. (Uni. of Toronto Press. Eds. D.A. Bromley and E.W. Vogt).

*2 S.I. DROZDOV Soviet Physics - J.E.T.P. 1, 588 and 599 (1955).

S.I. DROZDOV Soviet Physics - J.E.T.P. 7, 889 (1959).

E.V. INOPIN Soviet Physics - J.E.T.P. 4, 764 (1957)

J.S. BLAIR Phys. Rev. 115, 928 (1959)

*3 W.T. PINKSTON and G.R. SATCHLER Nucl. Phys. 27, 270 (1961).

*4 L.R. DODD and I.E. McCARTHY Proc. Int. Symp. on Direct Interactions and Nuclear Reaction Mechanisms, PADUA, 1962. (Eds. E. Clementel and C. Villi).

*5 A.J. KROMMINGA and I.E. McCARTHY Phys. Rev. Letters 6, 62, (1961).

*6 A.J. KROMMINGA and I.E. McCARTHY Nucl. Phys. 31, 678 (1962).

*7 V.F. WEISSKOPF Rev. Mod. Phys. 29, 174, (1957),

*8 M.G. MAYER and J.H.D. JENSEN "Elementary Theory of Nuclear Shell Structure". (John Wiley, New York, 1955).

D. INGLIS Handbuch der Physik P.H. XXXIX.

S. MOSZKOWSKI Handbuch der Physik P.H. XXXIX.

*9 S.G. NILSSON Dan. Mat.-Fys. Medd. 29, 16, (1955).

*9 J.P. ELLIOTT and B.H. FLOWERS Proc. Roy. Soc. A229, 536, (1955).
J.P. ELLIOTT Proc. Roy. Soc. A245, 128 and 562, (1958).

*10 N.K. GLENDENNING Phys. Rev. 114, 1297, (1959).

*11 C.A. LEVINSON and M.K. BANERJEE Ann. Phys. 2, 471 and 499 (1957) also Ann. Phys. 3, 67, (1958).
E.ROST and N. AUSTERN Phys. Rev. 120, 1375, (1960)

*12 S.T. BUTLER and O. HITTMAIR "Nuclear Stripping Reactions" (Horwitz, Sydney).
N. AUSTERN "Fast Neutron Physics" Vol. II (Interscience 1962).

*13 F. FESHBACH Ann. Rev. of Nucl. Sc. 8, 49, 1958.

*14 F.E. BJORKLUND, S. FERNBACH and N. SHERMAN Phys. Rev. 101, 1832 (1956).
F.E. BJORKLUND and S. FERNBACH Phys. Rev. 109, 1295 (1958).

*15 I.E. McCARTHY Phys. Rev. 128, 1237, (1962).

*16 I.E. McCARTHY Nucl. Phys. 11, 574, (1959).

*17 R.M. EISBERG, I.E. McCARTHY and R.A. SPURRIER Nucl. Phys. 10, 571 (1959).

*18 I.E. McCARTHY and D.L. PURSEY Phys. Rev. 122, 578, (1961).

*19 L.R.B. ELTON and L.C. GOMES Phys. Rev. 105, 1027 (1957).

*20 N. AUSTERN Ann. Phys. 15, 299, (1961)

*21 P. DAGLEY, W. HAEBERLI and J.X. SALADIN Nucl. Phys. 24, 353, (1961).

*22 A. AGODI and G. SCHIFFRER (private communication).

*23 A. AGODI and G. SCHIFFRER Nucl. Phys. 46, 545, (1963).

A. AGODI, R. GIORDANO and G. SCHIFFRER Phys. Letters 4, 253, (1963).

*24 S. MOSZKOWSKI Lawrence Radiation Lab. Report UCRL-5701.

*25 K.L. LIM and I.E. McCARTHY Proc. Int. Symp. on Direct Interactions and Nuclear Reaction Mechanisms, PADUA, 1962. (Eds. E. Clementel and C. Villi).

*26 L. ROSENFELD "Nuclear Forces" (North-Holland 1948).

*27 D.C. PEASLEE Phys. Rev. 124, 839, (1961).

*28 M.E. ROSE "Elementary Theory of Angular Momentum" (Wiley 1957).

A.R. EDMONDS "Angular Momentum and Quantum Mechanics" (Princeton U.P. 1957).

*29 R.J. EDEN Prog. Theor. Phys. 6, 26, (1957).

I.S. SHAPIRO Soviet Physics - Uspekhi 4, 674, (1962).

H.H. BARSCHALL Proc. Int. Conf. on Nucl. Physics, PARIS 1958. (Ed. P. Gugenberger).

A.E. GLASSGOLD Proc. Int. Conf. on Nucl. Physics PARIS, 1958. (Ed. P. Gugenberger).

A.E. GLASSGOLD Prog. In Nucl. Phys. 7, 123, (1958).

*30 E.P. WIGNER and L. EISENBUD "Nuclear Structure" (Princeton U.P.)

*31 V.F. WEISSKOPF and D.H. EWING Phys. Rev. 57, 472, (1940).

*32 J.P. BLASER, F. BOEHM, P. MARMIER and D.C. PEASLEE Helv. Phys. Acta 24, 3, (1951).

P.C. GUGELOT Phys. Rev. 81, 51, (1951).

E.R. GRAVES and L. ROSEN Phys. Rev. 89, 343, (1953).

*33 H.H. BARSCHALL Phys. Rev. 86, 431, (1952).

*34 P.C. GUGELOT Phys. Rev. 93, 425, (1954).

*35 S. FERNBACH, R. SERBER and T.B. TAYLOR Phys. Rev. 75, 1352, (1949).

*36 H. FESHBACH, C.E. PORTER and V.F. WEISSKOPF, Phys. Rev. 90, 166, (1953).

H. FESHBACH, C.E. PORTER and V.F. WEISSKOPF, Phys. Rev. 96, 448, (1954).

*37 M. WALT, J.R. BEYSTER and E.W. SALMI Phys. Rev. 104, 1319, (1956).

*38 D. SAXON Proc. Int. Conf. on Nucl. Structure, KINGSTON, 1960. (Uni. of Toronto Press Eds. D.A. Bromley and E.W. Vogt).

*39 N. HINTZ, C.D. KAVALOSKI, L.L. LEE Jr., and T. STOVALL, Proc. Rutherford Jub. Int. Conf. (Heywood, 1961).

*40 C.A. PEARSON, A.A.E.C. Report TM-197.

*41 P.E. HODGSON Proc. Int. Symp. of Direct Interactions and Nuclear Reaction Mechanisms, PADUA, 1962 (Eds. E. Clementel and C. Villi).

*42 G.R. SATCHLER Proc. Int. Symp. on Direct Interactions and Nuclear Reaction Mechanisms, PADUA, 1962. (Eds. E. Clementel and C. Villi).
N. AUSTERN, R. DRISKO, E.C. HALBERT and G.R. SATCHLER Phys. Rev. (in press)

*43 I.E. McCARTHY Phys. Rev. 134, B1285, 1964.

*44 A.B. CLEGG Physics Letters 7, 132, 1963.

*45 J.H.D. JENSEN in "Beta and Gamma Ray Spectroscopy", ed. K. SIEGBAHN p.415 (Interscience 1955).

*46 C.P. SWANN and METZGER Phys. Rev. 100, 1329 (1955).
F.J. SHORE, W.L. BENDEL and R.A. BECKER Phys. Rev. 83, 688 (1951).
F.J. SHORE, W.L. BENDEL, H.N. BROWN and R.A. BECKER Phys. Rev. 91, 1203 (1953).